

Investigating the cellular, molecular and immunological mechanisms of pathological filarial associated lymphatic remodelling

Thesis submitted in accordance with the requirements of the University of Liverpool for the degree of Doctor of Philosophy

by

Julio Furlong-Silva

August 2019

Declaration

I declare that the work presented in this thesis is all my own and that it has not been submitted for any other degree

.....

Acknowledgements

First and foremost, I am forever indebted to my primary supervisor Dr Joseph Turner, who has given me an innumerable amount of his time, patience and herculean support in completing this journey and thesis. No matter how bizarre, crazy or mind-blowingly expensive my ideas and thoughts for “the next big experiment”, he has always encouraged me and gave me the freedom to explore those avenues that I’m certain the vast majority of supervisors simply wouldn’t have entertained! I simply hope the work detailed in this thesis goes at least a small way to repaying that debt.

I would like to thank my secondary supervisor, Professor Mark Taylor for offering his time and support, but perhaps most usefully, teaching me how to cast a critical eye over my own work and to never forget how to place my work into ‘the bigger picture’. I also appreciate the support of my progress assessment panel team: Dr Alvaro Acosta-Serrano, Dr Steve Christmas and Dr James LaCourse all of which put up with my annual pestering emails, while donating their valuable time and effort to give me brilliant feedback and encouragement.

The financial support of the Liverpool School of Tropical Medicine Studentship and MRC was absolutely vital and all of the work in my thesis simply wouldn’t have happened if it wasn’t for them.

Special thanks to Dr Nicolas Pionnier and Dr Stephen Cross for their time and effort in training me in a variety of lab techniques, hopefully the progress from fresh faced student to hardened Flow cytometry warrior has filled you with pride. Thanks also goes to Miss Amy Marriott, Mr Shannon Quek (particularly for his R expertise!!) and Miss Anfal Yousef for sticking it out in the trenches with me and keeping me sane in my hours of need.

Last, but certainly not least, I am incredibly lucky to have the amazing support of my girlfriend; Miss Bethany McCann, my mum; Mrs Christine Silva, my dad,;Mr Jose Silva, my sister; Miss Jessica Silva and my best friend and cousin, Mr Benjamin Evans. There is no doubt I would not have made it this far without all of you, the words thank you will never be enough but always remember, without all of you, I am nothing.

Table of Contents

Declaration.....	2
Acknowledgements.....	3
Table of Contents.....	5
Figures and Tables	10
Abbreviations	13
Abstract.....	16
Introduction	18
1.1-The Global Burden, Consequences and Clinical Manifestations of Lymphatic Filariasis.....	19
1.2-The Filarial Life Cycle and aetiology of Filariasis	26
1.3-The human lymphatic system and lymphatic remodelling in health and disease	30
1.4-Lymphatic dysfunction, insufficiency and LE	36
1.5-Primary and secondary LE	37
1.6- Filarial LE, a neglected facet of a neglected tropical disease?	38
1.7- <i>in vitro</i> , <i>in vivo</i> and clinical evidence of a role for lymphatic remodelling in filarial infection and pathology	41
1.8-Filarial-associated lymphatic remodelling and implications for pathogenesis	44
1.9- Project Aims and Objectives	46
Characterisation of an inbred murine experimental model of filarial-induced lymphatic pathology	49
2.1 Introduction.....	50
2.1.1- Research Aims and Objectives	53
2.2- Methods	54
2.2.1- Mouse Maintenance	54
2.2.2- Parasite Life Cycle and Maintenance	54
2.2.3- Leg pathology model experimental infection.....	55
2.2.4-Intravital Near-Infrared (NIR) Imaging of lymphatic flow	55
2.2.5-Quantification of lymphatic remodelling and lymphatic insufficiency	56
2.2.6-Evan’s Blue dermal retention assay (modified Miles Assay).....	57
2.2.7-Epifluorescence Microscopy and quantitation of Lymphatic vessel width	58
2.2.8-Epifluorescence tracking of <i>BmL3</i> migration.....	59

2.2.9-Lymph node and cardiac blood sampling	59
2.2.10-Statistical Analysis	60
2.3- Results	63
2.3.1- Significant lymphatic remodelling and lymphatic insufficiency is evident post- infection with <i>B. malayi</i> larvae	63
2.3.2- <i>BmL3</i> migrate into pre-collector lymphatic channels, proximal to areas of lymphatic remodelling, as early as 3 hours following inoculation	64
2.3.3- Challenge filarial infection significantly increases lymphatic remodelling and lymphatic insufficiency compared to single infection ..	71
2.3.4- Aberrant lymphatics and lymphatic insufficiency persist 12 weeks following infection with <i>B. malayi</i> L3.	71
2.3.5- <i>BmL3</i> infection is associated with a significant lymphadenopathy and increased cellularity of local draining lymph nodes.	72
2.3.6- C57BL/6J mice demonstrate significantly elevated severities of lymphatic remodelling and insufficiency versus BALB/c mice following filarial infection	77
2.4- Discussion.....	82
2.5- Concluding remarks	95
Investigating the molecular mechanisms of filarial inflammatory associated lymphatic pathology.....	97
3.1- Introduction	98
3.2- Methods	100
3.2.1-Murine hind-limb infection model and associated pathological readouts.....	100
3.2.2-Cardiac blood sampling and harvesting of plasma	100
3.2.3-Multiplex Analysis of circulating angiogenic/lymphangiogenic molecules.....	100
3.2.4- Analysis of TGF- β and BMP-9/10 by Enzyme Linked Immunosorbent Assay (ELISA).....	100
3.2.5-VEGF-C Adenoviral infection experiments	101
3.2.6-Sunitinib intervention experiments.....	101
3.2.7-VEGFR-3-Fc and ALK-1-Fc chimera intervention experiments .	102
3.2.8-Statistical Analysis.....	102
3.3- Results	104
3.3.1- <i>BmL3</i> infection is associated with rapid upregulation of multiple circulating lymphangiogenic molecules.....	104

3.3.2- Sequential <i>BmL3</i> re-infection results in further upregulation of circulating lymphangiogenic molecules compared to primary <i>BmL3</i> infection	104
3.3.3- Increased filarial lymphatic pathology in C57BL/6J mice, compared to BALB/c mice, is associated with variation in circulating lymphangiogenic mediators.	107
3.3.4- Local upregulation of VEGF-C is sufficient to induce significant levels of lymphatic remodelling and pathological lymphatic insufficiency	110
3.3.5- Sunitinib treatment is insufficient to modify filarial-associated lymphatic pathology or circulating VEGF growth factors.....	115
3.3.6- <i>In vivo</i> administration of a sVEGFR3-Fc ‘trap’ failed to significantly modify circulating VEGF-C following <i>BmL3</i> infection.	116
3.3.7- Administration of an ALK-1-Fc ‘trap’ did not significantly impact on filarial associated lymphatic remodelling and insufficiency, following <i>BmL3</i> infection.	117
3.4- Discussion.....	122
3.5- Chapter concluding remarks	133
Cellular mediators of filarial inflammatory-associated lymphatic pathology	135
4.1- Introduction	136
4.2- Methods	139
4.2.1-Murine hind-limb infection model and associated pathological readouts.....	139
4.2.2-Lymphoid and lymphatic tissue harvest and single cell preparation	139
4.2.3-Flow cytometry	140
4.2.4-Fluorescent Antibody Cell Sorting (FACS) and subsequent cell secretion assays	140
4.2.5-Multiplex Analysis	141
4.2.6-Cell culture.....	141
4.2.7-Production of <i>Brugia malayi</i> L3 larval extract (<i>BmL3E</i>).....	142
4.2.8-Macrophage/ LEC co-culture proliferation assay	142
4.2.9- CCR2 and clodronate liposome monocyte/macrophage depletion experiments	143
4.2.10-Statistical Analysis	143
4.3- Results	146

4.3.1- <i>B. malayi</i> infection induces significant increases in multiple leukocyte populations within lymphatic / lymphoid tissues proximal to larval invasion.	146
4.3.2- The contribution of 'resident' Tim-4 ⁺ M ϕ to the overall sdLN M ϕ compartment is significantly diminished following <i>BmL3</i> infection.	146
4.3.3- C57BL/6J mice demonstrate more pronounced expansions of CD11b ⁺ Ly6C ⁺ CCR2 ⁺ inflammatory monocytes and Cd11b ⁺ MHCII ⁺ F/480 ⁺ M ϕ compared to BALB/c mice in lymphatic / lymphoid tissues proximal to <i>B. malayi</i> larval invasion	147
4.3.4- CD11b ⁺ Ly6C ⁺ CCR2 ⁺ monocytes, CD11b ⁺ MHCII ⁺ F480 ⁺ M ϕ 's and CD3 ⁺ T-cells are significant sources of lymphangiogenic molecules associated with filarial lymphatic pathology.	150
4.3.5- Depletion of phagocytic or CCR2 ⁺ cells significantly ameliorates <i>B. malayi</i> infection-associated lymphatic dilation and lymphatic insufficiency.	156
4.3.6 α -CCR2 and CL treatment results in significant reductions of a multitude of leukocyte populations in local sdLN's proximal to initial <i>BmL3</i> infection site	163
4.3.7 Exposure of monocyte-derived M ϕ to live <i>BmL3</i> or <i>BmL3</i> extract induce significant proliferation of lymphatic endothelial cells <i>in vitro</i>	163
.....	165
4.4- Discussion.....	167
4.5- Chapter Concluding Remarks	178
The role of host adaptive immune responses in induction of filarial inflammatory-associated lymphatic pathology.	179
5.1- Introduction	180
5.2- Methods	183
5.2.1-Mouse maintenance, Murine hind-limb infection model and associated pathological readouts.....	183
5.2.2-Skin draining Lymph Node (sdLN) Flow cytometry and Immunophenotyping	183
5.2.3-Multiplex analysis of plasma or human cell secretion samples..	184
5.2.4-Cell culture and maintenance	185
5.2.5-Macrophage/ LEC co-culture proliferation assay	185
5.2.6-Splenocyte recall assays	186
5.2.7-Statistical Analysis.....	187
5.3- Results	188
5.3.1- Ablation of adaptive immune responses results in significantly reduced lymphatic remodelling and insufficiency.....	188

5.3.2- <i>BmL3</i> infection induces significant expansion of IL-4, IL-13 and IL-10 expressing CD4 ⁺ T-cells in local draining lymph nodes.....	189
5.3.3- Impaired Th2 Adaptive immune responses in IL-4R α ^{-/-} mice abrogates filarial induced lymphatic remodelling and insufficiency following <i>BmL3</i> infection.	195
5.3.4- Lymphangiogenic mediators in circulation following <i>BmL3</i> infection are altered in IL-4R α ^{-/-} mice.	196
5.3.5- IL-4R α ^{-/-} mice demonstrate significantly lower expansions of M Φ 's, T and B-cells in lymphoid tissue local to inoculation sites following <i>BmL3</i> infection, than WT <i>BmL3</i> infected counterparts.	200
5.3.6- Macrophages in draining lymphoid tissues local to inoculation site express significantly higher levels of the alternatively activated macrophage markers CD206 and Relm- α	203
5.3.7- Human monocyte derived macrophages polarised with recombinant IL-4 and IL-13 induce significant LEC proliferation and secrete higher concentrations of lymphangiogenic molecules <i>in vitro</i>	203
5.4- Discussion.....	211
5.5- Chapter concluding remarks	221
Concluding remarks	222
6.1- A new perspective on the role of lymphatic remodelling in filarial associated lymphatic pathology.....	223
6.2- <i>BmL3</i> infection induces changes in expression of lymphangiogenic molecules which are implicated in lymphatic remodelling and pathology.	224
6.3- Host inflammatory Th2 adaptive immune responses to filarial infection- too much of a good thing?	226
6.4- Induction of filarial associated lymphatic remodelling and pathology- a conceptual model.	227
6.5- Future directions	230
6.5.1 Future experimental work to further characterise the drivers of filarial lymphatic pathology	230
6.5.2 Potential for novel anti-morbidity strategies against LF.....	232
Appendices	235
Appendix 1- Table of flow cytometry antibodies used, manufacturers and clones	235
Appendix 2- USB drive of relevant representative movies	236
REFERENCES	237

Figures and Tables

Figure 1.1: Global burden of Lymphatic Filariasis and associated pathologies	21
Figure 1.2: The Life cycle of filarial nematodes.....	29
Figure 1.3: A schematic of the human lymphatic architecture.....	35
Figure 2.1: Development of a filarial mouse pathology model	62
Figure 2.2: Lymphatic remodelling and insufficiency are significantly increased following <i>B. malayi</i> infection	66
Figure 2.3: Lymphatic insufficiency and dilation are significantly increased, while evidence of tortuous collateral lymphatics are manifest 14d post-infection compared to sham control.....	68
Figure 2.4: BmL3 migrate to lymphatic pre-collector channels proximal to areas of subsequent lymphatic remodelling 3-24 hours post infection	70
Figure 2.5: Challenge filarial infection significantly increases lymphatic remodelling and insufficiency	74
Figure 2.6: Lymphatic remodelling and insufficiency persist 12 weeks following infection with BmL3.	76
Figure 2.7: BmL3 infection results in lymphadenopathy and significant increases in sdLN cellularity	79
Figure 2.8: C57BL/6J mice are predisposed to more extensive lymphatic remodelling and insufficiency compared with BALB/c mice following <i>B. malayi</i> infection.....	81
Figure 3.1- BmL3 infection results in significant upregulation of multiple circulating lymphangiogenic molecules	106
Figure 3.2- BmL3 re-infection results in further upregulation of circulating lymphangiogenic molecules	109
Figure 3.3- BmL3 infection is associated with altered circulating levels of lymphangiogenic mediators in 'high pathology' C57BL/6J versus 'low pathology' BALB/c mouse strains.....	112

Figure 3.4- Local upregulation of VEGF-C alone is sufficient to induce significant lymphatic remodelling and associated pathological lymphatic dysfunction.	114
Figure 3.5- Sunitinib treatment does not modify filarial associated lymphatic pathology or reduce circulating VEGF-A-D.....	119
Figure 3.6- Administration of VEGFR-3 or ALK-1 –Fc traps do not significantly alter filarial lymphatic pathology.	121
Figure 4.1: Filarial Infection results in significant increases of multiple leukocyte populations in lymphatic / lymphoid tissues proximal to larval invasion	149
Figure 4.2: Local sdLN CD11b ⁺ Ly6C ⁺ CCR2 ⁺ monocytes and F/480 ⁺ M ϕ 's demonstrate more pronounced expansions in 'high pathology' C57BL/6J mice compared with 'low pathology' BALB/c mice.....	153
Figure 4.3: Macrophages, monocytes and T-cells derived from lymphatic / lymphoid tissues proximal to lymphatic pathology are significant sources of lymphangiogenic mediators following <i>B. malayi</i> infection.	155
Figure 4.4: Anti-CCR2 treatment significantly reduces circulating and local sdLN Cd11b ⁺ Ly6C ⁺ CCR2 ⁺ monocyte populations in BmL3 infected mice while CL reduces circulating Cd11b ⁺ Ly6C ⁺ CCR2 ⁺ monocytes.....	159
Figure 4.5: Depletion of phagocytes or CCR2 ⁺ monocytes significantly ameliorates filarial associated lymphatic insufficiency and local lymphatic vessel dilation post BmL3 infection.	161
Figure 4.6: α -CCR2 and CL treatment significantly reduces multiple leukocyte populations in sdLNs local to inoculation site.	162
Figure 4.7: Exposure of monocyte derived macrophages to BmL3E or Live L3 larvae induces a 'lymphangiogenic M ϕ phenotype' that drives significant survival/proliferation of LECs in vitro,	166
Figure 5.1: Defective adaptive Immune responses in Severe Combined Immuno-Deficient (SCID) mice results in significantly lower severity of lymphatic remodelling and insufficiency compared to Wild Type (WT) mouse counterparts, following filarial BmL3 infection.....	192

Figure 5.2: BmL3 infection induces a strong local Th2 adaptive immune response, 14dpi in sdLNs proximal to inoculation site concurrent with a mixed Th1/Th2 systemic response.....	194
Figure 5.3: Development of lymphatic remodelling and insufficiency following BmL3 filarial infection are ameliorated in the absence of IL-4R α immune responses.....	199
Figure 5.4: IL-4R α ^{-/-} mediated deficiency of Th2 adaptive immune responses significantly attenuates secretion of lymphangiogenic molecules linked with pathological filarial associated lymphatic remodelling, following BmL3 infection.....	202
Figure 5.5: IL-4R α ^{-/-} deficiency in C57BL/6J mice results in significantly reduced proliferation/recruitment of specific immune cells to local lymphatic / lymphoid tissues following BmL3 infection.	206
Figure 5.6: BmL3 infection in C57BL/6J mice induces an 'Alternatively Activated Macrophage (AAM ϕ)' phenotype in lymphatic / lymphoid tissues local to the BmL3 infection site.....	208
Figure 5.7: Exposure of monocyte derived macrophages to rIL-4 and rIL-13 induces significant proliferation of LECs in vitro	210
Figure 6.1: A conceptual model of early BmL3 associated lymphatic remodelling and pathology	230
Supplementary Figure S4.1: Gating strategy from flow cytometric immunophenotyping for determination of cell populations in sham and BmL3 infected sdLNs and proximal lymphatic/lymphoid tissues	145
Table 1.1: Dreyer classification of lymphoedematous pathologies associated with Lymphatic Filariasis.....	24
Table 2.1: Advantages and disadvantages associated with using current animal models of filarial infection.....	52

Abbreviations

AAM Φ , Alternatively-Activated Macrophage	CTLA, cytolytic T lymphocyte-associated Antigen
ad, Adenoviral vector	CXCL, CXC chemokine ligand
ADL, Adenolymphangitis	CXCR, CXC chemokine receptor
Amp B, Amphotericin B	Cy, Cyanine
Ab, antibody	d, day(s); deoxy; distilled
AF (number), AlexaFluor (number)	DMEM, Dulbecco's modified Eagle's medium
Ag, antigen	DMSO, dimethylsulfoxide
ALK-1, Activin like Kinase-1	DNA, deoxyribonucleic acid
Ang, Angiopoietin	EB, Evan's Blue
ANOVA, analysis of variance	EDTA, ethylenediaminetetraacetic acid
APC (cell), Ag-presenting cell	eF, eFluor
APC (fluorophore), Allophycocyanin	EGM-MV2- Endothelial Growth Medium- Modified Version 2
<i>Bm</i> L3, <i>Brugia malayi</i> L3 larvae	ELISA, enzyme-linked immunosorbent assay
<i>Bm</i> L3E, <i>Brugia malayi</i> L3 larval extract	FACS, fluorescence-activated cell sorting
BMP, Bone morphogenic Protein	FBS, foetal bovine serum
BSA, bovine serum albumin	FcR, Fc receptor
CCL, CC chemokine ligand	FGF, Fibroblast Growth Factor
CCR, CC chemokine receptor	FITC, fluorescein isothiocyanate
CD, Cluster of Differentiation	FLT3, fms-related tyrosine kinase 3
CD-L, Cluster of Differentiation-ligand	FOXP3, Forkhead box P3
CFU, colony-forming unit	FSC, Forward Scatter
CL, Clodronate liposomes	FVD, Fixable Viability Dye
CO ₂ , Carbon Dioxide	g, gram
Con A, concanavalin A	G-CSF, granulocyte Colony Stimulating Factor
CSF, colony-stimulating factor	
CTL, cytotoxic T lymphocyte	

GFP, green fluorescent protein

GM-CSF, granulocyte-macrophage Colony Stimulating Factor

GPELF, Global Programme for the Elimination of Lymphatic Filariasis

GST, glutathione S-transferase

H&E, hematoxylin and eosin

h, hour

HBSS, Hanks' balanced salt solution

adHMVEC(Ly), adult dermal Microvascular endothelial cell (lymphatic)

HEPES, N-2-hydroxyethylpiperazine-N'-2-ethanesulfonic acid

HRP, horseradish peroxidase

ICG, IndoCyanine Green

IAL, Inflammatory Associated Lymphangiogenesis

iLN, Iliac Lymph Node

i.p., intraperitoneal

i.v., intravenous

IFN γ , interferon gamma

Ig, immunoglobulin

IgH, Ig heavy chain

IL, interleukin

ILC, Innate Lymphoid Cell

L(number): Larval Stage

LE, Lymphoedema

LEC- Lymphatic Endothelial Cell

LEDC, Lower Economically Developed Country

LF, Lymphatic Filariasis

LN, Lymph Node

LPS, lipopolysaccharide

Ly6C, Lymphocyte antigen complex 6, locus C- Monocyte marker

Ly6G, Lymphocyte antigen complex 6, locus G, Neutrophil marker

mAb, monoclonal Ab

MAPK, mitogen-activated protein kinase

MCP, monocyte chemoattractant protein

M-CSF, macrophage Colony Stimulating Factor

MDA, Mass Drug Administration

MEK, mitogen-activated protein kinase kinase

MEM, minimum essential medium

mf, microfilariae

mg, milligram

MHC, major histocompatibility complex

min, minute

MIP, macrophage-inflammatory protein

ml, millilitre

M ϕ , Macrophage

n, number

ND, not determined

NF- κ B, nuclear factor κ B

ng, Nanogram

NIR, Near Infra-Red

NK, natural killer	PDE, Photo Dynamic Eye
NO, nitric oxide	PE, phycoerythrin
NS, not significant	PerCP, peridinin chlorophyll protein
OD, optical density	PFU, plaque-forming unit
p, probability	PG, prostaglandin
PBMC, peripheral blood mononuclear cell	Pg, Picogram
PBS, phosphate-buffered saline	
PHA, phytohemagglutinin	s, second
pi, Post Infection	s.c., subcutaneous
PI3K, phosphatidylinositol 3-kinase	SCID, severe combined immunodeficiency
pLN, Popliteal Lymph Node	SD, standard deviation
PMA, phorbol myristate acetate	SiglecF, Sialic acid-binding Ig-like lectin 8 eosinophil marker
PRL, Prolactin	siLN, Subiliac Lymph Node
Prox-1, Prospero Box-1	sdLN, Skin draining Lymph Nodes
PS, Penicillin streptomycin	THP-1, Immortalised monocyte-like cell line
R, receptor	v/w, volume to weight ratio (%)
r, recombinant	W, week (only with numbers)
RBC, red blood cell	WBC, white blood cell
RPMI, Roswell Park Memorial Institute	WHO, World Health Organisation
Rtki, Receptor Tyrosine Kinase inhibitor	α -, anti-
RELM- α , Resistin-like molecule alpha	μ g, microgram
RNA, ribonucleic acid	μ l, microlitre
rpm, revolutions per minute	VEGF Vascular Endothelial Growth Factor
s, Soluble	

Abstract

Pathological manifestations of Lymphatic filariasis (LF), namely: hydrocele and lymphoedema (LE), results in severe chronic morbidity, remaining a leading cause of global disability. Treatment for the ~40 million symptomatic LF patients worldwide is currently limited to morbidity management to slow progression of disease. There is an urgent need to identify and translate novel therapeutic strategies to improve on standard care and effectively reverse LF pathology. A novel *in vivo* murine limb pathology model, utilising *Brugia malayi* infective L3 larvae (*BmL3*) was developed and an *in vivo* intravital optical imaging system utilised to longitudinally track lymphatic alterations and developing pathology following infection. Lymphatic fluorescent reporter mice (*Prox1*-GFP) were also used to image changes in lymphatic architecture. Multiplex (Luminex) protein assays on harvested plasma were undertaken to investigate associations between changes in circulating lymphangiogenic factors and lymphatic remodelling following filarial infection. Immune-deficient murine knockout strains, targeted immune cell ablations, and manipulation of specific lymphangiogenic molecules were utilised in the model to investigate cellular, molecular and immunological mechanisms of lymphatic pathology. Significant lymphatic remodelling and lymphatic insufficiency were consistently observed as rapidly as 6 days following *BmL3* infection in lymphatic tissues where active parasitism could be determined by fluorescent *BmL3* labelling experiments. Severity of *BmL3* induced lymphatic remodelling and pathology was mouse strain-dependent and associated with significantly altered plasma concentrations of a milieu of lymphangiogenic factors including: Vascular Endothelial Growth Factors (VEGFA, C), Transforming Growth Factor- β superfamily members (BMP-10, endoglin, follistatin, sALK-1, TGF- β) and prolactin. Both elevated prolymphangiogenic secretions and pathology persisted for 12 weeks post-infection at a point where active parasitism was not evident (no adult infections or blood microfilaraemias). Monocytes and macrophages isolated from pathological lymphatic tissues and adjacent draining lymph nodes, secreted significant levels of prolymphangiogenic factors including sALK-1 and VEGF-C. Macrophages isolated from pathological lymphatic / lymphoid

tissues expressed markers consistent with blood monocyte recruitment and alternative activation. Clodronate liposome mediated ablations of phagocytic cells, including monocytes and macrophages or specific anti-CCR2 antibody ablation of CCR2⁺ monocytes in wild type (WT) mice also ameliorated filarial lymphatic insufficiency and dilation. *BmL3* infected Severe-Combined or Th2 adaptive immune deficient (SCID, IL-4R α ^{-/-}) mice displayed significantly abrogated lymphatic remodelling and pathology. Human lymphatic endothelial cells proliferated in response to monocyte-differentiated macrophage secretions after stimulation with live *BmL3*, L3 extracts or recombinant IL-4+IL-13. Together, the data demonstrates that lymphatic remodelling and insufficiency is rapidly induced following *BmL3* infection. Further, the data highlights a novel Th2/monocyte/macrophage signalling axis as a key driver of filarial lymphatic remodelling and pathology. Inhibiting, or reversing, filarial remodelling, through targeting the identified adaptive Th2 signalling mechanisms may represent novel therapeutic strategies to ameliorate LF-related pathology.

Chapter 1

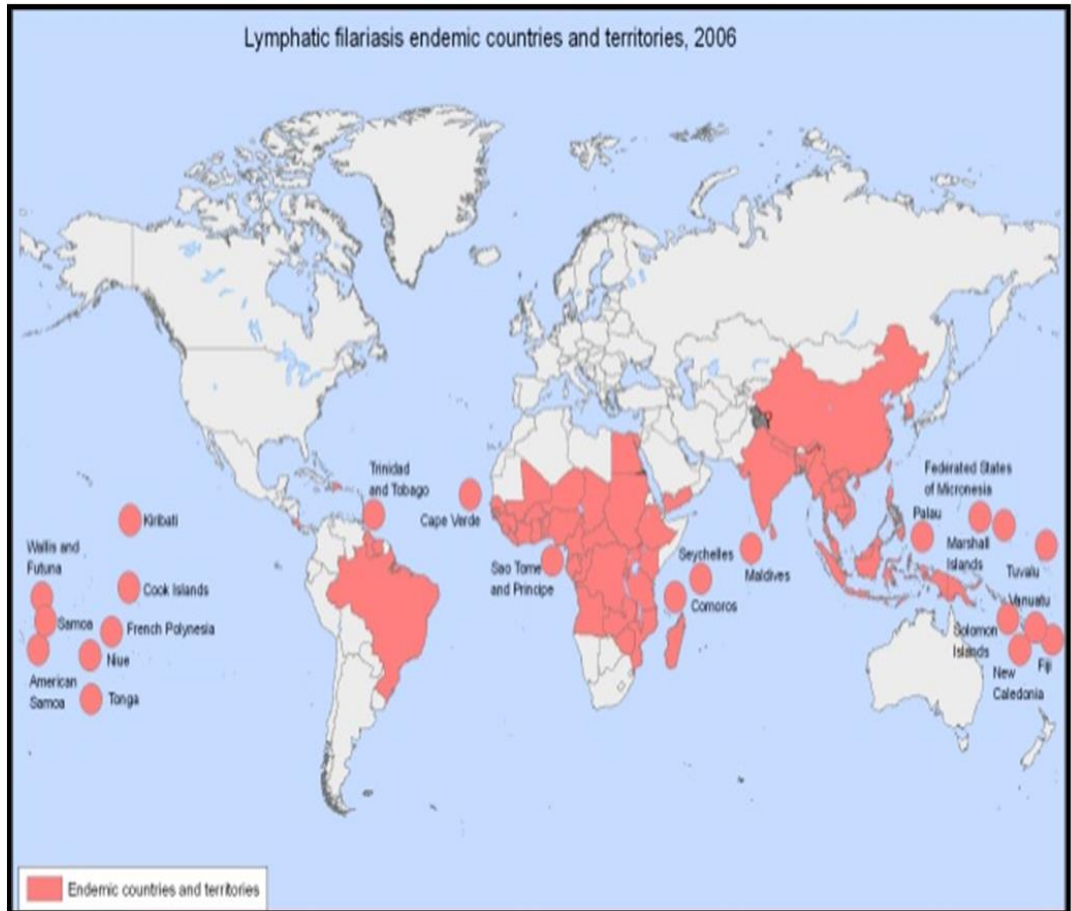
Introduction

1.1-The Global Burden, Consequences and Clinical Manifestations of Lymphatic Filariasis

Lymphatic Filariasis (LF) is a disease encompassing a group of clinical pathologies/symptoms, associated with parasitic infection of humans by the filarial nematode families: *Wuchereria bancrofti* (90% of cases), *Brugia malayi*, and *Brugia Timori* (Taylor, Hoerauf and Bockarie, 2010; Chandy *et al.*, 2011). Recent World Health Organization (WHO) estimates suggest that 68 million people remain infected with LF worldwide, with highest prevalence lying around the tropical belts of Africa, Asia and Latin America (Hotez *et al.*, 2008; Hotez and Kamath, 2009; Hotez, Savioli and Fenwick, 2012), while the WHO predicts 1.2 billion remain at high risk of infection (Michael, Bundy and Grenfell, 1996; Michael and Bundy, 1997) (Figure 1.1A). The high global burden of infection, the chronic nature of LF and its heavy concentration of infection in low and middle income countries (LF is endemic in 32 of the world's 38 lesser economically developed countries) makes it a primary contributor to neglected disease burden, subsequently ranking it as 4th highest, as ranked by highest causes of Disability Adjusted Life Years (DALYs), in the list of 13 neglected tropical diseases (NTDs) (Hotez *et al.*, 2007; Chandy *et al.*, 2011). While a proportion of those infected remain clinically asymptomatic, it is estimated that at least a 40 million patient subset suffer severely debilitating pathology and high morbidity as clinical manifestations of filarial infection (Nutman, 2013).

Clinically, LF manifests in a group of chronic and acute pathologies, often occurring months to years after initial infection (Pfarr *et al.*, 2009). While some success has been observed in reversing early stages of LF related pathology (Debrah *et al.*, 2006; Shenoy, 2008), progression to later stages results in incurable, chronic pathology. In addition, chronic LF related pathology persist beyond the clearing of active filarial infection through therapeutic intervention (Grenfell, Michael and Denham, 1991; Chan *et al.*, 1998). Chronic manifestations of LF include severe lymphoedema (LE) in: the limbs, genitals or breasts of individuals, resulting in severe disfigurement (Pani and Srividya, 1995) (Examples in figure 1.1B-C). In addition to

A



B



C




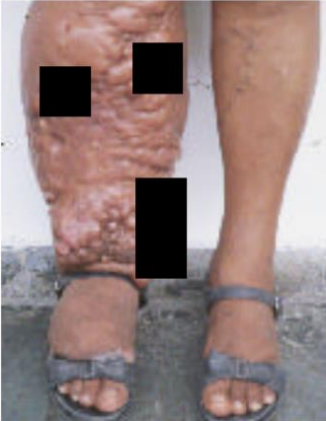



Figure 1.1: Global burden of Lymphatic Filariasis and associated pathologies

A) Map detailing the global distribution of LF endemic countries, notice the distribution round the tropical belts and correlation with lower economically developed countries. **B)** Images demonstrating the severely disfiguring effects of filarial lymphoedema (LE) / elephantiasis. The overt swelling leads to not only huge physical disability, but psychological disability, associated with mental health complications arising from disease as well as social stigma attached to LF patients. **C)** Scrotal lymphoedema, describe as hydrocoele. Hydrocoele is a common form of LF-related pathology with 25 million males estimated to suffer from this condition.

Images Sources: World Health Organization, 2019

LE, affected limbs often display progressively worse skin abnormalities, namely severe skin pitting, thickening (hyper-keratosis and hyper-pigmentation), fibrosis and localised inflammation (Partono, 1987). Other chronic manifestations can include acute swelling of the penis and scrotum, a condition known as hydrocoele that is thought to affect around 27 million males globally (Nutman, 2013). Due to the spectrum of lymphoedematous pathology observed in LF, Dreyer and colleagues (Gillespie, 2004) have characterised a sliding scale of filarial related lymphoedema, classified in stages 1-7 as shown in Table 1 . Importantly, recent work has suggested revisiting this classification by addition of a “Stage 0”, taking into account patients who do not present with clinical symptoms, but present with “covert” or “sub-clinical” pathologies (Douglass *et al.*, 2017). These “Stage 0 sub-clinical pathologies”, described as changes to skin elasticity, firmness, increased tissue “free fluid” and possible alterations to the lymphatic architecture is argued to be a key window in which therapeutic interventions may prevent progression to later stages of severity (Douglass *et al.*, 2019).

STAGE	DESCRIPTION	EXAMPLE
1	Mild lymphoedema which is reversible overnight, rarely have acute attacks, entry lesions or odour	 <p>Fig. 23 -</p>
2	Mild lymphoedema which is not reversible overnight. Very occasional acute attacks, entry lesions or mild bad odour	
3	Noticeable lymphoedema which is not reversible overnight. Presence of shallow skin folds and occasional acute attacks, entry lesions and bad odour	
4	Severe lymphoedema which is not reversible overnight. Clear presence of knobs/swellings or protrusions on skin. Frequent entry lesions and bad odours which may be occasionally accompanied by acute attacks	
5	Severe lymphoedema not reversible overnight. Many deep skin folds/pitting with common entry lesions and bad odour. Occasional to frequent acute attacks	



6	Severe lymphoedema not reversible overnight. Small clustered round protrusions/knobs give rise to appearance of “mossy foot”. Lymphoedema can extend to above the knee. Frequent entry lesions, bad odour and acute attacks	
7	Severe lymphoedema not reversible overnight. Severe disability to patient who cannot adequately perform simple daily routines. Extremely large affected limb which extends above knee with deep skin folds, thickening and pitting. Frequent entry lesions, bad odour and acute attacks	

Table 1.1: Dreyer classification of lymphoedematous pathologies associated with Lymphatic Filariasis.

Description of different stages of filarial LE increasing in severity. Some data suggests therapeutic intervention at earlier stages can arrest progression or even be reversed while later stages are irreversible and lifelong in duration. Images and descriptions from (Dreyer *et al.*, 2001)

The high prevalence of LF in lesser economically developed countries (LEDC's) in conjunction with associated high morbidity results in significant impacts on patient household income, due to lost earning opportunity from being unable to work as well as carer duties. This has led to LF being described as a "disease of poverty" (Durrheim *et al.*, 2004). Aside from physical morbidity, LF pathology is associated with accompanying secondary complications including an incredibly high psychological burden through mental health problems, associated with levels of disfigurement (Zeldenryk *et al.*, 2011; Ton, Mackenzie and Molyneux, 2015) and marginalisation from communities due to the social stigma attached to LF (Weiss, 2008).

Chronic infection is often accompanied by acute, 'inflammatory episode' type manifestations of LF, although such episodes are also observed following initial infection in asymptomatic patient cohorts. The most common acute manifestation is adeno-lymphangitis (ADL) characterised by: systemic fever, lymphadenopathy of affected lymph nodes (LN's), and general inflammation and pain of affected limbs (Shenoy, 2008). It is hypothesised that ADL 'episodes' are a result of inflammatory reactions to filarial worm death events and the associated release of antigens, triggering inflammatory immune responses (Kar, Mania, & Kar, 1987). Additional evidence suggests that ADL may be triggered by secondary bacterial infections, either from loss of skin barrier protection in patients suffering from high grade lymphoedemas, or due to improper clearance/dysfunction of lymphatic drainage (lymphostasis) in affected limbs providing an ideal environment for opportunistic bacterial and fungal infection (Pani *et al.*, 1995). In chronic cases of LF, it is believed that recurring attacks of ADL is a contributing factor to the worsening severity or 'grade' of lymphoedema in affected limbs (Pani *et al.*, 1995.). The severity of ADL episodes has resulted in it being highlighted as the single largest cause of lost wages in LEDC countries by LF patients (Ramaiah *et al.*, 1998; Krishnamoorthy, 1999).

The extremely high morbidity and socio-economic burden of LF results in it consistently being ranked as a leading cause of global disability (Ottesen,

2000). The high prevalence and global concentration of endemicity of LF in LEDC's, results in it ranking highly in the list of neglected tropical diseases (NTDs). Resultantly, the World Health Organization produced an ambitious policy of the elimination of LF as a public health problem, creating the Global Programme to Eliminate Lymphatic Filariasis (GPELF) in 2000, which initially targeted global 'elimination' (reduction of transmission to <1%) by 2020 (Ottesen, 2006; Addiss and Brady, 2007; Hotez *et al.*, 2007). Elimination efforts centre around preventing transmission by mass drug administration (MDA) with standard anti-filarial drugs and latterly bednet distribution. After 13 years, estimates of LF infection had effectively halved, from 120 to 67 million (Ramaiah and Ottesen, 2014). While excellent progress has been achieved in halting disease transmission and eradication of active infection, due to MDA drugs having no curative effects on LF morbidity, the 40 million pathology cases persist with no measurable drop in pathology cases over the same 13 year period (Ramaiah and Ottesen, 2014).

1.2-The filarial life cycle and aetiology of filariasis

LF is transmitted through mosquito vectors. Infectious, third-stage filarial larvae (L3) infect the host when L3 infected mosquitoes take a second blood meal. L3 larvae migrate from the bite site into subcutaneous tissues (Taylor, Hoerauf and Bockarie, 2010). L3 larvae penetrate the surrounding dermal lymphatic capillaries before migrating through pre-collector and collector lymphatic vessels to reside in the host peripheral lymphatics and LNs proximal to the infection site. During migration, the filarial larvae undergo a series of moults from L3 to L4 stage, before reaching a final adult male or female stage, where they reside in 'worm nests' (dilated lymphatic channels) (R. K. Shenoy *et al.*, 2007; Pfarr *et al.*, 2009). Male and female worms sexually reproduce resulting in the release of microfilariae (mf) into the host vascular systemic circulation. It has been well documented that the highest concentration of mf in circulation coincides with night-time hours, while lower to no circulating mf is observed in day time hours. This is a process known as periodicity (Paily, Hoti and Das, 2009) and is thought to coincide with periods of highest mosquito activity, maximising the chance of a successful

infection from blood meals. Mf infect mosquito vectors upon these further blood meals, where they unsheathe and migrate through the proventriculus and cardiac portion of the mosquito's midgut, reaching the thoracic muscles. Here, the MF grow firstly into L1 larvae before developing into infective L3 larvae, where the cycle can repeat through further bloodmeals on animal hosts from infected mosquitos (Paily, Hoti and Das, 2009). The life cycle is summarised in figure 1.2 where the key lymphatic structures involved in the infection process are highlighted and discussed.

Populations in filarial endemic areas are known to fall into three distinct subsets (Partono, 1987; Ottesen, 1992; Chandy *et al.*, 2011): (1) so called 'endemic normals' or 'putative immunes' are individuals repeatedly exposed to filarial infection, as assessed by parasite-specific antibody responses, but fail to establish active infection and thus are considered to be naturally immune, (2) 'Asymptomatic carriers' are individuals carrying active filarial infection, testing positive for mf in their blood (and therefore classed as microfilaraemic) but exhibit no clinical manifestations or pathology related to disease and (3) pathological filariasis where patients often have low or even an absence of mf in the blood 'amicrofilaraemic', may or may not be positive for adult infection and suffer a sliding scale of clinical disease, ultimately culminating in LE and elephantiasis (Partono, 1987; Pfarr *et al.*, 2009). Filariasis is known to be the leading cause of secondary LE (acquired rather than genetically predisposed primary / congenital) globally (Shenoy, 2008).

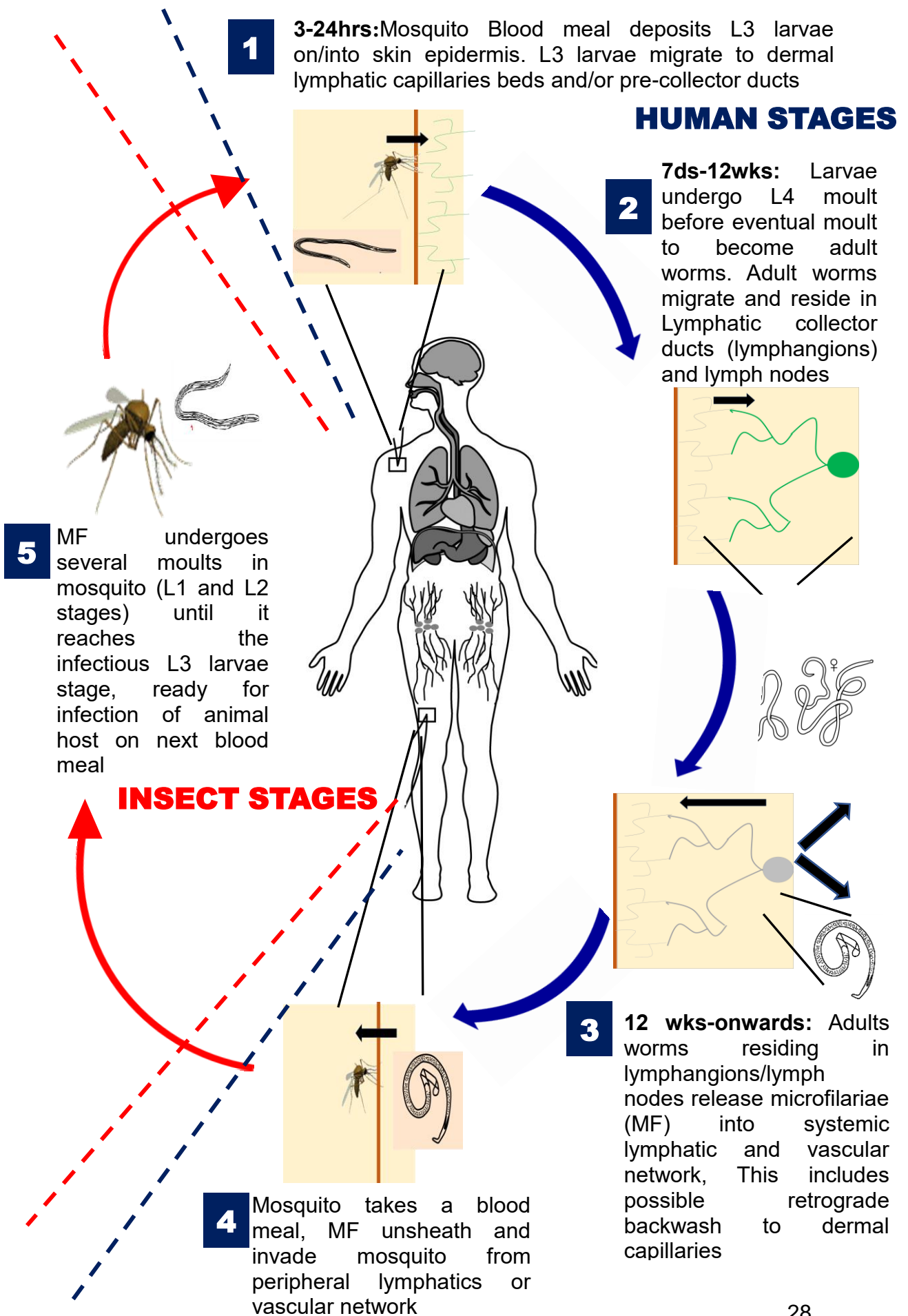


Figure 1.2: The Life cycle of filarial nematodes

Schematic detailing the filarial life cycle and where they reside in the lymphatic architecture during the varying life stages.

Image adapted from life cycle figure displayed at:
https://www.cdc.gov/parasites/lymphaticfilariasis/biology_w_bancrofti.html

Accessed: 20/03/2019

1.3-The human lymphatic system and lymphatic remodelling in health and disease

The lymphatic vessels, together with blood vessels, form the human vascular system. Once thought of as a passive conduit, maintaining homeostasis by resorbing extravasated and interstitial fluid, as well as aiding in the absorption of proteins, lipids and macromolecules from the intestine, the lymphatic system is now implicated in playing an important role in a variety of functions including immunity and immunomodulation (Randolph *et al.*, 2017). It is currently agreed that the three main functions of the lymphatic vasculature are: 1) Control absorbance of nutrients from the blood into peripheral tissues, as well as act as a 'highway' by transporting small molecules such as chemokines and cytokines in interstitial fluid (Vranova and Halin, 2014), 2) A transport network for the trafficking of immune cells, particularly from the peripheral tissues to lymph nodes, where appropriate immune responses are coordinated and, 3) Maintenance of fluid homeostasis, transporting interstitial fluid back to systemic blood circulation via the thoracic duct.

While the blood and lymphatic vasculature often work in conjunction, structurally, there are key differences between the two, most notably the pressurised pump system of the blood vasculature contrasts the unidirectional passive flow of the lymphatics (Randolph *et al.*, 2017). Lymph fluid enters the lymphatic vasculature via the complex, branched network of collecting lymphatic capillaries. Lymphatic capillaries consist of a single cell layer of Lymphatic Endothelial Cells (LECs), anchored to discontinuous basement membrane as well as extracellular matrix (ECM). In contrast to blood capillaries, lymphatic capillaries lack pericytes and are held together by weak intercellular "button like" junctions between LECs (Coso, Bovay and Petrova, 2014). Together, the single cell layer and weak junctions allow antigens, small molecules and immune cells easy entrance to the lumen of lymphatic capillaries entering the lymph fluid. Collected lymph in capillary beds then travel into lymphatic pre-collector ducts which, together with LECs, are sparsely covered by smooth muscle cells which produce contractility that

propels the lymph forward to lymphatic collector ducts (Alitalo, 2011). Retrograde channel flow is prevented in capillary beds, as well as the pre-collector and collector vessels through intraluminal valves that line the lymphatic vessels (Bazigou *et al.*, 2014). Collecting lymphatic vessels act as final, primary vessels of the hierarchal capillary-pre-collector-collector structure and are more continuously lined by smooth muscle cells, which together with proximal skeletal muscle and arterial pulsations, provide the contractile function required for unidirectional lymph propulsion (Coso, Bovay and Petrova, 2014). Collecting lymphatic vessels channel lymph into the subcapsular sinus of draining lymph nodes, which act as sentinels of immune surveillance by monitoring antigens passing through lymph and coordinating appropriate immune responses from incoming migrating immune cells (Liao and Padera, 2013). 'Filtered' efferent lymph fluid leaving lymph nodes channel through further collecting vessels before finally draining into blood systemic circulation, through the thoracic ducts which channels lymph into the subclavian veins. An overview of the lymphatic architecture can be found in figure 1.3.

Pre-natal lymphangiogenesis is responsible for the preliminary construction of the lymphatic vascular system (Semo, Nicenboim and Yaniv, 2016). The lymphatic architecture, however, remains highly dynamic with frequent remodelling of lymphatic vessels and associated architecture occurring in response to a variety of stimuli including: tissue injury, wound healing and inflammation (Flister *et al.*, 2010; Lund *et al.*, 2012; Coso, Bovay and Petrova, 2014; Hirosue *et al.*, 2014; Vranova and Halin, 2014). Lymphatic remodelling, induced by post-natal lymphangiogenesis, is crucial to maintain physiological homeostasis and optimal function in humans (Tammela and Alitalo, 2010). Post-natal lymphangiogenesis and associated lymphatic remodelling is usually initiated by the sprouting of novel vessels from the existing lymphatic architecture (Tammela and Alitalo, 2010). In order for sprouting initiation to occur, careful molecular regulation must promote the proliferation and subsequent survival of existing LECs at the points of sprouting (Tammela, Petrova and Alitalo, 2005). Further, migration and subsequent recruitment of: LECs (Coso, Bovay and Petrova, 2014), bone

marrow progenitor cells (Lee *et al.*, 2010.; Maertens *et al.*, 2014) , as well as the trans-differentiation of myeloid derived macrophages into LECs (Attout *et al.*, 2009; Ran and Montgomery, 2012) have all been demonstrated to be important in the initial sprouting steps of lymphangiogenic mediated lymphatic remodelling. The 'immature' newly sprouted vessels then undergo a 'maturation' step involving correct valvular development (Kazenwadel *et al.*, 2012; Sabine *et al.*, 2012; Bazigou *et al.*, 2014), tube formation and recruitment of smooth muscle cells (Sweet *et al.*, 2015) to become fully functioning, novel lymphatic vessels. Finally, correct lymphatic patterning is crucial for the functionality of the novel lymphatic vessels (Gale *et al.*, 2002; Liebl *et al.*, 2015). Mutations in any of the key genes identified in the regulation of lymphatic sprouting, valvular development, recruitment/migration and lymphatic patterning have been intrinsically linked with dysfunctional lymphatics and development of primary LE.

While the above demonstrates the importance of lymphatic remodelling in homeostasis and health, aberrant or dysregulated lymphatic remodelling has been implicated in a range of varied pathologies. Several 'Hallmarks' of pathological lymphatic remodelling have been defined. Lymphatic dilation, sometimes described as lymphangiectasia, is the abnormal widening of lymphatic channels (Faul *et al.*, 2000; Bellini *et al.*, 2006; Wang and Oliver, 2010). Dilation of lymphatic vessels in the lungs (pulmonary lymphangiectasia) has been demonstrated to cause severe respiratory distress and render individuals highly susceptible to infection, primary pulmonary lymphangiectasia has a high mortality rate and is a leading cause of neonatal death (Esther and Barker, 2004; Bellini *et al.*, 2006). Lymphatic remodelling can also manifest in neovascularisation and hyperplasia, defined by aberrant growth of LECs and dysregulated lymphangiogenesis, leading to poorly functioning immature lymphatics that manifest as increased lymphatic vessel density (Cursiefen *et al.*, 2004; Attout *et al.*, 2009; Park, Lee and Yoon, 2011). Lymphatic neovascularisation is commonly observed in the affected skin of psoriasis and thought to contribute to disease pathogenesis (Kunstfeld *et al.*, 2004). Hyperplasia and neovascularisation is significantly associated with diseases as diverse as: arthritic joints (Zhang *et al.*, 2007),

allergy (including asthma) (Kim *et al.*, 2010; Moldobaeva *et al.*, 2017) and inflammatory bowel disease (Alexander *et al.*, 2010; Linares and Gisbert, 2010). Finally, tortuous collateral lymphatic vessels, described as aberrantly patterned or shaped dysfunctional vessels (Liu, Yan and Wu, 2012) is a key facet of pathological lymphatic remodelling (Gale *et al.*, 2002).

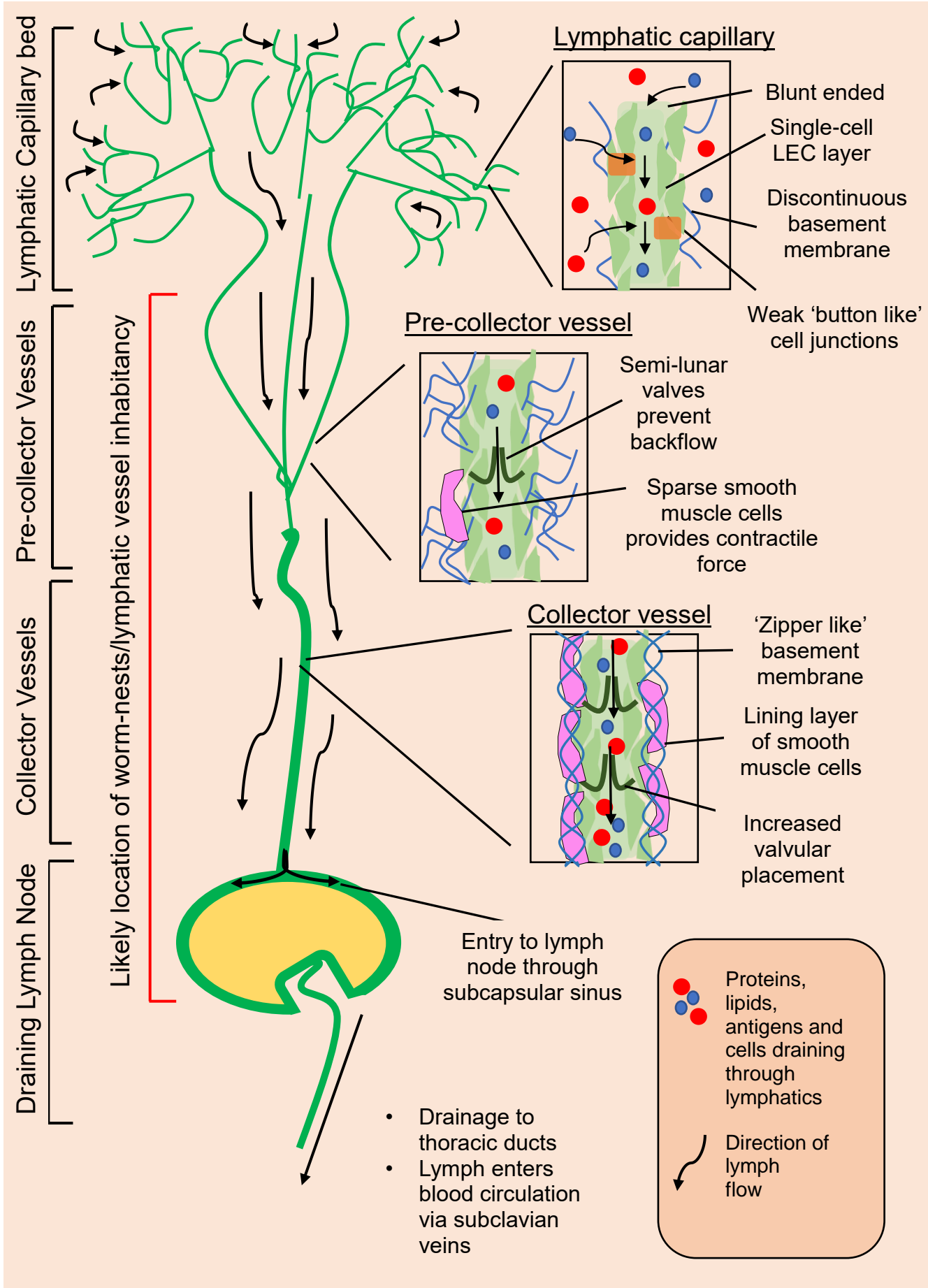


Figure 1.3: A schematic of the human lymphatic architecture

Diagrammatic representation of human lymphatic architecture. The blunt ended, single cell layer held together by weak button junctions and discontinuous basement membrane of lymphatic capillaries allows interstitial lymph fluid to easily diffuse across into the lumen of vessels. Lymph flow then travels unidirectionally across hierarchically organised vessels structures from branching lymphatic capillaries that converge into larger pre-collector vessels before finally adjoining to main collector vessels. Unidirectional flow is maintained by: placement of semi-lunar valves that prevent retrograde travel in pre-collector and collector lymphatic vessels, the lining of these vessels with smooth muscle that provides a contractile force and exterior surrounding skeletal muscles that contribute to the contractile force and pressure gradient. The size and integrity of lymphatic vessels increases across the hierarchal structure, with an eventual 'zipper like' basement membrane in the main collector vessels preventing lymph extravasation.

1.4-Lymphatic dysfunction, insufficiency and LE

Correct lymphatic function is crucial for fluid balance, homeostasis and a variety of other functions. Dysfunction of lymphatic vessels, or disruption to the normal lymphatic architecture, often lead to perturbations in normal homeostatic lymphatic drainage, resulting in lymphatic insufficiency. Lymphatic insufficiency results in the breakdown of proper lymph fluid clearance, resulting in aberrant retention, or pooling of lymph fluid (known as lymphostasis). This can result in areas where lymphatic drainage is no longer able to fulfil the demand of building up interstitial or extravasated fluid. The causes of lymphatic dysfunction are hugely varied and still not fully understood. Mutations in the key regulatory drivers of lymphangiogenesis can result in poorly developed, immature or improperly patterned lymphatic vessels and architecture, resulting in poorly functioning vessels, that are insufficient to handle drainage demand of lymph fluid (Mellor *et al.*, 2011; Brouillard, Boon and Vikkula, 2014). Additionally, perturbations to lymphatic contractility can result in lymphatic dysfunction, characterised by the breakdown of the normal pumping action of lymphatic vessels to transport fluid along the lymphatic system, resulting in retarded lymph drainage and further insufficiency (Zawieja *et al.*, 2012; Chakraborty, Davis and Muthuchamy, 2015). Impairments to the normal function of lymphatic valves (valvular dysfunction) is an additional, well characterised cause of dysfunction. Valvular insufficiency allows aberrant retrograde travel of lymph fluid back into pre-collector vessels of capillaries (Petrova *et al.*, 2004; Zawieja, 2009) resulting in the retardation, or complete breakdown of unidirectional lymphatic drainage. Finally, dilation of lymphatic vessels have been demonstrated to contribute to dysfunction. Aberrant dilation can result in a weakening of necessary intraluminal pressure, created by lymphatic vessel contractile forces (Zawieja, 2009; Zawieja *et al.*, 2012). The weakened pressure results in perturbed lymph flow rates which can contribute to lymphatic insufficiency.

The main pathological manifestations of lymphatic insufficiency and dysfunction is the development of LE. LE is characterised as abnormal,

severe swelling, and subsequent disfigurement, of peripheral areas of the body, most often in limbs (Grada and Phillips, 2017). Overt LE develops when venous capillary filtration and extravasation, resulting in formation of interstitial fluid, is greater than the capacity of the lymphatics to drain away the formed fluid, resulting in its aberrant retention. The resultant lymphostasis, in the local lymphatic architecture results in extravasation into surrounding interstitial spaces which contributes to a build-up of permanently retained/pooling of lymph (Carlson, 2014). The progressive aggregation of undrained lymph fluid results in continual swelling of the surrounding affected areas, while inflammation and resultant inflammatory cell infiltrates, with deposition of soluble inflammatory mediators, often observed in the static lymph fluid (Grada and Phillips, 2017), further exacerbate pathology. Additional contributions to swelling frequently occur post-establishment of LE as the static fluid becomes prone to secondary opportunistic bacterial and fungal infections, resulting in painful inflammatory episodes (Myers, 2018) . In conclusion, whilst the pathophysiology of LE is still not fully understood, it is commonly agreed a break down in lymphatic function (lymphatic dysfunction) induces a state of lymphatic insufficiency, where net drainage is lower than net build-up of interstitial fluid. Chronic insufficiency is a trigger for numerous co-factors leading to the development of LE.

1.5-Primary and secondary LE

LE can be classified into primary (congenital) and secondary, (acquired) forms. The latter is induced when damage due to trauma, surgery or infection, results in the development of lymphatic dysfunction and oedema (Grada and Phillips, 2017). Primary LE is most often a result of genetic mutations that results in aberrant development of a functional lymphatic network, leading to poor lymphatic drainage and insufficiency (Adamczyk *et al.*, 2016). Lymphoedema distichiasis syndrome results in patients developing spontaneous LE often around puberty, usually in the limbs, due to mutations in the Fork-head box protein C2 (FOXC2) gene (Mellor *et al.*, 2011). Defective FOXC2 signalling has been demonstrated to result in abnormal development of lymphatic vessel valves, causing lymphatic

dysfunction, retrograde lymph travel and insufficiency that leads to LE (Petrova *et al.*, 2004). Milroy disease results in overt LE from birth due to a severely dysfunctional, and poorly developed, lymphatic system (Brice *et al.*, 2005). Genetic studies have found high association between mutations in the Vascular Endothelial Growth Factor Receptor (VEGFR)3 gene and Milroy syndrome (Ferrell *et al.*, 1998; Karkkainen *et al.*, 2000; Ghalamkarpour *et al.*, 2006). Cell surface-expressed VEGFR3 signals upon binding to its ligands VEGF-C and VEGF-D. VEGF-C, in particular, has been demonstrated to be a key driver of pre- and post-natal lymphangiogenesis (Oh *et al.*, 1997; Skobe *et al.*, 2001) with defective signalling demonstrated to result in poorly developed lymphatics (Ghalamkarpour *et al.*, 2006)

Secondary LE is the more common cause of lymphoedema with estimates between 180-250 million cases worldwide (Rockson and Rivera, 2008). In high income countries, the most common cause of secondary LE is either cancer mediated lymphatic remodelling, or medical intervention for the treatment of cancer, such as surgical resection of cancerous and sentinel lymph nodes (DiSipio *et al.*, 2013; Mortimer, 2013). Both results in significant injury, or changes, to the local lymphatic architecture which results in the development of lymphatic dysfunction and insufficiency (Mortimer and Rockson, 2014). The most common cause of all secondary LE, however, is as a result of LF, which is in turn referred to as filarial LE (Warren *et al.*, 2007; Pfarr *et al.*, 2009). Filarial LE is often progressive and clinically graded by: severity of swelling / disfigurement, thickness of skin and degree of pitting/sclerosis in the skin of affected areas (Pani and Srividya, 1995). While there has been a degree of success in reversing milder, earlier gradings of LE, the later, more severe grading (also known as elephantiasis) is irreversible and highly debilitating (Shenoy, 2008; Nutman, 2013).

[1.6- Filarial LE, a neglected facet of a neglected tropical disease?](#)

Significant progress has been made in eliminating filarial infection worldwide, with programmes such as Global Programme for the Elimination of Lymphatic Filariasis (GPELF) making commendable progress towards the elimination of LF as a public health problem by the WHO's original 2020

target. Such success has risen from a strategy which aims to prevent the transmission of LF, involving mass drug administration programmes (MDA) of anti-filarial drugs - displaying microfilaricidal activity (effective against mf) - along with overlapping mosquito vector control measures, typically through distribution of long-acting insecticide impregnated bednets (Gyapong *et al.*, 2005; Hoerauf, 2006). To date, of the 73 countries targeted for MDA and blocking of transmission, only 18 have completed interventions and subsequent surveillance to confirm elimination, including Korea and China (Cheun *et al.*, 2009; De-Jian, Xu-Li and Ji-Hui, 2013). Although a further 22 countries are forecast to achieve elimination by the 2020 milestone, having already delivered MDA in disease endemic areas, 33 countries have been unable to achieve 100% geographical coverage for MDA programmes. Worryingly, 10 countries are yet to start any MDA programmes or have been unable to provide evidence that MDA is not required (Alexander, 2015). That 58% of the countries involved are failing to implement measures necessary for the blocking of filarial transmission, 4 years before the deadline paints a dim outlook for the success of the 2020 target for elimination. These figures confirm that, despite excellent progress, LF remains an enduring global health problem and at-risk populations continue to remain extremely vulnerable to the development of the highly disabling, life-long pathologies associated with filarial infection.

Irrespective of the time-frame for successful elimination of LF parasitic infection, LF patients displaying pathology will endure often irreversible, life-long disability. The progress in treatment for the estimated 40 million cohort who suffer with high morbidity has been far more disappointing than the demonstrable success in LF elimination. Current treatment strategies mainly involve management of the symptoms, namely intense physiotherapy, heating or cooling and analgesics to the affected swollen limbs (Addiss and Brady, 2007). Good hygiene practices to the affected limbs and use of prophylactic antibiotics have also seen partial success in reducing further acute inflammatory attacks associated with filarial LE (Ottesen, 2006). A recent emphasis has been given to the self-care and management of LE symptoms by the patient, namely remedial exercises and practicing good

hygiene to affected areas (Douglass, Graves and Gordon, 2016). Surgical intervention is an effective anti-morbidity intervention for hydrocoele (hydrocoelelectomy) (Shenoy, 2008). Hydrocoelelectomy is not, however, readily accessible in hard-to-reach areas where health resources are limiting (Stanton *et al.*, 2015).

There is currently a paucity of research into novel and affordable therapies that ameliorate filarial LE and elephantiasis. Recent work has demonstrated that chemical intervention, during early stages of infection and before clinical manifestations of pathology, can be effective in reversing changes in skin firmness and subclinical changes to the lymphatic architecture (termed “covert pathology”). The authors argue halting these sub clinical pathologies are useful in preventing the development of later clinical LE pathologies (Douglass *et al.*, 2019) . Further, it has been demonstrated that doxycycline is able to halt and even reverse early stages of filarial LE, independent of its antibiotic or filaricidal mode of actions (Debrah *et al.*, 2006, 2009; Mand *et al.*, 2012). Promisingly, doxycycline has shown measurable anti-morbidity success in phase II clinical trials (Mand *et al.*, 2012). The anti-morbidity mode of action of doxycycline, however, is poorly understood, while efficacy has only been demonstrated in patients with lower grade LE, with less success on more severe, higher LE grades.

Vascular and Lymphatic remodelling is regarded as a key ‘hallmark’ along the pathway to LF pathology (Addiss and Brady, 2007) and as such may be considered as a viable LF anti-morbidity drug strategy. Unfortunately, vascular remodelling processes in LF remain poorly elucidated, partly due to a lack of adequate preclinical model systems to mechanistically study LF disease aetiology. Furthermore, there is conflicting evidence across secondary LE model systems as to whether lymphatic remodelling events are causal factors in the development of lymphoedematous pathology, are a part of host repair mechanism which prevents more severe disease and could be harnessed for therapeutic potential or are merely ‘epiphenomena’ which are not causal in pathology development. What is clear, especially in a ‘post-elimination era’ is that there is a requirement for more effective anti-

morbidity strategies that could alleviate filarial LE to improve the quality of life of those afflicted with life-long disability.

1.7- *In vitro*, *in vivo* and clinical evidence of a role for lymphatic remodelling in filarial infection and pathology

The events and mechanisms that lead to pathology and subsequent morbidity in LF remain poorly elucidated. There is some evidence to suggest worm inhabitation of the peripheral lymphatics and their so called 'worm nests' lead to progressive physical damage and blockage of the lymphatic architecture, which contributes to lymphatic dysfunction and LE (Dreyer *et al.*, 2000; Nutman, 2013). In addition to direct worm mediated damage, emerging evidence suggests that inflammatory immune responses to dying or dead worms, or release of the endosymbiotic *Wolbachia* bacteria inside filarial worms results in indirect, off target or 'collateral' damage to the lymphatics leading to lymphatic dysfunction (Babu and Nutman, 2014). Nevertheless, these findings cannot reconcile the fact that both these events occur in all cases of filarial infection, yet only a subset of patients display clinical pathology. Key questions remain unanswered about the complex relationship between the parasitic worm, the lymphatic niche in which they inhabit and the immune microenvironment to which they are exposed. The events and crosstalk that occurs at this interface, and what determines an asymptomatic or pathological outcome remains an area of great scientific interest.

Lymphatic remodelling is regarded to be a key event which facilitates the manifestation of pathology in LF. *In vitro* evidence has demonstrated that co-culturing of live worms, or their soluble extracts and antigens, with LECs induced activation, proliferation and tube formation (Bennuru and Nutman, 2009a). Such evidence implicates filarial infection with the ability to induce lymphatic remodelling in the host. Interestingly, initial studies involving filarial E/S products and LECs failed to induce the direct activation or proliferation (Weinkopff and Lammie, 2011), although later work by the same group showed filarial E/S products were able to stimulate primary human monocytes (from peripheral blood mononuclear cells (PBMCs)) to produce

lymphangiogenic mediators *in vitro*, which when cultured with LECs stimulated proliferation and tube formation (Weinkopff *et al.*, 2014). This perhaps reconciles findings in which plasma from LF infected patients were able to induce proliferation of LECs in culture (Bennuru and Nutman, 2009b; Bennuru *et al.*, 2010). Importantly, these findings suggest a significant and complex interplay between filarial worms and the host immune system which results in lymphatic remodelling during LF. Studies have demonstrated that asparingyl Transfer RiboNucleic Acid (tRNA) synthase, a 'physiocrine' product released from worms, can directly induce proliferation in Human Umbilical Vascular Endothelial Cell (HUVEC) assays (Jothi *et al.*, 2016) suggesting vascular remodelling is induced following infection and parasite mediated signalling. Further experiments that investigate the effect of this 'physiocrine' on LEC cells may yield an additional effect on lymphatic remodelling. The aforementioned *in vitro* evidence is strengthened by data acquired from *in vivo* models. Experimental intra-lymphatic infections into inguinal lymphatic ducts demonstrated a significant increase in lymphatic dilation, in Severe Combined ImmunoDeficient (SCID) or athymic mouse models (Vincent *et al.*, 1984; Nelson *et al.*, 1991). Interestingly this dilation was not limited to the immediate 'worm nest', where the worms localised, but the entire length of infected ducts, while chemotherapeutic removal of the worms led to a reversal of dilation (Vickery *et al.*, 1991). Such dilation seems to be a hallmark of filarial infection as similar observations have been made in Mongolian jirds (Ah and Thompson, 1973) and feline (Denham and Fletcher, 1987; Grenfell, Michael and Denham, 1991) infection models. Of particular note were studies demonstrating initial lymphatic remodelling (in forms of dilation), but absence of pathological manifestations in immunodeficient mice, which upon immune reconstitution with immune-competent splenocytes resulted in significant fibrosis, lymphatic remodelling and manifest pathology (Vickery *et al.*, 1991). This could suggest that while initial lymphatic remodelling could be directed by filarial signals or 'toxins', adaptive immune responses are necessary to initiate larger scale lymphatic remodelling or changes to the architecture that is concomitant with pathological manifestations.

Overt lymphatic remodelling has also been demonstrated as a feature of filarial infection from clinical observations. Research involving a small number (n=15) of filarial patients utilised histological methods on patient skin explants to demonstrate a significant increase in vasculitis, vascular fibrosis and vessel diameter in filarial infected patients (Case *et al.*, 1991). Additionally, marked dilation of worm inhabiting lymphatic vessels was observed in LF patients (Freedman *et al.*, 1994). Surprisingly, limb scintigraphy demonstrated that 'asymptomatic' filarial patients also display a degree of either remodelling of the normal lymphatic architecture or dilation of lymphatic vessels (Freedman *et al.*, 1995; Noroes *et al.*, 1996; Shenoy *et al.*, 2008; Kar *et al.*, 2017). Ultrasonographical analysis of filarial-infected hydrocoele patients have strengthened the association of active infection with lymphatic remodelling, with marked dilation and tortuosity observed in infected scrotal lymphatics (Amaral *et al.*, 1994; Noroes *et al.*, 1996). Additionally, excised infected lymph nodes that have undergone histological analysis lead to observations of marked lymphatic hyperplasia and dilation (Jungmann, Figueredo-Silva and Dreyer, 1991). Mechanistically, serum comparisons between endemic normal and both microfilaraemic and pathology displaying patient groups demonstrated significantly higher plasma levels of factors: VEGF-A, VEGF-C, VEGF-D sVEGFR3 and Ang1/2 in filarial-infected microfilaraemic and pathology cohorts (Alexander Yaw Debrah *et al.*, 2007; Debrah *et al.*, 2009; Bennuru *et al.*, 2010). These identified factors are known to be key drivers of lymphangiogenesis that can lead to lymphatic remodelling events (Lohela *et al.*, 2009). Higher circulating levels of these factors in infected patients would suggest potential for lymphangiogenic remodelling, stimulated either directly by the worms (i.e. induction of growth factors derived from parasitized lymphatic tissue), or indirectly through an immune response to worm infection. Supporting evidence has come from work undertaken by Debrah *et al.* who observed significantly higher serum levels of VEGF-A in filarial infected patients suffering from hydrocoele pathology than uninfected counterparts (A Y Debrah *et al.*, 2007). Treatment of these patients with macrofilaricidal drugs, leading to worm clearance, positively correlated with significant reductions of serum VEGF-A, VEGF-C and sVEGFR3 post treatment (Debrah *et al.*, 2009).

These studies perhaps provide more compelling and direct evidence that worm presence leads to an increase in lymph/angiogenic factors and subsequent angiogenic/lymphangiogenic remodelling.

1.8-Filarial-associated lymphatic remodelling and implications for pathogenesis

Whilst there is substantial evidence that lymphatic remodelling is a key 'hallmark' that occurs following filarial infection, what is less understood, is the causality of this remodelling in progression from a 'grade 0' or asymptomatic state to overt lymphoedematous disease. The prevailing theory states that lymphatic damage or perturbation initiates lymphatic remodelling and dilation, driven by filarial adult inhabitation. The accumulation of this damage and subsequent lymphatic remodelling contributes to a 'pathway' that leads to pathological manifestations (Dreyer *et al.*, 2000; Chakraborty *et al.*, 2013; Nutman, 2013). Studies that demonstrate significantly higher circulating plasma pro-lymphangiogenic VEGF-C and VEGF-A in LF patients compared to uninfected controls (A Y Debrah *et al.*, 2007; Bennuru *et al.*, 2010) would suggest that an association exists between increased stimulation of lymphatic remodelling and lymphatic dysfunction/pathology. Importantly, doxycycline treatment has demonstrated an ability to significantly reduce serum levels of these lymphangiogenic factors, which was associated with amelioration of severity of lymphoedema and morbidity (Debrah *et al.*, 2006, 2009). In addition, this amelioration was observed in filarial LE patients in the absence of active filarial infection, suggesting the doxycycline mode-of-action was independent from its adult worm curative activity (Mand *et al.*, 2012). Together, these studies would suggest that reducing lymphatic remodelling by targeting the drivers of lymphangiogenesis could be a novel strategy to ameliorate lymphatic insufficiency and dysfunction associated with filarial infection. Research in oncology has demonstrated that aberrant lymphatic remodelling, in the form of a tumour's ability to 'hijack' lymphangiogenesis, is essential for tumour vascularisation, survival and metastasis (Skobe *et al.*, 2001; Hanahan and Weinberg, 2011; Ran and Montgomery, 2012)

The evidence above associating severity of LE with pro-lymphangiogenic mediators and evidence of pronounced lymphatic remodelling would support that remodelling / lymphangiogenesis is pathological in nature. This is in contrast, however, to the theory in other areas of LE research. Primary LE has been directly linked with genetic mutations in a host of pro-lymphangiogenic signalling pathways, preventing either development, of the lymphatic architecture (Brice *et al.*, 2005; Mellor *et al.*, 2011), or appropriate functional lymphatic remodelling. These aberrant mutations often result in severe lymphatic insufficiency and dysfunction. It can, however be argued that primary LE reflects more initial failure to develop lymphatics, rather than lack of remodelling. Recent studies, however, have demonstrated that secondary LE, acquired following surgical excision of tumour tissue in breast cancer, can arise due to mutations which render the VEGFR3 gene dysfunctional thus severely reducing the ability to remodel lymphatics following the injury resulting in failure of restoration of lymphatic drainage (Newman *et al.*, 2012). Additionally, exogenous VEGF-C administration in an established murine tail model of secondary LE significantly increased rates of lymphatic remodelling, resulting in amelioration of lymphoedematous pathology (Jin da *et al.*, 2009; Visuri *et al.*, 2015). Co-administration of an anti-VEGF-C neutralising antibody in the same model abrogated this improvement (Jin da *et al.*, 2009). Elegant studies that overexpressed the VEGF-C gene in the same murine model of LE, also lead to significant amelioration (Yoon *et al.*, 2003). Recent research following filarial infected patient cohorts have observed a significant increase in forkhead box protein C2 (*foxc2*) and fms-like tyrosine kinase 4 (*flt4- also known as vascular endothelial growth factor receptor 3(vegfr3)*) gene mutations in pathology displaying cohorts, when compared to asymptomatic and non-infected cohorts. Such genes have been implicated as important intermediaries in the correct regulation and mediation of lymphangiogenic/ angiogenic programmes. Sheik *et al.* suggests that pathology arises as a result of aberrant function of these genes, leading to improper or complete abrogation of lymphatic remodelling that would usually repair worm mediated damage of lymphatics following filarial infection (Sheik *et al.*, 2015). Together, this would suggest that lymphatic remodelling, rather than contributing to filarial

pathology, may be a host compensatory mechanism to repair filarial damage of the lymphatics, thus acting in a therapeutic capacity.

From the evidence presented above, it is clear that lymphatic remodelling is highly regulated and the context of its activation can result in both pathological and therapeutic outcomes. This perhaps is best demonstrated in a review suggesting the 'double-edged sword' effect of lymphatic remodelling (Kim, Kataru and Koh, 2014). Equally as clear, however is that lymphatic remodelling is an important event, that occurs following filarial infection. Although there is tentative evidence that infers a role for worms themselves as well as the host immune response in lymphatic remodelling events, the exact contributors and the regulatory mechanisms that govern this important event remains elusive. In addition, whether the observed lymphatic remodelling in LF is a contributor to future pathology, or compensatory in nature to prevent pathological development, is highly debated and poorly defined. Defining a 'developmental timeline' of lymphatic remodelling following infection and how it is regulated both in terms of cellular and molecular mechanisms will aid in understanding the contribution of remodelling to filarial pathology. However, this is extremely challenging in human infections both due to uncertainty of degree of prior exposure and for ethical considerations post-diagnosing active infection. A better understanding of the processes that lead to lymphatic remodelling as a key event of LF may yield novel therapeutic strategies, that could ultimately result in new treatments to alleviate LF morbidity.

1.9- Project Aims and Objectives

The overarching aim of my PhD project is to assess how filarial infection induces lymphatic remodelling and test whether lymphatic remodelling events are pathological, or a result of tissue repair pathways to prevent the development of lymphatic pathology. With better knowledge of how lymphatic remodelling relates to pathology, it is hoped that manipulation of this process could potentially yield future therapeutic strategies to combat LF associated-morbidity.

My project will look to address the question outlined above, by dissecting the potential role of host innate and adaptive immune response mechanisms in lymphatic remodelling, both on a cellular and molecular level. Preliminary objectives will be as follows:

- Develop a murine filarial leg infection model which allows longitudinal imaging of the lymphatics *in vivo*, thus allowing the tracking of changes to the lymphatic architecture following infection.
- Evaluate the consequences of filarial-associated lymphatic remodelling by:
 - Using imaging techniques in the model to quantify changes to the lymphatic architecture and its effect on lymphatic drainage/performance.
 - Investigate gross histological and anatomical changes following lymphatic remodelling.
 - Evaluate whether remodelling leads to signs of pathology development.
- Investigate how host immune responses may contribute to lymphatic remodelling following infection (immune-competent vs immunocompromised mice)
- Investigate adaptive and innate immune mechanisms that may play a role in lymphatic remodelling. This will be achieved through investigating:
 - Systemic immune cytokine and angiogenic/lymphangiogenic profiles following infection.
 - Immuno-phenotyping of adaptive and innate immune cells in the lymphatic network proximal to infection sites.
 - Isolation of important immune cells in filarial infection for investigation of their angiogenic/lymphangiogenic expression profiles/
- Based on findings from objectives above, make use of murine-specific reagents and evaluate their effect on lymphatic remodelling. It is hoped lymphatic remodelling can be manipulated (increased or suppressed) as a therapeutic target for the alleviation of pathology in

LF. Some preliminary manipulations that could be investigated include:

- Use of mouse knockout lines for important immune pathways.
- Blocking antibodies or traps to manipulate host immune responses or lymphangiogenic networks that contribute to filarial associated lymphatic remodelling.

Chapter 2

Characterisation of an inbred murine experimental model of filarial-induced lymphatic pathology

Chapter abstract

120 million people are estimated to be infected with Lymphatic filariasis (LF) globally, while a 40 million patient subset present with the severely disabling pathology of lymphoedema, contributing to high levels of LF related morbidity. Lymphatic remodelling is a well-documented hallmark of LF patients, yet what drives its induction, and its causal link with aetiology of disease, is poorly defined. An immune competent murine model of *Brugia malayi* filarial infection was developed and validated to allow investigation of the longitudinal development of lymphatic remodelling. In addition, the association between magnitude of lymphatic remodelling and lymphatic insufficiency was investigated. The model indicated that onset of lymphatic remodelling occurs rapidly (as little as 6 days) post-infection and is highly associative with the degree of lymphatic insufficiency. Lymphatic remodelling and insufficiency persisted long-term (16 weeks) in animals with no evidence of adult infection. Severity of remodelling and insufficiency was dependent on the murine strain utilised and was increased after challenge infection, suggesting host adaptive immune responses influenced pathology. Lymphatic remodelling, and related insufficiency, is a consistent event that rapidly occurs following infection with infective *B.malayi* L3 larvae. Furthermore, the developed model enables the future interrogation of molecular, cellular and immunological mechanisms driving filarial-associated lymphatic pathology, with the objective to yield new therapeutic strategies to ameliorate LF morbidity.

2.1 Introduction

As discussed in chapter one, lymphatic remodelling is a well-documented, feature of patients infected with lymphatic filariasis (LF), observed in both individuals with overt LE (Dreyer *et al.*, 2000; Figueredo-Silva *et al.*, 2002; Chakraborty *et al.*, 2013) as well as 'latent stage 'asymptomatic' (Freedman *et al.*, 1995; Kar *et al.*, 2017) infected patients. With a mixed and variable history of exposure and complications such as annual MDA treatments and/or secondary microbial skin infections, it is not possible to accurately interrogate causal mechanisms of lymphatic remodelling in natural human infections. In addition, the presence of lymphatic remodelling in both patient cohorts raises the question as to whether remodelling is responsible for, or contributes to the more advanced lymphoedematous pathological manifestations of LF.

While the causal mechanisms of lymphatic remodelling remains undefined, it has been hypothesised to be driven both by direct stimulation from active filarial secretions of invading parasites (Shenoy, 2008; Bennuru and Nutman, 2009a; Weinkopff *et al.*, 2014) as well as possible host responses against filarial infection (Babu and Nutman, 2012, 2014). A pervading theory in the field states that long term inhabitation of the lymphatic architecture by filarial worms ,and subsequent damage caused by their motility and moulting, leads to the accumulation of lymphatic remodelling events, that tips the balance towards a lymphoedematous pathological outcome (Bennuru and Nutman, 2009a; Taylor, Hoerauf and Bockarie, 2010). Conversely, Dreyer and colleagues propose that the bridging link between almost universal lymphatic remodelling in symptomatic and asymptomatic cohorts, and subsequent development of pathology, is attributed to other co-factors including worm death events and the proceeding host inflammatory reaction to filarial antigenic release (Dreyer *et al.*, 2000; Figueredo-Silva *et al.*, 2002).

In depth immunological studies have shown the strength and type of adaptive immune responses may be critical, with strengthened inflammatory Th-1 and Th-17 responses associated with LE pathology, while more "regulatory" or "modified" Th-2 responses dominate asymptomatic LF

outcomes (King *et al.*, 1993; Taylor *et al.*, 2005; Babu and Nutman, 2014). Pfarr and colleagues, meanwhile, hypothesise that the intracellular bacterial symbiont *Wolbachia* and inflammatory events against them may play an important role in remodelling and the driving of subsequent pathology (Bandi, Trees and Brattig, 2001; Mand *et al.*, 2009). A general consensus in the field of filariasis, therefore, links active parasitism of the lymphatics with adult parasites and consequential host inflammation, with the triggering of remodelling that eventually contributes to the development of LE (Nutman, 2013). In contrast, studies investigating the mechanisms of secondary LE, not induced by filarial infection, supports a role for increased lymphatic remodelling as a compensatory, wound healing mechanism to restore lymphatic function, following damage or injury to the lymphatic architecture (Jin da *et al.*, 2009; Visuri *et al.*, 2015).

A major hurdle in researching the link between remodelling and pathology is that most research is based on clinical observations, that only occur long after initial infection events. Establishing when remodelling occurs on the 'pathway' to pathology, therefore, is difficult to achieve. Several permissive animal models exist that may allow interrogation of this question, including gerbils (McCall *et al.*, 1973; Figueredo-Silva *et al.*, 2002), rats (Ahmed, 1967; Benjamin and Soulsby, 1976; Lawrence and Denham, 1993), ferrets (Hines *et al.*, 1989; Jackson-Thompson *et al.*, 2018) and lymphopenic mouse strains (Vincent *et al.*, 1984; Nelson *et al.*, 1991; Vickery *et al.*, 1991; Lawrence, 1996) yet significant drawbacks exist in all cases. In the case of gerbils, rats and ferrets, the lack of available reagents and ability to easily genetically manipulate these model organisms make it difficult to mechanistically interrogate filarial lymphatic remodelling. Conversely, the use of immunodeficient mouse strains removes facets of the host response which may play a vital role in the induction of lymphatic remodelling and possible pathology. A table summarising the advantages and disadvantages of the current animal models of *Brugia malayi/ pahangi* filarial infection are summarised in the table below.

Animal Model	Advantages	Disadvantages
Gerbils	-Permissive- can attain full life cycle	-Large, expensive to house in experimental conditions -Lack of immunological/experimental reagents which are gerbil specific -Lack of established genetic knockout/knockin strains
Ferrets	-Permissive- can attain full life cycle -Filarial LE pathology can be experimentally emulated	-Large, expensive to house in experimental conditions -Lack of immunological/experimental reagents which are ferret specific -Lack of established genetic knockout/knockin strains
Rats	-Partially permissive- larvae develop to adult worms	-Not fully permissive, microfilariae are not released by adult worms into circulation -Large, expensive to house in experimental conditions -Not as comprehensive range of immunological reagents or knockouts in rats
Immunodeficient mice strains	-Partial permissive- can attain full life cycle in ~50% of animals -Can emulate early lymphatic pathology (lymphatic vessel dilation)	-Loss of components of host immune response to LF

Table 2.1: Advantages and disadvantages associated with using current animal models of filarial infection

With the discussed lack of an optimal animal model, development of a murine immunocompetent mouse model facilitating the longitudinal interrogation of filarial associated lymphatic remodelling, would be of potential utility to investigate the relationship between lymphatic remodelling and pathological consequences in terms of lymphatic function. Such a model would allow for improved interrogation of the cellular and molecular mechanisms regulating filarial associated lymphatic remodelling. The utilisation of: well established genetic knock-in or knock-out lines, and well characterised murine antibody reagents could facilitate thorough characterisation of lymphatic remodelling and their role in filarial infection. Ultimately, clarifying the link between lymphatic remodelling and pathology, and utilisation to explore host mechanisms regulating lymphatic pathology, may yield novel therapeutic strategies to combat filarial disease.

2.1.1- Research Aims and Objectives

The aims of this research chapter, therefore, will be to develop a novel inbred, immunocompetent, murine pathology model of *B. malayi* filarial infection (*BmL3*) that allows longitudinal tracking of potential changes to the lymphatic architecture. The model will be utilised to interrogate:

1. Whether there is evidence of host lymphatic remodelling post *BmL3* infection and, if so, determine the dynamics of pathology induction and resolution post-infection.
2. If there is evidence to support that lymphatic remodelling is associated with lymphatic insufficiency
3. How challenge infection or host genetic variation, in the form of varying inbred strains of mice, impacts on the development and severity of lymphatic remodelling

2.2- Methods

2.2.1- Mouse Maintenance

All procedures involving the use of laboratory animals were performed in a pathogen free facility at The Biomedical Services Unit (BSU), University of Liverpool. All animal procedures were approved by the Animal Welfare Committee of University of Liverpool and The Animal Welfare and Ethics Review Board of Liverpool School of Tropical Medicine (LSTM), and were carried out in accordance with The Use of Animals in Scientific Procedures Act (UK Home Office).

Male Immuno-competent C57BL/6J Prox-1^{GFP} transgenic mice were bred in house for *B. malayi* infection experiments and were created using out-bred Prox1-GFP FVB/N:CD1 cross mouse breeding pairs (A kind gift from the Hong lab, UCLA (Choi *et al.*, 2011)) back-crossed onto C57BL/6J mice for six generations. Following six generations of back-crossing, resultant homozygous Prox-1^{GFP} offspring were selected for future breeding pairs. Male BALB/c and C57BL/6J mice were purchased from Charles River (Margate,UK); all were 6-12 weeks at the start of each experiment. Male Mongolian gerbils were purchased from Charles River (Margate,UK) and were typically 8-12 weeks old at point of infection.

2.2.2- Parasite Life Cycle and Maintenance

The life cycle of *B. malayi* (*Bm*) was maintained in mosquitoes and Mongolian gerbils. Mongolian gerbils were initially infected intraperitoneally (i.p) with 400 *B. malayi* infective L3 larvae (*Bmi*L3) and left for 12 weeks to establish fecund adult infection. Microfilariae (mf) were collected from infected Mongolian gerbils via catheterisation involving anaesthetisation with isoflurane followed by peritoneal washes with Roswell Park Memorial Institute (RPMI) 1640 media (ThermoFisher Scientific) to harvest Mf. Mf were subsequently purified, using PD10 column size exclusion chromatography (Amersham), enumerated by microscopy and mixed with heparinised human blood to a final concentration of 15–20,000 mf/ml. Mf spiked human blood

was then fed to female *Aedes aegypti* mosquitoes through an artificial membrane feeder (Hemotek) and reared for 14 days with daily sugar-water feeding to allow development of mf to the infective *BmiL3* stage. Following 14-day incubation *BmiL3* were collected from infected mosquitoes by physical crushing of infected mosquitoes following immobilisation by chilling at 4°C for 10 minutes, followed by concentration using a Baermann's apparatus and RPMI media. *BmiL3* were utilised for either downstream experiments or used to infect naïve Gerbils to maintain the life cycle

2.2.3- Leg pathology model experimental infection

Mice were sedated using isoflurane general anaesthetic and 100 *B. malayi* L3 larvae (*BmL3*) per mouse divided over two injection sites in a volume not exceeding 50µl/injection. 50 *BmL3*, were injected subcutaneously (sc.), using a 35-gauge needle (Sigma, Dorset) attached to a 1ml capacity syringe (BD Biosciences, UK) into the left hind leg of mice on top of the foot and 50 sc. caudal to the left knee joint. Sham-infected control mice received equal volumes of sterile Roswell Park Memorial Institute 1640 (RPMI) at both sc. injection sites. Mice were left for varying time points from 6 days to 16 weeks before sacrifice via schedule one method of rising concentration of CO₂ (3 minutes 0-100% CO₂ followed by 2 minute 100% cycle) and subsequent exsanguination through standard cardiac puncture technique, prior to dissection and tissue sampling. Figure 2.1A shows a diagrammatic representation of the developed model.

2.2.4-Intravital Near-Infrared (NIR) Imaging of lymphatic flow

Mice infected as described above were maintained under isoflurane anaesthetic to allow equal volume (20µl) s.c. injections of a prepared 1mg/ml solution in ddH₂O of clinical-grade angiographic contrast agent indocyanine green (ICG; 'cardio-green') (Sigma, Dorset UK) into the dorsal area of both left and right hind feet. As the ICG is drained away from injection site through the lymphatics, a Photo Dynamic Eye (PDE) near infra-red (NIR) optical imaging device (Hamamatsu Photonics, Hertfordshire) was used to observe in real time the near infrared fluorescent signal emitted from the ICG. Mice

were imaged from above and placed in 4 different viewpoints: Dorsal (mouse's back pointing upwards), ventral (mouse's stomach pointing upwards), left (mouse placed on side with left hind leg pointing upwards) and right (mouse placed on side with left hind leg pointing upwards) (Figure 2.1B). A digital moving image of approximately 3 minutes per mouse was recorded, using an EasyCap DC60 USB Video Capture Card Adapter (Softonic, Barcelona) that converted footage from the PDE imaging device directly to ImageJ software (NIH, USA) via the IJwebcam plugin. A resolution setting of 720 x 480 at 60 fps was utilised, encompassing all 4 viewpoints described and completed movies saved directly into .Tiff file format. The imaging method was applied either at single time points or longitudinally, where indicated ranging from 6 days to 16 weeks pi.

2.2.5-Quantification of lymphatic remodelling and lymphatic insufficiency

High resolution (720 x 480) still images from all 4 viewpoints per mouse were obtained from the imaging movies by pausing the digital moving image on the most representative example of all 4 viewpoints as described above. Downstream analysis was undertaken directly in ImageJ (NIH, USA) (described below), while representative images for figures were screen captured by using Snipping Tool (Windows, USA) and saved as a .Jpeg image at native 720 x 480 resolution. To avoid bias in analysis, images were blinded using the Filename Randomiser ImageJ macro. Briefly, Tiff moving image files were masked to assigned random letter/number sequences and a "key" file generated to allow deciphering of relevant files post analysis. Atypical 'aberrant' lymphatic patterns (not present in naïve mice) were quantified by tracing from the images obtained in all 4 viewpoints using ImageJ software (NIH, USA) (Figure 2.1C). Traced lymphatics were reported as a length measurement (arbitrary units- Pixels)- with higher lengths reporting higher quantities of aberrant lymphatic channels. Measurements from all four view-points were plotted into separate dot-plot graphs using GraphPad Prism Version 5 Software (GraphPad Software, La Jolla USA)

For lymphatic insufficiency measurements, paused representative stills from the ventral viewpoint (see figure 2.1D) were analysed in ImageJ (NIH, USA).

A polygon selection region of interest (ROI) was used to trace round the left- and right-hindfoot, from below the popliteal lymph node (pLN) down to above the injection site (Figure 2.1D) and the “mean pixel fluorescent intensity measurement” obtained using the standard “measure> mean grey value” tool from ImageJ (NIH, USA). ImageJ calculates this measurement by assigning pixels in the ROI a “brightness” value between 0-255 and reporting the mean value from total number of pixels. Because ICG dye emits NIR fluorescence which is registered on the PDE imaging device, an increased “mean pixel intensity”, equates to more ICG retention in the ROI. The intensities were reported as a ratio of the right (uninfected) hind lower limb : left (infected) hind lower limb, the equations used to calculate the Right/Left leg ratio is described below:

$$\text{Ratio Value} = \frac{\text{Mean ROI Fluorescent Intensity RIGHT LIMB}}{\text{Mean ROI Fluorescent Intensity LEFT LIMB}}$$

A ratio value less than one (0.999-0) is indicative of ICG retention in the left (infected limb) while ratio values above one (>1) suggest retention of ICG in the right (uninfected foot)

2.2.6-Evan’s Blue dermal retention assay (modified Miles Assay)

A modified Miles Assay (Radu and Chernoff, 2013) was utilised whereby mice infected for 14 days, following *BmL3* or sham infection as described previously, were maintained under isoflurane anaesthetic and a sc. injection of 10µl (using a NanoFil 100µl sub-microlitre injection syringe (World Precision Instruments, USA) for precise delivery) of 1% Evan’s Blue (Sigma, Dorset UK) w/v in sterile dulbecco’s Phosphate Buffered Media (dPBS) (Sigma, UK) administered in the dorsal foot pocket of the left hind leg. Following a 20-minute draining period, mice were euthanized using schedule one method of a rising concentration of CO₂ followed by confirmation of death. The skin of the left hind leg between the knee and ankle joint was carefully excised and transferred to 1ml of dPBS (Sigma, UK) for an incubation period of 20 minutes before removal. A 100µl sample of the PBS

from the incubated skin section was then transferred to a flat bottom 96 well plate (Starlab, Milton Keynes) and absorbance read on a VarioSkan (ThermoFisher, UK) plate reader at 620nm.

2.2.7-Epifluorescence Microscopy and quantitation of Lymphatic vessel width

The C57BL/6J Prox-1^{GFP} transgenic mice utilised in the pathology model results in any Prox-1 expression being visible due to Bacterial Artificial Chromosome (BAC) transgenic knock-in of a GFP fluorescent tag to the promoter region of the *prox-1* gene. Prox-1 is a master transcription factor for the lymphatic endothelium lineage and results in visualisation of the mouse's lymphatic architecture when visualising GFP epifluorescence by fluorescence microscopy.

Following various time points of the pathology model, mice were euthanised using schedule one method of a rising concentration of CO₂ followed by confirmation of death. Skin samples were removed at areas of aberrant lymphatics (with equivalent areas used in sham control mice) and mounted onto a wooden board. Epifluorescence was then visualised using a fluorescent stereo-dissecting microscope (Leica Microsystems, Milton Keynes). Between 15 and 30 images were taken per mouse in these areas and saved as .BMP image files before blinding, utilising the same Filename Randomiser Macro in ImageJ as described above. Lymphatic channels representative of the captured individual image were then measured for lymphatic channel aperture using the 'straight line' measuring tool in ImageJ (NIH, USA). All image measurements across the 15-30 images per mouse were then pooled to allow calculation of an average lymphatic width of these measurements to be reported.

In other experiments the popliteal lymph node (pLN, Iliac (iLN) and sub-iliac (siLN) lymph nodes from sham and 14dpi infected mice were dissected and placed on petri dishes ready for epifluorescence microscopy using a fluorescent stereo-dissecting microscope (Leica Microsystems, Milton Keynes). An image of the lymph node was taken in the GFP channel and an area measurement obtained in ImageJ using the Prox-1 fluorescence as a guideline for the perimeter of the lymph nodes.

2.2.8-Epifluorescence tracking of *BmL3* migration

BmL3 larvae were harvested and separated into 200 *BmL3* aliquots. Aliquots were washed in RPMI 1640 (Sigma, Dorset) followed by staining in a 150 μ M solution of Alexa Fluor™ 546 NHS Ester (Succinimidyl Ester) (Thermofisher, UK) in Fluorobrite DMEM (Thermofisher, UK) for 2 hours. Following staining, *BmL3* larvae were washed once in RPMI 1640 (Sigma, Dorset) before resuspension in approximately 50 μ l of RPMI 1640 (Sigma, Dorset) and drawing up into 35-gauge needle (Sigma, Dorset) 1ml capacity syringes (BD Biosciences, UK).

C57BL/6J Prox-1^{GFP} transgenic mice were injected sc with 400 *BmL3* across two sites- 200 into the dorsal pocket of the foot and 200 in a pocket caudal to the left knee joint. Mice were left for 3 hours, 24 hours, 48 hours or 6 days pi followed by euthanasia using schedule one method of a rising concentration of CO₂ and confirmation of death. Epifluorescence microscopy was undertaken, utilising a fluorescent stereo-dissecting microscope (Leica Microsystems, Milton Keynes), to locate *BmL3* in the 'dsRed' filter channel. Fluorescent *BmL3* were checked for location in relation to initial inoculation sites and common areas of lymphatic remodelling as visualised under PDE ICG imaging. Fluorescent *BmL3* were also checked for co-localisation with Prox-1^{GFP} expressing lymphatic channels. Where colocalization was found, images were taken or a time-course of images obtained to create moving images using manufacturer's software.

2.2.9-Lymph node and cardiac blood sampling

At varying time points following the pathology model described above, mice were sacrificed utilising schedule 1 method of rising CO₂ overdose and was immediately followed by blood collection, using standard cardiac puncture techniques, into heparinised collection tubes (Starstedt, Germany). Following cardiac punctures, left (infected) side popliteal, iliac and sub-iliac lymph nodes were dissected and a single cell suspension created by teasing apart of nodes on top of a 40 μ m cell sieve (Sigma, Dorset) followed by maceration of remaining lymph node tissue through the sieve using the handle of 2ml

syringes (Sigma, Dorset). The resultant single cell suspension was then centrifuged and resuspended in PBS (Sigma, Dorset) + 5% Foetal Bovine Serum + 2mM EDTA and aliquoted into equal cell numbers ready for proceeding cell cytometry. A manual total viable cell count was undertaken on pooled lymph node single cell suspensions to gain a measurement of LN cellularity per mouse. This was done by mixing LN suspensions 1:1 0.1% trypan blue (Sigma, Dorset): cell suspension (for dead cell differentiation) followed by mounting onto Kova Glasstic slides (Sigma, UK) for counting under a x10 light microscope

2.2.10-Statistical Analysis

All statistical analysis was undertaken using Prism software (Graphpad software, San Diego). All continuous data was tested for normal distribution using the Kolmogorov-Smirnov test for equal variance. Where data was normally distributed, a two-tailed independent Student's t-test was used to test for significant differences between two groups. Where data was found to be not normally distributed, a log transformation of the data was first attempted and data re-tested for normal distribution. If data continued to be not normally distributed after log transformation, a two-tailed non-parametric Mann-Whitney U test was used to test for significant differences between two groups. Where more than 2 groups were being compared, a One-way ANOVA was utilised with a Tukey's post-hoc comparisons test to measure differences in parametric data, while a Kruskal-Wallis test was used for non-parametric data with Dunn's post-hoc multiple comparisons test. The mean along with the standard error of the mean (SEM) are reported in all data unless otherwise stated. Significance is indicated as *= $P < 0.05$, **= < 0.01 , ***= < 0.001 in all figures unless stated otherwise.

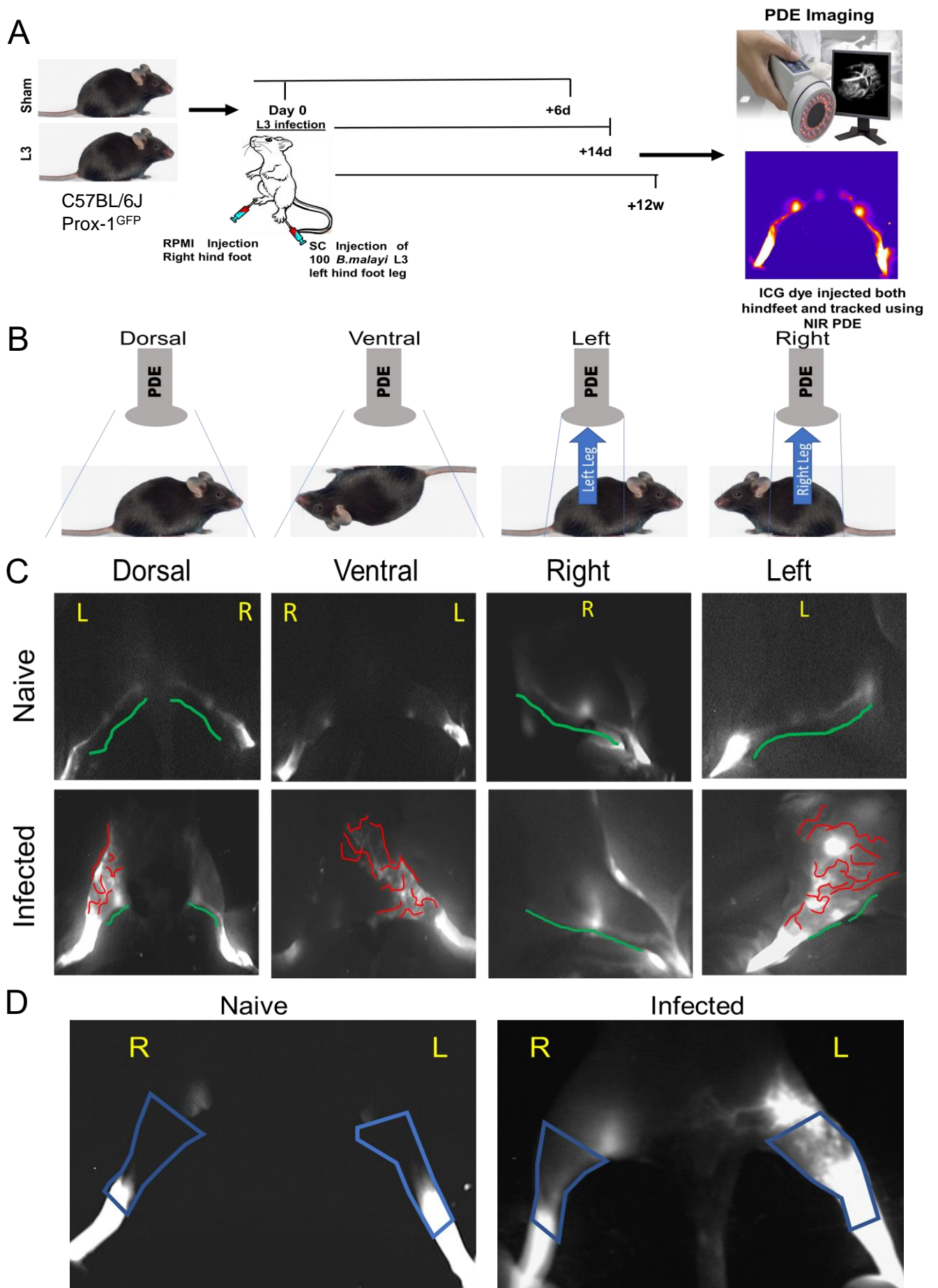


Figure 2.1: Development of a filarial mouse pathology model

A) Schematic of the developed mouse pathology model where mice were subcutaneously infected with 100 *BmL3* into the dorsal pocket of the left hind foot (50 L3) and pocket caudal to left hind foot knee (50 L3) followed by incubation for various time points before PDE NIR intravital imaging. **B)** Diagrammatic representation of the 4 viewpoints used to image mice hind legs. **C)** Illustration of the method used to quantify aberrant lymphatics across the 4 view-points. High quality still of the imaging movies are captured in all 4 view-points, normal lymphatic channels observed in naïve mice are highlighted in green and not traced/measured. Aberrant lymphatic vessels observed- defined as not present normally in naïve mice- are highlighted in red and would be traced and reported as a length measurement (Arbitrary unit: pixels) using ImageJ. **D)** Illustration of lymphatic insufficiency measurement taken from the ventral viewpoint. A polygonal area selection is made in ImageJ from just below the popliteal lymph node down to just above the injection site in both hind legs. The average pixel intensity is measured in both and reported as a ratio of right uninfected leg: left infected leg. Numbers below one would suggest aggregation of ICG in the left infected limb, numbers above one would suggest aggregation of ICG in right uninfected limb.

2.3- Results

2.3.1- Significant lymphatic remodelling and lymphatic insufficiency is evident post- infection with *B. malayi* larvae

To investigate whether lymphatic remodelling was induced post-infection with *BmL3*, lymphatics were imaged longitudinally in the hind legs of infected and naïve mouse groups between 6 days and 12 weeks post-infection (pi) utilising PDE NIR optical imaging of ICG lymphatic drainage. Additionally, lymphatic vessels were visualised using GFP epifluorescence at +14 days pi for measurement of lymphatic channel density and aperture. As an additional measure to investigate if infection lead to lymphatic insufficiency, an Evan's Blue dermal retention assay was undertaken at 14 days pi.

Novel, aberrant lymphatics were significantly higher in *BmL3* infected mice groups, compared to sham infected counterparts, at both 6 and 14 days pi in dorsal (Sham: 2.5 ± 1.9 A.U. vs 6 day: 331.4 ± 43.2 , $P < 0.001$, vs 14 day: 79.3 ± 25.2 $P < 0.001$), ventral (Sham: 10.4 ± 8.232 A.U: vs 6 day: 546.3 ± 64.9 A.U $P < 0.0001$, vs 14 day: 252.0 ± 31.00 A.U $P < 0.001$) and left viewpoints (Sham: 2.2 ± 2.2 A.U: vs 6 day: 602.2 ± 87.3 A.U $P < 0.0001$, vs 14 day: 374.5 ± 57.7 A.U $P < 0.0001$) , (Figure 2.2A&B.). Six day infections displayed significantly higher novel aberrant lymphatics than 14 day infections in ventral (6 day: 546.3 ± 64.9 A.U vs 14 day: 252.0 ± 31.0 A.U $P < 0.0001$) and left (6 day: 602.2 ± 87.3 A.U vs 14 day: 374.5 ± 57.7 A.U $P < 0.001$) viewpoints (Figure 2.2A&B). Additionally, the ratio of ICG fluorescence in right versus left limbs were significantly lower in *BmL3* infected mice, compared to sham infected controls at both 6 (Sham: 0.9 ± 0.1 R/L ratio vs 6 days: 0.3 ± 0.1 R/L ratio $P < 0.001$) and 14 days pi. (Sham: 0.9 ± 0.06 R/L ratio vs 14 days: 0.6 ± 0.06 R/L ratio $P < 0.01$)(Figure 2.2C.). At 14 days pi, a significant accumulation of Evan's Blue was apparent in limb dermal tissues in *BmL3* infected mice, compared to sham infected controls (Sham: 0.06 ± 0.01 O.D. 620nm vs *BmL3*: 0.1 ± 0.02 $P < 0.001$, Figure 2.3C&D).

Following previously established qualitative classification of pathologies indicative of dermal backflow and lymphatic insufficiency (Yamamoto *et al.*,

2011), all three grades: 'splash' 'stardust' and 'diffuse' were consistently observed in *BmL3* infected mouse cohorts as early as 14dpi (Figure 2.2D)

Apertures of Prox1-GFP⁺ dermal lymphatic channels were significantly larger in *BmL3* infected mice compared to sham-infected controls at 14 days pi, (Figure 2.3A&B; Sham: 43.3±3.7 μm vs *BmL3*: 96.8±4.9μm, P<0.001). Further, epifluorescent visualisation of Prox1-GFP⁺ dermal lymphatic channels consistently demonstrated the presence of tortuous collateral lymphatics in *BmL3* infected mice, which were absent in sham infected counterparts (Figure 2.3E)

2.3.2- *BmL3* migrate into pre-collector lymphatic channels, proximal to areas of lymphatic remodelling, as early as 3 hours following inoculation

To investigate the time-course of *BmL3* migration, confirm presence of *BmL3* in the lymphatic channels and in which lymphatic areas they reside, *BmL3* were protein labelled with AlexaFluor546 amine-reactive dye and inoculated into the left hind-limb of CB57/6J Prox-1^{GFP} mice and their locations tracked 3 hour and 24 hours after infection, using epifluorescence microscopy (Schematic shown in figure 2.4A).

Highly motile *BmL3* were observed inside host lymphatic pre-collector and collector channels as early as 3 hours pi. and resided in areas proximal to confirmed zones of common lymphatic remodelling as imaged by PDE NIR optical imaging of ICG lymphatic drainage (Figure 2.4B&C). The highest number of intra-lymphatic larvae were observed 24 hours pi, with numbers dropping following this time point (Laboratory observation, data not shown). Motile worms were observed as late as 6 days following infection, although numbers of observed intra-lymphatic larvae declined rapidly following 48 hours. The numbers of motile larvae visualised at both injection sites, with localisation outside of lymphatic vessels, were highest 3 hours pi. ,decreasing in number up to 48 hours pi. No larvae could be visualised 4dpi or 6dpi at injection sites (Laboratory observation, data not shown).

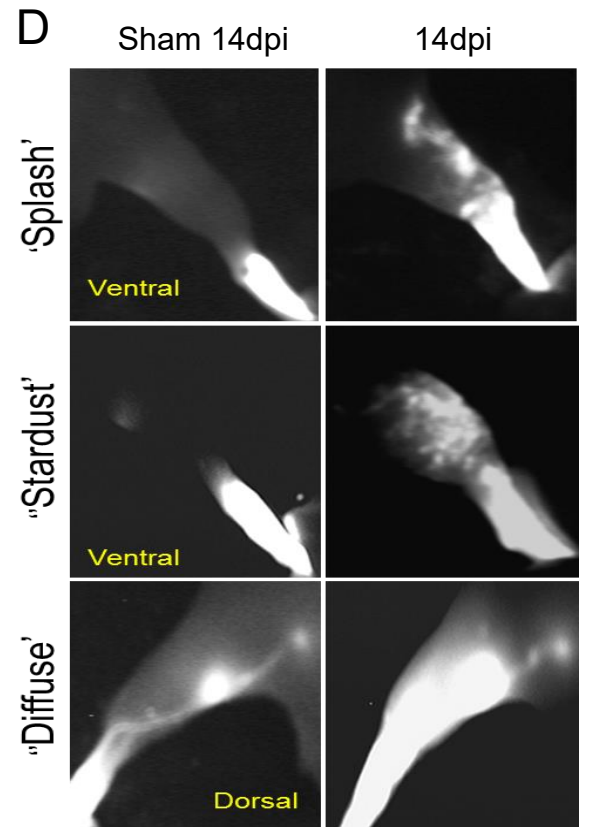
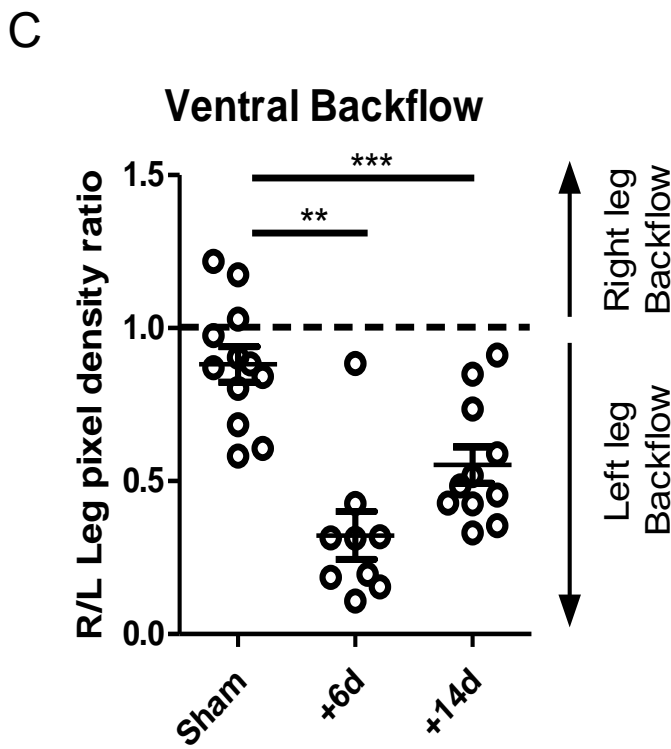
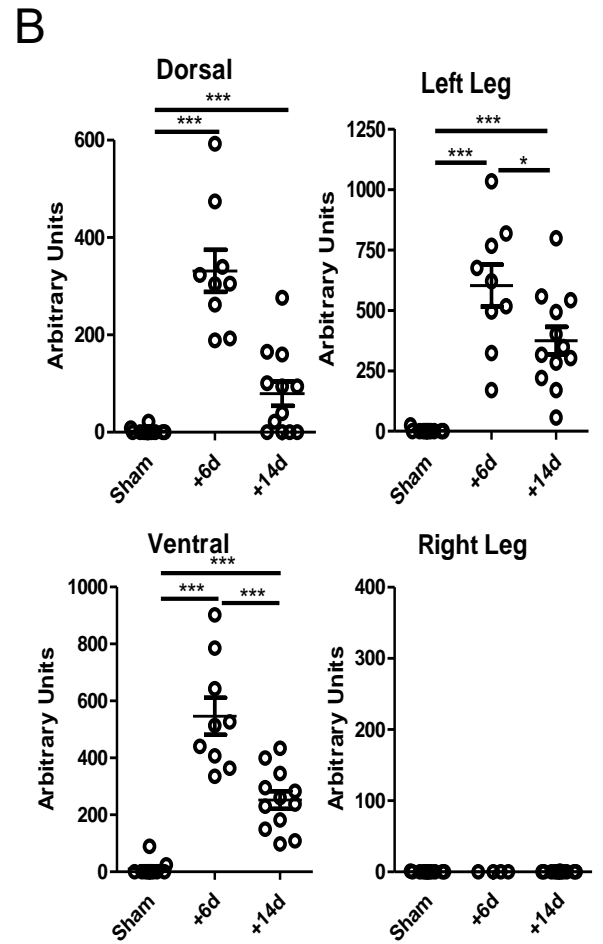
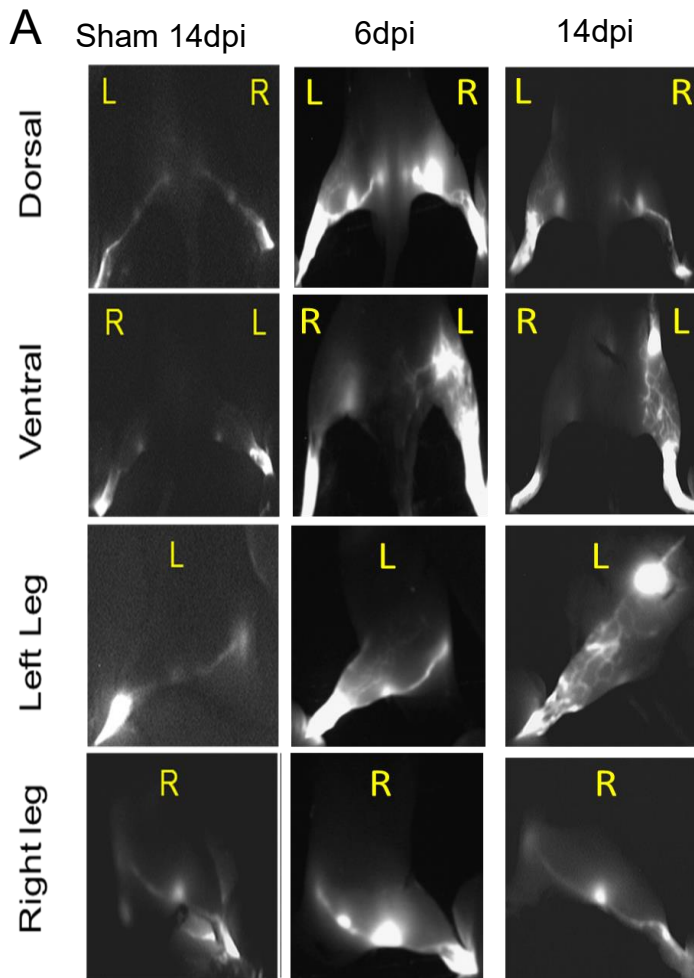
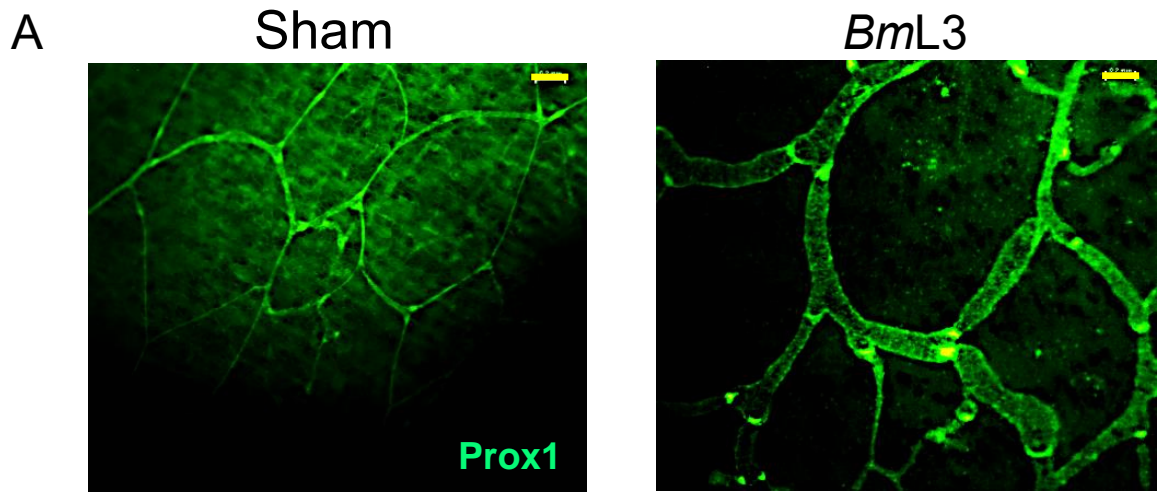
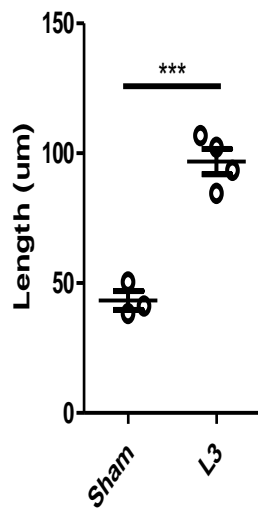


Figure 2.2: lymphatic remodelling and insufficiency are significantly increased following *B. malayi* infection

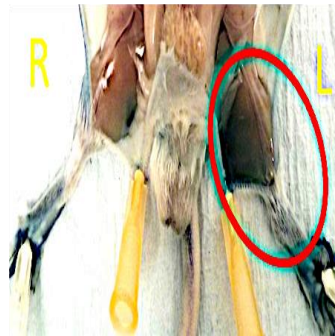
A) Representative images taken from PDE imaging and analysed for aberrant lymphatics and lymphatic insufficiency **B)** Quantification of aberrant lymphatics in dorsal, ventral, left leg and right leg or **C)** ventral backflow at indicated time-points post-infection with 100 *BmiL3* compared to sham infection controls **D)** Representative examples of all three observed qualitative grade pathologies, defined in previous ICG studies as measures of lymphatic insufficiency Data plotted is the number of ICG positive pixel arbitrary units within aberrant lymphatic channels (B) or the ratio of ICG positive pixel arbitrary units between right and left limbs in a ROI above the injection site and below the pLN per mouse (C). Horizontal bars indicate mean \pm SEM per group. Data was pooled from either two or three individual experiments. Significance is indicated *=P<0.05, **=P<0.01, ***=P<0.001, One Way ANOVA with Tukey's multiple comparisons tests.



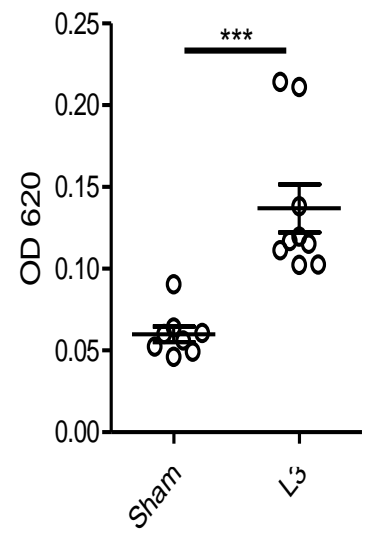
B Average Lymphatic Width



C



D Limb Backflow



E

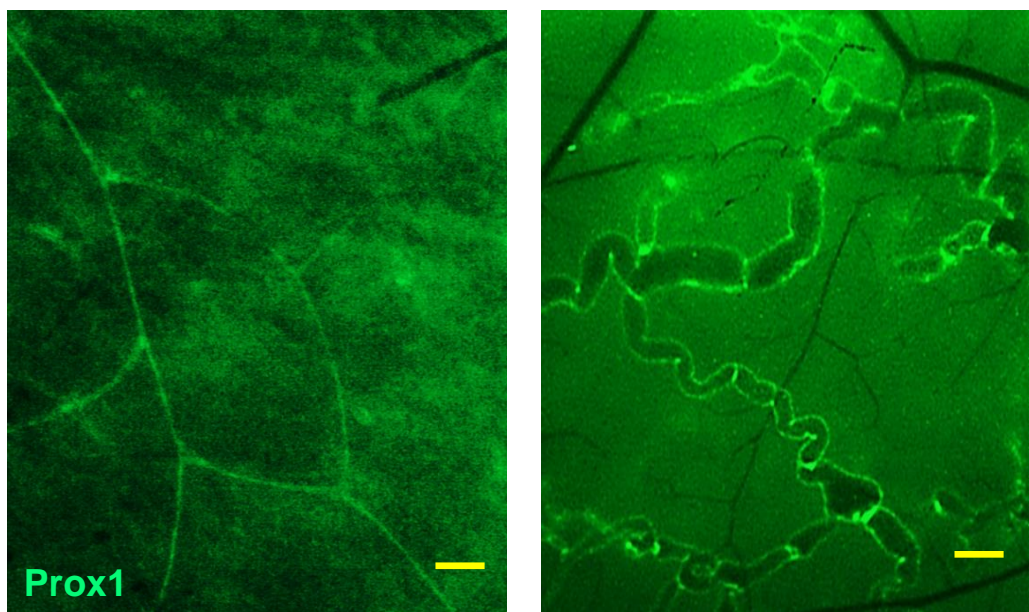


Figure 2.3: Lymphatic insufficiency and dilation are significantly increased, while evidence of tortuous collateral lymphatics are manifest 14d post-infection compared to sham control

A) Representative images of Prox-1 GFP epifluorescence in zones of dermis corresponding with ICG remodelling at 14 dpi with 100 *BmL3* or corresponding zones in sham infected animals. **B)** Lymphatic aperture measurements of Prox-1 GFP epifluorescence in zones of dermis corresponding with ICG remodelling at 14 dpi with 100 *BmL3* or corresponding zones in sham-infected animals. **C)** Representative image of limb lymphatic backflow in an infected and uninfected limb, 14 dpi with 100 *BmL3*, visualised by modified Mile's Assay where 10µl of Evan's Blue was injected subcutaneously into the left hindlimb of experimental mice, followed by a timed drainage period of 20 minutes. Subsequent necropsy to excise the left hind-limb skin from ankle to below knee joint was then undertaken. **D)** Quantification of Evan's Blue dermal backflow in excised lower hind-limb skin, 14 days post-infection with 100 *BmL3*, versus sham infection controls. Data is optical density at 620nm following extraction of dye in PBS per mouse. **E)** Representative example of tortuous collateral lymphatics as observed in *BmL3* infected mice utilising epifluorescence microscopy 14dpi. Scale bars (yellow bars) represent 200µm. Horizontal bars represent mean ±SEM where data is pooled from 2 individual experiments (D) or derived from a single experiment (B). Significance is indicated ***P<0.001, determined by student two tailed t-test

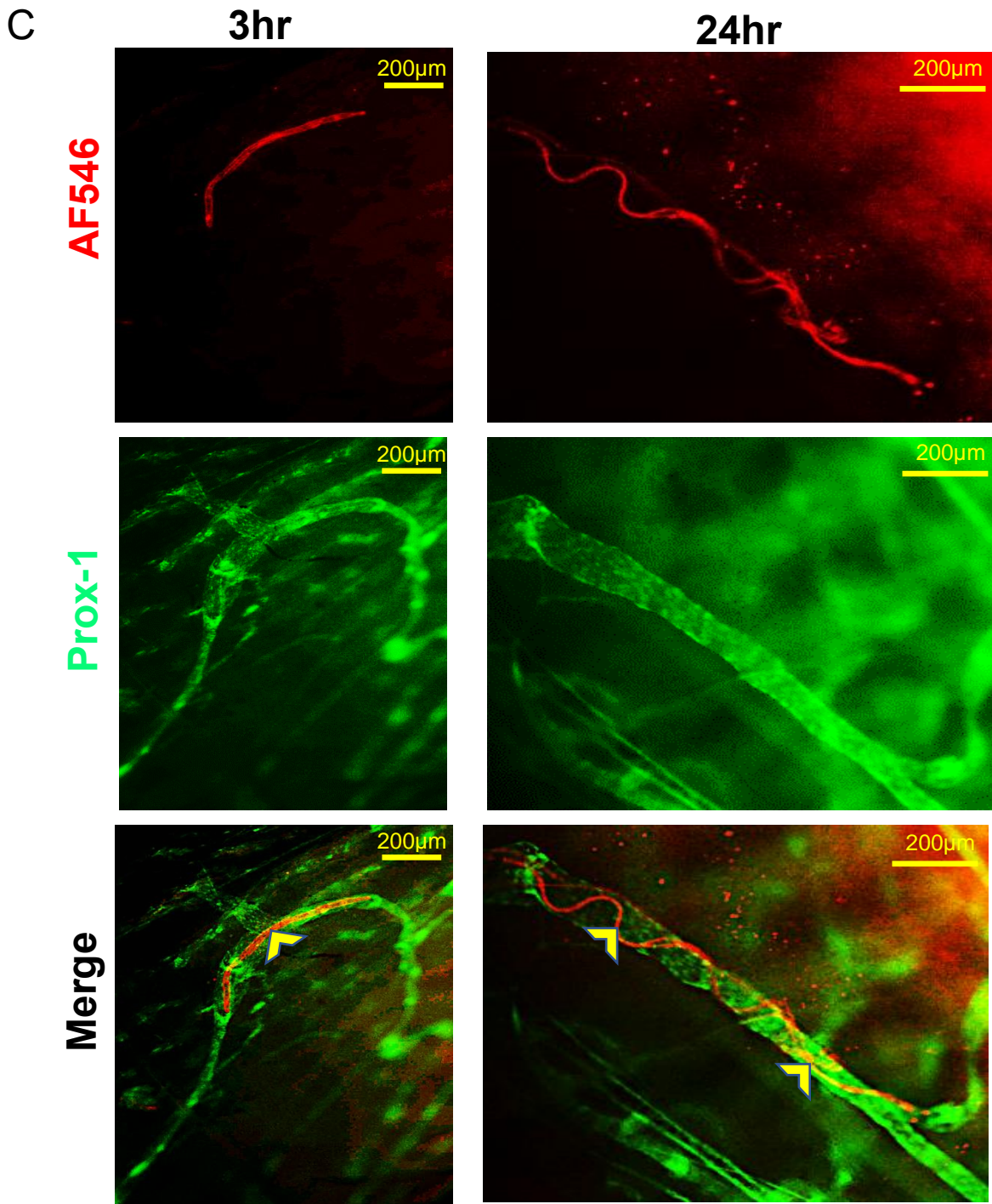
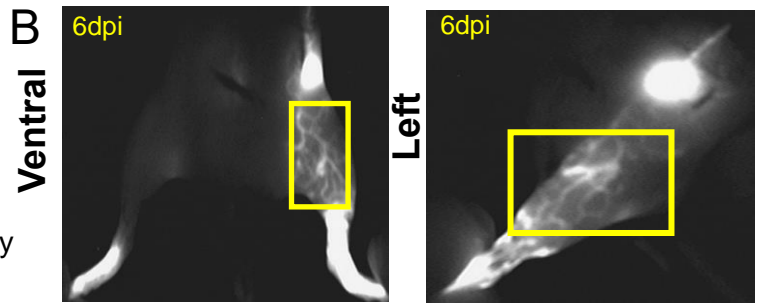
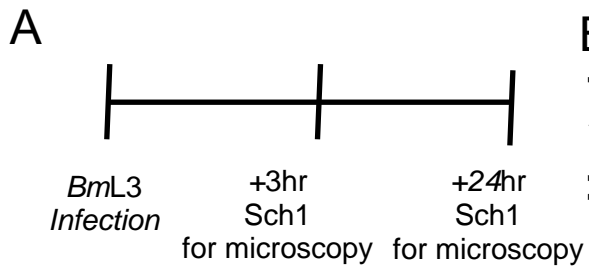


Figure 2.4: *BmL3* migrate to lymphatic pre-collector channels proximal to areas of subsequent lymphatic remodelling 3-24 hours post infectionError! Bookmark not defined.

A) Schematic of experiment timeline. **B)** NIR intravital imaging of ICG lymphatic drainage with yellow boxes demonstrating areas examined for *BmL3* infection. **C)** Prox-1 GFP lymphatic channels and AF546 stained epifluorescence. Representative images of *BmL3* located inside lymphatic pre-collector channels (arrows indicate *BmL3* location).

2.3.3- Challenge filarial infection significantly increases lymphatic remodelling and lymphatic insufficiency compared to single infection.

Following characterisation that lymphatic remodelling occurred as soon as 6 days post-filarial infection, the impact of re-infection was evaluated. Following an initial infection (as described above), a further inoculation of *BmL3* larvae was administered after a 2-week interval. PDE imaging was undertaken two weeks later (Schematic shown in figure 2.5A).

Challenge infections (*BmL3x2*) significantly increased the extent of lymphatic remodelling, defined by increased incidence of aberrant lymphatics, in dorsal (*BmL3*: 79.3±25.2 A.U vs *BmL3x2*: 435.9±68 A.U P<0.001, left (*BmL3*: 374.5±57.7 A.U vs *BmL3x2*: 790.1±82.1 A.U P<0.001) and ventral (*BmL3*: 252±31.0 A.U vs *BmL3x2*: 758.5±157.7 A.U P<0.001) viewpoints compared with single infection alone (Figure 2.5B&C). Left Leg / Right leg ROI ICG fluorescence, measured by PDE NIR imaging, between a single and challenge infection was not significantly different, although both single and double infections mediated a significant biased accumulation of ICG in the infected limb compared to sham infected controls (Figure 2.5D; *BmL3*: 0.55±0.06 and *BmL3x2* 0.45±0.04 R/L ratio vs sham: 0.88±0.06, P<0.001 and P<0.0001, respectively.)

2.3.4- Aberrant lymphatics and lymphatic insufficiency persist 12 weeks following infection with *B. malayi* L3.

To investigate whether the acute lymphatic remodelling and lymphatic insufficiency phenotype post-*BmL3* infection was a transient and resolving event or led to long-lasting alterations, infected and sham infected mice were allowed to reach 12 week pi before subsequent PDE imaging (Schematic shown in figure 2.6A). In susceptible animal models, including immunodeficient mice and Mongolian gerbils, adult *B. malayi* develop to patent adult infections before 12 weeks. Mice that had been inoculated with *BmL3* were checked for infection status through blood thick smears and all mice were confirmed as microfilariae (mf) negative (6 mice) at 12wpi. Further careful examination of hind-limb lymphatics confirmed an absence of active intra-lymphatic infection at 12 wpi (laboratory observations, data not shown).

Despite the infection negative status at 12 wpi (laboratory observation following thick blood smears of cardiac punctures from appropriate mice), mice that had been inoculated with *BmL3* displayed significantly higher aberrant lymphatics compared to sham counterparts in dorsal (Figure 2.6B&C; 12 weeks: 190.6 ± 81.8 A.U vs sham: 0.2 ± 0.2 A.U $P < 0.05$) ventral (12 weeks: 830.5 ± 162.6 A.U vs sham: 0.2 ± 0.2 A.U $P < 0.0001$) and left viewpoints (12 weeks: 682.5 ± 165.4 A.U vs sham: 0.2 ± 0.2 A.U $P < 0.001$). Further, there were no significant differences in dorsal, ventral or left viewpoints between mouse groups who had received prior inoculations either at 2 or 12 weeks (Figure 2.6B&C). In addition, left leg fluorescence/right leg fluorescence (R/L leg ratio) was significantly lower in the 12 week pi mouse group compared to sham controls and no significant differences in R/L leg ratio were apparent in 2 week versus 12 week pi mouse groups (Figure 2.6D; 12 week: 0.4 ± 0.05 R/L ratio vs Sham: 0.9 ± 0.06 , $P < 0.0001$).

2.3.5- *BmL3* infection is associated with a significant lymphadenopathy and increased cellularity of local draining lymph nodes.

Fourteen days post-infection with 100 *BmiL3* or sham inoculates, skin draining lymph nodes (sdLN) of the infected left leg (pLN, iLN, and siLN) were excised and total sdLN area determined utilising Prox-1GFP epifluorescence as a guide. A pooled, single cell suspension of sdLN per mouse was then prepared and quantified by cell counting.

At 14 dpi the areas of the pLN, iLN, and siLN proximal to the inoculation site were significantly increased compared to sham infection controls (Figure 2.7A&B; pLN : *BmL3* 2.9 ± 0.15 mm² vs Sham 0.9 ± 0.15 mm² $P < 0.01$, iLN: *BmL3* 7.5 ± 0.89 mm² vs Sham 2.0 ± 0.09 mm² $P < 0.01$, siLN: 3.5 ± 0.4 mm² vs sham: 0.69 ± 0.08 mm² $P < 0.0001$). Furthermore, cellularity of the pooled sdLN were significantly increase in infected mice, compared to sham controls (Figure 2.7C; *BmL3*: $1.9 \times 10^7 \pm 5.0 \times 10^6$ vs $6.1 \times 10^6 \pm 2.4 \times 10^5$ cells, $P < 0.05$).

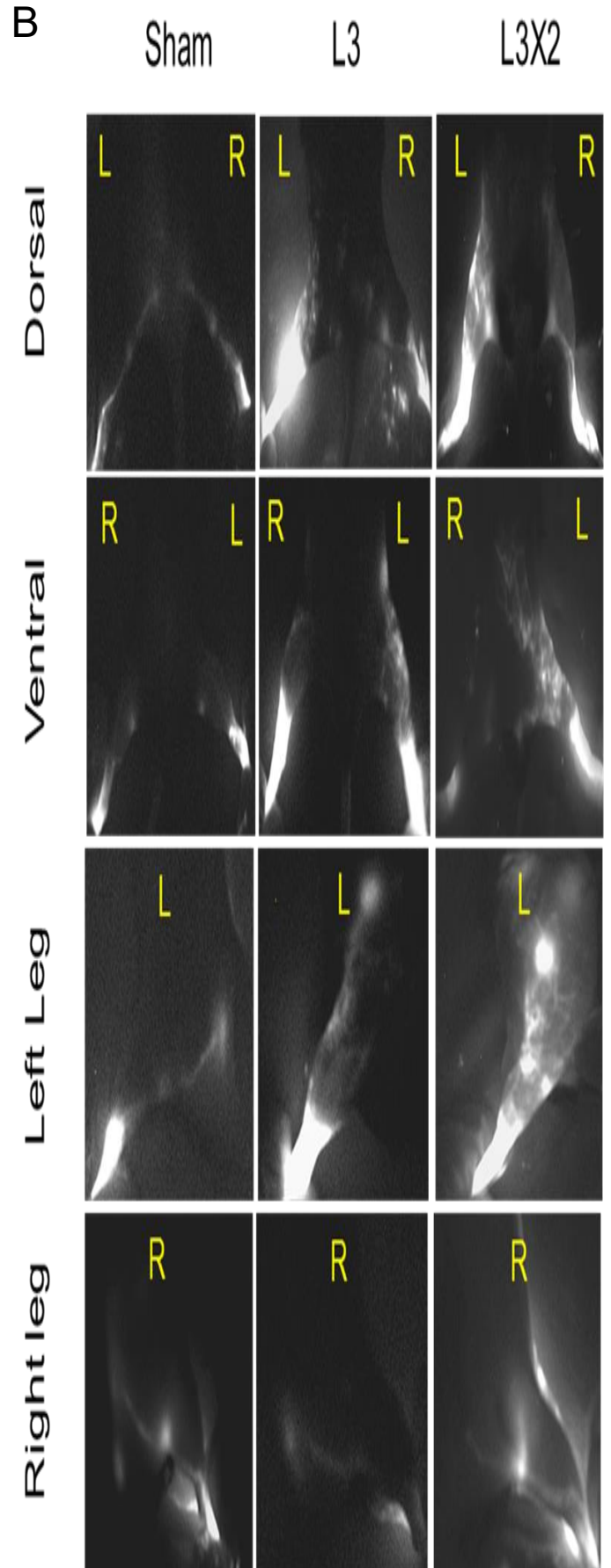
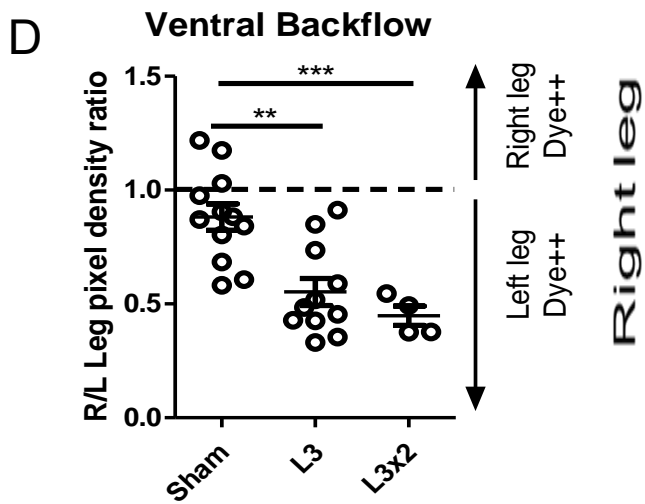
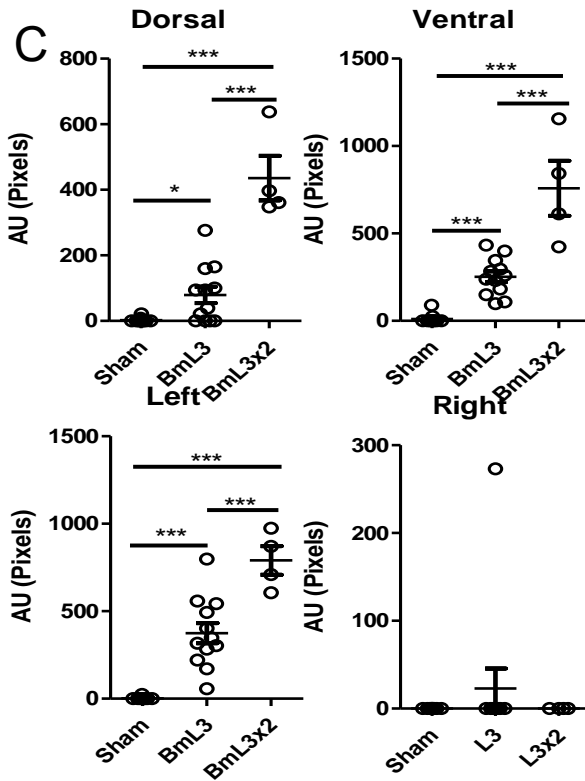
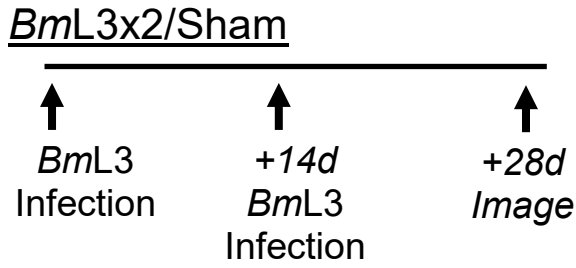
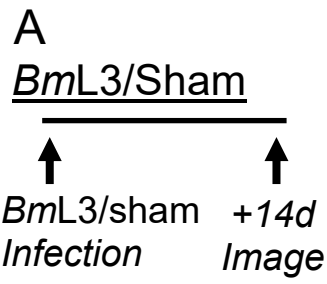


Figure 2.5: Challenge filarial infection significantly increases lymphatic remodelling and insufficiency

A) Schematic of experimental time-line. Sham infections followed *BmL3* timeline. **B)** Representative images from PDE analysis. **C)** Quantification of aberrant lymphatics in dorsal, ventral, left leg and right leg or, **D)** dermal backflow from primary (*BmL3*) vs challenge infection (*BmL3x2*) compared to sham infection controls. Data plotted is the total ICG positive pixel arbitrary units defining aberrant lymphatic channels (C) or the ratio of ICG positive pixel arbitrary units between right and left limbs in a ROI above the injection site and below the pLN per mouse (D). Horizontal bars indicate mean \pm SEM per group. Data was pooled from either three individual experiments (primary infection and sham data reused from figure 2.2B-C) or a single experiment (challenge). Significance is indicated *=P<0.05, **=P<0.01, ***=P<0.001 derived from 1 Way ANOVA with Tukey's multiple comparisons tests.

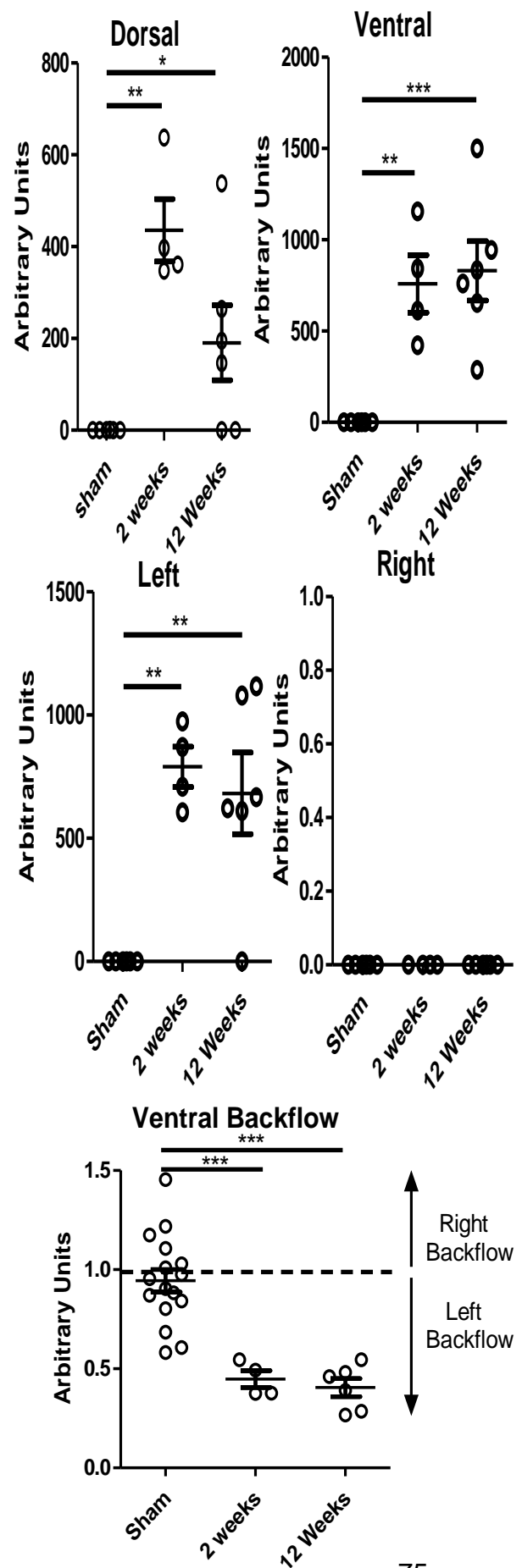
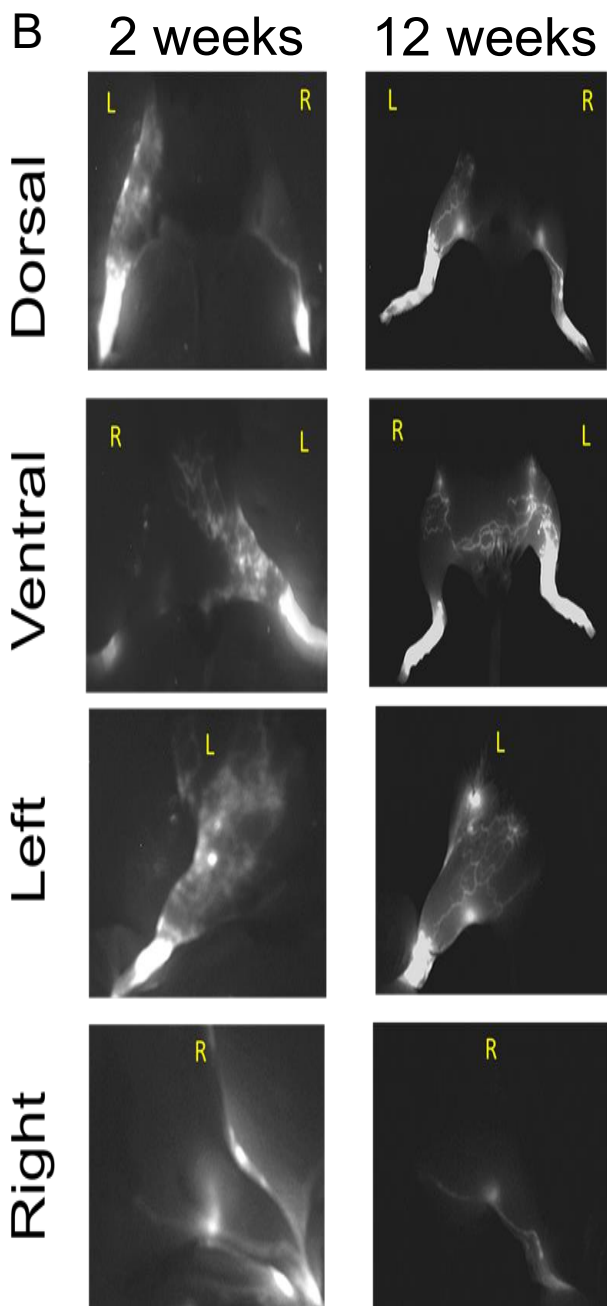
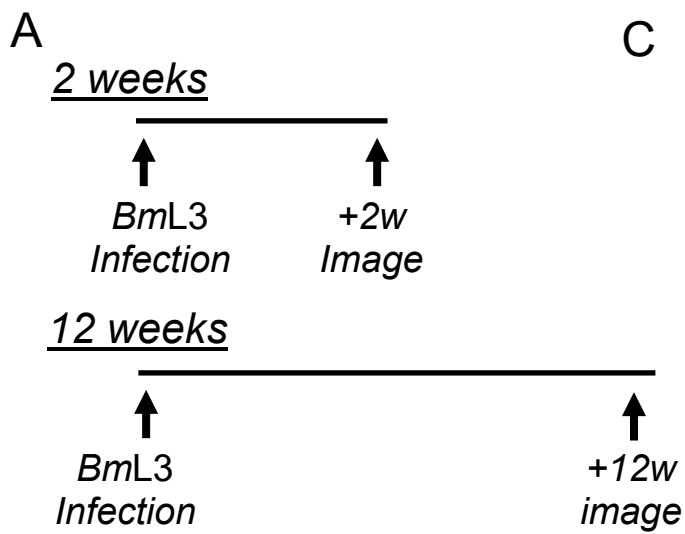


Figure 2.6: Lymphatic remodelling and insufficiency persist 12 weeks following infection with *BmL3*.

A) Schematic of experimental time line. **B)** Representative PDE images PDE analysis. **C)** Quantification of aberrant lymphatics in dorsal, ventral, left leg and right leg or, **D)** dermal backflow from 2 weeks vs 12 weeks compared to sham infection controls. Data was pooled from 2 (2+12 weeks) or 3 (sham) individual experiments. Horizontal bars represent mean \pm SEM. Significance is indicated as *= $P < 0.05$, **= $P < 0.01$, ***= $P < 0.001$ derived from One Way ANOVA with Tukey's multiple comparisons tests.

2.3.6- C57BL/6J mice demonstrate significantly elevated severities of lymphatic remodelling and insufficiency versus BALB/c mice following filarial infection

Potential host strain variation in filarial-associated lymphatic remodelling and insufficiency was explored by comparing pathologies 14 dpi between commercially-supplied BALB/c and C57BL/6J mouse cohorts.

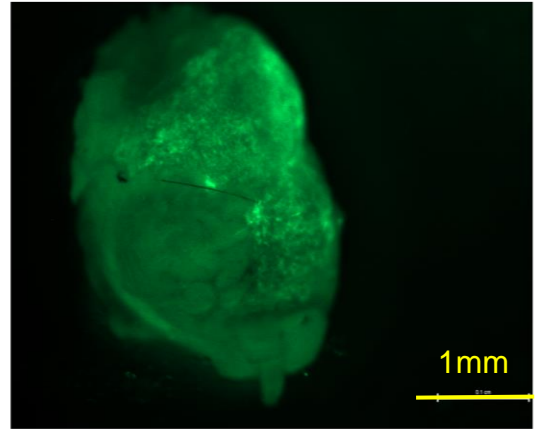
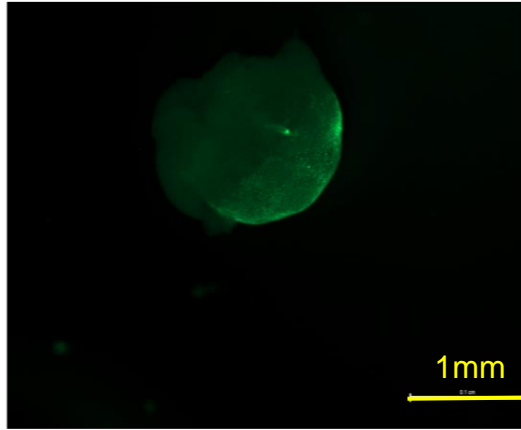
C57BL/6J *BmL3* infected mice were found to display significantly higher levels of aberrant lymphatics in dorsal (BALB/c *BmL3*: 27.9 ± 16.3 A.U vs C57BL/6J *BmL3*: 284.0 ± 72.3 A.U $P < 0.001$), ventral (BALB/c *BmL3*: 231.6 ± 33.0 A.U vs C57BL/6J *BmL3*: 611.6 ± 101.6 A.U $P < 0.001$) and left leg (BALB/c *BmL3*: 150.8 ± 44.4 A.U vs C57BL/6J *BmL3*: 656.7 ± 109.8 A.U $P < 0.001$) viewpoints of PDE imaging, when compared to BALB/c infected mice (Figure 2.8A&B). Both C57BL/6J and BALB/c *BmL3* infected mice demonstrated a significant change in the ratio of R/L leg ICG accumulation (Figure 2.8C; BALB/c Sham: 1.080 ± 0.08 R/L ratio vs BALB/c *BmL3*: 0.44 ± 0.09 , $P < 0.001$, CB57/6J Sham: 0.99 ± 0.03 R/L ratio vs CB57/6J *BmL3*: 0.57 ± 0.09 , $P < 0.001$), however C57/6J *BmL3* infected mice retained significantly higher levels of Evan's Blue in the dermis of infected limbs compared to BALB/c infected mice (Figure 2.8D; BALB/c *BmL3*: 0.11 ± 0.01 OD_{620} vs CB57/6J *BmL3*: 0.17 ± 0.03 , $P < 0.05$)

A

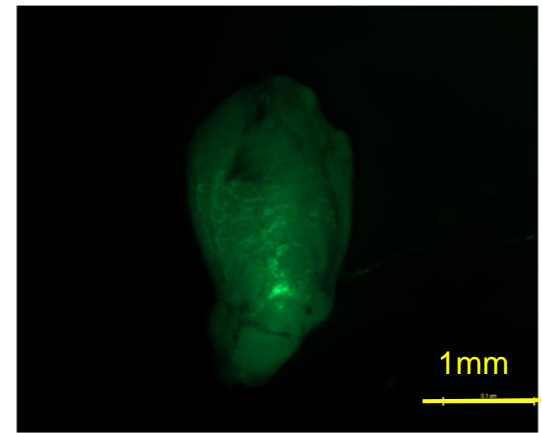
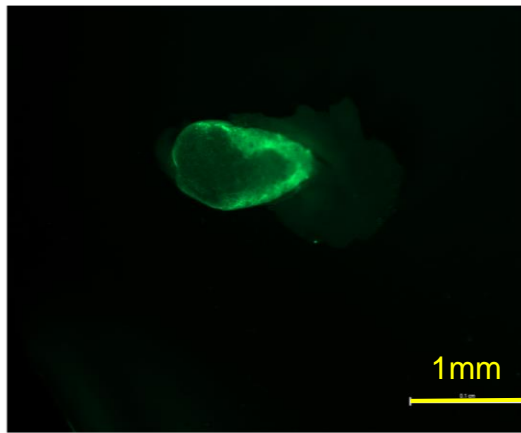
Sham

L3

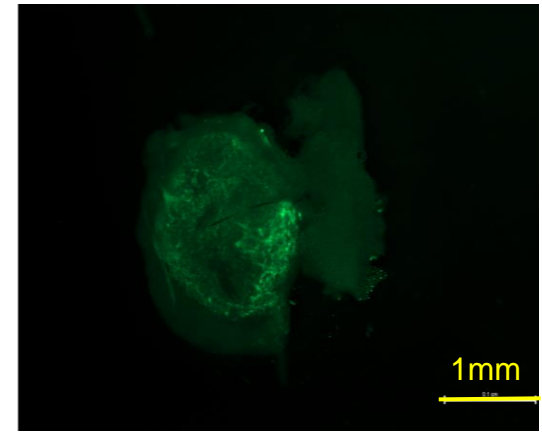
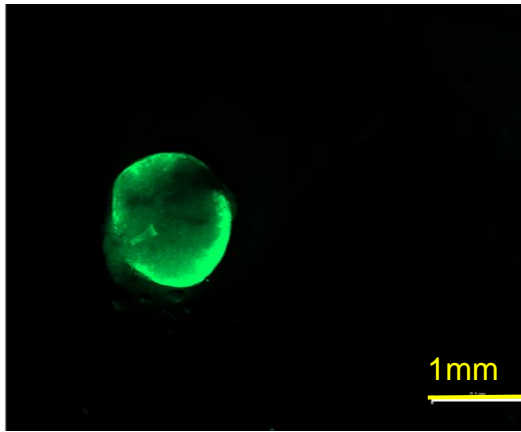
Iliac



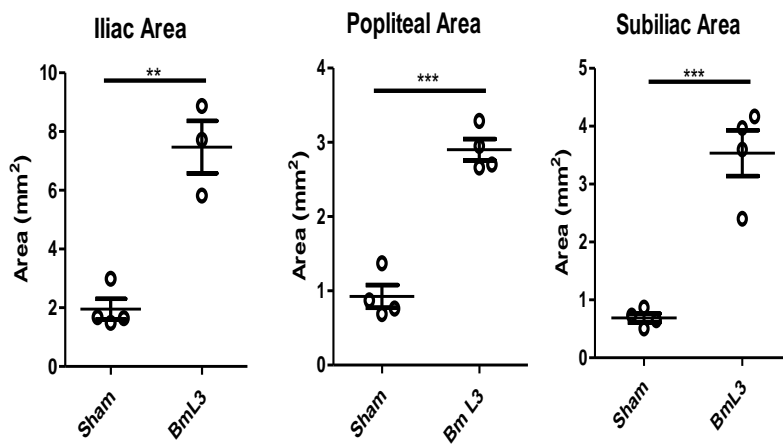
Sub-Iliac



Popliteal



B



C

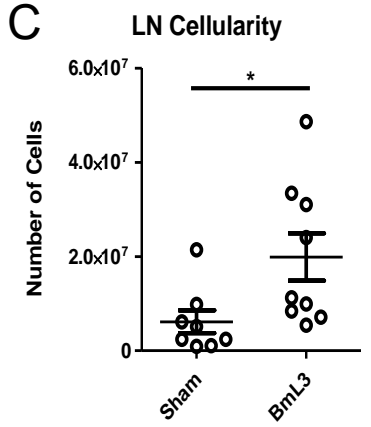
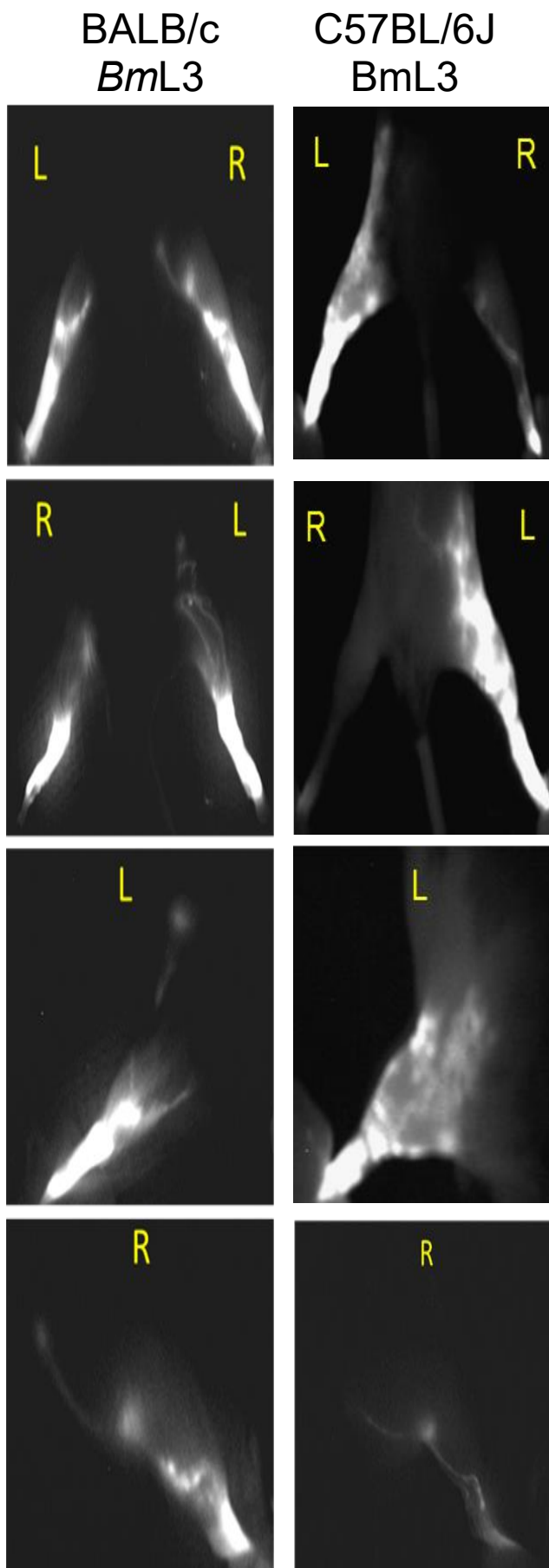


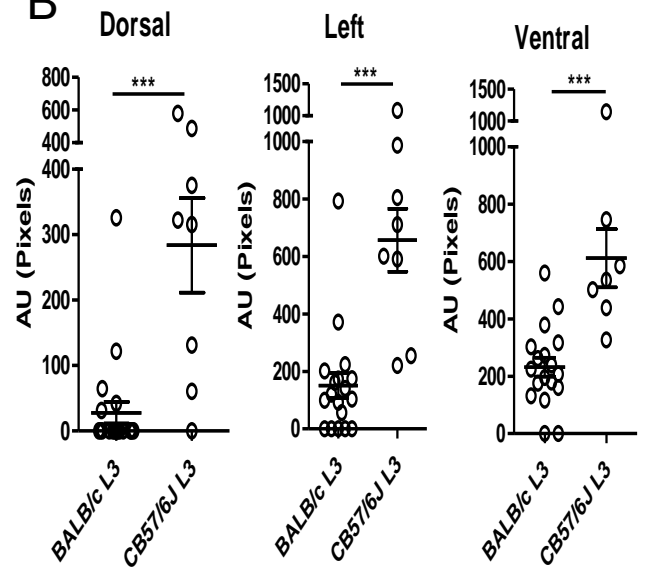
Figure 2.7: *BmL3* infection results in lymphadenopathy and significant increases in sdLN cellularity

A) Representative Prox-1^{GFP} images of sdLNs (pLN, iLN, siLN) between infected and *BmL3* infected counterparts. **B)** Area measurements of sham vs *BmL3* pLN, iLN and siLN (n=3 per group) **C)** Cellularity measurements of pooled sdLNs (n=8-9 per group). Data is from a single experiment (A+B) or 3 individual experiments (C) Horizontal bars represent the mean \pm SEM with significance indicated as *= $P < 0.05$, **= $P < 0.01$ ***= $P < 0.001$ derived from student's two tailed t-test.

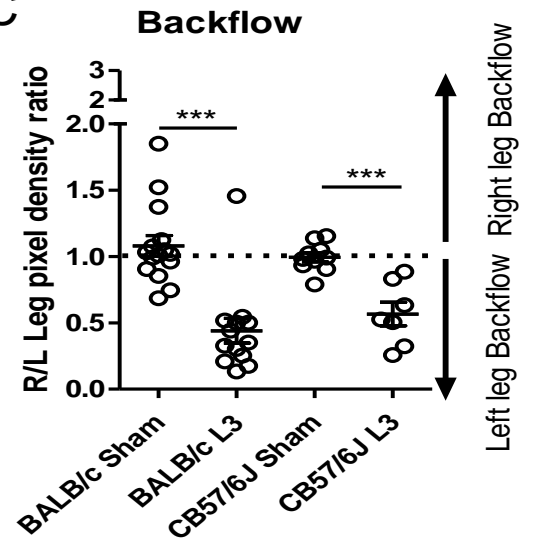
A



B



C



D

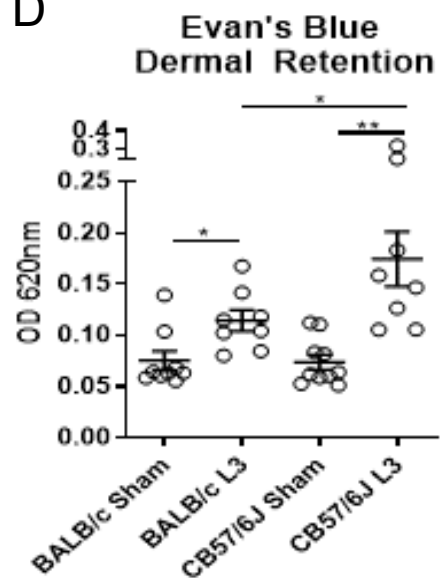


Figure 2.8: C57BL/6J mice are predisposed to more extensive lymphatic remodelling and insufficiency compared with BALB/c mice following *B. malayi* infection.

A) Representative images of mouse groups from PDE imaging **B)** quantification of aberrant lymphatics in dorsal, ventral and left leg viewpoints or **C)** dermal backflow from 14 days post-infection comparing *BmL3*. infected BALB/C vs C57BL/6J groups **D)** Quantification of Evan's Blue dermal backflow in excised lower hind-limb skin. Horizontal bars represent the mean \pm SEM, data shown is pooled from 3 independent experiments. Significance is indicated as *= $P < 0.05$ **= $P < 0.01$ ***= $P < 0.001$ derived from one-way ANOVA with Tukey's multiple comparisons post-hoc test.

2.4- Discussion

Lymphatic remodelling, encompassing lymphatic vessel dilation, lymphatic neovascularisation, lymphadenitis and the presence of tortuous collateral lymphatics, is a key hallmark observed in patients suffering from filarial infection (Figueredo-Silva *et al.*, 2002; Baluk *et al.*, 2005; Shenoy, 2008; Nutman, 2013). The pervasive theory in the field hypothesises that changes to the lymphatic architecture are a result of progressive damage to existing lymphatics, as a consequence chronic inhabitation of live fecund adult filarial worms (Nutman, 2013). Dreyer and colleagues speculate that these lymphatic remodelling events also require death events of pre-established adult infections, either natural or drug-induced, that cause bolus release of toxic and antigenic material and consequent immune responses to drive pathological manifestations observed in LF (Dreyer *et al.*, 2000). Currently, it is impossible to accurately delineate the relative impact of each of the different filarial life cycle stages on the ensuing lymphatic remodelling and pathologies evident in naturally infected human populations. The introduction described an inadequacy of current animal models to interrogate the temporal induction of lymphatic remodelling, the role of remodelling in lymphatic dysfunction, and immune-dependent mechanisms that potentially drive remodelling processes

The first objective of the thesis was to assess the initial impact of filarial larval invasion on lymphatic remodelling and possible pathology in a novel, immunocompetent murine model of infection. The data collected indicates that significant alterations to the lymphatic architecture are manifest as early as 6 days following infection. Homeostatic hind-limb lymphatic drainage consistently shows linear, single channel flow from the foot injection site, firstly to the popliteal lymph node followed by subsequent flow via another single efferent collector channel to the iliac lymph node (Example shown in sham infection representative image in figure 2.2A). The linear patterns of 'normal lymphatic flow' observed are replicated in human studies, reporting similar 'linear flow patterns' in 'normal' subjects imaged using similar methods of NIR intravital imaging (Yamamoto *et al.*, 2011; Narushima *et al.*, 2015). In contrast, filarial infection resulted in overt changes with many

“micro-channels” becoming visible at 6 and 14 days pi (Figure 2.2A). These channels create areas of “webbing” across the dorsal and ventral hind limb that did not appear to connect to existing draining lymph nodes. Devised quantification methods of intravital imaging enabled thorough characterisation of infection-associated lymphatic remodelling. This quantification showed significant increases in aberrant lymphatics compared to sham controls at both 6 days and 14 days. Aberrant lymphatics were observed in 100% of mice infected at this early time point. The pattern of aberrant lymphatics (Figure 2.2A, 2.3A) are similar to ‘tortuous collateral lymphatics’ observed in LF patients (Case *et al.*, 1991, 1992; Freedman *et al.*, 1994; Shenoy, 2008). Further, lymphatic patterns visualised in the C57BL/6J mouse model of filarial infection displayed resemblance to those reported in non-LF LE patients, utilising the same imaging techniques of ICG lymphangiography (Mihara *et al.*, 2012). The common ‘lymphatic backflow patterning’s’ putatively named ‘splash’ and ‘starburst’, both of which positively correlated with grades of lymphatic insufficiency, were consistently observed in the filarial mouse model (Yamamoto *et al.*, 2011; Narushima *et al.*, 2015). This would suggest that the lymphatic remodelling observed are pathological in nature, contributing to lymphatic insufficiency rather than suggested ‘compensatory’ therapeutic remodelling hypothesised to ‘repair’ lymphatic insufficiency in models of surgically-induced LE (Haiko *et al.*, 2008; Alitalo, 2011; Lähteenvuo *et al.*, 2011). The apparent lack of connection of these novel lymphatics to any existing draining lymphatics would suggest that rather than diverted lymphatic drainage into pre-existing proximal lymphatic channels, caused by an infection-mediated occlusion of normal lymphatic flow, the aberrant lymphatic channels are potentially novel neovascularisation events stimulated by the invasion of *BmL3* into the lymphatic architecture. No significant increases in aberrant lymphatics were observed in the control right hind-limb in infected mice, nor in sham counterparts (Figure 2.2B) signifying that filarial infection induces very focal changes to the lymphatic architecture and associated lymphatic function, localised to sites of initial parasitism. Significantly higher levels of aberrant lymphatics were observed at the earlier 6-day time point, compared to mouse cohorts imaged at 14 days pi (Figure 2.2B). While, initially, this would

suggest a pattern of resolution of lymphatic remodelling, further investigation of imaging (Figure 2A) would suggest a higher degree of dilation of lymphatic channels at the 14 day time point. This results in a larger spread of ICG fluorescence which masks adjacent lymphatic channels, resulting in a falsely low level of aberrant lymphatics being reported, particularly in lower parts of the hind limb. Potentially, this masking reveals a sensitivity issue of the PDE imager, where the higher fluorescence overtakes the resolution limit, thus yielding artificially lower levels of aberrant lymphatics at 14 days, compared to 6. Regardless, the observations of sustained remodelling in long-term infection experiments indicates a failure to resolve aberrant lymphatic formation or insufficiency post-14 days.

The use of the Prox-1GFP reporter mouse on the C57BL/6J background strain provided a useful tool to visualise, via epifluorescence, the lymphatic micro-architecture, as Prox-1 is a common transcription factor exclusive to the lymphatic endothelial cell lineage (Partanen and Paavonen, 2001; da Cunha Castro and Galambos, 2009). Visualisation of the common areas in which these aberrant lymphatic channels allowed clear visualisation of the aberrant lymphatics channels which were consistently observed to be pre-collector lymphatic vessels, sometimes termed “lymphangions”, adjoined by lymphatic valves, located in the subcutaneous tissues (laboratory observation, representative examples shown in figure 2.3A&E). In contrast, fewer abnormalities were observed either in the blind-ended dermal lymphatic capillary beds prior to the pre-collecting ducts, or the larger collector vessels to which the pre-collector vessels supply (laboratory observation, data not shown). These aberrant channels were highly abnormal and bore similarity to described ‘tortuous collateral lymphatic channels’ in histological studies of patients suffering from filarial LE. The aberrant channels consistently displayed areas of gross dilation, followed by areas of irregular constriction, and is in stark contrast to the uniform, linear channels observed in uninfected mice (shown in figure 2.3E). Additionally, quantifying the aperture of channels in areas of most pronounced ICG lymphatic remodelling confirmed a ~2-fold average dilation of the subcutaneous lymphatics in areas proximal to the initial filarial infection.

With evidence suggesting early onset lymphatic remodelling, it was important to investigate if remodelling was significantly associated with physical inhabitation of *BmL3* in the affected local lymphatic architecture. Utilisation of the Prox-1GFP reporter mouse on the C57BL/6J to visualise lymphatic channels and the staining of live *BmL3* before inoculation allowed the tracking of migrating larvae from the initial infection site shortly after inoculation. These experiments demonstrated *BmL3* rapidly migrate from subcutaneous dermal tissues into lymphatic channels as early as 3-hours pi (figure 2.4C). Previous findings from *Brugia pahangi* infections in gerbils demonstrate rapid migration from skin tissue injection sites into lymphatic vessels, but more commonly to the popliteal or sub-iliac lymph nodes themselves (Ah and Thompson, 1973; Chirgwin *et al.*, 2006), around 3 days post infection. Further, both studies demonstrate migration away from initial injection site as little as 3 hours post infection (Chirgwin *et al.*, 2006). The data described is generally in concordance with these studies, although faster migration of larvae, more commonly to lymphatic vessels proximal to sdLN's (as little as 3 hours) rather than sdLNs themselves were observed. *BmL3* proximal to sdLNs were consistently found to inhabit lymphatic channels proximal to areas of observed lymphatic remodelling, inferring remodelling is rapidly initiated upon invasion of *BmL3* into lymphatic channels. Furthermore, microscopy revealed evidence of remodelling in uninhabited lymphatic architecture, proximal to *BmL3* resident lymphatic channels.

The rapid onset of all three aforementioned 'hallmarks' of lymphatic remodelling, as little as 6 days pi, while corroborating the hypothesis that remodelling, notably lymphangiectasia, is a consequence of filarial inhabitation of lymphatic vessels, contradicts the pervading theory that inhabitation and resultant damage occurs over a longer time period (Jungmann, Figueredo-Silva and Dreyer, 1991; Noroes *et al.*, 1996; Dreyer *et al.*, 2000). Whilst no overt rupturing, or obvious damage to the lymphatic architecture, in areas of lymphatic remodelling were observable, it is possible that the initial L3 invasion into and subsequent migration within pre-collectors may induce lymphatic tissue damage. Parasite-mediated damage could

trigger a disproportionate 'runaway' wound healing response leading to remodelling. Further, or in addition, lymphatic remodelling could be induced directly by filarial signals, such as excretory/secretory proteins with lymphangiogenic potential, as has been previously reported (Shenoy *et al.*, 2008; Weinkopff *et al.*, 2014). Finally, the host anti-filarial immune response could trigger inflammatory-associated lymphangiogenesis (IAL) that is a well-known 'hallmark' documented in a range of inflammatory conditions including infection (Flister *et al.*, 2010; Abouelkheir, Upchurch and Rutkowski, 2017).

The data together would suggest that remodelled lymphatics, in contrast to being a consequence of long term damage due to adult inhabitation, is a very early "seeding event", actively initiated either by larvae themselves or host immune responses, on a 'timeline' to pathology. A pertinent question to investigate would therefore be what are the divergent events following the ubiquitous initial lymphatic remodelling and early pathology, between hosts that later develop pathology and more asymptomatic groups that appear to tolerate active infections without overt LE. (Freedman *et al.*, 1994, 1995; Kar *et al.*, 2017)

A key objective upon observation of rapid and significant lymphatic remodelling, post filarial infection, was to investigate the consequences of such overt remodelling and whether it may contribute to lymphatic dysfunction. Overt LE is the major pathology associated with LF, while LE itself is often one of the final stages of a varied group of sub-pathologies (Pani and Srividya, 1995; Nutman, 2013). LE is clinically described as the extravasation of lymphatic fluid into the interstitial spaces surrounding lymphatic vessels (Grada and Phillips, 2017). The accumulating factors leading to this end stage can be complex, but it is generally agreed a disruption of normal lymph flow and resultant perturbation of homeostatic lymphatic flow- leads to aberrant accumulation of lymph in lymphatic channels (lymphostasis) (Brouillard, Boon and Vikkula, 2014; Carlson, 2014). One of the largest contributing factors to lymphostasis is lymphatic vessel dysfunction. Dysfunction can occur due to: damage to the lymphatic vessel valves that direct lymph flow, leading to valvular insufficiency and lymph backflow (Petrova *et al.*, 2004), hyperplasia/aplasia/dilation of lymphatic

endothelial cells comprising lymphatic vessels (Kesler *et al.*, 2013), obliteration or blockages to the lymphatic architecture, dysfunction in lymphatic vessel contractility (Zawieja *et al.*, 2012) and, breakdown in the integrity of lymphatic channels that results in a 'leaky phenotype' allowing lymph extravasation. Lymphoedema often develops over a "timeline of pathology" and initiates following events which cause lymphatic dysfunction- even if associated dysfunction does not immediately manifest as clinical lymphoedema. Onset of lymphatic dysfunction in the presence of rapidly remodelled lymphatics in the murine model following *B. malayi* infections would suggest, rather than being a compensatory repair mechanism, the remodelling observed may be a pathological contributor to later LF related pathology.

PDE imaging 6 and 14 days following filarial infection demonstrated a clear retention or "pooling" of the fluorescent dye in the lower left infected hind-limb, which was completely absent in the healthy uninfected right leg. Additionally, this retention was not observed in sham infected mouse cohorts. Investigators of human, non-filarial LE patients, using similar intravital imaging methods, observed aggregations of ICG dye which was indicative of the dye escaping into interstitial spaces after irregular lymphostasis and lymphatic dysfunction in these channels (Narushima *et al.*, 2015). Further a positive correlation between severity of dye aggregation with higher grades of LE and lymphatic dysfunction was determined (Yamamoto *et al.*, 2011). A method was devised to allow quantification of the retention of ICG dye at or above the injection site which demonstrated a significantly higher aggregation of dye in the left infected leg in infected mouse cohorts (as shown by a significantly lower R/L fluorescence leg ratio) compared to sham controls at both 6 and 14 days pi. This suggests the rapid initiation of lymphatic remodelling following filarial infection is highly coincident with the onset of significantly impeded lymphatic drainage. Further strengthening of these assertions came from Evan's Blue dermal retention assays which quantitatively measured the volume of Evan's Blue that persisted in the lower limb skin (knee to ankle joint) following injection into the foot. At 14 days post-filarial infection, significantly larger quantities of

Evan's blue aggregated within the lower hind-limb of infected mice than sham controls cohorts. Thus two measures of lymphatic function in the model indicate that normal homeostatic lymphatic drainage of the lower limb is perturbed following filarial infection, indicative of lymphatic dysfunction. Further the observed dysfunction is highly associated with significant levels of lymphatic remodelling these assertions are strengthened by recent work which demonstrate similar findings of mechanical damage, associated with both filarial entry, and movement through the lymphatics in a *litomosoides* rodent model (Kilarski *et al.*, 2019)). These were frequently observed in pre-collector vessel areas, matching with where the majority of observed lymphatic remodelling is observed in the developed *brugian* leg pathology model

Taken together, filarial infection not only results in rapid onset lymphatic remodelling, but is coincident with development of early lymphatic insufficiency, disrupting homeostatic lymph drainage. It can be postulated that rapid, novel remodelling of lymphatic channels impedes normal lymph clearance, with nascent, immature vessels lacking the proper structure or smooth muscle cells required for efficient pumping and lymphatic transport of lymph fluid. Additionally, remodelling of local lymphatic channels into a more dilated phenotype is coincident with significantly elevated Evan's Blue fluid retention in the dermis, This might indicate that remodelled, dilated lymphatics become more 'leaky', allowing lymph to escape channels into surrounding interstitial spaces. Whilst insufficiency and 'leakiness' occurred very early following infection and persisted for 12 weeks (the longest time-point scrutinised), pathology remained 'sub-clinical', in so much as overt swelling of the affected limb (ie LE) was not apparent in the first 12 weeks after infection.

Almost all *BmL3* infected BALB/c and C57BL/6 mice (>95%) displayed significant lymphatic alterations and associative pathological insufficiency. Extrapolating to human infection, this suggests that rapid onset of lymphatic remodelling may occur early and in a large proportion of filarial infected subjects. Therefore, many filarial infected individuals (especially younger LF patients who are less infection-experienced) may still exhibit "covert",

subclinical pathology manifest as lymphatic insufficiency/ lowered lymphatic draining efficiency. This is supported by clinical findings which demonstrated filarial antigen positive, asymptomatic patients, display profound lymphatic alterations (Amaral *et al.*, 1994; Freedman *et al.*, 1994, 1995; Noroes *et al.*, 1996; R K Shenoy *et al.*, 2007). Further, so called “covert pathology”, in terms of subtle changes to fluid retention and skin elasticity has been characterised in asymptomatic filarial infected cohorts (Douglass *et al.*, 2017). This raises the possibility that identifying both early filarial infection (ie pre-patent infections) and individuals with covert lymphatic insufficiency and interventions aimed at blocking progression at the “covert pathology” stage may be a promising therapeutic strategy to prevent future development of pathological manifestations. Recent work adds strength to this prospect in which chemotherapeutic treatment at these early stages ameliorated filarial “covert pathology” (Douglass *et al.*, 2019)

Emerging evidence suggests that the lymphatic architecture is highly dynamic with post-natal lymphangiogenesis occurring in response to inflammatory stimuli (Vranova and Halin, 2014; Abouelkheir, Upchurch and Rutkowski, 2017). It is thought inflammatory responses induce the increases in lymphatic flow in areas of infection, either through dilation or extranodal lymphatic vessel or neo-lymphangiogenesis, primarily to increase trafficking of immune effector cells to areas of need, coordinating an appropriate and robust immune response (Kim, Kataru and Koh, 2014). Additionally, evidence suggests inflammatory-induced lymphatic remodelling aids in the increase of trafficking of antigens or antigen presenting cells to local lymph nodes, thus acting as a bridging arm mediating innate and adaptive immune responses to infection, shaping the most appropriate immune response (Soderberg *et al.*, 2005; Qi, Kastenmüller and Germain, 2014). Finally, inflammatory associated lymphangiogenesis (IAL) can increase lymphatic flow both through lymph nodes, thus optimising antigen presentation and appropriate immune responses (Liao *et al.*, 2015)-, and through infection sites thus clearing antigens and cellular debris/damage in the resolution phase of infection (Abouelkheir, Upchurch and Rutkowski, 2017). It is clear, therefore, that IAL is a necessary component of inflammation and the correct host

immunological response yet, significantly, resolves resulting in restoration of normal lymphatic flow and architecture, as part of return to homeostasis.

Long term infections utilising the established model were undertaken to interrogate whether the rapid onset of lymphatic remodelling, and associated lymphatic insufficiency, following filarial infection was a transient mechanism involved with homeostatic IAL. Such remodelling would presumably enter a resolution phase upon clearance of infection and therefore be a separate mechanism to filarial induced lymphatic remodelling. Immunocompetent CB57/6J and BALB/c mouse strains are known to be resistant to filarial infection, and whilst CB57/6J mice clear larval infections at an earlier time-point compared with BALB/c mice, the BALB/c background still remains resistant to long-term, fecund infections (Lawrence, 1996). Permissiveness to fecund infection requires the ablation of adaptive immune responses, as observed in athymic nude or Severe Combined Immuno-Deficient (SCID) mice, where successful establishment of microfilariae (mf) producing fecund adult infections occurs in approximately 90% of infected cohorts (Nelson *et al.*, 1991). Twelve week infections in the CB57/6J mouse strain is therefore an appropriate time frame by which filarial infection would be effectively cleared and resolution of IAL achieved, while mice who have not effectively cleared infection at this time point will have established a fecund infection and begin to release detectable mf into the bloodstream as well as large, 5cm adult *B. malayi* worm nests apparent in infected lymphatics (Vincent, Sodeman and Winters, 1980; Vincent *et al.*, 1984). Cardiac punctures and subsequent thick blood smears revealed that all mice were mf negative, with no evidence of adult worm intra-lymphatic infections suggesting all mice in the 12-week cohort had effectively cleared filarial infection at this late time point. PDE imaging of 12 week infected mice, while demonstrating a significantly higher amount of lymphatic remodelling compared to sham counterparts, showed no significant difference in aberrant lymphatics between 2-week and 12-week infected mouse cohorts. Additionally, the retention of ICG dye in the infected foot, analysed by PDE imaging and quantification of R/L leg fluorescence, remained significantly higher in 12-week infected mice compared to sham controls, with no significant difference

observed between 2-week and 12-week infections. Taken together these data suggests, in contrast to acute IAL, both the observed filarial induced lymphatic remodelling and associated insufficiency persists long term and does not resolve, even in the absence of active filarial infection.

With only approximately 30-40% of LF patients suffering LE pathology, a key unanswered question is what diverging mechanisms occur which pushes filarial infection from asymptomatic, altered lymphatics and “covert pathology”, to symptomatic overt LE. It is highly likely, in endemic areas of filarial infection, that individuals would be subjected to multiple infection events across their lifetime. With the data suggesting strong persistence of altered lymphatics, post-clearance of filarial infection, thus the impact of multiple infections on severity of lymphatic remodelling and dysfunction was investigated. Experiments involving sequential *BmL3* inoculations suggested that mice groups subjected to two individual *BmL3* (*BmL3x2*) infection events developed significantly higher levels of aberrant lymphatics compared to mice subjected to a single inoculation alone (*BmL3*). Scrutiny of larger sample sizes may resolve this trend, while the addition of an Evan’s Blue dermal retention assay for challenge infections may further elucidate whether multiple infection events worsens lymphatic insufficiency. Taken together, the data provides evidence that additional *BmL3* infections result in progressively higher remodelling of local lymphatics, potentially worsening the level of lymphatic dysfunction in the infected area. Considering the data, the accumulation of ever more remodelled and dysfunctional lymphatic architecture could pave the way to a critical ‘tipping-point’ that results in more profound collapse of lymphatic drainage and subsequent symptomatic LE. Endemic patients, however, live in areas at high risk of infection throughout their lifetimes with the chance of reinfection in most patients relatively high, including non-pathology displaying ‘asymptomatic’ groups. Furthermore, there are reported cases of non-endemic patients suffering from filarial LE and pathology often after historic travel to endemic countries and becoming infected (Jones, 2014). Therefore, while continuous infections may significantly contribute to later pathology and lymphatic dysfunction through higher levels of lymphatic remodelling, it cannot by itself be the sole driving

mechanism to the development of filarial LE. Instead, immunological, molecular, cellular or genetic mechanisms in addition to lymphatic remodelling events must play a significant role in determining later manifestation of pathology as also postulated in Dreyer's model for filarial pathogenesis (Dreyer *et al.*, 2000).

To begin to understand the possible immune component to the observed lymphatic pathology, experiments were undertaken to investigate changes to the local immunological environment, following filarial challenge at the early 2-week time point. Filarial infection into the two sites in the left hind-limb results in marked lymphadenopathy to all 3 draining: popliteal, iliac and sub-iliac lymph nodes (LNs), demonstrated by the significant increases in LN area in BmL3 infected mice, compared to sham controls, 2 weeks following infection. This was further corroborated when all draining lymph nodes were pooled and a single cell suspension created, showing a significant increase in cellularity of the LN's in *BmL3* infected mice compared to sham controls. These results would suggest that filarial infection is either inducing significant cellular migration to/from, trafficking to/from or proliferation in the three LN's local to the infection site. LN's act as sentinels in the host immune system, playing a key role in immune surveillance to possible pathogenic threat, by scanning for antigens in lymphatic fluid that flows through them (Liao and Padera, 2013). More pertinently, draining LN's play a key role in coordinating early immune responses to possible threat, helping to shape innate and adaptive immune responses to the most appropriate type against the pathogen encountered (Chang and Turley, 2015). Rapid increases in LN size and cellularity following filarial challenge would suggest significant activation of a robust host immune response at this early time-point. For lymphadenopathy to occur, it is often necessary for the lymphatic vessels, supporting LN architecture and intranodal functions, to rapidly remodel and vascularise in order to sustain higher influx of cells, antigens and debris flowing through them (Angeli *et al.*, 2006). While such lymphatic remodelling is associated with a normal immune response and IAL, it is further evidence of filarial infection inducing a significant change to the pre-existing lymphatic architecture very shortly after infection.

A final objective in this chapter was to investigate if the severity of lymphatic remodelling, and associated lymphatic insufficiency significantly varies in the murine model depending on genetic background of inbred mice. Experiments utilising the established model were undertaken to evaluate differences between purchased C57BL/6J and BALB/c mice strains in relation to severity of early onset lymphatic remodelling and degree of associated pathology related lymphatic insufficiency. *BmL3* infected, commercially purchased and therefore outsourced, C57BL/6J mice displayed similar levels of aberrant lymphatics to the *BmL3* infected, bred in-house, Prox-1^{GFP} C57BL/6J mouse cohorts previously used. This suggests the reproducibility of observed aberrant lymphatics and insufficiency following *BmL3* infection, across varying sources of C57BL/6J mice, ruling out the possibility that the observed differences are a result of the genetic manipulation of the in-house colony. This assertion was further strengthened by the data demonstrating significantly increased aberrant lymphatics, PDE imaged aggregation of dye in inoculated hind limb and increased Evan's Blue dermal retention in *BmL3* infected BALB/c mice compared to sham control BALB/c counterparts, suggesting filarial induced lymphatic remodelling and pathological lymphatic insufficiency is repeatable across differing genetic mouse strain backgrounds. Interestingly, *BmL3*-infected C57BL/6J mice displayed significantly higher levels of PDE imaged aberrant lymphatics and increased Evan's Blue dermal retention than *BmL3* infected BALB/c counterparts. This infers that the C57BL/6J mouse strain develop a more severe filarial associated lymphatic pathology phenotype compared to BALB/c counterparts following *BmL3* infection, as demonstrated by higher levels of lymphatic remodelling and insufficiency.

The strain-dependent difference in filarial lymphatic pathology is suggestive that severity of remodelling and insufficiency is significantly influenced by host responses to filarial infection. Previous literature advocates quite marked phenotypic variation, particularly in relation to host anti-filarial immunological responses, between the two mouse strains utilised. Early work from Lawrence and colleagues noted a lack of surviving larvae post-infection on the C57BL/6J murine background compared to other inbred

strains (Lawrence *et al.*, 1995). In studies comparing the kinetics of filarial clearance between BALB/c and CB57/6J mice, Rajan and colleagues described significantly faster clearance of *B. malayi* filarial infection in CB57/6J mice than BALB/c counterparts, owing to the more 'vigorous' host immunological response in CB57/6J cohorts (Shenoy *et al.*, 1998). Further observations from the same group showed differences in susceptibility to infection on the two backgrounds, even in adaptive immune deficient SCID variants of the strains, suggesting differences in innate immune responses also exist between the two strains (Rajan *et al.*, 1999). Work examining susceptibility to *B. pahangi* infection in varying inbred mouse strains demonstrated higher parasite recovery in BALB/c mice, compared to B.6 backgrounds, with authors speculating genetic differences in T-cell responses being a key component (Howells *et al.*, 1983). In *Litomosoides sigmodontis*, a rodent filarial parasite used as a laboratory model of human filarial parasites, C57BL/6J mice are considered refractory- with the parasite unable to establish fecund infection while BALB/c mice are considered relatively permissive, establishing fecund infection and release of circulating microfilariae in >50% of infections (Graham *et al.*, 2005). The C57BL/6J strain becomes susceptible to fecund filarial infection in *L. sigmodontis* upon ablation of IL-4 cytokine responses- a key driver of CD4+ T cell helper 2 "Th2" adaptive immunity (Le Goff *et al.*, 2002). Further, manipulation of IFN- γ (a prototypic "Th1" cytokine) also renders mice more susceptible to experimental *L. sigmodontis* infection (Gentil, Hoerauf and Pearlman, 2012). This indicates both arms of the adaptive immune response are initiated following filarial infection leading to a state of non-permissiveness. This may also be explained by variation in regulatory adaptive immune responses between BALB/c and C57BL/6J strains. For instance, regulatory CD4+ T cells "T-regs" are elevated in BALB/c mice following *L. sigmodontis* infection and their specific ablation leads to increased Th2 adaptive immunity and control of infection (Taylor JI, 2005). Further, recruitment of 'regulatory' monocytes/macrophages in BALB/c mice, rather than the local *in situ* proliferation of resident 'Th2-activated' macrophages in C57BL/6J mice are hypothesised to influence the degree of immunological resistance to

experimental *L. sigmodontis* infection (Campbell *et al.*, 2018). Taken together, there is clear evidence of marked immunological dichotomies that consequently shape immunity/susceptibility to filarial parasitic infection between the two strains. The significant differences in lymphatic remodelling and resultant insufficiency observed between BALB/c and C57BL/6J strains, suggests initial host adaptive immune responses may also play a key role in dictating severity of lymphatic pathology following larval filarial infection.

2.5- Concluding remarks

Despite remodelling of the lymphatic architecture remaining a clear “hallmark” of LF infection, its role in pathological development remains elusive, primarily due to a lack of adequate animal models that can longitudinally interrogate lymphatic remodelling events and possible associations with pathology. The successful development of a novel murine infection model in this chapter demonstrated that rapid and profound changes to the lymphatic architecture occur as early as 6-days post infection, and in response to the L3 larval stage of filarial infection. This not only contrasts a long-standing pervading theory that lymphatic remodelling is a long-term consequence of adult infections, but robust evidence presented demonstrates clear early associations between observed lymphatic alterations and development of pathological lymphatic insufficiency and dysfunction. The consistency in which lymphatic alterations and insufficiency was observed suggests, regardless of symptomatic or asymptomatic outcome, a degree of “covert pathology” exists in all filarial infected patients. In addition, the data presented demonstrates that the severity of this pathological remodelling and insufficiency is variable; challenge infections significantly worsens filarial lymphatic pathology, while significant differences in severity of lymphatic pathology and insufficiency exist between inbred murine strains. Together these findings demonstrate differences in host genetics and immune responses to *BmL3* infections determine, not only degree of lymphatic remodelling, but the severity of ensuing pathological lymphatic insufficiency.

Proceeding chapters will utilise the developed tractable limb pathology model to investigate the cellular, molecular and immunological drivers of *BmL3*

associated lymphatic pathology. Interrogation of the inducers of lymphatic remodelling could ultimately yield novel, promising therapeutic strategies aiming to target early lymphatic remodelling events, to attempt to prevent, ameliorate, or even reverse future pathological manifestations of LF

Chapter 3

Investigating the molecular mechanisms of filarial inflammatory associated lymphatic pathology.

In Chapter two, a development of a novel murine limb infection model was established indicating infection with *Brugia malayi* filarial L3 (*BmL3*) infective stage larvae rapidly induce lymphatic remodelling and lymphatic insufficiency. The rapid induction of lymphatic pathology in response to *BmL3* infection and the molecular mechanisms that mediate it remain poorly understood. Utilising the novel murine *BmL3* infection model, multiplex analysis was undertaken to investigate associations between induction of filarial-associated lymphatic pathology and alterations in circulating levels of angiogenic/lymphangiogenic molecules. *BmL3* infection rapidly induced the upregulation of a milieu of lymphangiogenic mediators. Further, specific angiogenic/lymphangiogenic molecules: VEGF-C, members of the TGF- β superfamily and prolactin were further increased following multiple infections, or preferentially elevated in C57BL/6J *versus* BALB/c mice, coincident with increased patterns of pathology. Administration of an adenoviral VEGF-C expression vector to locally upregulate VEGF-C was, on its own, sufficient to induce significant levels of lymphatic remodelling and pathological insufficiency in the hind limb and to levels comparable to *BmL3* infection. Taken together, these data identify a milieu of lymphangiogenic molecules that are important in the mediation of filarial associated lymphatic remodelling and insufficiency, providing new insights into the molecular mechanisms driving pathology. Targeted manipulation of these signalling pathways to inhibit the induction of lymphatic remodelling and insufficiency, following *BmL3* infection, may represent a novel therapeutic strategy to prevent the onset of future pathological manifestations of lymphatic filariasis.

3.1- Introduction

Clinical studies on lymphatic filariasis (LF) infected patient cohorts have identified associations between filarial infection and significant elevation of a number of circulating growth factors, known to induce lymphatic remodelling including: Vascular Endothelial Growth Factors A, C & D (VEGF-A,C,D), soluble VEGF Receptor-3 (VEGFR-3), Fibroblast Growth Factor-2 (FGF-2), Angiopoietins 1 and 2 (Ang-1/2) and Placental growth factors (PIGF) (Debrah *et al.*, 2006, 2009; A Y Debrah *et al.*, 2007; Bennuru *et al.*, 2010; Babu *et al.*, 2012). Six-week doxycycline antibiotic treatment is associated with reduced elevated serum VEGF-C/VEGFR-3 at a time-point preceding clinical improvements in LF pathology (Debrah *et al.*, 2006, 2009). These studies identify a potential causal role for increased lymphangiogenic molecules in inducing filarial-associated pathological lymphatic remodelling. The direct targeting of these factors may represent a therapeutic strategy to ameliorate LF related pathology.

Work to date, however, is based on the premise that filarial-induced lymphatic remodelling occurs within a chronic time-frame, primarily as a result of adult inhabitation, death and chronic inflammatory events within lymphatic vessels (Chakraborty *et al.*, 2013; Nutman, 2013). Clinical studies have only investigated growth factor changes following detection of patent adult filarial infection, or long after the manifestation of often irreversible symptomatic LF pathology (hydrocele / elephantiasis). Chapter two demonstrated that rapid onset of lymphatic remodelling, concurrent with pathological lymphatic dysfunction, is manifest following infection with the infective L3 larval stage of *Brugia malayi* (BmL3). Similarly, lymphatic alterations and lymphatic insufficiency are manifest in LF-infected children some of whom are 'asymptomatic' at the level of clinical presentation of lymphoedema (LE) (Kar *et al.*, 2017). The prevention, or reversal, of this early 'seeding' lymphatic remodelling could present a novel therapeutic strategy to potentially block development of later pathological manifestations of lymphatic filariasis (LF). A knowledge gap, therefore, exists in defining the molecular signalling events that drives the induction and maintenance of

filarial inflammatory-associated lymphatic pathology following initial larval-stage infections.

The overarching aim of the research detailed within this chapter was to utilise the developed filarial lymphatic pathology model (defined in chapter two) to evaluate potential molecular mechanisms driving induction of filarial-associated lymphatic pathology. Specific objectives were:

- To identify circulating lymphangiogenic molecules that are altered following induction of early filarial-associated lymphatic pathology.
- To evaluate whether differences in filarial-associated pathology apparent between mouse genetic backgrounds, or following larval re-infections, are associated with magnitude of circulating lymphangiogenic molecules.
- To experimentally reduce or enhance identified specific-lymphangiogenic molecules to evaluate their effect on filarial-associated lymphatic remodelling and pathology.

3.2- Methods

3.2.1-Murine hind-limb infection model and associated pathological readouts

The murine experimental model of filarial-induced lymphatic was utilised throughout this chapter, methods can be accessed from chapter 2.2.1-2.2.7

3.2.2-Cardiac blood sampling and harvesting of plasma

14 days post infection (or other time points as specified) in the previously described pathology model, mice were sacrificed utilising Schedule 1 method of rising CO₂ overdose. Blood withdrawal was undertaken immediately following confirmation of cessation of life, using standard cardiac puncture techniques, into heparinised anti-coagulant collection tubes (Starstedt, Germany) and placed on ice until centrifugation.

Collected blood was centrifuged at 2000rpm for 10 minutes, the serum above pelleted blood cells was then harvested into clean 1ml Eppendorf tubes (Sigma, Dorset) and stored at -80°C for later multiplex analysis.

3.2.3-Multiplex Analysis of circulating angiogenic/lymphangiogenic molecules

Harvested plasma was thawed slowly and kept on ice throughout. A multiplex immunoassay for 25 growth factor analytes (MILLIPLEX MAP Mouse Angiogenesis/Growth Factor Magnetic Bead Panel, Merck, Germany) was undertaken following manufacturer's protocol.

The prepared multiplex immunoassay was read on a Bioplex 200 suspension array system (Biorad, Watfrod, UK). Data was analysed in real time using Luminex XPONENT software (Luminexcorp, Netherlands). Analyte concentrations were either reported as a fold change from the mean serum concentration of relevant sham control groups or analyte concentration levels depending on experiment.

3.2.4- Analysis of TGF- β and BMP-9/10 by Enzyme Linked Immunosorbent Assay (ELISA)

Thawed plasma was either analysed directly (BMP-9/10) or first activated (TGF- β) by addition of 1M Hydrochloric Acid (HCL) (Sigma, Dorset) for 5 minutes immediately followed by addition of 1.2M Sodium Hydroxide (NaOH)/0.5M (Sigma, Dorset). Circulating concentrations of TGF- β and BMP-9/10 were analysed by utilising relevant Duo-set ELISAs (RnD systems, Abingdon) as per manufacturer's instructions.

3.2.5-VEGF-C Adenoviral infection experiments

Adenoviral vectors (ad) encoding full length VEGF-C (adVEGF-C) or full length GFP (adGFP) were constructed by Vector Development Lab, Texas. adVEGF-C and adGFP were reconstituted in Dulbecco's Phosphate Buffered saline (dPBS) (Sigma, Dorset) and further diluted when required to create final viral dosages of 5×10^{10} , 5×10^9 or 1×10^8 viral particles/injection.

C57BL/6J mouse cohorts were administered bi-daily viral doses or sham control (dPBS (Sigma, Dorset) of an equal volume utilised in adenoviral injections), subcutaneously into the left hind limb as previously described (Chapter 2). 6 days after initial injection, mice underwent PDE intravital imaging as previously described (chapter 2), followed by an Evan's Blue dermal retention assay (described in chapter 2).

3.2.6-Sunitinib intervention experiments

Sunitinib malate (Selleckchem, Munich) was reconstituted in a liquid suspension of: 0.5% Carboxy-Methyl Cellulose (CMC; Sigma, Dorset), 0.4% Benzyl Alcohol (Sigma, Dorset), 0.5% Tween80 (Sigma, Dorset), 0.5% Sodium Chloride (NaCl; Sigma, Dorset) in double distilled water (ddH₂O). C57BL/6J mice were placed into sham control, *BmL3* infected + Sunitinib and *BmL3* infected + Vehicle control groups followed by SC injection of 100 *BmL3* larvae or sham RPMI into the left hind limb of relevant groups as previously described in chapter 2.

On the same day as *BmL3*/sham infection, Sunitinib malate at 40mg/kg, or 0.5% CMC, 0.4% Benzyl Alcohol, 0.5% Tween80 0.5% NaCl only vehicle control was administered by oral gavage to relevant mice and continued

daily for the length of the experiment. 14 days following infection, all mouse groups were PDE imaged as described in chapter 2, followed by Schedule 1 for lymph node harvest and other experimental end point readouts as detailed in chapter 2. A schematic of the experiment plan can be seen in Figure 3.5A.

3.2.7-VEGFR-3-Fc and ALK-1-Fc chimera intervention experiments

Recombinant Mouse VEGFR-3/Flt-4-Fc chimera (RnD systems, Abingdon, Cat #:743-R3-100) and Recombinant Mouse ALK-1-Fc chimera (RnD systems, Abingdon, Cat #:770-MA-100) were resuspended in sterile dPBS (Sigma, Dorset). C57BL/6J mice were randomised into sham control, *BmL3* infected + vehicle control (dPBS), *BmL3* + VEGFR-3-Fc chimera and *BmL3* + ALK-1-Fc follow by relevant SC injection with 100 *BmL3* larvae, or sham RPMI into the left hind limb as previously described in chapter 2.

On the same day as infection, 65µg of VEGFR-3-Fc chimera or ALK-1-Fc chimera, or equal volumes of dPBS only were injected to relevant groups subcutaneously using the same injection sites utilised for *BmL3* infection (as previously described in Chapter 2). Injections were continued bi-daily for the length of the experiment. 6 days post infection, all mouse groups were PDE imaged followed by undertaking of an Evan's Blue dermal retention assay as previously described in chapter 2. Cardiac blood sampling was also undertaken for analysis of circulating serum sALK-1 and VEGF-C levels. A schematic of the experiment plan can be seen in Figure 3.6A

3.2.8-Statistical Analysis

All continuous data was tested for normal distribution using the Kolmogorov-Smirnov test for equal variance. Where data was normally distributed, a two-tailed independent Student's t-test was used to test for significant differences between two groups. Where data was found to be not normally distributed, a log transformation was first performed and normality retested. Data that remained not normally distributed following log transformation underwent non-parametric Mann-Whitney U tests to test for

significant differences between two groups. Where more than 2 groups were being compared, a One-way ANOVA was utilised with a Tukey's post-hoc comparisons test to measure differences in parametric data, while a Kruskal-Wallis test was used for non-parametric data with Dunn's post-hoc multiple comparisons test. The mean along with the standard error of the mean (SEM) are reported in all data unless otherwise stated. Significance is indicated as *=P<0.05, **=0.01, ***=0.001 in all figures unless stated otherwise.

3.3- Results

3.3.1- *BmL3* infection is associated with rapid upregulation of multiple circulating lymphangiogenic molecules

Fourteen days following infection, *BmL3* infected cohorts displayed significant increases in circulating : VEGF-C ($2.5\pm 1.3-4.4$ median fold-increase \pm IQR, $P<0.001$), sALK-1 ($1.5\pm 0.9-2.9$, $P<0.05$), Prolactin ($1.6\pm 0.8-3.2$, $P<0.05$), Follistatin ($1.3\pm 0.9-2.4$, $P<0.05$), Angiopoietin-2 ($1.2 \pm 1-1.6$, $P<0.05$) and TNF- α ($1.4\pm 1.1-2.1$, $P<0.05$) compared to sham controls (Figure 3.1A&B). Additionally, *BmL3* infected cohorts displayed significantly decreased circulating endoglin (Figure 3.1A-B; $0.83\pm 0.50-0.96$, $P<0.05$).

3.3.2- Sequential *BmL3* re-infection results in further upregulation of circulating lymphangiogenic molecules compared to primary *BmL3* infection

Fourteen days following final inoculation of primary infected (*BmL3x1*) or re-infected (*BmL3x2*) mice, circulating levels of sALK-1 ($5.5\pm 2.6-15$ vs $1.5\pm 0.9-1.3$, $P<0.05$), prolactin ($6.3\pm 3.1-9.3$ vs $1.6\pm 0.83-3.2$, $P<0.05$) and HGF ($2.2\pm 1.9-7.3$ vs $0.7\pm 0.4-$, $P<0.01$) were significantly upregulated in *BmL3x2* versus *BmL3x1* infection groups, normalised to infection controls (Figure 3.2B&C). In addition, *BmL3x2* infected mice had significantly decreased levels of CXCL3 ($0.48\pm 0.3-0.6$ vs $1\pm 0.7-1.6$, $P<0.05$). Circulating levels of: sALK-1 ($6.3\pm 3.1-9.3$, $P<0.01$) and HGF ($2.2\pm 1.9-7.3$, $P<0.01$) were all significantly increased from sham infection control mice (Figure 3.2B&C).

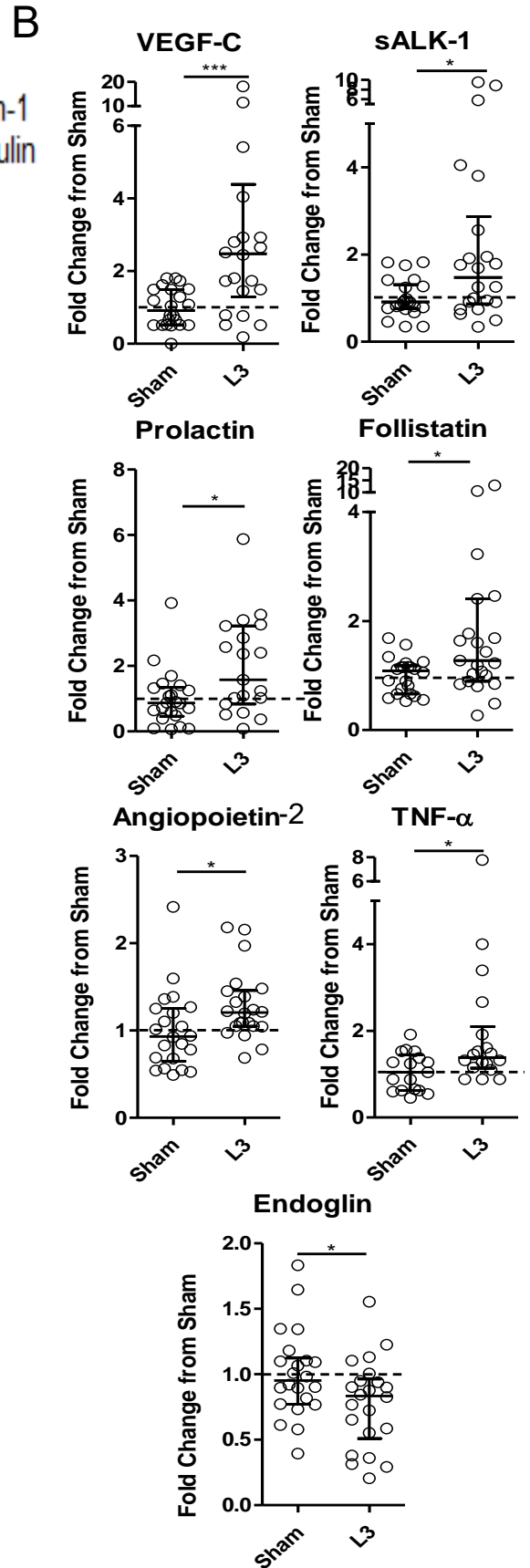
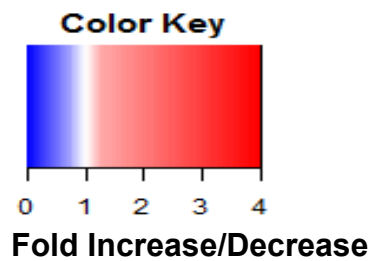
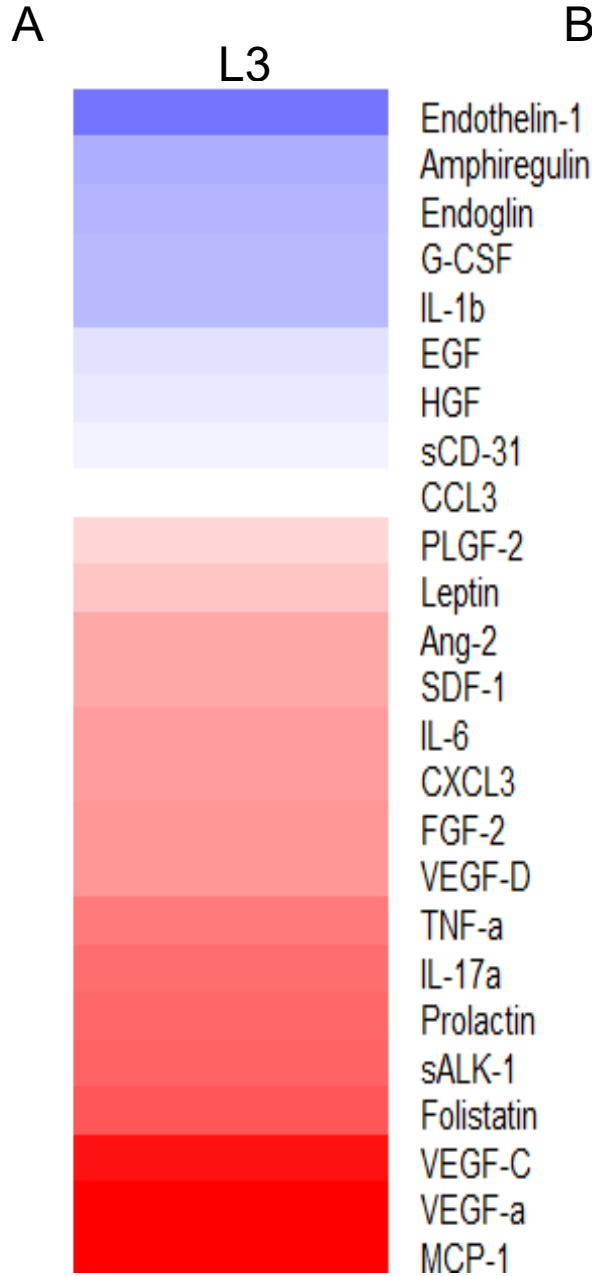


Figure 3.1- *BmL3* infection results in significant upregulation of multiple circulating lymphangiogenic molecules.

A) Heatmap displaying mean fold-change of circulating growth factors 14 dpi with 100 *BmL3* in C57BL/6J mice compared with sham infection controls. Red indicates increases while blue expresses decreases compared to controls. **B)** Individual analytes attaining statistical significance are displayed, plotting fold change from mean sham control concentration. Data is pooled from 3 individual experiments. Horizontal bars plot median \pm interquartile range (IQR). Statistical significance is noted as $*$ = $P < 0.05$, $***$ = $P < 0.01$ derived from Mann-Whitney tests.

3.3.3- Increased filarial lymphatic pathology in C57BL/6J mice, compared to BALB/c mice, is associated with variation in circulating lymphangiogenic mediators.

To further investigate the role of identified lymphangiogenic molecules in the induction of filarial associated lymphatic pathology, C57BL/6J, which demonstrate a higher severity of lymphatic pathology (Chapter 2), and BALB/c mouse strains were compared.

BmL3 infected C57BL/6J mice had significantly higher upregulation of: VEGF-C ($2.5 \pm 1.3-4.4$ vs $0.6 \pm 0.5-1.6$, $P < 0.01$), sALK-1 ($2.4 \pm 0.86-2.8.6$ vs $1.3 \pm 1-1.7$, $P < 0.05$), SDF-1 ($1.1 \pm 0.8-1.5$ vs $0.6 \pm 0.4-0.9$, $P < 0.001$) and Angiopoietin-2 ($1.2 \pm 1-1.45$ vs $0.9 \pm 0.7-1.1$, $P < 0.01$) compared to *BmL3* infected BALB/c mice (Figure 3.3A&B). In addition, compared to *BmL3* BALB/c mice, *BmL3* C57BL/6J mice displayed significantly lower downregulation of Endoglin (Figure 3.3A&B; $0.83 \pm 0.5-1$ vs $1 \pm 0.7-1.3$, $P < 0.05$).

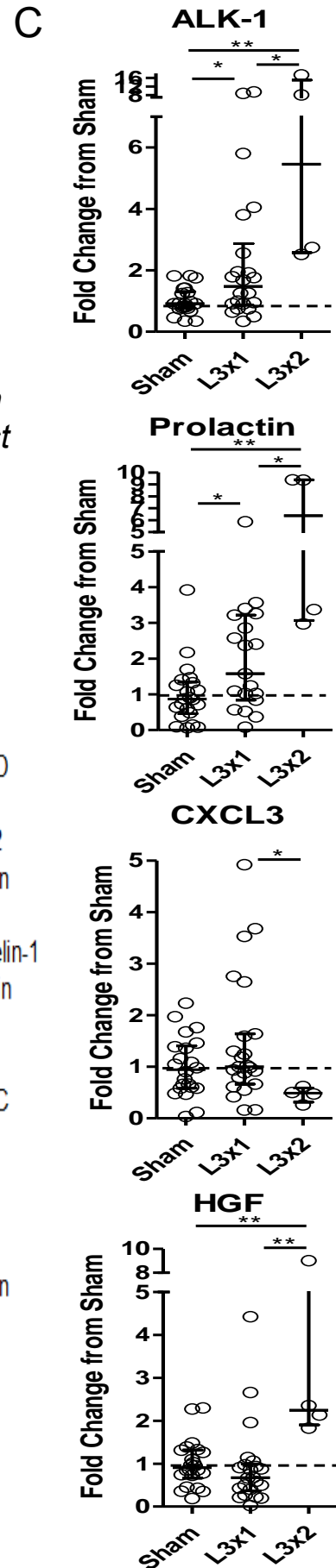
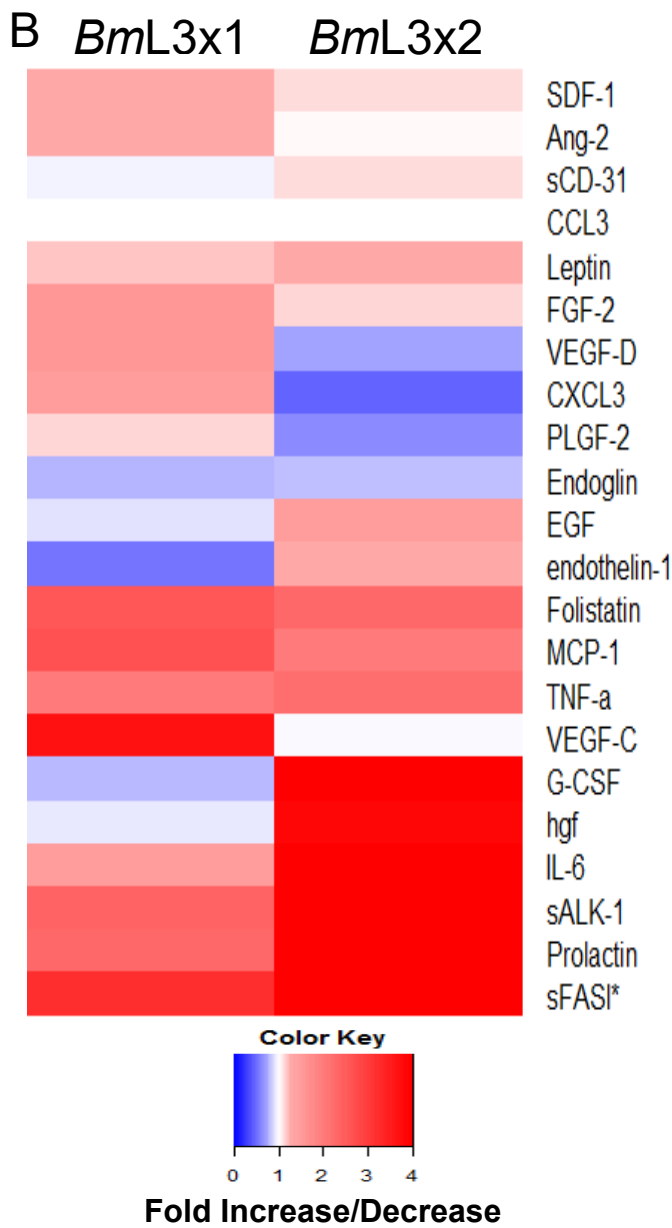
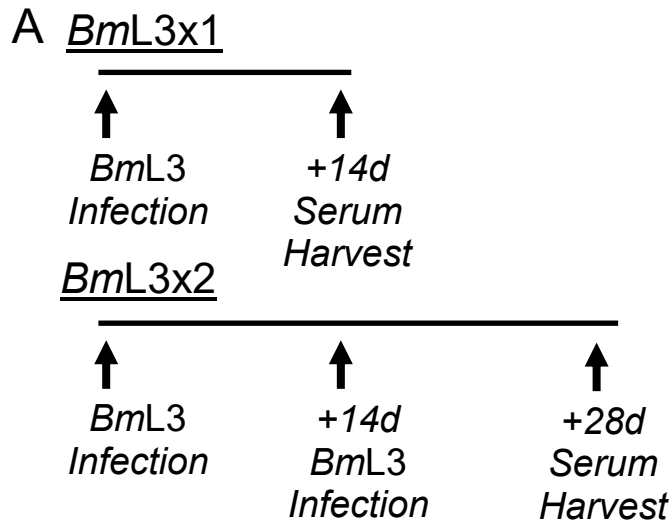


Figure 3.2- *BmL3* re-infection results in further upregulation of circulating lymphangiogenic molecules.

A) Schematic of experimental plan. **B)** Heatmap displaying mean fold change of circulating mediator level in re-infected (*BmL3x2*) mice compared to primary infected (*BmL3x1*) mice normalised to sham control mean analyte concentration. Red indicates increases while blue indicates decreases compared to infection controls **C)** Individual data of analytes attaining statistical significance. Plots are fold-change from mean concentration of sham control. Data is pooled from 3 individual experiments (sham and L3x1) or a single experiment (L3x2). Horizontal bars represent median value \pm interquartile range (IQR). Statistical significance is indicated as *= $P < 0.05$, **= $P < 0.01$, ***= $P < 0.001$ derived from Kruskal Wallis test followed by Dunn's multiple comparisons test between specified groups.

3.3.4- Local upregulation of VEGF-C is sufficient to induce significant levels of lymphatic remodelling and pathological lymphatic insufficiency

VEGF-C is a well-defined lymphangiogenic mediator and was one of the most consistently systemically upregulated factors examined in C57BL/6J mice following larval infection. To investigate impact of localised upregulation of VEGF-C in limb lymphatics and lymphoid tissues, varying titres of adenovirus particles expressing VEGF-C (adVEGF-C), an adenovirus that induces overexpression of VEGF-C upon infection of cells (Enholm *et al.*, 2001; Lähteenvuo *et al.*, 2011), were inoculated into the left hind limb of naive C57BL/6J mice. A schematic of experiment can be seen in figure 3.4A

No significant difference was observed in aberrant lymphatics, in any plane of view, between mice inoculated with high titre (5×10^{10}) control adenovirus expressing GFP (adGFP) and sham-infection controls (Figure 3.4B&C). Compared to adGFP controls, mice inoculated with 5×10^{10} adVEGF-C had significantly increased aberrant lymphatics in dorsal, ventral and left viewpoints (dorsal: 299.5 ± 65.1 vs 3.4 ± 3.4 A.U, $p < 0.05$; ventral: 257.7 ± 46 vs 48.00 ± 40 A.U., $p < 0.05$; left: 329.1 ± 78.4 vs 29.1 ± 29.1 A.U, $p < 0.01$), determined by PDE imaging (Figure 3.4B&C). 5×10^9 particle adVEGF-C mice also displayed significantly higher aberrant lymphatics, compared to 5×10^{10} adGFP controls, in dorsal, ventral and left viewpoints (dorsal: 94.9 ± 24.2 A.U, $p < 0.05$; Ventral: 264.3 ± 52.7 A.U, $p < 0.01$; Left: 281.7 ± 59.6 A.U, $p < 0.01$). 1×10^8 adVEGF-C inoculated cohorts displayed significantly higher aberrant lymphatics than adGFP inoculated controls viewed ventrally (193.4 ± 49.8 A.U, $p < 0.05$). Magnitude of lymphatic remodelling was VEGF-C dose-dependent with 5×10^9 adVEGF-C inoculated mice displaying significantly lower aberrant lymphatics than 5×10^{10} adVEGF-C inoculated mice in the dorsal aspect (94.9 ± 24.2 vs 299.5 ± 65.1 A.U, $P < 0.01$), whilst 1×10^8 adVEGF-C inoculated mice displayed significantly lower aberrant lymphatics compared to 5×10^9 adVEGF-C inoculated animals in dorsal and Left PDE imaged planes of view (dorsal: 11.4 ± 11.4 vs 94.9 ± 24.2 A.U., $P < 0.05$; Left: 56.2 ± 26.1 vs 281.7 ± 59.6 A.U, $P < 0.01$) (Figure 3.4C).

A

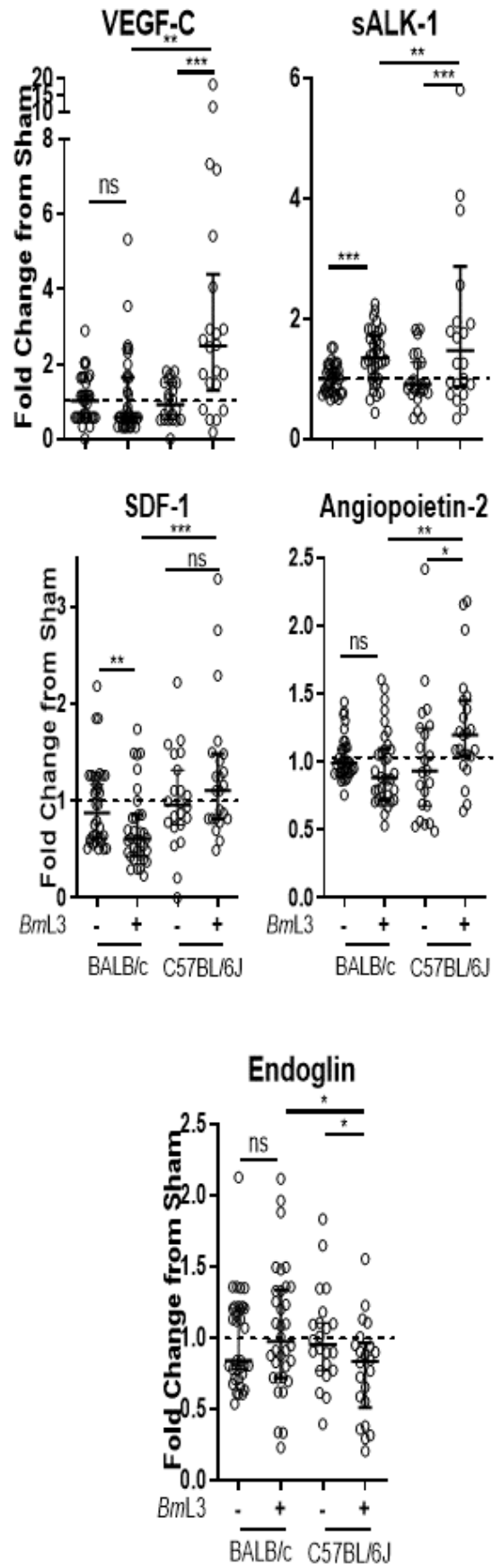
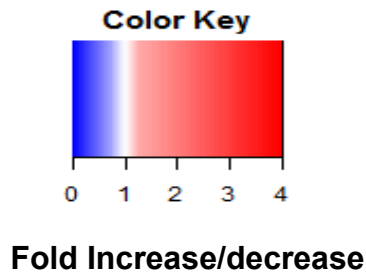


Figure 3.3- *BmL3* infection is associated with altered circulating levels of lymphangiogenic mediators in ‘high pathology’ C57BL/6J versus ‘low pathology’ BALB/c mouse strains.

A) Heatmap depicting upregulation/downregulation of circulating lymphangiogenic mediators from BALB/c and C57BL/6J mice 2 weeks following subcutaneous infection with 100 *BmL3*. Mean fold-change increases (red) and decreases (blue) are shown normalised to sham-infected control groups. **B)** Individual analytes achieving statistical significance plotted as fold-changes from corresponding sham infected controls. Data is pooled from three individual experiments with horizontal bars representing the median value \pm IQR. Statistical significance is represented as *=P<0.05, **=P<0.01, ***=P<0.001 derived from Mann-Whitney tests.

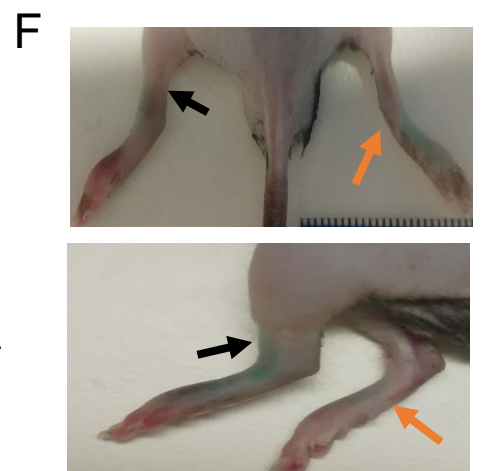
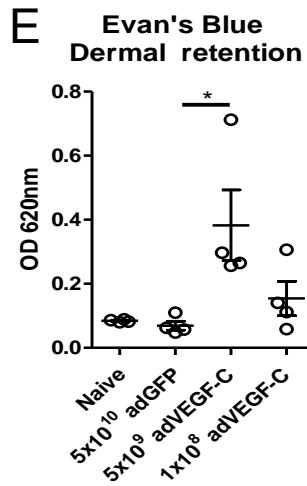
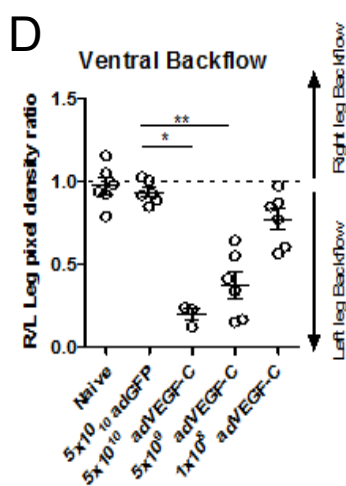
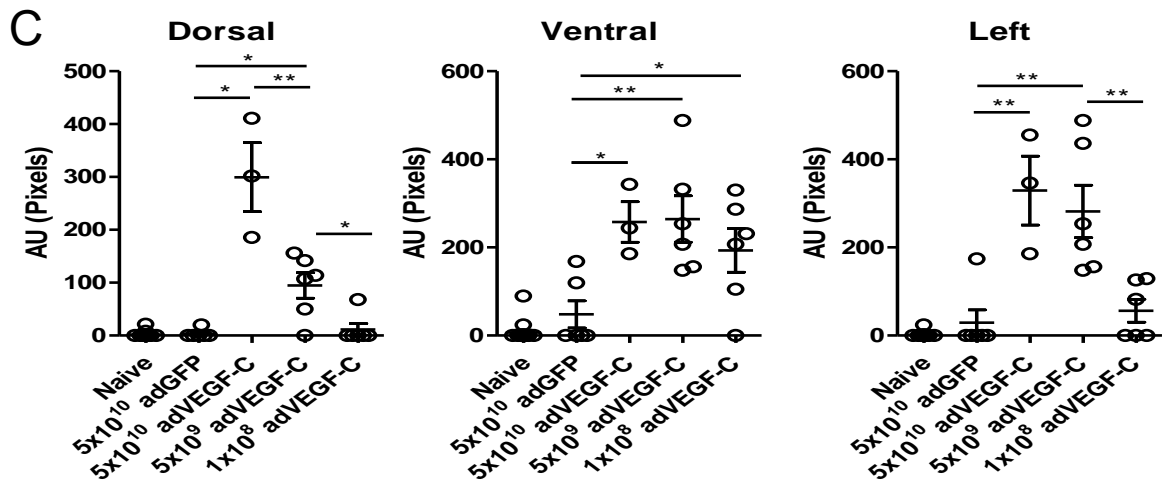
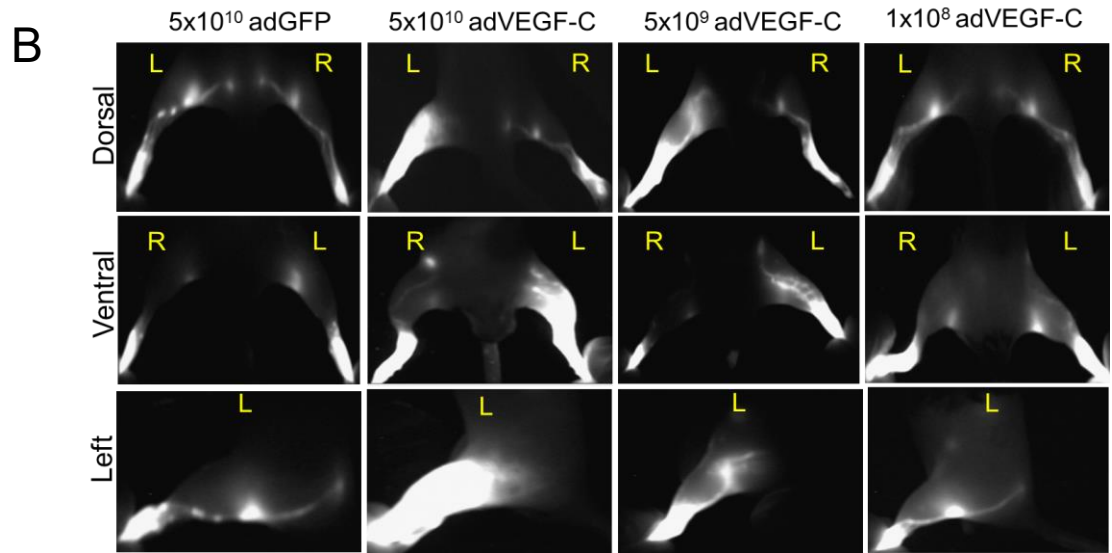
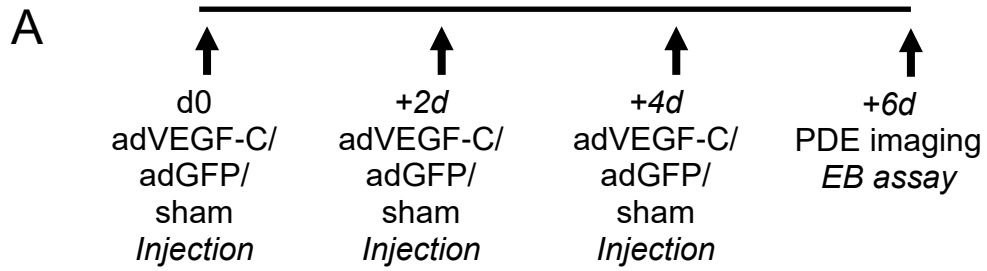


Figure 3.4- Local upregulation of VEGF-C alone is sufficient to induce significant lymphatic remodelling and associated pathological lymphatic dysfunction.

A) Schematic of experimental plan. C57BL/6J mice (n=3-6) were administered bi-daily subcutaneous injections of: 5×10^{10} viral units of adGFP, 5×10^{10} , 5×10^9 or 1×10^8 viral units of adVEGF-C, or sham-injections. **B)** Representative images from near infrared intravital PDE imaging of the dorsal, ventral and left viewpoints, **C)** quantitation of aberrant lymphatics in all groups derived from PDE imaging analysis across the 3 imaged viewpoints, **D)** quantified lymphatic insufficiency measurements taken from PDE imaging of the ventral viewpoint, **E)** Evan's Blue lower limb retention, as measured from Evan's Blue dermal retention assay and, **F)** Examples of lymphoedematous pathological manifestations (black arrows: injected left hind limb, orange arrows: sham injected right hind limb) 6 days post-inoculation. Data is pooled from 2 individual experiments (B-D) or a single experiment (E) from groups of 3 mice. Graph horizontal bars plot mean \pm SEM and statistical significance represented as: *=P<0.05, **=P<0.01 derived from a Kruskal Wallis test followed by Dunn's multiple comparisons post-hoc test between specified groups.

PDE lymphatic ventral backflow measurements revealed no significant difference between adGFP- and sham-inoculated mice (Figure 3.4D). Contrastingly, ICG accumulation in injected hindlimbs were significantly lower in 5×10^{10} and 5×10^9 adVEGF-C groups, compared to 5×10^{10} adGFP controls (Figure 3.4D; 5×10^{10} adVEGF-C: 0.2 ± 0.04 and 5×10^9 adVEGF-C: 0.38 ± 0.08 vs 5×10^{10} adGFP: 0.94 ± 0.03 R/L ratio, both $P < 0.001$). However, 5×10^{10} and 5×10^9 adVEGF-C inoculations induced significant retention of ICG in infected hindlimbs compared to 1×10^8 adVEGF-C inoculated mice (Figure 3.4D; 5×10^{10} adVEGF-C: 0.2 ± 0.04 and 5×10^9 adVEGF-C: 0.38 ± 0.08 vs 1×10^8 adVEGF-C: 0.77 ± 0.07 R/L ratio, $P < 0.001$ and $P < 0.01$, respectively). No significant difference was observed in ratio of ICG accumulations in right versus left hindlimbs between 1×10^8 adVEGF-C and 5×10^{10} adGFP inoculated mice. The Evan's Blue (EB) dermal retention assay revealed no significant difference in EB accumulations between sham and 5×10^{10} adGFP groups, while significantly higher OD⁶²⁰ EB retention was observed in 5×10^9 adVEGF-C inoculated mice compared to 5×10^{10} adGFP inoculated controls (Figure 3.4E; 0.38 ± 0.11 vs 0.07 ± 0.01 OD⁶²⁰, $P < 0.05$). Significant oedema was manifest in the injected left hind limb of mice receiving 5×10^{10} adVEGF-C doses, while no physical differences in limb swelling or size could be detected at lower adVEGF-C particle titres (Figure 3.4F).

3.3.5- Sunitinib treatment is insufficient to modify filarial-associated lymphatic pathology or circulating VEGF growth factors.

To investigate if inhibition of VEGF signalling would result in significant changes to filarial associated lymphatic remodelling and insufficiency, Sunitinib, a small molecule receptor tyrosine kinase inhibitor that inhibits downstream signalling of all three VEGF receptors (VEGFR1-3) (Roskoski, 2007), was administered following *BmL3* infection (Schematic of experiment shown in figure 3.5A).

At 14dpi, PDE imaging indicated that irrespective of sunitinib treatment, *BmL3* infected mouse groups had significantly higher aberrant lymphatics in dorsal, ventral and left viewpoints compared to sham infected controls (Figure 3.5B&C). No significant difference in aberrant lymphatics were

observed between L3+Vehicle and L3+Sunitinib treated mice (Figure 3.5B&C). In addition, L3+Veh and L3+Sun groups displayed higher ICG dye retention in the left (infected) limb than sham infection controls (Figure 3.5D; 0.58 ± 0.11 and 0.54 ± 0.07 vs 0.98 ± 0.07 R/L leg ratio, both $P < 0.001$). No significant difference in ICG dye retention in the left limb was observed between L3+Veh and L3+Sun groups (Figure 3.5D). In addition, at 14dpi, circulating VEGF-C was elevated in both L3+Veh and L3+Sun groups. VEGF-A, VEGF-C and VEGF-D in circulation was not modified by sunitinib treatment compared to L3+Veh groups (Figure 3.5E).

3.3.6- *In vivo* administration of a sVEGFR3-Fc 'trap' failed to significantly modify circulating VEGF-C following *BmL3* infection.

In an attempt to specifically reduce bioavailable VEGF-C following *BmL3* infection, a Mouse VEGFR3-Fc chimera was administered in the infection model followed by imaging of pathological readouts at 6dpi. The VEGFR3-Fc chimera is an extracellular domain portion of Mouse VEGF Receptor 3- the receptor for the ligand VEGF-C (Lohela *et al.*, 2009)- fused to the Fc chain of mouse IgG1, that sequesters VEGF-C, preventing VEGF-C/VEGFR-3 interactions and thus downstream VEGF-C signalling (Takahashi, 2011).

At 6dpi, a non significant elevation of circulating VEGF-C was observed in *BmL3* infected groups, compared to sham controls, while no significant difference in VEGF-C serum concentrations were observed between *BmL3* infected and *BmL3* + VEGFR3-Fc mouse cohorts (Figure 3.6F). PDE imaging demonstrated *BmL3* infected cohorts administered: vehicle control (*BmL3*) and *BmL3* administered VEGFR3-Fc (*BmL3*+sVEGFR3-Fc) displayed similar significantly increased aberrant lymphatics compared with sham infected controls, with no significant differences in aberrant lymphatics observed between *BmL3* and *BmL3*+sVEGFR3-Fc cohorts (Figure 3.6B&C). *BmL3* and *BmL3*+sVEGFR3-Fc mice also displayed similar limb ICG retention (Figure 3.6D). Additionally, the Evan's blue dermal retention assay demonstrated that *BmL3* and *BmL3*+sVEGFR3-Fc mice displayed a similar elevated retention of EB dye compared to sham infection controls (Figure 3.6E)

3.3.7- Administration of an ALK-1-Fc ‘trap’ did not significantly impact on filarial associated lymphatic remodelling and insufficiency, following *BmL3* infection.

To investigate if increased concentrations of sALK-1 could affect filarial associated pathology following *BmL3* infection, a ALK-1-Fc chimera was administered to a mouse cohort following *BmL3* infection and PDE imaging and associated pathological readouts undertaken 6dpi. The ALK-1-Fc chimera is the extracellular domain of ALK-1 fused to the Fc chain of mouse IgG1 which will sequester ALK-1 ligands: Bone Morphogenic Protein- 9 (BMP-9), Bone Morphogenic Protein- 10 (BMP-10), and Transforming Growth Factor- β (TGF- β), thus reducing receptor ligand interaction and inhibiting downstream signalling.

BmL3 infected mice, administered with ALK-1-Fc (*BmL3*+sALK-1-Fc), displayed significantly higher circulating serum levels of sALK-1 than *BmL3* infected mice alone (Figure 3.6G; 2589 ± 927 vs 105 ± 12 pg/ml, $P < 0.001$). While no significant difference was observed in circulating ALK-1 ligands: TGF- β and BMP-9 between sALK-1-Fc and vehicle treated infected groups (Figure 3.6G). *BmL3*+sALK-1-Fc treated mice displayed significantly reduced circulating BMP-10 compared to vehicle treated infected counterparts (Figure 3.6G; 50 ± 22 vs 7 ± 3 .pg/ml, $P < 0.05$). PDE imaging demonstrated that both *BmL3* and *BmL3*+sALK-1-Fc mice displayed significantly higher aberrant lymphatics compared to infection controls, while no significant difference was observed between *BmL3*+sALK-1-Fc and *BmL3* or *BmL3*+sVEGFR3-Fc groups (Figure 3.6B&C). Additionally, both *BmL3* and *BmL3*+sALK-1-Fc mice displayed higher infected limb ICG retentions compared with infection controls, with no significant differences apparent between *BmL3* and *BmL3*+sALK-1-Fc groups (Figure 3.6D). Similarly, the Evan’s blue dermal retention assay demonstrated that both *BmL3* and *BmL3*+sALK-1-Fc groups displayed a similar increased EB dye dermal retention than sham infection controls (Figure 3.6E).

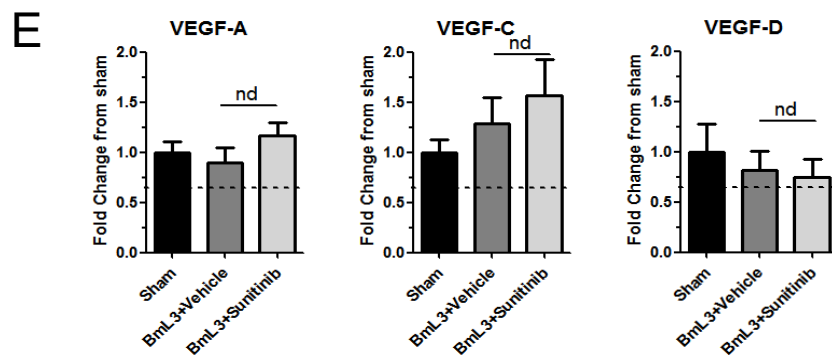
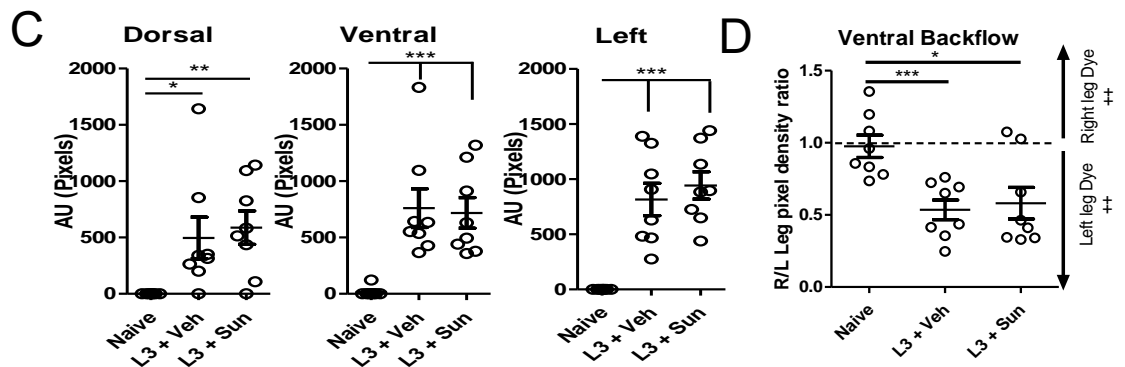
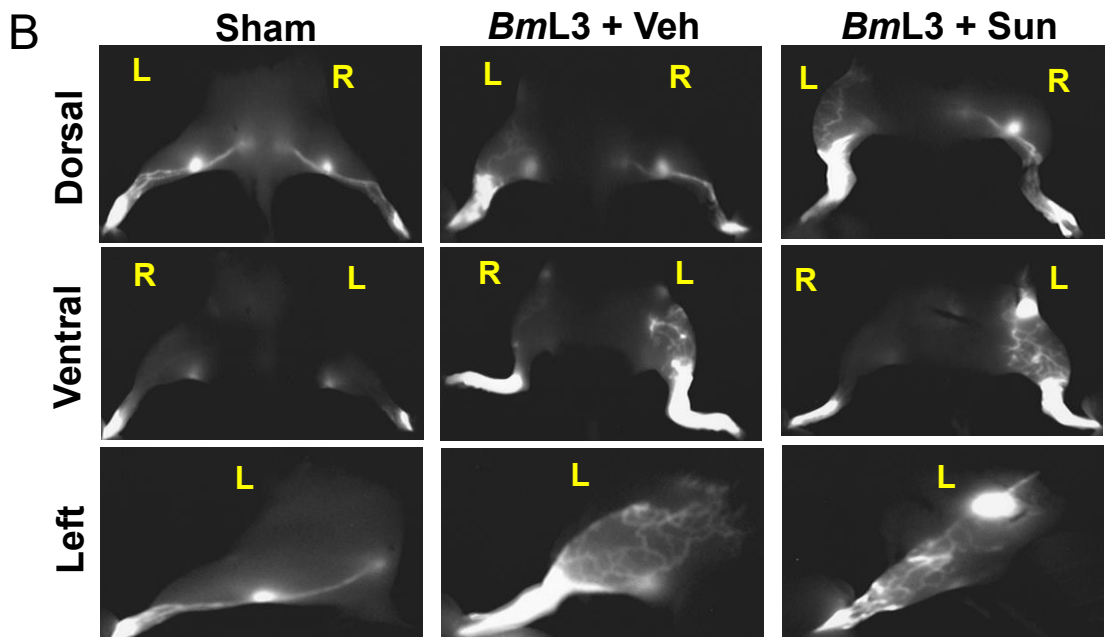
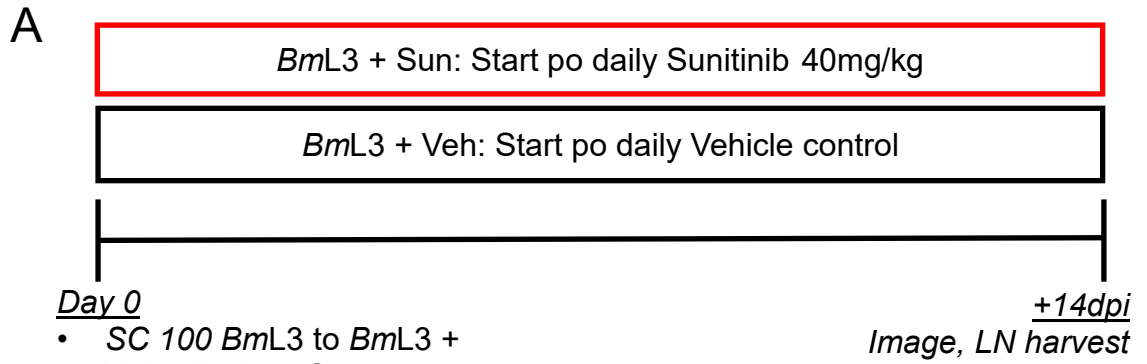
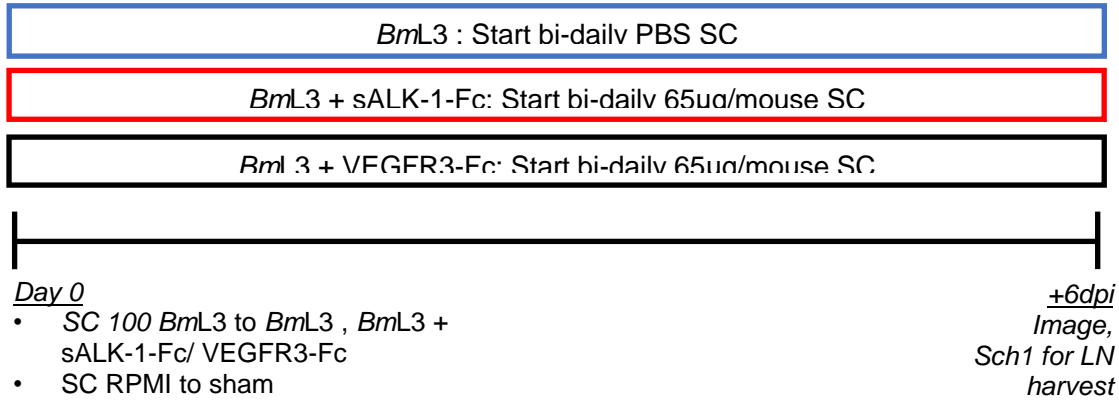


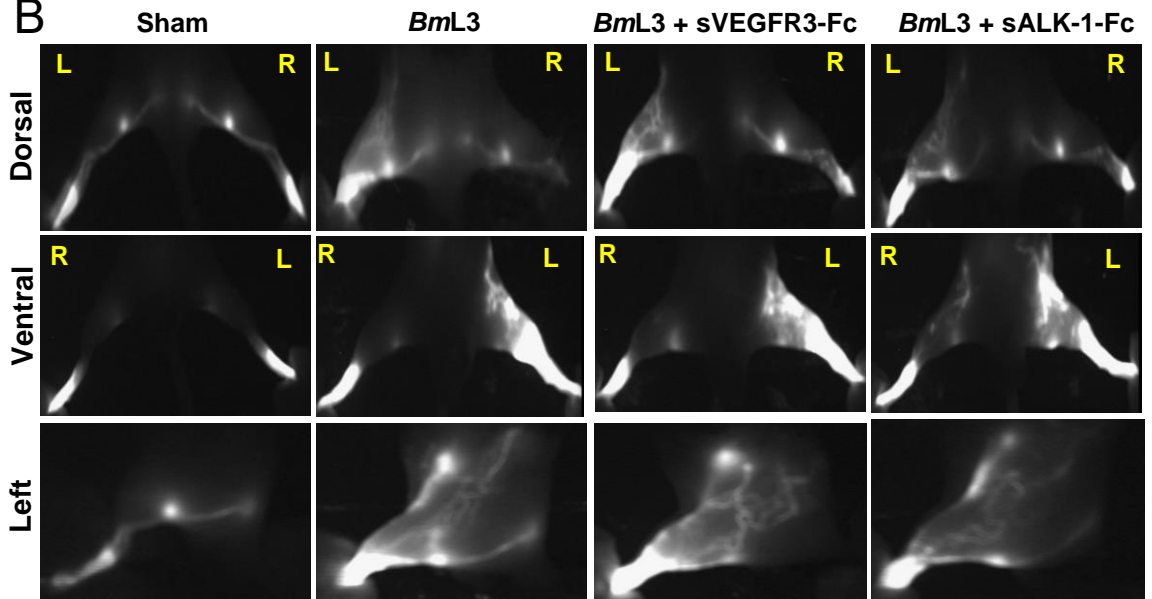
Figure 3.5- Sunitinib treatment does not modify filarial associated lymphatic pathology or reduce circulating VEGF-A-D.

A) Schematic representation of experimental plan. **B)** Representative images from near infrared intravital PDE imaging of the dorsal, ventral and left viewpoints of relevant treatment groups **C)** Quantitation of aberrant lymphatics in all groups derived from PDE imaging analysis across the 3 imaged viewpoints **D)** Quantified lymphatic insufficiency measurement of all groups taken from PDE imaging of ventral viewpoint. Data is from a single experiment. **E)** Serum VEGF-A,C and D levels of all groups quantified by multiplex analysis and expressed as fold change from sham infection control group. Graph horizontal bars are mean \pm SEM with statistical significance represented as: *=P<0.05, **=P<0.01, ***=P<0.001 derived from a one-way ANOVA with Tukey's multiple comparison post-hoc test.

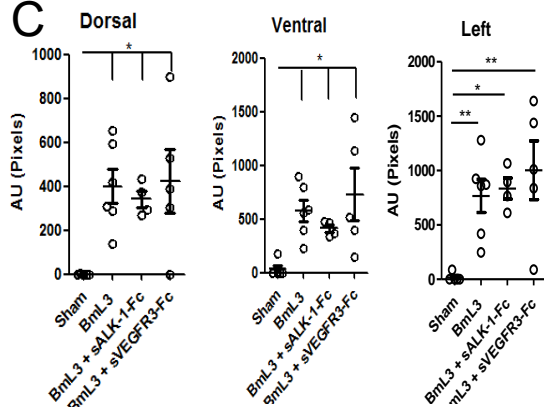
A



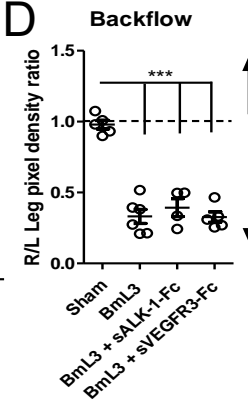
B



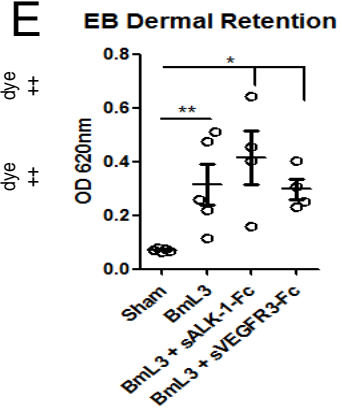
C



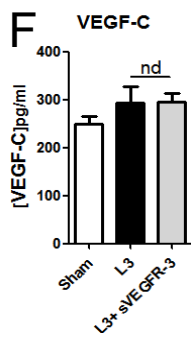
D



E



F



G

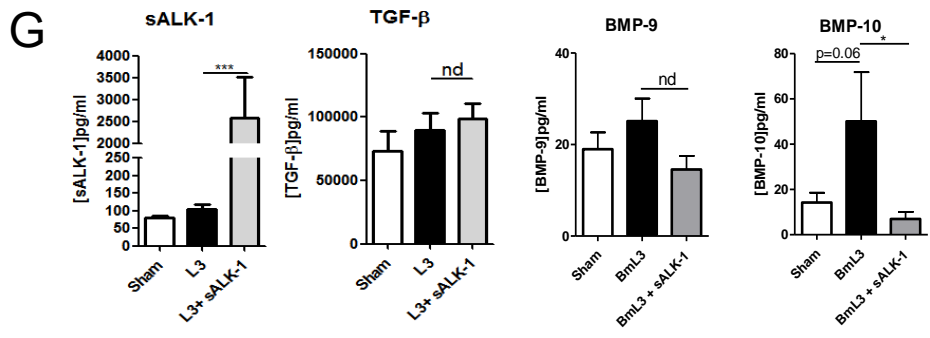


Figure 3.6- Administration of VEGFR-3 or ALK-1 -Fc traps do not significantly alter filarial lymphatic pathology.

A) Schematic representation of experimental plan. **B)** Representative images from near infrared intravital PDE imaging of the dorsal, ventral and left viewpoints of relevant treatment groups **C)** Quantitation of aberrant lymphatics in all groups derived from PDE imaging analysis across the 3 imaged viewpoints **D)** Quantified lymphatic insufficiency measurement of all groups taken from PDE imaging of ventral viewpoint **E)** Quantified dermal retention of Evan's blue following dermal retention assay **F)** Quantified circulating concentrations of VEGF-C following sVEGFR-3-Fc chimera treatment. **G)** Quantified circulating concentrations of sALK-1 and its ligands following sALK-1-Fc treatment Data is pooled from two individual experiments. Horizontal bars are mean \pm SEM with statistical significance represented as: *=P<0.05, **=P<0.01, ***=P<0.001 derived from a one-way ANOVA with Tukey's multiple comparisons post-hoc test.

3.4- Discussion

Chapter two demonstrated that *BmL3* infection induces rapid lymphatic remodelling, resulting in significant pathological lymphatic dysfunction, possibly forming the basis for the development of later lymphoedematous pathology. Therefore, a key research question investigated here was to interrogate the molecular mechanisms that mediate the rapid induction of lymphatic remodelling and dysfunction following filarial larval infection. As discussed in detail in Chapter 1, the molecular regulation of post-natal lymphangiogenesis and lymphatic remodelling is highly complex which, despite increasing research interest in the field, remains to be fully elucidated. Induction of lymphangiogenesis, and changes to the lymphatic architecture, is highly regulated with dynamic interplay between pro-lymphangiogenic signals and the downregulation of 'regulatory' inhibitory signals of lymphangiogenesis (Coso, Bovay and Petrova, 2014). Further, induction of lymphangiogenesis appears to be highly context dependent, with combinations of several identified lymphangiogenic cues required to induce: lymphatic endothelial cell proliferation, lymphatic vessel sprouting and lymphatic patterning, occurring to specific stimuli and the surrounding microenvironment (Linares and Gisbert, 2010; Tammela and Alitalo, 2010). In filariasis, clinical studies have demonstrated that significant changes in circulating concentrations of several known lymphangiogenic factors between uninfected healthy individuals and filariasis patients presenting with forms of lymphoedema or changes to the lymphatic architecture (A Y Debrah *et al.*, 2007; Debrah *et al.*, 2009; Bennuru *et al.*, 2010; Anuradha *et al.*, 2012; Babu *et al.*, 2012; Jensen *et al.*, 2015). However it is not known whether any of these mediators are functionally important in induction or progression of filarial LE.

The novel murine limb pathology model developed in chapter two provides a tractable *in vivo* model to begin to interrogate molecular mediators of lymphatic pathology following filarial infection. Longitudinally tracking changes of circulating levels of lymphangiogenic molecules after *BmL3* infection, and how these changes correlate with observed lymphatic

remodelling and dysfunction enables associative evidence to be ascertained between pathology and potential host lymphangiogenic factors that mediate them, following early filarial infection.

Following 14 days post *BmL3* infection, utilising a focused protein array of known angiogenic/lymphangiogenic growth factors, significant upregulation of circulating: Vascular Endothelial Growth Factor-C (VEGF-C), soluble Activin Like Kinase 1 (sALK-1), Prolactin, Follistatin, Angiopoietin 2, and Tumour Necrosis Factor- α (TNF- α) were observed compared to sham-infected controls. The significant upregulation of this milieu of factors, concurrent with the described lymphatic remodelling, dysfunction and pathology in the *B. malayi* larval lymphatic infection model (chapter 2), promotes a role for these molecules in induction of filarial pathology.

From re-infection experiments, further increases in sALK-1 and prolactin in circulation were apparent, concomitant with increased lymphatic remodelling, compared to primary infections. The association between higher lymphatic remodelling/insufficiency and higher levels of sALK-1 and prolactin may suggest a dose-dependent effect in the induction of pathological lymphatic remodelling. This strengthens the evidence for the functional importance of these molecules in the mediation lymphatic remodelling and insufficiency.

Comparing circulating levels of lymphangiogenic factors between 'high pathology' C57BL/6J mice and 'low pathology' BALB/c mice post-*B. malayi* L3 infection, weaker upregulation of VEGF-C, sALK-1 and Angiopoietin-2 in BALB/c mice was evident. Additionally, a trend toward lower levels of prolactin in BALB/c mice was identified (seen in figure 3.3A). Taken together, the data further demonstrates a possible concentration-dependent effect of these molecules, where increased concentrations result in the induction of higher magnitudes of lymphatic remodelling and dysfunction.

VEGF-C, a member of the VEGF superfamily, is a ligand that when bound to its primary receptor, VEGFR-3, induces lymphangiogenesis (Lohela *et al.*, 2009). In humans, mutations in VEGF-C or VEGFR3 genes results in congenital primary lymphoedematous pathologies linked to poorly developed lymphatic networks (Evans *et al.*, 2003; Ghalamkarpour *et al.*, 2006; Gordon

et al., 2013; Nadarajah *et al.*, 2018), while VEGF-C overexpression in murine models demonstrate aberrantly increased lymphatic vessel density and lymphatic hyperplasia (Goldman *et al.*, 2005). VEGFR-3 is highly expressed on lymphatic endothelial cells (LECs), which upon ligation of VEGF-C induces: LEC proliferation (Veikkola *et al.*, 2003), migration (Ochi *et al.*, 2007) and sprouting from existing lymphatic vessels (Karkkainen *et al.*, 2004; Xu *et al.*, 2010), allowing remodelling of the existing lymphatic architecture as well as induce the formation of new channels. Further it has been demonstrated that endothelial cells upregulate production of VEGF's in response to VEGFR ligation (Lee *et al.*, 2007). There is a well-established role for VEGF-C in post-natal lymphatic remodelling and lymphangiogenesis, as part of homeostatic mechanisms particularly in the context of wound healing (Saaristo *et al.*, 2006; Bao *et al.*, 2009; Zhao *et al.*, 2014) and inflammatory-associated lymphangiogenesis, as a necessary stage of inflammation (Kubo *et al.*, 2002; Kataru *et al.*, 2009) . Importantly, there is evidence implicating VEGF-C signalling in pathological lymphangiogenesis and remodelling, such as in organ transplant rejections (Hajrasouliha *et al.*, 2012; Mertlitz *et al.*, 2017), metastasis of tumours (Skobe *et al.*, 2001; Su *et al.*, 2007), psoriasis (Kunstfeld *et al.*, 2004; Liew *et al.*, 2012) and rheumatoid arthritis (Paavonen *et al.*, 2002; Wauke *et al.*, 2002; Zhang *et al.*, 2007). The pleiotropic nature of VEGF-C, therefore may imply that its role in induction of lymphatic remodelling and lymphangiogenesis is a double-edged sword, where depending on context, it can both ameliorate or contribute to pathology (Kim, Kataru and Koh, 2014).

Studies specific to LF have demonstrated significantly increased serum VEGF-C concentrations in both symptomatic and 'asymptomatic' LF patients (with assumed covert manifestations of aberrant remodelling), compared to endemic control group (A Y Debrah *et al.*, 2007; Bennuru *et al.*, 2010). The data presented is in concordance with these studies, with significantly increased serum VEGF-C observed. Importantly, however, the data suggests that significantly increased VEGF-C secretion occurs rapidly, and in response to much the earlier life cycle stage *BmL3* larval infection. Further, VEGF-C upregulation was concurrent with significant levels of lymphatic

remodelling and dysfunction, suggestive of a role for VEGF-C in the induction of these pathological processes. This data corroborates earlier studies demonstrating reversal of lower grade LF related lymphoedema following doxycycline administration associated with reversal of elevated serum VEGF-C levels (Debrah *et al.*, 2006, 2009; Mand *et al.*, 2012).

The subcutaneous infection of a VEGF-C overexpressing adenoviral vector (adVEGF-C) in identical infection sites utilised for *BmL3* infection delivers VEGF-C protein secretions (Saaristo *et al.*, 2002) targeted to similar anatomical areas exposed to migrating infective *BmL3* larvae. In these experiments, a maximal dose of a GFP-overexpressing adenoviral vector (adGFP) was utilised as a control, accounting for potential lymphatic remodelling or insufficiency that may occur due inflammatory host responses and possible inflammatory-associated lymphangiogenesis to adenoviral infection. However, AdGFP cohorts displayed no significant changes in aberrant lymphatics or aberrant retention of ICG dye compared to sham inoculations, demonstrating that adenoviral infection alone does not induce any measurable lymphatic remodelling or insufficiency. In contrast, adVEGF-C infected cohorts displayed significantly increased levels of both lymphatic remodelling and pathological insufficiency. Further, administration of increased concentrations of adVEGF-C viral units resulted in correspondingly higher levels of aberrant lymphatics, with most the severe level of remodelled lymphatics observed in cohorts administered the maximal 5×10^{10} PFU dose. Therefore, upregulation of local VEGF-C signalling alone can sufficiently drive pathological lymphatic remodelling and dysfunction in a dose-dependent manner. Maximal doses of adVEGF-C administration resulted in manifestation of overt lymphoedema in the infected limb at the early 6 day time point, while 'mid' doses recapitulated levels of lymphatic remodelling and insufficiency similar to that observed in filarial infected mice at the same time point. In contrast to this data, previous research has demonstrated VEGF-C administration ameliorates, and even reverses, lymphoedematous pathology in an acquired lymphoedema murine tail model (Chavez-Rueda *et al.*, 2005; Jin da *et al.*, 2009) as well as in a pig lymph node excision LE model (Lähteenvuo *et al.*, 2011). A contrasting study, however,

demonstrated worsening of lymphoedema following VEGF-C administration in the same tail lymphoedema model (Gousopoulos *et al.*, 2017), better aligning with the data described. Notably, the exogenous administration of VEGF-C in the aforementioned studies was preceded by an injury event resulting in disruption to the lymphatic network which results in lymphatic insufficiency and eventual development of lymphoedema. This differs substantially to administration of VEGF-C to un-manipulated 'healthy lymphatics'. The dichotomy in therapeutic outcome could therefore be explained by the 'type' of secondary lymphoedema in which administration of VEGF-C is delivered. In a situation where augmented lymphangiogenesis would be desirable, to 'reconnect' or 'repair' the existing lymphatic network following overt injury, increased VEGF-C levels mediating lymphangiogenesis and remodelling would be beneficial. In contrast, unregulated, aberrantly increased VEGF-C signalling in healthy subjects- a situation more akin to what is encountered following *BmL3* infection- ,would result in aberrantly increased lymphatic remodelling in the absence of overt lymphatic injury, disrupting normal lymphatic homeostasis and driving lymphatic insufficiency. Experiments undertaken by Saaristo *et al* (2002) strengthens this concept, reporting pathological changes to blood vasculature following adenoviral administration of VEGF-C to healthy mouse subjects.

With local upregulation of VEGF-C signalling alone demonstrated to induce remodelling and pathological insufficiency, it was hypothesised that perturbing VEGF-C and/or its downstream signalling cascade during early *BmL3* infection may be a valid therapeutic target to inhibit filarial associated lymphatic remodelling, therefore ameliorating development of pathology. Studies in oncology have previously assessed a strategy involving the blockade of VEGF signalling. Such blockade has shown to be highly effective in reducing both blood and lymphatic vascularisation of tumours as well as inhibiting metastasis (Ellis and Hicklin, 2008). The result is the clinical development of several classes of biological and small molecule drugs as anti-cancer therapies indicated for a diverse range of tumours from renal

cancers to neuroblastomas (Ferrara, Hillan and Novotny, 2005; Cardones and Banez, 2006).

The startling success of these 'anti-angiogenic and anti-lymphangiogenic' drugs provides a rationale for the use of these drugs to block VEGF-C signalling, therefore inhibiting lymphatic remodelling and insufficiency following filarial infection. Sunitinib, a receptor tyrosine kinase (rtki) inhibitor is a small molecule that has shown efficacy as a pan-VEGF inhibitor (Chow and Eckhardt, 2007). This is achieved by inhibiting downstream signalling of all three VEGF receptors thus blocking VEGF signalling which mediates angiogenesis and lymphangiogenesis (Roskoski, 2007; Takahashi, 2011). With VEGF-C known to be the main ligand for VEGFR-3, effective sunitinib treatment would inhibit downstream VEGF-C signalling, which would be hypothesised to inhibit filarial associated lymphatic remodelling. A number of monoclonal antibodies, designed to block ligation of the VEGF ligands to the appropriate VEGFR receptor have also reached the clinic; bevacizumab, a monoclonal antibody against VEGF-A has shown success in blocking tumour vascularisation (Ferrara, Hillan and Novotny, 2005). A strategy to sequester the released pool of VEGF molecules, resulting in vastly decreased VEGF signalling, has been successful. Aflibercept was created by ligating the extracellular binding domain of VEGF receptors 1 and 2 to the Fc region of human IgG1 (Byrne *et al.*, 2013), this results in a decoy receptor that binds any released VEGF-A, and to a lesser extent C, preventing signalling with functional VEGFR1-2 receptors resulting in the inhibition of angiogenesis and lymphangiogenesis (Takahashi, 2011). More specific targeting of VEGF-C in anti-lymphangiogenic therapies has been achieved by a similar sequestration strategy, involving the fusing of VEGFR-3 (the main receptor for VEGF-C) to an Fc region (Wang, Zhang and Groopman, 2004; Emami-Naeini *et al.*, 2014).

Both Sunitinib and a VEGFR-3 -Fc chimera were utilised as a potential therapeutic intervention to prevent filarial lymphatic pathology in the developed *BmL3* pathology model. Disappointingly, neither administration of Sunitinib or the VEGFR-3-Fc chimera had any significant effect on the severity of lymphatic remodelling or pathological insufficiency following *BmL3*

infection, when compared to *BmL3* infected vehicle controls. Further, surprisingly, neither intervention disrupted the circulating levels of the target VEGF-C molecule. It is therefore likely that both Sunitinib and VEGFR-3-Fc chimera treatments failed to adequately block, or alter VEGF-C signalling in the experimental model, therefore making inferences from the data unreliable. Future experiments to confirm, or validate, that inhibitor reagents used bind to their relevant ligands, or mediate their relevant biological effect may help to determine the failure of both these intervention experiments. While efficacy of sunitinib to block VEGF mediated LEC proliferation was validated *in vitro* (data not shown, undertaken by colleagues), the expense of the VEGFR3-Fc chimera resulted in only sufficient amounts for the *in vivo* experiments could be purchased, resulting in a lack of validation *in vitro*. Nevertheless, relatively high dosages of both were utilised in the study, and in line with dosages utilised in previous studies that demonstrate *in vivo* efficacy (O'Farrell *et al.*, 2003; Benedito *et al.*, 2012). Further work to optimise, and then validate, a treatment concentration and administration regime that demonstrates efficacy in blocking VEGF-C signalling in the model will be required before results from any experimental repeat prove reliable. Use of the adVEGFC *in vivo* lymphoedema model should assist in assessing effective VEGF-C-based antiangiogenic treatment approaches. Alternatively, a strategy utilising mouse strains with conditional knockout of VEGF-C (VEGF-C^{flox/flox} - (Aspelund *et al.*, 2014) or VEGFR-3 (VEGFR-3^{flox/flox} - (Haiko *et al.*, 2008)) signalling may prove a better strategy to better control of VEGF-C signalling following *BmL3* infection, thus providing proof of concept that VEGF-C blockade could significantly lower filarial associated lymphatic remodelling and pathology.

ALK-1 is a member of the Transforming Growth Factor- β (TGF- β) receptor superfamily (Graham and Peng, 2006), with conflicting evidence for its role in lymphangiogenesis and lymphatic remodelling. Recent studies suggest ligation of endothelial cells expressing the receptor ALK-1 with its primary ligand, Bone Morphogenic Protein-9 (BMP-9) results in signalling that inhibits lymphatic vessel formation, LEC proliferation and reduction of Prox-1 expression- the major transcription factor of lymphatic endothelial cell lineage

(Yoshimatsu et al., 2013.). Conversely, BMP-9/ALK-1 signalling has been shown to be important for normal lymphatic vessel patterning and function. BMP-9 knockout mice demonstrate marked lymphatic drainage insufficiency, due to aberrant lymphatic vessel patterning and loss of lymphatic vessel maturation, with visible valvular defects (Levet *et al.*, 2013). BMP-9/ALK-1 signalling has also been demonstrated to be important for early postnatal lymphatic patterning, with interruption of ALK-1 signalling, utilising an ALK-1 Fc chimera that binds ALK-1 ligands and prevents downstream signalling, resulting in abnormalities in the lymphatic architecture of the retina and tail (Niessen *et al.*, 2010). Finally, it has been proposed that LEC ALK-1 receptor ligation with TGF- β itself may be required for sprouting lymphangiogenesis and functional dermal lymphatic patterning, both of which are severely disrupted following TGF- β blockade (James, Nalbandian and Mukoyama, 2013). Contrasting studies, however, have demonstrated that TGF- β signalling inhibits LEC proliferation and results in loss of lymphatic endothelial cell identity (Kasten *et al.*, 2009). Upregulation of circulating soluble ALK-1 (sALK-1) co-incident with induction of filarial lymphatic pathology may suggest a functional role of this soluble receptor in filarial-induced lymphatic remodelling, yet further work is required to understand the relevance of this circulating soluble version of ALK-1. Most research to date focuses on the membrane bound receptor form of ALK-1 and resultantly, the biological role for sALK-1 remains poorly understood. As has been shown with various soluble version of receptors, such as sVEGFR3 (Singh *et al.*, 2013; Emami-Naeini *et al.*, 2014), sALK-1 may act as a decoy receptor, reducing downstream ALK-1 signalling by binding to, and thus sequestering circulating ligands (such as BMP-9/BMP-10 and TGF- β) which have demonstrable roles in the induction of lymphangiogenesis. Alternatively, the increased levels of circulating sALK-1 may reflect an upregulation of membrane-bound ALK-1 expression, following engagement with ALK ligands and ALK-1 signalling. The contrasting role of ALK-1 in lymphangiogenesis described in the literature may suggest a temporal aspect for ALK-1 signalling, were the regulated timing and strength of ALK-1 signalling, at varying stages of lymphangiogenesis dictate the development of functional lymphatic channels.

Similar to VEGF-C blockade, ALK-1 inhibitors are currently the focus of clinical trials as a novel anti-angiogenic/lymphangiogenic therapy for cancer (Jimeno *et al.*, 2016; Burger *et al.*, 2018). The ALK-1 trap, comparable to VEGFR-Fc chimeras, aims to sequester ALK-1 ligands; BMP-9 and BMP-10 which are strong stimulators for both angiogenesis and lymphangiogenesis (Niessen *et al.*, 2010; Levet *et al.*, 2013). This served as a rationale for administration of an ALK-1-Fc chimera as an intervention in the established infection model. ALK-1-Fc chimera administration to *BmL3* infected mice resulted in further significantly increased levels of circulating serum sALK-1, compared to *BmL3* infected mice alone. Due to associations between increased sALK-1 level and higher magnitudes of lymphatic remodelling and insufficiency, it was hypothesised that sALK-1-Fc administration may result in enhanced severity of observed lymphatic remodelling and insufficiency. Despite the successful delivery of the chimera following infection, no significant effect on filarial associated lymphatic remodelling, or insufficiency was observed compared to *BmL3* infected + vehicle treated mice. The associated costs of the ALK-1-Fc chimera, similar to the VEGFR-3-Fc chimera, resulted in purchasing of only a limited quantity, sufficient for a single *in vivo* experiment only. As a result, the lack of validation of the purchased ALK-1-Fc to bind to its targets means a failure of the reagent cannot be discounted, with further *in vitro* experiments to prove binding activity to ALK-1 ligands: BMP-9, BMP-10 and TGF- β advisable. Nevertheless, comparable doses to those utilised in previous *in vivo* studies with success were utilised (Mitchell *et al.*, 2010; Ricard *et al.*, 2012). While circulating TGF- β levels were not significantly altered in this study, it is postulated that the increased sALK-1 concentrations following infection may act to sequester an increased systemic release of its secondary ligand, TGF- β . With TGF- β demonstrated to act as a significant inhibitor of lymphangiogenesis (Kasten *et al.*, 2009), increased sALK-1 may remove the 'inhibitory breaks' of lymphangiogenesis, enabling lymphatic remodelling to occur. This may, however be dose-dependant and while the two-fold increase observed following infection may be optimal to remove TGF- β mediated inhibition, the ten-fold increase observed following sALK-1-Fc administration may, in addition to TGF- β sequestration, also strongly

sequester lymphangiogenic ligands BMP-9 and BMP-10. The resultant removal of not only inhibitory signals, but also stimulatory ligands could result in no net change to remodelling, as was observed. Possible evidence of this is demonstrated by the significantly lower circulating BMP-10 and a non-significant trend suggesting lower BMP-9 in sALK-1-Fc treated infected animals compared to vehicle treated infected counterparts. With circulating lymphangiogenic BMP-10 demonstrating a non-significant trend suggesting increased levels following *BmL3* infection, and the administered trap successful in significantly lowering circulating BMP-10. Alternatively, as the sAlk-1-Fc administration failed to effect filarial lymphatic pathology, this may be evidence of redundancy of BMP9/10 lymphangiogenic signalling pathways in induction of filarial associated lymphatic remodelling pathology. Conversely, it is possible the high *BmL3* numbers used in the inoculations provided too strong a stimulus for lymphatic remodelling and pathology (with resultant strong upregulation of the milieu lymphangiogenic signals discussed in this chapter) to be overcome by blockade of one pathway alone. Further intervention experiments utilising lower *BmL3* inoculations, or using the “low pathology” BALB/c background instead of the “high pathology” C57BL/6J strain used in these experiments may result in significantly altered filarial lymphatic pathology following treatment. Further, the failure to affect filarial associated lymphatic pathology with an intervention targeting a single lymphangiogenic pathway suggests a combinatorial approach, with therapies designed to inhibit several of the identified lymphangiogenic pathways may be more effective in reducing lymphatic pathology following *BmL3* infection. A potential more effective and achievable therapeutic approach might be to target the upstream inflammatory processes driving secretions of pro-lymphangiogenic factors (discussed in chapters 4 & 5).

While little research has been undertaken to investigate the role of prolactin in lymphangiogenesis, a role for prolactin on the induction of angiogenesis has been demonstrated. Genetic deletion of the prolactin receptor in mice resulted in vascular defects and lack of normal angiogenesis of the corpus luteum (Grosdemouge *et al.*, 2003), while over expression of prolactin, utilising intramuscular injection of prolactin cDNA fused with a

cytomegalovirus promoter, resulted in significant vascular development in the testes of mice (Ko, Ahn and Cho, 2003). Prolactin injection in an *in vivo* chick chorioallantoic membrane resulted in markedly higher lymphangiogenesis and endothelial cell migration, which was prevented with addition of a prolactin inhibitor (Reuwer *et al.*, 2012). Importantly, prolactin has been shown to indirectly induce angiogenesis by stimulating the release of growth factors such as VEGF-A (observed to be upregulated following *BmL3* infection, albeit not with statistical significance) on a multitude of cells including the epithelium and macrophages (Malaguarnera *et al.*, 2004). With VEGF ligands often showing affinity for multiple VEGFR receptors, it is possible prolactin indirectly stimulates lymphangiogenesis through a prolactin/VEGF/VEGFR3 signalling pathway, contributing to *BmL3* induced lymphatic remodelling. Additionally, VEGF-A has been demonstrated to indirectly induce lymphangiogenesis in the cornea through chemotactic recruitment of macrophages that appear necessary for corneal lymphatic remodelling (Cursiefen *et al.*, 2004). Prolactin stimulated release of VEGF-A may be important for recruitment of cellular drivers of lymphatic remodelling, while prolactin may be necessary itself to correctly programme monocytes and macrophages into phenotypes of lymphangiogenic potential (Malaguarnera *et al.*, 2004). It is clear, however, that the role of prolactin in filarial lymphatic pathology needs further investigation, as proteolytically cleaved 16K fragments of prolactin have demonstrated potent anti-lymphangiogenic potential *in vitro* and *in vivo* (Kinet *et al.*, 2011). Additionally, prolactin has been implicated in regulation of immune responses, promoting the survival of T-cells (Carreño *et al.*, 2005) and differentially modulating CD4⁺ T-cell responses depending on concentration (Chavez-Rueda *et al.*, 2005; Legorreta-Haquet *et al.*, 2012). It is therefore possible that observed upregulation of prolactin is a consequence of a role in the immune response to early filarial infection, rather than mediation of lymphatic remodelling, with further work required to delineate the two.

3.5- Chapter concluding remarks

With prior studies demonstrating a causal link between increased lymphangiogenic mediators and filarial associated lymphatic remodelling, a key objective within this chapter was to better elucidate the driving molecular mechanisms involved in mediating lymphangiogenesis and lymphatic remodelling, observed to rapidly occur following filarial larval infection. The developed model in chapter two provided a tractable system to longitudinally track changes to the lymphatic architecture following filarial infection, thus allowing investigation of whether the observed rapid induction of lymphatic remodelling and dysfunction was associated with significant alterations to circulating lymphangiogenic molecules. The data described in the chapter successfully identified a milieu of lymphangiogenic factors which were differentially expressed following *BmL3* infection. Further, changes to these lymphangiogenic factors were significantly associated with alterations to the lymphatic architecture and pathological lymphatic insufficiency.

VEGF-C, a well characterised inducer of lymphangiogenesis was observed to consistently be significantly upregulated, concurrent with the onset of lymphatic remodelling and pathology, while experimentally induced local upregulation of VEGF-C in absence of *BmL3* infection was enough to recapitulate similar levels of lymphatic remodelling and pathology observed in filarial infected mice. Of interest, a host of less well characterised molecules such as prolactin, TGF- β family members (such as sALK-1) and Follistatin were all demonstrated to be significantly changed following infection, highlighting the complexity of the potential regulating molecular mechanisms that mediate filarial associated lymphatic remodelling. While targeted manipulation of the two most consistently upregulated molecules, VEGF-C and sALK-1, failed to significantly alter remodelling or pathology in *BmL3* infected cohorts, experimental difficulties encountered does not rule these molecules out as functional mediators of filarial associated lymphatic pathology and distinct experimental approaches will be required in the future to investigate their functional roles.

The data together reveals a host of molecules that potentially play a key role in mediating filarial associated lymphatic remodelling. Specifically targeting of these molecules, to prevent development of lymphatic remodelling and associated insufficiency following filarial infection, highlights a potential novel therapeutic strategy to stop later pathological manifestations of LF. Further work, however, will be required to fully understand the contribution of identified molecules in the lymphangiogenic processes that drives the observed post-natal lymphatic remodelling. Better knowledge of how the identified molecules affect: LEC proliferation, migration as well as lymphatic patterning and vessel maturation following filarial infection may yield a more focused list of candidate molecules as therapeutic targets.

Chapter 4

Cellular mediators of filarial inflammatory-associated lymphatic pathology

Prior work has defined rapid onset of lymphatic remodelling and associated lymphatic insufficiency, following *B. malayi* larval L3 (*BmL3*) infection (chapter 2), while upregulation of multiple lymphangiogenic mediators implicated in filarial associated lymphatic remodelling were defined in chapter 3. In this chapter, the murine *B. malayi* lymphatic pathology model was utilised to interrogate inflammatory cell population dynamics following *BmL3* infection, while purifications of inflammatory cell populations were undertaken to characterise their secretion of lymphangiogenic mediators. *BmL3* infection resulted in significant expansion of Cd11b⁺Ly6C⁺CCR2⁺ monocytes in skin draining Lymph nodes (sdLNs), proximal to infection, which were demonstrated to secrete significant concentrations of lymphangiogenic molecules associated with the initiation of lymphatic pathology. C57BL/6J mice, predisposed to a more extensive filarial-infection associated lymphatic pathology, displayed significantly increased expansions of monocyte and macrophage populations than 'low-pathology' BALB/c mice following *BmL3* inoculations. Subsequently, clodronate and anti-CCR2 ablation experiments were undertaken to investigate the impact of monocyte/macrophage lineage cells and CCR2⁺ inflammatory monocytes on development of filarial-associated lymphatic pathology. Ablation of macrophage and/or CCR2⁺ monocyte populations in proximal lymphatic channels and sdLNs local to *BmL3* inoculation resulted in significant amelioration of lymphatic dilation and insufficiency. Together, the data demonstrates a novel role for recruited monocytes and macrophages in contributing to lymphatic pathology. Targeting the recruitment or differentiation of these monocyte/macrophage populations may yield a novel therapeutic approach to inhibit development of filarial associated pathology.

4.1- Introduction

Chapter two detailed the development of a novel murine filarial infection model which enabled robust interrogation of the early stages of lymphatic pathology following filarial larval invasion. The model demonstrated rapid onset remodelling of the lymphatic architecture, coinciding with significant lymphatic dysfunction, as early as 6 days following filarial infection. Chapter three detailed investigations into the molecular mechanisms mediating lymphangiogenic events that contribute to filarial infection associated lymphatic pathology. This resulted in the characterisation of lymphangiogenic mediators and pathways demonstrated to be implicated in the initiation of lymphatic remodelling and associated insufficiency following filarial infection. With the data suggesting significant increases of a milieu of growth factors, hormones and cytokines associated with lymphangiogenesis, a key objective in this chapter was to investigate the cellular sources of these molecules.

Cellular mediators have been identified in other settings of lymphangiogenesis resulting in post-natal lymphatic remodelling including: 'wound healing' macrophages (Krzyszczuk *et al.*, 2018), other cells of myeloid origin (Zumsteg and Christofori, 2012) and B-cells (Angeli *et al.*, 2006). Despite this, the cellular mechanisms implicated in filarial infection-associated lymphatic remodelling remain poorly defined. It is postulated that filarial adult excretory/secretory products (E/S products) may include molecules with direct angiogenic / lymphangiogenic potential and may directly mediate 'early' dilation through direct signalling with lymphatic endothelial cells (LECs) lining lymphatic vessels (Higazi *et al.*, 2003). Additionally, studies have demonstrated the ability of *B. malayi* parasite homogenates to directly activate LECs, thus inducing lymphangiogenesis and remodelling (Bennuru and Nutman, 2009a). Conversely, more recent studies dispute this finding, showing no evidence for LEC activation with excretory secretory products of filarial parasites (Weinkopff and Lammie, 2011). Instead, data from the same lab argues a crucial role for monocytes, where adult *B. malayi* ES products stimulated primary human monocytes (PBMCs) to produce lymphangiogenic mediators in concentrations that

stimulated LEC proliferation *in vitro* (Weinkopff *et al.*, 2014). This would perhaps suggest an underappreciated role for host immune cells in being a causal driver of lymphatic remodelling following filarial infection, that is postulated to increase the risk of lymphatic filariasis (LF) related pathology. An evident role for inflammatory immune cells (particularly of leukocyte origin) in driving the remodelling of the lymphatic architecture following experimental bacterial infection already exists (Kataru *et al.*, 2009).

Clinical studies enrolling patients suffering with chronic LF can only adequately interrogate associations between lymphatic remodelling and inflammatory cell recruitment at the point of adult parasitism, long after initial filarial L3 larval infection. The developed model (chapter 2), however, clearly demonstrates rapid alterations to the lymphatic architecture, in response to *BmL3* larval invasion to lymphatics proximal to infection site. The early local cellular events which may contribute to the observed early lymphatic pathology remain uncharacterised.

In chapter 3, systemic upregulation of a number of pro-lymphangiogenic host mediators were demonstrated following inoculation with *BmL3*. With lymphadenopathy apparent in the sdLN proximal to parasitized and remodelled lymphatics, host immune cells are a potential major source of these growth factors. Investigation into molecular/cellular signalling axes driving filarial-infection associated lymphatic pathology could yield novel cellular therapeutic targets.

The objectives of this chapter were to:

- Investigate early changes to lymphoid and myeloid leukocyte cell populations proximal to areas of *BmL3* lymphatic infection, utilising the established murine experimental pathology model.
- Compare whether there are differences in the magnitude of lymphoid and myeloid leukocyte cell populations post-infection in C57BL/6J 'high pathology' versus BALB/c 'low pathology' mouse strains
- Interrogate if specific leukocyte cell types secrete significant quantities of lymphangiogenic molecules implicated in the development of pathology

- Determine a direct role for specific leukocyte populations in filarial lymphatic remodelling, by investigating the ability of filarial-stimulated cell populations to mediate proliferation of lymphatic endothelial cells (LEC).
- Investigate if ablations of specific leukocyte cell populations, proximal to *BmL3* infection, influences the development of filarial infection associated lymphatic pathology

4.2- Methods

4.2.1-Murine hind-limb infection model and associated pathological readouts

The murine experimental model of filarial-induced lymphatic pathology was utilised throughout this chapter, methods can be accessed from chapter 2.2.1-2.2.7

4.2.2-Lymphoid/ lymphatic and blood tissue harvest and single cell preparation

Following inoculation of 100 *BmL3* and at time points varying from 6 days post infection (dpi)-14dpi, mice were sacrificed using Sch1 method of rising concentration of CO₂ followed by confirmation of kill. Inoculated limb skin draining lymph nodes (sdLNs) i.e.. popliteal (pLN), iliac (iLN) and sub-iliac (siLN) were carefully excised from mice along with their relevant afferent and efferent lymphatic channels. A single cell suspension was created by teasing apart sdLN's and channels on top of a 40 µm cell sieve (Sigma, Dorset) followed by physical maceration of remaining lymph node tissue through the sieve, using the handle of sterile, 2ml syringes (Sigma, Dorset). The resultant single cell suspension was re-suspended in Dulbecco's Phosphate Buffered Saline (dPBS) (Sigma, Dorset) + 5% Foetal Bovine Serum (FBS) + 2mM EDTA and aliquoted into equal cell numbers, ready for proceeding cell cytometry or FACs. A measurement of total cellularity was obtained by a manual cell count on sdLN single cell suspensions, using a haemocytometer in a 1:1 cell sample:2% w/v Trypan Blue (Sigma, Dorset) solution for Live/Dead cell differentiation..

In experiments where blood immunophenotyping was undertaken, blood samples, acquired utilising cardiac puncture at necropsy, was first depleted of red blood cells (RBCs), utilising RBC lysis buffer (Biolegend, London) as per manufacturer's protocol. Following depletion, blood samples were resuspended in Dulbecco's Phosphate Buffered Saline (dPBS) (Sigma, Dorset) + 5% Foetal Bovine Serum (FBS) + 2mM EDTA and aliquoted into equal volumes of 100µl, ready for proceeding cell cytometry.

4.2.3-Flow cytometry

Cell suspension samples, prepared as above, were placed on ice throughout the proceeding staining steps. Blocking of Fc regions was undertaken by a 20 minute incubation with rat anti-mouse Cluster of Differentiation(CD)16/32 CD16/32 Fc-block (eBioscience, Hatfield UK) followed by a subsequent 30 minute incubation of samples with efluor 450 fixable viability dye (eBioscience, Hatfield UK) for live/dead cell differentiation. Subsequent cell surface staining was undertaken for 30 minutes using the following rat monoclonal antibodies: Ly6G Phycoerythrin(PE) (ebioscience, Hatfield), Ly6C PerCyP5.5 (eBioscience, Hatfield), Rat IgG1 Allophycocyanine APC Isotype control (eBioscience, Hatfield), Rat IgG1 Fluorescein (FITC) Isotype control (eBioscience, Hatfield), CD4 APC (eBioscience, Hatfield), Chemokine receptor-2 (CCR2) Phycoerythrin-Cyanine7 (PE-Cy7) or CCR2 AlexaFluor 700 (AF700) (eBioscience, Hatfield), CD11b AlexaFluor 488 (AF488) or CD11b PerCyP5.5 (eBioscience, Hatfield), B220 APC (eBioscience, Hatfield), CD3 PE (Biolegend, London), F/480 Brilliant Violet 711 (BV711) (Biolegend, UK), MHCII APC (eBioscience, Hatfield), Tim-4 PE-Cy7 (eBioscience, Hatfield). Surface-antibody labelled cell suspension samples were then fixed for 40 minutes using the Forkhead box P3 (FoxP3) Fixation/Permeabilisation Kit (eBioscience, Hatfield), followed by immediate acquisition undertaken on a Becton Dickinson (BD) LSRII Flow cytometer (BD Biosciences, Berkshire, UK). Data was analysed using Flowjo software (BD Biosciences, Berkshire, UK). The gating strategy utilised is outlined in supplementary figure 4.1 below, while antibody clones are listed in appendix 1.

4.2.4-Fluorescent Antibody Cell Sorting (FACS) and subsequent cell secretion assays

Following surface staining with specific antibodies, lymphatic/lymphoid cell suspensions from individual *BmL3* or sham infected mice were cell sorted using a Becton Dickinson FACSAria II (BD Biosciences, Berkshire, UK) to

≥95% purity into ice cold dPBS (Sigma, Dorset) + 40% FBS Serum + 2mM EDTA to maintain maximum cell viability. The gating strategy used to sort cells into: Monocytes, B-cells, T-cells, and macrophages is outlined in Figure S4.1 below. Following cell sorting, cells were resuspended into RPMI 1640 (Sigma, Dorset) supplemented with: 10% FBS (Sigma, Dorset), Penicillin / Streptomycin at 100 I.U./mL (Sigma, Dorset) and Amphotericin B 2.5mg/L (Sigma, Dorset). Purified B and T-cells were plated out at 1×10^6 cells in 250µl, while monocytes and macrophages were plated out at 2.5×10^5 cells in 100µl into flat-bottom 96 well plates (Starlab, Milton Keynes). Plated purified cell populations were incubated at 37°C, 5% CO₂ for 72 hours before plate centrifugation and harvesting of cell supernatants. Collected supernatants were frozen at -70°C for future analysis.

4.2.5-Multiplex Analysis

Concentrations of a panel of angiogenic/lymphangiogenic analytes were probed for cell sorted culture supernatants (as described above) using the MAGMAP-24k multiplex full panel (Merck Millipore, East Midlands), as per manufacturer's instructions, and analysed using a Bioplex 200 (Biorad, Hertfordshire). Analyte expression was normalised to analyte secretion/ 1×10^6 cells after accounting for initial supernatant volume and cell concentrations. Data was then plotted by sorted cell population with between 3 and 5 individual mouse cell sorted sdLN populations used as replicates.

4.2.6-Cell culture

Primary (adult) Dermal Lymphatic Human Micro-Vascular Endothelial Cells (HMVECdLy: LECs) were purchased from Lonza (Slough, UK) and were maintained and passaged in fully supplemented Endothelial Growth Medium-2 Bullet kit (EGM-2)(Lonza, Slough UK). THP-1 monocytes were a kind gift from Professor Giancarlo Biagini (LSTM, UK) and passaged using Roswell Park Memorial Institute (RPMI) 1640 (Sigma, Dorset) supplemented with: 10% FBS (Sigma, Dorset), Penicillin / Streptomycin 100 I.U./mL (Sigma, Dorset) and Amphotericin B 2.5mg/L (Sigma, Dorset) All cells were maintained at 37°C, 5% CO₂.

4.2.7-Production of *Brugia malayi* L3 larval extract (BmL3E)

Batches of between 1000 and 2000 *Brugia malayi* L3 larval were washed 3 times in dPBS (Sigma,Dorset) before re-suspension in between 200µl-500µl E-toxate ultra-pure water (Sigma,Dorset). Resuspended larvae were left in constant motion using a tube roller at 4 °C overnight. The following day, samples were sonicated (using a Vibracell sonicator (Jencons)) for 5 minutes, and repeated for 3 sonication cycles to ensure full lysis of larvae and extraction of water-soluble macromolecules. BmL3E protein concentrations were quantified using a BCA assay (ThermoFisher, UK), as per manufacturer's protocol, before being frozen at -20°C until utilised in assays.

4.2.8-Macrophage/ LEC co-culture survival/proliferation assay

Thp-1 monocytes were plated into the cell inset of 6 well trans-well plates (Sigma, Dorset) at 1×10^6 cells/well and differentiated into adherent "M0" macrophages using 10ng/ml PMA (Sigma,Dorset) for 24 hours. Following differentiation, macrophage insets were washed in PBS before stimulation with either 10µg/ml of BmL3E, 10 live *Brugia malayi* L3 larvae (L3) or media only (M0) for 48 hours. On the intermediate day, LECs were seeded separately on the bottom of fresh 6 well trans-well plates at 8×10^4 cells/well. Following 48-hour stimulation, L3/BmL3E/M0-activated macrophage insets and LEC adherent layers were washed, before addition of the inserts onto the top of LEC wells, creating a LEC/Macrophage co-culture. A 20% EGM-2, 80% Endothelial basal media (EGM-2 without addition of any growth supplements, +0.1% FBS only) mix was used as the culture media. LEC wells without macrophage inserts plated in: 80:20 media alone or full EGM-2 were used as negative (negligible growth) and positive (maximal growth) controls respectively. All LEC/Macrophage co-culture wells and LEC control wells were incubated for 72 hours at 37°C, 5% CO₂. Following incubation, macrophage inserts were discarded and LEC cells dissociated from wells using 1x Trypsin/EDTA solution (Thermofisher, UK). All LEC samples were manually counted using a haemocytometer in a 1:1 cell sample: 2% Trypan

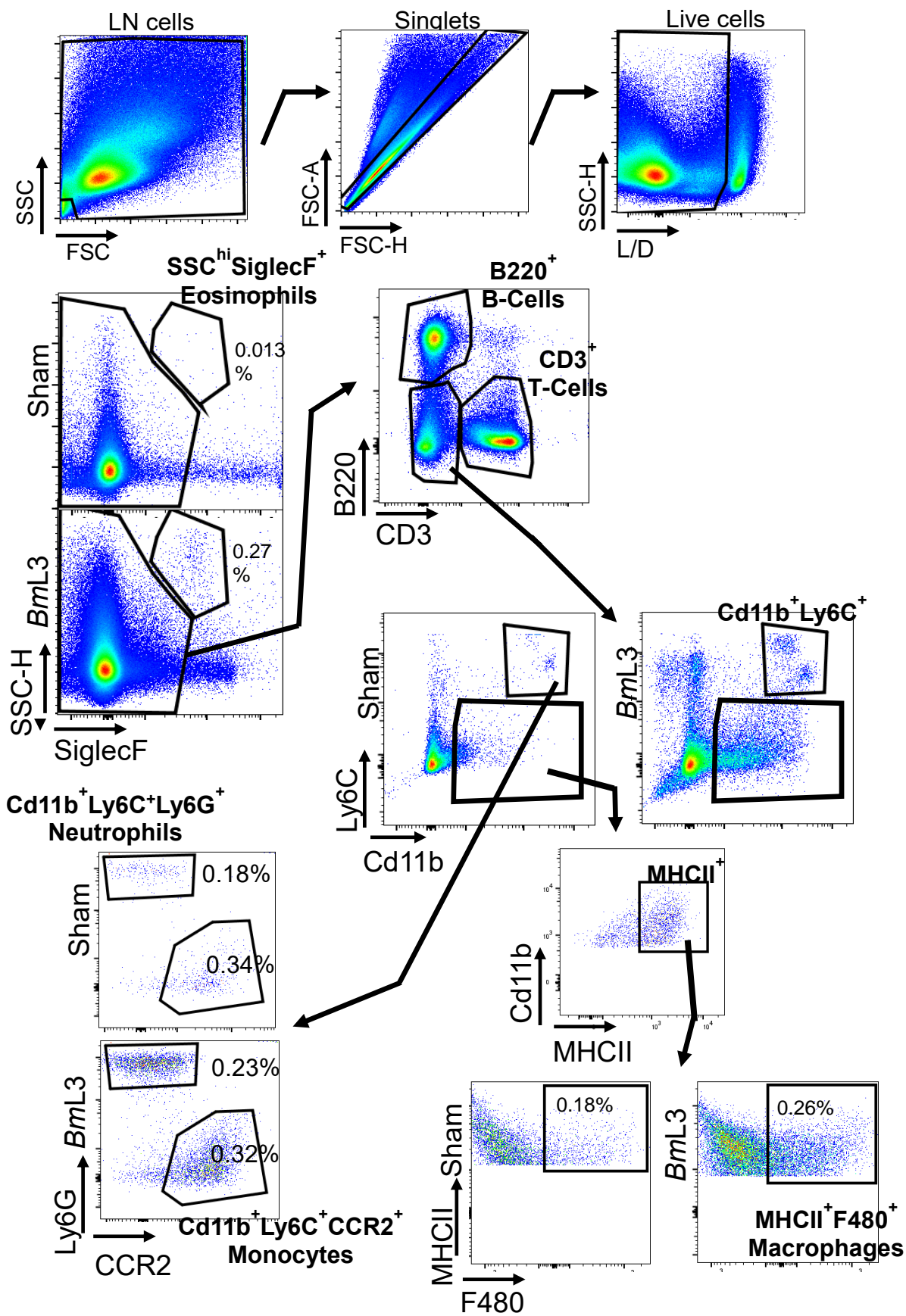
Blue (Sigma, Dorset) solution for Live/Dead cell differentiation. A schematic summary of the assay can be found in Figure 4.7A

4.2.9- CCR2 and clodronate liposome monocyte/macrophage depletion experiments

Following inoculation of 100 *BmL3* into the left hind limb, infected mice were administered either: MC-21 rat anti-mouse CCR2 depleting antibody (a well characterised depleting antibody (Frade *et al.*, 1997) and a kind gift from Professor Matthias Mack) intraperitoneally (i.p.) daily at an amount of 65µg per injection, or clodronate liposome suspensions (Liposoma, supplied by Professor Nico Van Rooijen, VU University Medical Centre, Netherlands) at a concentration of 5mg/ml further diluted 1:2 in dPBS (Sigma, Dorset), subcutaneously (s.c.) across the two infection sites (s.c. top of foot, s.c. caudal to knee joint) every three days. Both mouse groups, together with *BmL3* infected only and sham infected groups were treated for 6 days followed by intravital PDE imaging and other end-point readouts as previously described (2.2.2-2.2.7)

4.2.10-Statistical Analysis

All continuous data was tested for normal distribution using the Kolmogorov-Smirnov test for equal variance. Where data was normally distributed, a two-tailed independent Student's T-Test was used to test for significant differences between two groups. Where data was found to be not normally distributed, a log transformation was first attempted and data re-tested for equal variance. If data remained non-parametric, a two-tailed Mann-Whitney U test was utilised to test for significant differences between two groups. Where more than 2 groups were being compared, a One-way ANOVA was utilised with a Tukey's post-hoc comparisons test to measure differences in parametric data, while a Kruskal-Wallis test was used for non-parametric data with Dunn's post-hoc multiple comparisons test. The mean along with the standard error of the mean (SEM) are reported in all data unless otherwise stated. Significance is indicated as *= $P < 0.05$, **= 0.01 , ***= 0.001 in all figures unless stated otherwise.



Supplementary Figure S4.1: Gating strategy from flow cytometric immunophenotyping for determination of cell populations in sham and *BmL3* infected sdLNs and proximal lymphatic/lymphoid tissues

Immune cell populations from sdLN and proximal lymphatic collecting channels of *BmL3* and Sham infected mice underwent immunophenotyping utilising flow cytometry. The gating strategy utilised is displayed with % live cell populations shown representative of data acquired. Percentages are derived as percentage of total live cells from acquired sample. Percentages of individual cell populations were used to derive final cell numbers from manual live cell counts of total sdLN suspensions as described in methods.

4.3- Results

4.3.1- *B. malayi* infection induces significant increases in multiple leukocyte populations within lymphatic / lymphoid tissues proximal to larval invasion.

To explore a possible role of immune cells in mediating filarial-associated lymphatic pathology, the population dynamics of local leukocyte populations following *BmL3* infection were investigated. sdLN's (pLN, iLN, siLN) proximal to the infection site, along with connecting lymphatic vessels, were harvested and flow-cytometric immunophenotyping undertaken on *BmL3* and sham control mouse cohorts 14 dpi.

BmL3 infected mice were observed to have significantly increased: CD3⁺ T lymphocytes ($1.8 \pm 1.9 \times 10^7$ vs $7.1 \pm 0.6 \times 10^6$ cells, $P < 0.001$), B220⁺ B lymphocytes ($2.4 \pm 0.2 \times 10^7$ vs $2.2 \pm 5.1 \times 10^6$ cells, $P < 0.001$), Cd11b⁺MHCII⁺F4/80⁺ macrophages (M ϕ) ($2.8 \pm 0.5 \times 10^6$ vs $1.6 \pm 0.3 \times 10^6$ cells, $P < 0.05$), CD11b⁺Ly6C⁺CCR2⁺ "inflammatory monocytes" ($7.7 \pm 1.1 \times 10^4$ vs $2.7 \pm 0.4 \times 10^4$ cells $P < 0.001$) and SiglecF⁺SSC^{hi} eosinophils ($4.9 \pm 1.0 \times 10^4$ vs $2 \pm 0.47 \times 10^3$ cells $P < 0.001$) and CD11b⁺Ly6G⁺Ly6G⁺ neutrophils ($1.05 \pm 0.28 \times 10^5$ vs $2 \pm 0.23 \times 10^4$ cells $P < 0.05$) compared to sham control counterparts (Figure 4.1A).

4.3.2- The contribution of 'resident' Tim-4⁺ M ϕ to the overall sdLN M ϕ compartment is significantly diminished following *BmL3* infection.

To investigate if the significant increase of total macrophage populations in sdLN and adjoining lymphatic tissue are due to *in situ* proliferation of resident macrophages or derived from recruited monocytes, Tim-4 macrophage expression, a marker of macrophage residency (Davies *et al.*, 2011; Shaw *et al.*, 2018), was compared. Following 14 day *BmL3* infection, the percentage of macrophages that were Tim-4⁺ was significantly reduced, compared to sham infected counterparts (Figure 4.1B&C; 40.5 ± 6.2 vs 83.1 ± 2.5 % Tim-4⁺ M ϕ , $P < 0.01$).

4.3.3- C57BL/6J mice demonstrate more pronounced expansions of CD11b⁺Ly6C⁺CCR2⁺ inflammatory monocytes and Cd11b⁺MHCII⁺F4/80⁺ M ϕ compared to BALB/c mice in lymphatic / lymphoid tissues proximal to *B. malayi* larval invasion

To investigate if the predisposition to increased lymphatic pathology in C57BL/6J versus BALB/c mice was associated with differences in the quantity or quality of leukocyte increases in lymphatic / lymphoid tissues proximal to sites of initial *B. malayi* larval invasion, flow-cytometric immunophenotyping of infected limb sLN and lymphatic channels isolated at 14dpi were undertaken.

BmL3-infected C57BL/6J and BALB/c mouse cohorts (C57BL/6J L3, BALB/c L3) both displayed significantly increased cellularity within sampled lymphatic / lymphoid tissues compared with respective sham controls (Figure 4.2A; C57BL/6J: $5.5 \pm 0.6 \times 10^7$ vs $2.2 \pm 0.4 \times 10^7$ cells $P < 0.001$, BALB/c: $5.0 \pm 0.8 \times 10^7$ vs $1.5 \pm 0.2 \times 10^7$ cells, $P < 0.001$). No significant differences in cellularity between *BmL3* infected C57BL/6J and BALB/c mouse cohorts were observed (Figure 4.2A).

C57BL/6J *BmL3* infected mice demonstrated a significantly higher fold-change increase (compared to sham controls) of CD11b⁺Ly6C⁺CCR2⁺ monocytes compared with BALB/c *BmL3* infected animals (Figure 4.2B, C57BL/6J: 4.9 ± 0.9 vs BALB/c: 2.2 ± 0.5 fold change, $P < 0.05$). A significantly higher fold-change in CD11b⁺MHCII⁺F4/80⁺ macrophages was also observed in C57BL/6J mice compared with BALB/c animals following *BmL3* infection (Figure 4.2B; C57BL/6J: 2.9 ± 0.5 vs BALB/c: 1.2 ± 0.4 fold change, $P < 0.05$). Comparatively, there were no significant differences in fold-change of B220⁺ B cells or CD3⁺ T cells between C57BL/6J and BALB/c mouse groups following infection (Figure 4.2B).

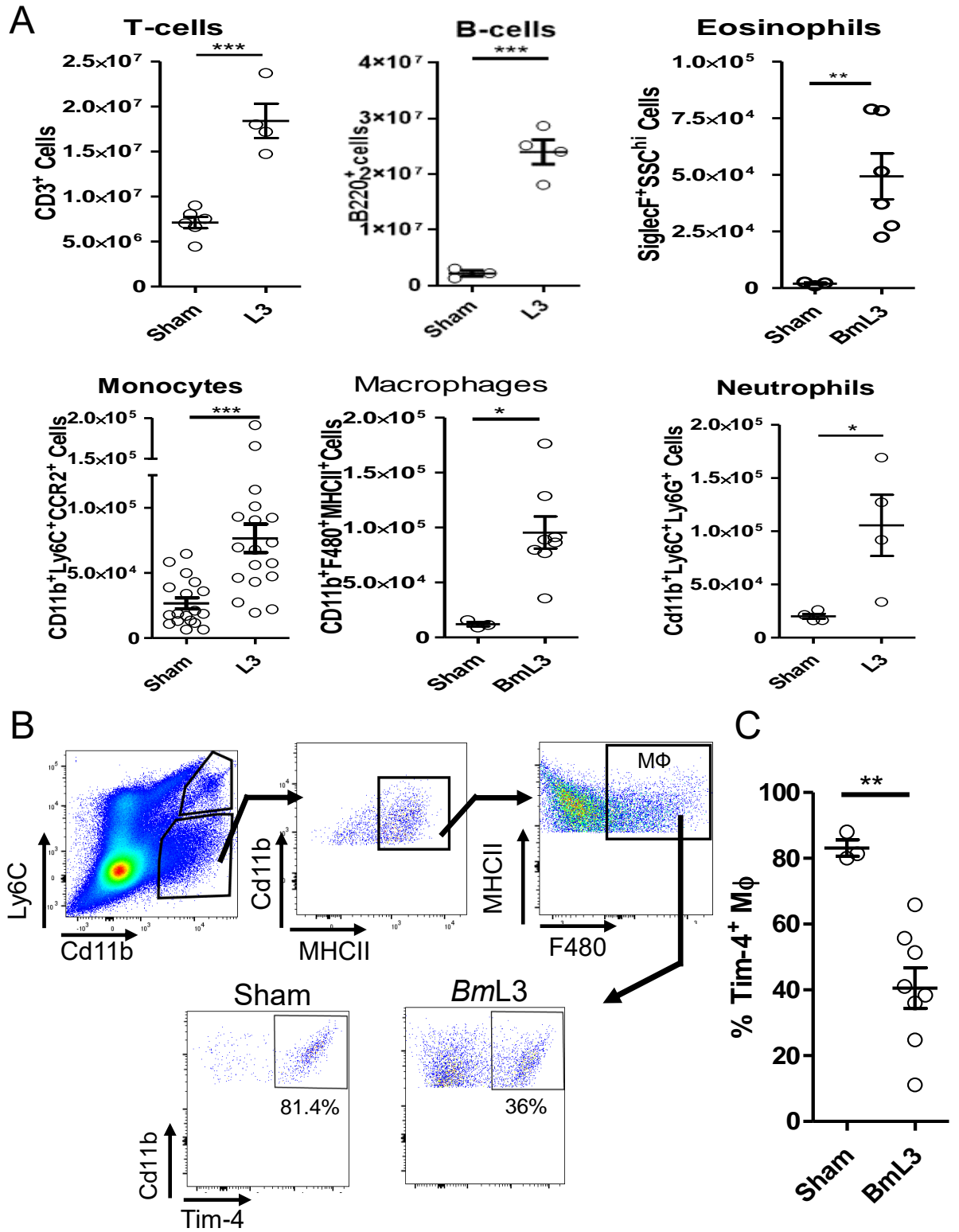


Figure 4.1: Filarial Infection results in significant increases of multiple leukocyte populations in lymphatic / lymphoid tissues proximal to larval invasion.

A) Quantification of immune cell populations from sdLN and proximal lymphatic collecting channels of *BmL3* and Sham infected mice. **B)** Gating strategy utilised to determine Tim-4 expression on macrophages. % Shown are representative values and demonstrate percentage of macrophages that are Tim-4⁺ **C)** Quantified Tim-4⁺ macrophage expression. Horizontal bars represent the mean \pm SEM. Data is pooled from 3 (monocytes) individual experiments (N=18 mice/group), 2 individual experiments (eosinophils and macrophages) (N=3 mice/group) or a single experiment (T-cells, B-cells, Neutrophils and Tim-4⁺ macrophage expression) (N=3-4 mice/group). Significance is indicated as **=P<0.01, ***=P<0.001 derived from a student two-tailed t-test (T+B-cells, Monocytes and Macrophages or a Mann Whitney Test (Eosinophils and Neutrophils).

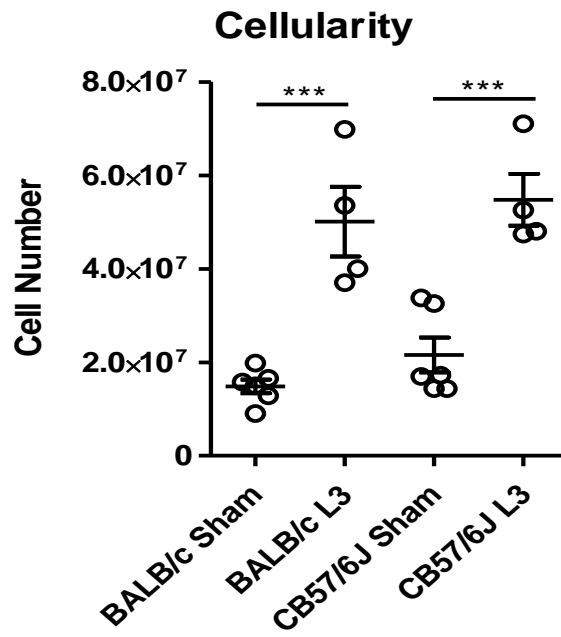
4.3.4- CD11b⁺Ly6C⁺CCR2⁺ monocytes, CD11b⁺MHCII⁺F480⁺ MΦ's and CD3⁺ T-cells are significant sources of lymphangiogenic molecules associated with filarial lymphatic pathology.

Localised cellular sources of circulating lymphangiogenic mediators following *B. malayi* infection (defined in chapter 3) were investigated. LN and lymphatic vessels, proximal to infection, were dissected from *BmL3*-infected or sham infected mice 14dpi and resultant suspensions were cell-sorted using Fluorescent Antibody Cell Sorting (FACS) into: CD11b⁺Ly6C⁺CCR2⁺ inflammatory monocytes, CD3⁺ T lymphocytes, B220⁺ B lymphocytes and CD11b⁺MHCII⁺F4/80⁺ macrophages. The purified immune cell populations were subsequently cultured for 72 hours *ex vivo* followed by Luminex analysis on culture supernatants to quantify secretions of a panel of known angiogenic/lymphangiogenic molecules. Diagrammatical representation of sorting experiments are shown in figure 4.3A

At 14 dpi, isolated CD11b⁺Ly6C⁺CCR2⁺ monocytes secreted significantly higher concentrations of sALK-1 (140.2 IQR:102-182 vs 0 IQR:0-0.75 pg/ml/10⁶ cells P<0.05), prolactin (376.9 IQR: 221- 403 vs 8.8 IQR: 1.7- 16 pg/ml/10⁶ cells P<0.05), amphiregulin (35.3 IQR:30-39 vs 0 IQR: 0- 0.75 pg/ml/10⁶ cells P<0.001), IL-6 (17.2 IQR:6-43 vs 0 IQR- 0-0.75 pg/ml/10⁶ cells P<0.05) compared to sham-infected unsorted lymphatic / lymphoid cell suspensions (Figure 4.3B). Additionally, marginal non-significant increased secretions of: CXCL-1 were recorded when comparing CD11b⁺Ly6C⁺CCR2⁺ monocyte cultures from infected mice with sham-infected counterparts (Figure 4.3B). Purified CD3⁺ T cells secreted significantly higher: amphiregulin (16.8 IQR:14-191.3 vs 0 IQR:0-0.75 pg/ml/10⁶ cells P<0.05), IL-6 (25.4 IQR:13-53 vs 1.186 IQR:0.1-1.8 pg/ml/10⁶ cells P<0.05), Prolactin (102.4 IQR:93-122 vs 17.2 IQR:3-23 pg/ml/10⁶ cells P<0.05), sALK-1 (60.5 IQR:36-64 vs 4.7 IQR:1-12 pg/ml/10⁶ cells P<0.05) and CXCL-1 (36.3 IQR:16-70 vs 0 IQR:0-3.7 pg/ml/10⁶ cells P<0.05) compared with sham-infected purified CD3⁺ T-cell suspensions (Figure 4.3B). Purified B220⁺ B-cells from infected mice secreted significantly higher: Amphiregulin (11.4 IQR:7-12 vs 0 IQR:0-0.75 pg/ml/10⁶ cells P<0.05), Prolactin (82.9 IQR:44-

112 vs 14.4 IQR:7-17 pg/ml/10⁶ cells P<0.05) and IL-6 (20.6 IQR:11-67 vs 0 IQR:0-0.4 pg/ml/10⁶ cells P<0.05) compared to purified sham infected cell counterparts. Finally, CD11b⁺MHCII⁺F480⁺ macrophages from *BmL3* infected mice secreted significantly higher VEGF-C than sham infected counterparts (Figure 4.3B; 264.7 IQR:188-286 vs 154.8 IQR:122-162 pg/ml/10⁶ cells P<0.05)

A



B

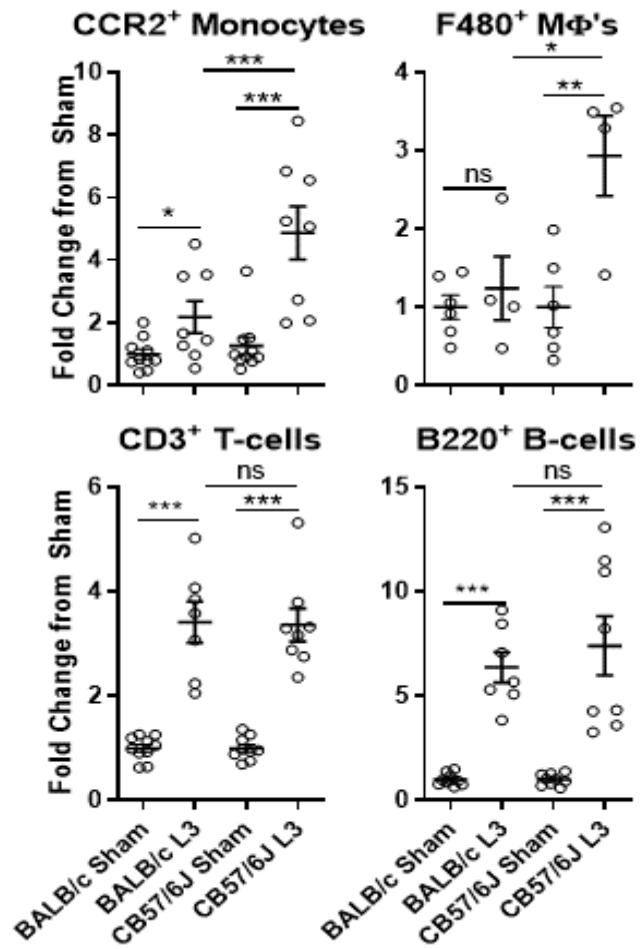


Figure 4.2: Local sdLN CD11b⁺Ly6C⁺CCR2⁺ monocytes and F/480⁺ M Φ 's demonstrate more pronounced expansions in 'high pathology' C57BL/6J mice compared with 'low pathology' BALB/c mice.

A) Quantification of inoculated limb sdLN pooled total cellularity (number of cells) and **B)** sdLN individual immune cell populations between 14dpi BALB/c and CB57/6J mouse strains inoculated with 100 *BmL3*. Fold change increases from relevant sham infected mouse groups are plotted for individual immune cell populations. Horizontal bars represent the mean \pm SEM with data pooled from two individual experiments. Significant differences are indicated as *=P<0.05 ***=P<0.001 derived from a One-way ANOVA with Tukey's post-hoc test (B) or student two-tailed t-test (C)

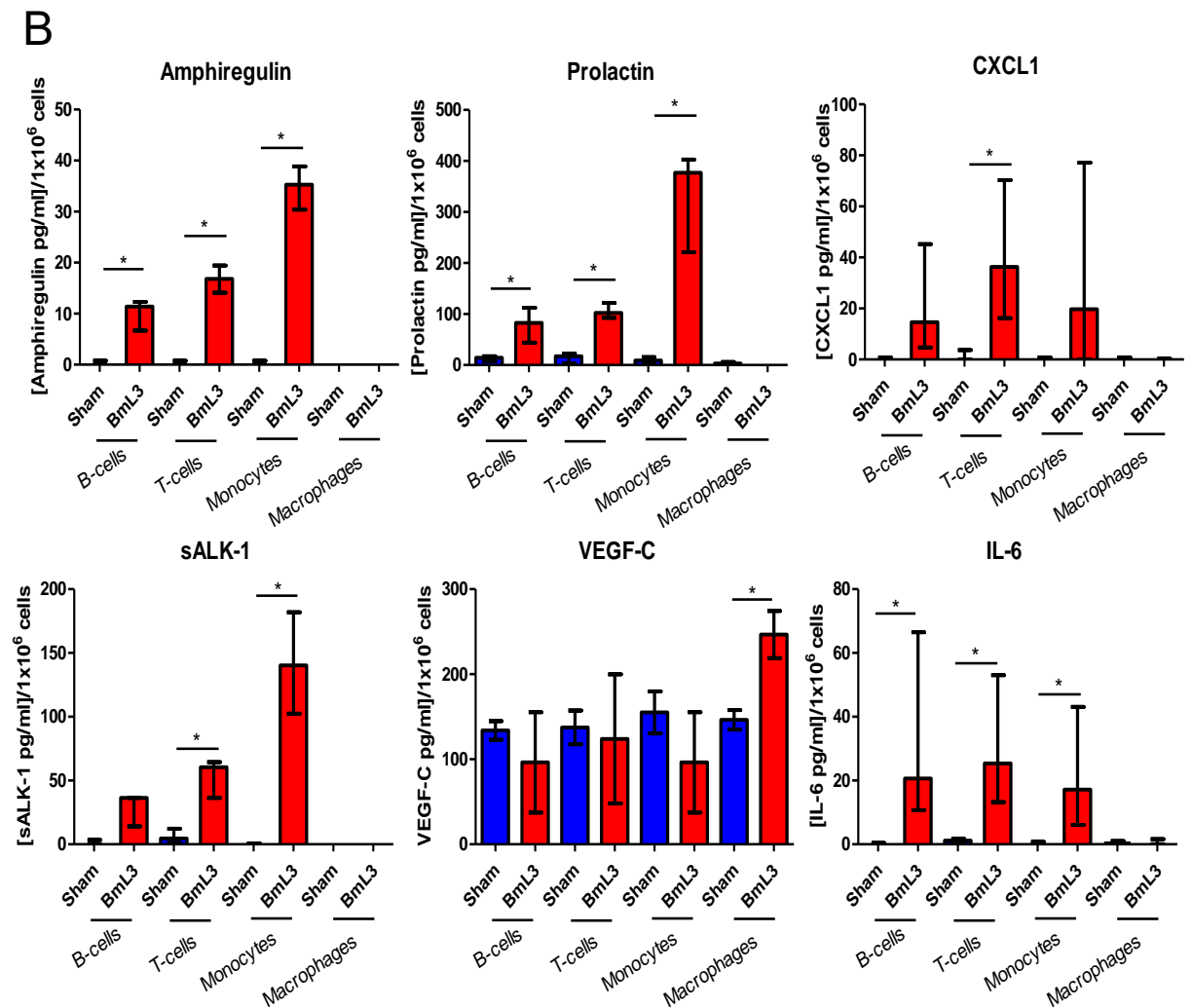
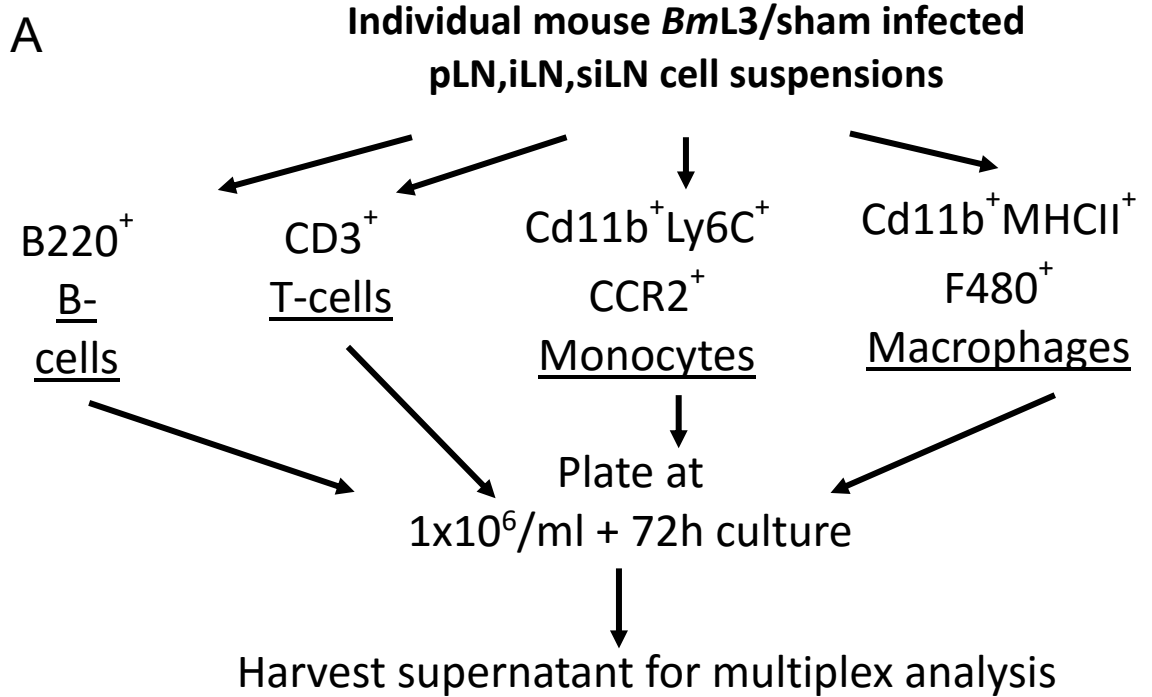


Figure 4.3: Macrophages, monocytes and T-cells derived from lymphatic / lymphoid tissues proximal to lymphatic pathology are significant sources of lymphangiogenic mediators following *B. malayi* infection.

A) Schematic representing workflow of cell sorted cells from mice inoculated with 100 *BmL3* or sham control 14dpi B) Quantification of lymphangiogenic molecule secretion from purified cell populations (red) compared to relevant purified sham infected cell populations (blue). Secretions were normalised to secreted concentration of analyte in pg/ml per 1×10^6 cells ($[\text{analyte pg/ml}] / 1 \times 10^6 \text{ cells}$). Bars represent the median \pm Interquartile range, with significance indicated as *= $P < 0.05$ **= $P < 0.01$ ***= $P < 0.001$ derived from Mann Whitney tests comparing purified infected cell populations to relevant purified sham control populations.

4.3.5-Depletion of phagocytic or CCR2⁺ cells significantly ameliorates *B. malayi* infection-associated lymphatic dilation and lymphatic insufficiency.

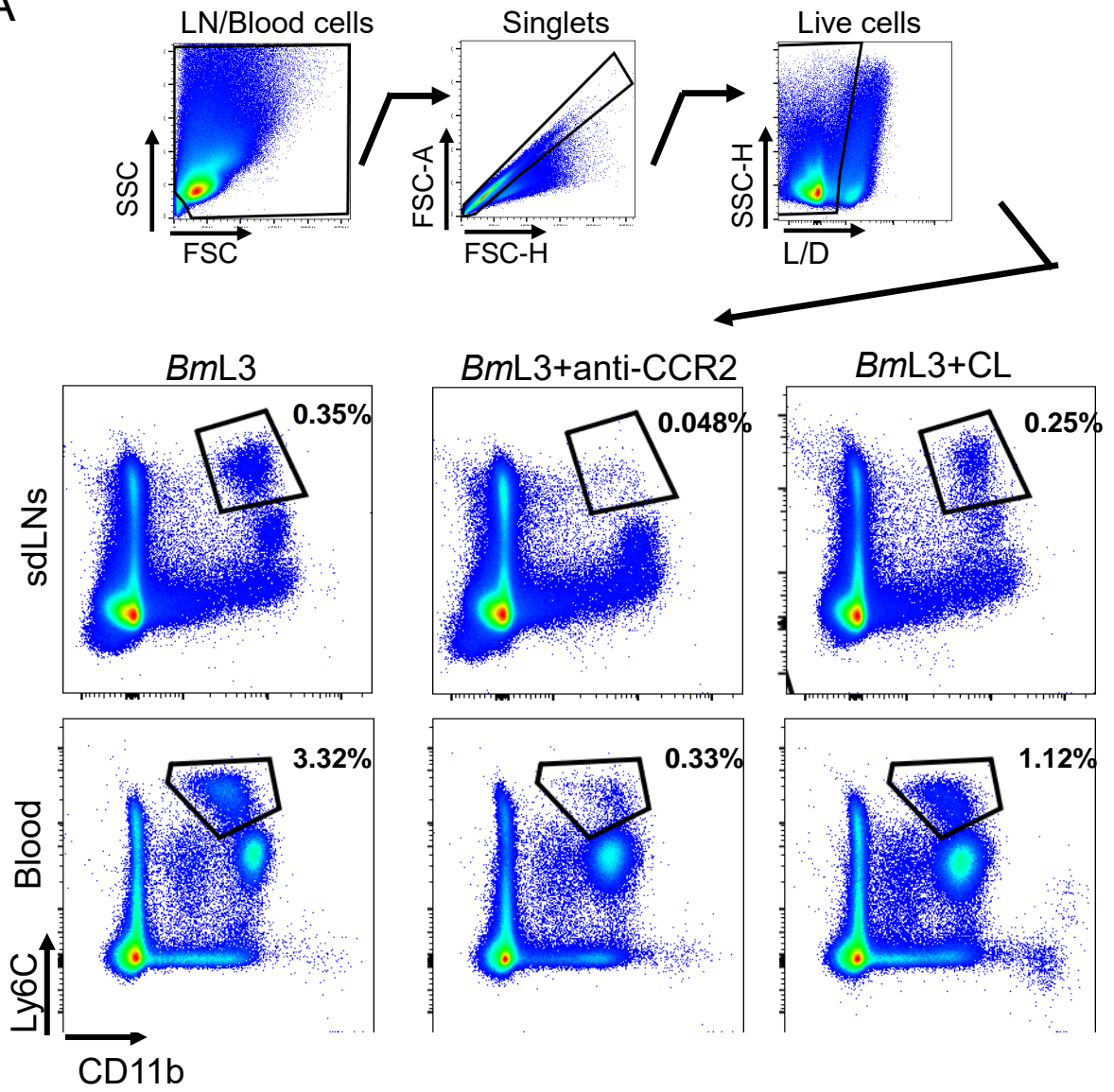
To test whether local increases in either total phagocytic cells, including monocytes and M ϕ , or specific increases in CD11b⁺Ly6C⁺CCR2⁺ monocytes impacted on the extent of lymphatic remodelling and insufficiency following *BmL3* infection, CB57/6J or CB57/6J Prox-1^{GFP} mice were either administered: subcutaneous clodronate liposomes (CL) at initial inoculation site every three days or daily intraperitoneal anti-CCR2 depleting antibody. Treated mice were compared with *BmL3* infection or sham infection controls. CCR2⁺ monocyte depletion was confirmed by flow cytometric immunophenotyping of circulating blood, or lymphatic / lymphoid cell suspensions. Anti-CCR2 (α -CCR2) and CL treated *BmL3* infected mice demonstrating a significant decrease in % CCR2⁺ monocytes in blood (Figure 4.4C; 0.51 ± 0.1 and 1.2 ± 0.4 vs 2.7 ± 0.28 %WBC cells) compared to *BmL3* infected counterparts, while a significant decrease of total CCR2⁺ monocytes in lymphoid/lymphatic tissue proximal to *BmL3* inoculation site was observed post anti-CCR2 antibody treatment (Figure 4.4B; $9.9 \times 10^3 \pm 1940$ vs $5.0 \times 10^4 \pm 4417$ CD11b⁺Ly6C⁺CCR2⁺ cells, $P < 0.05$).

Corroborating data detailed in chapter 2, *BmL3*-infected mouse cohorts displayed significantly increased aberrant lymphatics across dorsal, ventral and left limb PDE-imaged viewpoints compared to sham infected controls (all $P < 0.001$, Figure 4.5A). Additionally, *BmL3* infected mice demonstrated significantly higher retention of fluorescence in the infected left foot up to the pLN (significantly decreased Right/Left foot ratio) (Representative ICG examples 4.5B, $P < 0.001$, Figure 4.5B&C), while significantly higher Evan's Blue was measured in a dermal retention assay compared to sham control mouse groups ($P < 0.05$, Figure 4.5D). Finally, via epifluorescence microscopy analysis, significantly larger apertures of lymphatic vessels, in areas of lymphatic remodelling, were apparent in *BmL3* infected mice, compared with sham infection controls (Representative images 4.5E, $P < 0.01$, Figure 4.5E&F).

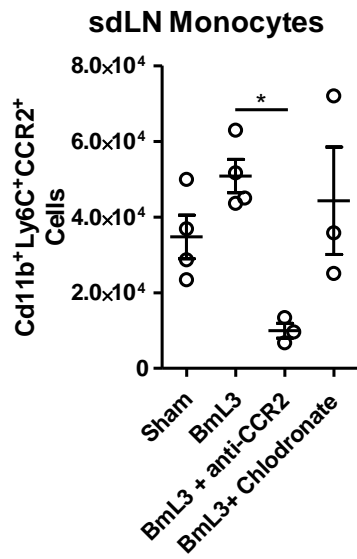
No changes were apparent in aberrant lymphatic patterns, discernible by PDE lymphangiography, between mice infected with *BmL3* and treated with CL or α CCR2-depleting antibody and infection controls (Figure 4.5A). Also, no significant difference in right leg/left leg ICG fluorescent ratio was observed between *BmL3* and *BmL3*+CL mouse groups (Figure 4.5C), however, significantly less Evan's Blue accumulation was apparent in *BmL3*+CL mice compared to *BmL3* infection controls (Figure 4.5D; 0.1 ± 0.04 vs 0.3 ± 0.05 , OD⁶²⁰, $P < 0.05$). *BmL3*+ α CCR2 mouse cohorts displayed significantly less retention of ICG fluorescence in the ROI in the infected left foot up to below the pLN, compared with *BmL3* infection controls (Figure 4.5B&C; 0.6 ± 0.1 vs 0.2 ± 0.03 R/L leg ratio, $P < 0.05$). Additionally, significantly less Evan's Blue accumulated in the surrounding dermis in areas proximal to remodelled lymphatics in the *BmL3*+ α CCR2 mouse group compared to *BmL3* infection controls (Figure 4.5D; 0.1 ± 0.02 vs *BmL3*: 0.3 ± 0.05 OD⁶²⁰, $P < 0.001$). No significant difference was apparent when comparing Evan's Blue retention between *BmL3*+ α CCR2 infected mice and sham infection controls (Figure 4.5D).

Via Prox-1^{GFP} visualisation of lymphatic collecting vessels proximal to *BmL3* infection, a significant decrease in average lymphatic apertures was detected in areas where remodelling was apparent, in both L3+CL and L3+ α CCR2 groups, compared to *BmL3* infection controls (Representative images figure 4.5E. figure 4.5F; average aperture *BmL3* infections: 97.2 ± 8.5 vs 77.1 ± 4.8 , or 75.2 ± 4.4 μ m *BmL3*+CL or *BmL3*+ α CCR2, respectively, both $P < 0.05$).

A



B



C

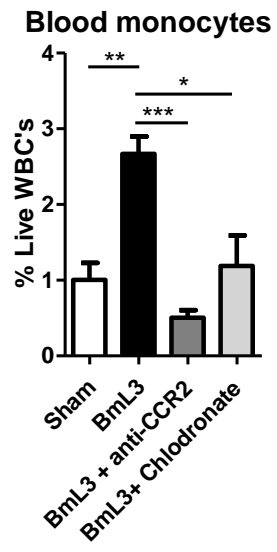


Figure 4.4: Anti-CCR2 treatment significantly reduces circulating and local sdLN Cd11b⁺Ly6C⁺CCR2⁺ monocyte populations in *BmL3* infected mice while CL reduces circulating Cd11b⁺Ly6C⁺CCR2⁺ monocytes.

Sham infected mice were compared with mice inoculated with 100 *BmL3* and treated with either: anti-(α)CCR2 ablating antibody i.p. daily (L3+ α CCR2), clodronate liposomes (CL) s.c. every 3 days (L3+CL) or no further treatment (L3). 2dpi: **A**) Gating strategy used to phenotype both circulating blood and local sdLN Cd11b⁺Ly6C⁺CCR2⁺ monocytes along with representative flow plots demonstrating Cd11b⁺Ly6C⁺CCR2⁺ monocytes (CCR2⁺ expression was confirmed on the Cd11b⁺Ly6C⁺ gate) percentages shown demonstrate percentage of total live cells **B**) Quantified Cd11b⁺Ly6C⁺CCR2⁺ monocytes as total cell number in lymphoid and lymphatic tissues proximal to *BmL3* infection site **C**) Quantified Cd11b⁺Ly6C⁺CCR2⁺ monocytes as percentage of White blood cell (WBC) compartment of blood horizontal lines represent mean \pm SEM while bars plot mean \pm SEM Data is from a single experiment (N=3-4 mice/group) with statistical significance indicated as *=P<0.05 **=P<0.01 ***=P<0.001 derived from a one-way ANOVA with Tukey's multiple comparisons post-hoc test.

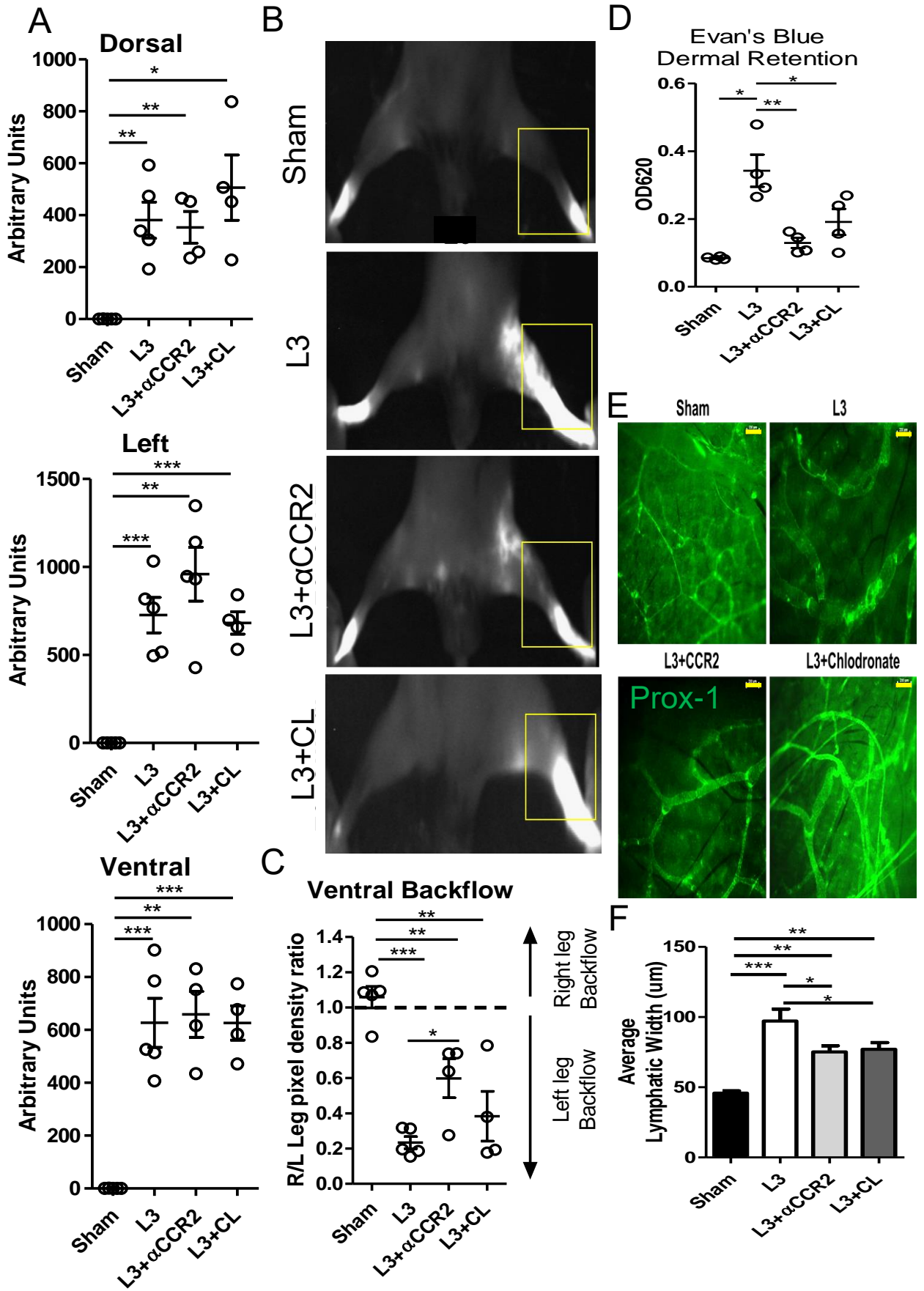


Figure 4.5: Depletion of phagocytes or CCR2⁺ monocytes significantly ameliorates filarial associated lymphatic insufficiency and local lymphatic vessel dilation post *BmL3* infection.

Sham infected mice were compared with mice inoculated with 100 *BmL3* and treated with either: anti-(α)CCR2 ablating antibody i.p. daily (L3+ α CCR2), clodronate liposomes (CL) s.c. every 3 days (L3+CL) or no further treatment (L3). 6dpi: **A)** Quantification of aberrant lymphatics using PDE imaging in dorsal, ventral and left leg viewpoints **B)** Representative PDE images demonstrating lymphatic insufficiency- yellow box highlights differences in ICG retention between groups **C)** Quantification of lymphatic insufficiency using ICG fluorescence ratio of ROI from ankle to below pLN between mouse groups **D)** Evan's Blue Dermal retention assay quantifying Evan's Blue retention in inoculated limb 6dpi **E)** Representative Prox-1^{GFP} fluorescence microscopy images from all experimental groups demonstrating differences in lymphatic vessel aperture. Yellow scale bar is 100 μ m **F)** Lymphatic aperture measurements of Prox-1 GFP epifluorescence in zones of dermis corresponding with ICG remodelling or matched zones in sham-infected animals. Horizontal lines of **(A),(C)** and **(D)** represent mean \pm SEM while bars plot mean \pm SEM in **(F)**, Data is from a single experiment with statistical significance indicated as *=P<0.05 **=P<0.01 ***=P<0.001 derived from a one-way ANOVA with Tukey's multiple comparison post-hoc test.

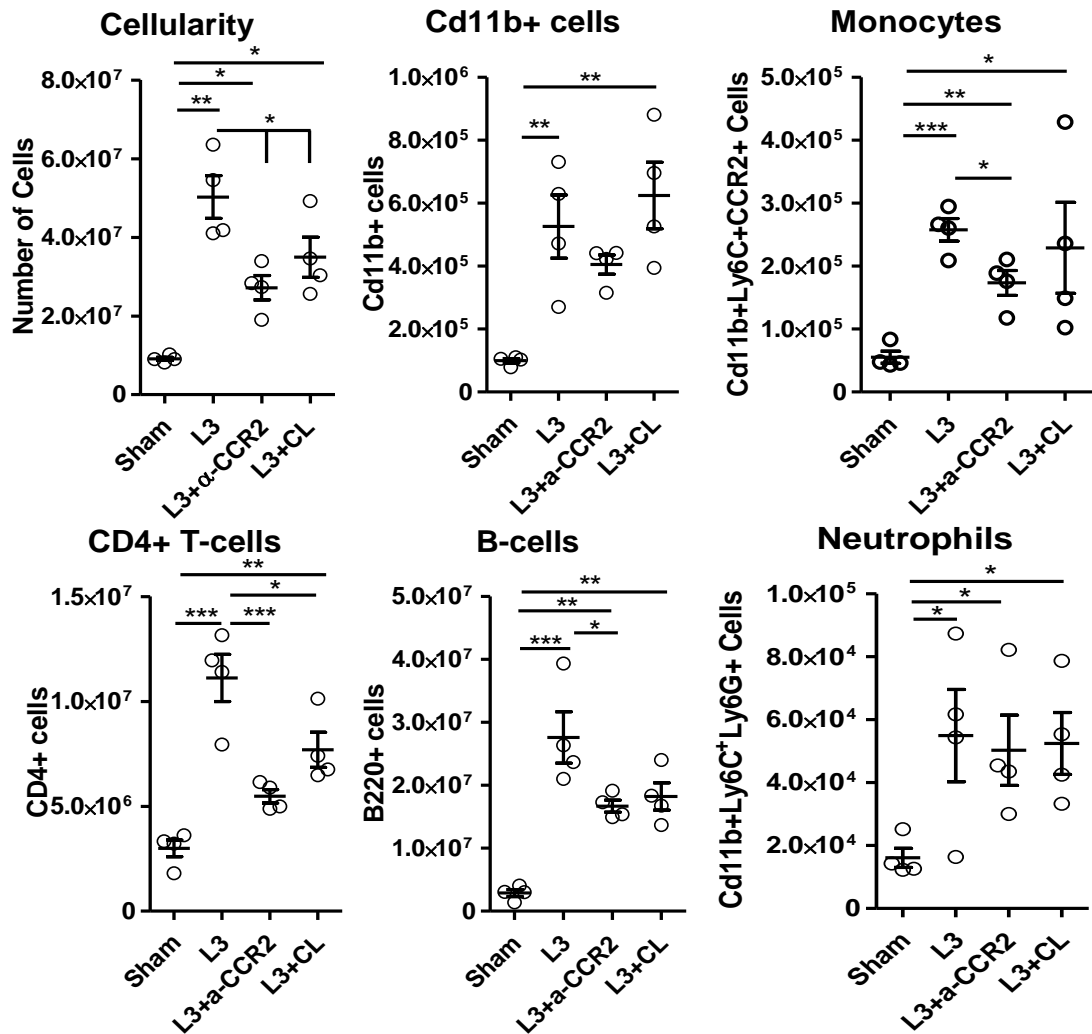


Figure 4.6: α-CCR2 and CL treatment significantly reduces multiple leukocyte populations in sdLNs local to inoculation site.

Mouse groups were subcutaneously infected in the left hind limb with 100 *BmL3* or sham controls. Mouse groups were then either administered chlodronate SC into infected hind limb (L3+CL) every 3 days, anti-CCR2 depleting antibody (L3+α-CCR2) IP every day or PBS SC into infected hind limb (L3) every 2 days. 6dpi, flow cytometric immunophenotyping was undertaken on dissected draining LN's and lymphatic vessels of the infected limb on all groups for comparison of cell populations. All graphs plot the mean ± SEM, each data point plotted represents a single mouse (N=4 or 5 per group). Data is from a single experiment * = P < 0.05 ** = P < 0.01 *** = P < 0.001 derived from a One-way ANOVA with Tukey's multiple comparisons test.

4.3.6 α -CCR2 and CL treatment results in significant reductions of a multitude of leukocyte populations in local sdLN's proximal to initial *BmL3* infection site.

To investigate the effect of monocyte depletion on early immune cell dynamics to *BmL3* infection, sdLNs of all mouse groups were immunophenotyped at experimental end point (6dpi)

Both CL and α -CCR2 treated *BmL3* infected cohorts demonstrated significantly reduced total sdLN cellularity compared to *BmL3* infected only mice (Figure 4.6; $3.5 \times 10^7 \pm 3.1 \times 10^6$ and $2.7 \times 10^7 \pm 3.1 \times 10^6$ vs $5 \times 10^7 \pm 5.4 \times 10^6$ cells respectively, $P < 0.05$). In addition, CL treated groups demonstrated significantly reduced CD4⁺ T-cell populations compared to *BmL3* infected only ($7.7 \times 10^6 \pm 8.4 \times 10^5$ vs $1.1 \times 10^7 \pm 1.1 \times 10^6$ CD4⁺ T-cells) (Figure 4.6). α -CCR2 treated infected mouse cohorts demonstrated significant reductions in sdLN: Cd11b⁺Ly6C⁺CCR2⁺ monocyte ($1.7 \times 10^5 \pm 2 \times 10^4$ vs $2.6 \times 10^5 \pm 1.8 \times 10^4$ Cd11b⁺Ly6C⁺CCR2 cells, $P < 0.05$), CD4⁺ T-cells ($5.5 \times 10^6 \pm 3.2 \times 10^5$ vs $11 \times 10^7 \pm 1.1 \times 10^6$ CD4⁺ T-cells, $P < 0.001$) and B220⁺ B-cells ($1.7 \times 10^7 \pm 9.6 \times 10^5$ vs $2.8 \times 10^7 \pm 4.1 \times 10^6$ B220⁺ B-cells, $P < 0.05$) compared to *BmL3* infected mice (Figure 4.6). Marginal non-significant decreases of total Cd11b⁺ cells were recorded when comparing α -CCR2 treated mice to infected only counterparts (Figure 4.6).

4.3.7 Exposure of monocyte-derived M ϕ to live *BmL3* or *BmL3* extract induce significant LEC survival/proliferation of lymphatic endothelial cells *in vitro*

To further investigate if monocytes/macrophages stimulated with L3 larval material could directly contribute to lymphatic endothelial activation, an *in vitro* co-culture proliferation assay was developed. Human THP-1 monocytes were differentiated into M ϕ before stimulation with *BmL3* extract (*BmL3E*) or live *BmL3* followed by addition in co-culture to human lymphatic endothelial cells (LECs). LEC survival/proliferation in the presence of unstimulated M ϕ , *BmL3E*- or *BmL3*-stimulated M ϕ were then compared (Schematic of co-culture assay displayed in Figure 4.7A).

No significant fold change increase in LEC numbers (from basal media controls) were observed between LECs cultured with basal medium alone and LECs co-cultured with THP-1 differentiated, unstimulated M ϕ ('M0' (Figure 4.7B). LECs co-cultured with THP-1 differentiated M ϕ stimulated with *BmL3E* displayed a significantly increased fold-change in LEC cell number, compared to both LECs co-cultured in basal medium only (2.2 ± 0.3 vs 0.9 ± 0.03 fold-change, $P < 0.001$) or M0 (1.1 ± 0.04 fold-change, $P < 0.001$, Figure 4.7B). Additionally, LECs co-cultured with THP-1 differentiated M ϕ stimulated with live *BmL3* displayed a significantly higher fold-change in proliferation, compared to either LECs co-cultured in basal medium (1.9 ± 0.1 fold-change increase, $P < 0.001$) or LECs cultured in the presence of M0 (1.9 ± 0.1 fold-change increase, $P < 0.001$, Figure 4.7B)

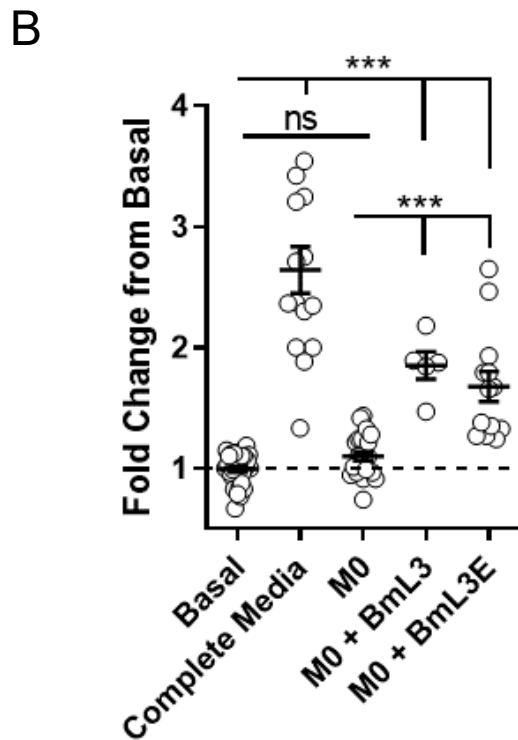
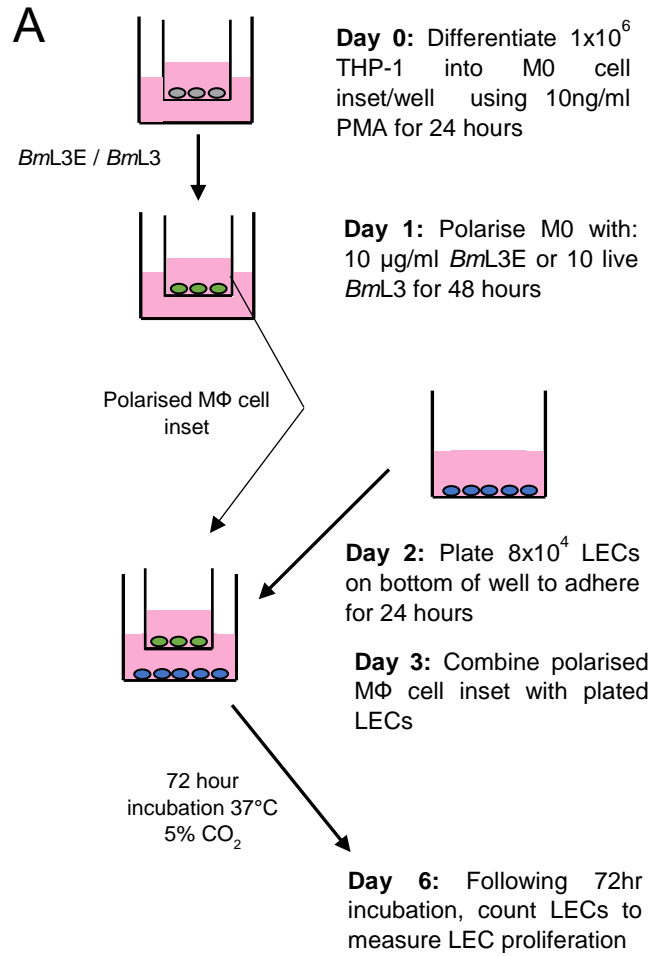


Figure 4.7: Exposure of monocyte derived macrophages to *BmL3E* or Live L3 larvae induces a 'lymphangiogenic M ϕ phenotype' that drives significant survival/proliferation of LECs *in vitro*.

A) Schematic of the developed THP-1 monocyte/macrophage co-culture assay with Lymphatic Endothelial Cells (LECs) **B)** Quantification of LEC proliferation, normalised as fold-change increase from basal medium control cultures. Horizontal bars represent the mean \pm SEM. Data is pooled from a single (live L3) or 2 (all other conditions) individual experiments with significance indicated as ***=P<0.01, ns=non-significant derived from a one-way ANOVA with Tukey's multiple comparison post-hoc test.

4.4- Discussion

Data discussed in Chapter 2 demonstrates the rapid onset of lymphatic pathologies following filarial *BmL3* infection, while Chapter 3 elucidated some of the lymphangiogenic molecules that are significantly upregulated, and therefore associated with pathology. The primary aim of this chapter, was to interrogate the cellular sources of these highly angiogenic/lymphangiogenic molecules and the cellular mechanisms that may regulate their release into the microenvironment proximal to the site of filarial infection *BmL3* larval infection.

Infecting *B.malayi* filarial larvae will be exposed to distinct cellular microenvironments as migration through dermal tissues, cutaneous tissues and peripheral lymphatics progresses in the first 24-48h (Demonstrated in chapter 2). *BmL3* invasion and establishment into the draining pre-collecting lymphatic vessels, results in physical interaction with lymphatic endothelial cells (LECs) lining lymphatic vessels. Data from Chapter two suggests a robust and rapid activation of host immune responses following filarial infection, while there is established literature that details induction of a robust multi-faceted primary adaptive immune response to filarial larval infection (Allen and Maizels, 2011; Babu and Nutman, 2014). Resultant host early innate and then augmented adaptive immune activation, will expose larvae to a repertoire of recruited effector immune cells as part of robust anti-parasitic host responses, including: T-cells (Babu and Nutman, 2003), B-cells (Hussain and Ottesen, 1985), monocytes (Babu, Kumaraswami and Nutman, 2009), eosinophils (Chirgwin *et al.*, 2005; Turner *et al.*, 2018) and neutrophils (Al-Qaoud *et al.*, 2000; Tamarozzi *et al.*, 2016) which have all been shown to play a role in host anti-filarial responses.

The central hypothesis of this research chapter proposed that facets of the host immune response and relevant immune effector cells recruited to the site of larval infection are causal in induction of lymphatic pathology. This hypothesis was based on host-strain differences in magnitude of pathology development and prime / challenge infections could induce increases in lymphatic remodelling (chapter 2).

Immunophenotyping of lymphatic and lymphoid tissues proximal to *BmL3* infection demonstrated significant expansion of a typical adaptive immune response including T-cell and B-cells, 14 dpi. Additionally, significant expansions in $\text{Cd11b}^+\text{Ly6C}^+\text{CCR2}^+$ 'inflammatory' monocytes and $\text{Cd11b}^+\text{MHCII}^+\text{F480}^+$ $\text{M}\phi$ following *BmL3* inoculation were observed, demonstrating active recruitment, or proliferation, of these myeloid cells at sites proximal to filarial infection. "Classical" CCR2^+ monocytes are of bone marrow myeloid lineage that circulate in the bloodstream (Guilliams, Mildner and Yona, 2018). In response to infection, activated monocytes undergo rapid proliferation, before subsequent recruitment to areas local to infection, mediated by migration along chemokine gradients such as the ligand to CCR2 , CCL2 (Shi and Pamer, 2011). Because monocytes recruited to sites of infection can trans-differentiate into inflammatory DC or $\text{M}\phi$, which can subsequently drain to be retained in the local LN (Shi and Pamer, 2011), increases in CD11c or $\text{CD11b}^+\text{MHCII}^+\text{F4/80}$ cells observed by 14dpi may putatively derive from the recruited inflammatory monocyte pool.

The marked loss of tissue residency marker Tim-4^+ from the total $\text{M}\phi$ compartment, coupled with a significant increase of non-tissue resident Tim-4^- $\text{M}\phi$ post *BmL3* infection would be indicative of the strong expansion of the $\text{M}\phi$ compartment in sdLNs being primarily derived from recruited inflammatory monocytes. With recent work questioning the reliability of Tim-4 as a residency marker (Campbell *et al.*, 2018), however, further studies including: use of other identifying tissue residency markers such as GATA6 and CD102 (Rosas *et al.*, 2014; Bain *et al.*, 2016), or bone marrow chimeras to precisely track macrophage origin may better strengthen the assertion that the increase in $\text{M}\phi$ is inflammatory monocyte derived. Recruited monocytes and terminally-differentiated DC or $\text{M}\phi$ of monocytic origin can influence immune priming events in the initiation of an adaptive immune response within LN. Therefore, it is also plausible that recruited CCR2 inflammatory monocytes influence the degree of CD3 and B220 lymphocyte expansions recorded following *BmL3* infection.

To further investigate the possible contribution of these immune cell expansions in filarial lymphatic pathology, the predisposition of BALB/c and

CB56BL/6J mice to low or high pathology development, respectively, was exploited. While expansion of T-cells, B-cells and DC were all non-significantly different between the BALB/c and C57BL/6J *BmL3* infected mouse groups, significantly higher increases of Cd11b⁺Ly6C⁺CCR2⁺ monocytes and CD11b⁺MHCII⁺F4/80 M ϕ in the high pathology C57BL/6J mice was demonstrable, 14dpi with *BmL3*. This suggested a possible functional role of both CD11b⁺Ly6C⁺CCR2⁺ monocytes and/or CD11b⁺MHCII⁺F4/80 M ϕ in inducing or augmenting pathology post-filarial infection.

Several studies have established the role for M ϕ in the host immune response to filarial infection, with evidence suggesting divergent roles dependent on polarisation of the macrophage. Evidence has suggested a pro-inflammatory role for 'Classically activated' M ϕ (sometimes referred to as 'M1'), differentiating in response to worm inhabitation and death (Rajan *et al.*, 1996), thus acting as an effector mechanism for filarial clearance. Conversely, macrophages have been implicated in facilitating chronic filarial infection by permitting filarial immune evasion, often through macrophage mediated CD4⁺ T-cell hypo-responsiveness/tolerance after polarisation to a regulatory 'alternatively activated macrophage' (AAM) phenotype (sometimes referred to as 'M2') (Taylor *et al.*, 2006). This is likely to be an over simplification of macrophage heterogeneity following filarial infection, however, as recent work in our lab has identified that rapid expansion of macrophages, concomitant with polarisation to an AAM ϕ phenotype occurs following filarial infection and is crucial in recruiting eosinophils to the site of infection that facilitates worm expulsion (Turner *et al.*, 2018). Further, variation in plasticity and origin of AAM ϕ in response to filarial infection, at least following parasitism of serous cavities, is implicated in relative susceptibility or resistance (Campbell *et al.*, 2018)

To investigate if the recruited CCR2⁺ monocytes or CD11b⁺MHCII⁺F4/80 M ϕ demonstrated pro-lymphangiogenic phenotype upon *BmL3* infection, supernatants harvested from *ex-vivo* cultured purified cell populations from *BmL3* or sham infected cohorts were assayed for concentrations of

lymphangiogenic molecules identified as increased in circulation of mice post-infection (chapter 3). Data from these experiments demonstrated that CD11b⁺Ly6C⁺CCR2⁺ inflammatory monocytes recruited to sites of *BmL3* infection secreted increased quantities of sALK-1, prolactin, IL-6 and amphiregulin, when compared to purified monocyte secretions from sham animals. Additionally, CD11b⁺MHCII⁺F4/80 M ϕ from *BmL3* infected cohorts were shown to secrete significantly higher quantities of VEGF-C than sham controls. The evidence presented above demonstrates that the *BmL3* induced increase in the M ϕ compartment is likely driven by recruitment and differentiation of inflammatory CCR2⁺ monocytes. Together, the data is suggestive of a cellular mechanism by which recruited monocytes themselves, or their differentiation into macrophages, release a milieu of highly lymphangiogenic molecules which directly mediate early filarial associated lymphatic remodelling. In addition to the roles of M ϕ in immune/inflammatory mediation- recent work has identified a role for M ϕ in both vascular remodelling/angiogenesis and lymphatic remodelling/lymphangiogenesis.

In the context of inflammatory-associated lymphangiogenesis (IAL), elegant studies have shown that recruited M ϕ can both secrete a milieu of factors that contribute to increased lymphangiogenesis (Including VEGF-C and Angiopoietin-2) in areas of infection (Kataru *et al.*, 2009; Ran and Montgomery, 2012), as well as undergo trans-differentiation themselves into a lymphatic endothelial cell progenitor which facilitates in vessel sprouting and growth (Maruyama *et al.*, 2005; Hall *et al.*, 2012). Further, M ϕ drive changes to the extracellular matrix (ECM) through secretion of matrix metalloproteases, such as matrix metalloprotease 9 (MMP-9), degrading established ECM to facilitate novel remodelling of lymphatic and vascular channels during lymphangiogenesis.(Böhmer *et al.*, 2010). In oncology, work has shown that macrophages recruited to the tumour microenvironment are 'hijacked' into a highly angiogenic/lymphangiogenic phenotype termed 'Tumour-Associated Macrophages' (TAMs). TAMs have been shown to degrade extracellular matrix (Huang *et al.*, 2002) and secrete a variety of growth factors that facilitate vascular remodelling/angiogenesis, including

factors identified to be increased following *BmL3* infection including bFGF-2, and VEGFs (Lewis *et al.*, 2000; Ly *et al.*, 2010; Riabov *et al.*, 2014). Additionally, studies have elucidated a role for inflammatory monocytes, specifically Tie-2 expressing monocytes (TEMs), with the ability to drive lymphangiogenesis and thus remodelling of the lymphatic architecture in the tumour microenvironment, (De Palma *et al.*, 2005; Venneri *et al.*, 2007). Taken together, the identified pro-lymphangiogenic/angiogenic monocytes and macrophages that are recruited proximal to areas of *BmL3* infection play as strong contributing role to the observed lymphatic pathology following filarial infection

Purified and assayed cell secretions of CD3⁺ T-cells and B220⁺ B-cells from *BmL3* infected cohorts demonstrated that they also secrete significant quantities of: amphiregulin, prolactin and IL-6 (T and B-cells) as well as CXCL-1 and sALK-1 (T-cells) compared to purified sham counterparts. This is indicative of a potential role of T and B-cells in filarial associated lymphatic remodelling, however the near two fold lower secreted concentrations when compared to monocytes and macrophages may suggest these cells are less important contributors to the highly lymphangiogenic milieu that is secreted in response to *BmL3* infection and mediates the significant pathological remodelling observed. Previous work has implicated a role for CD4⁺ T-cells in driving fibrosis and lymphoedema, as depletion resulted in attenuated levels of pathology (Zampell *et al.*, 2012). This is further supported from studies involving filarial infection of lymphocyte deficient mice strains, where lymphoedematous pathology is only manifest upon reconstitution of lymphocyte populations by adoptive transfer (Vincent *et al.*, 1984; Bosma and Carroll, 1991). T-cells have also been implicated in inducing angiogenesis through direct secretion of VEGFs, driving vascular remodelling (Mor, Quintana and Cohen, 2004) although increased secretion of VEGF-s by purified CD3⁺ T-cells was not observed in this study. Alternatively, studies have shown that excess lymphangiogenesis, that contributes to lymphoedematous pathologies in a mouse model, requires cooperation between CD4⁺ T-cells and macrophages, with ablation of CD4⁺ T-cell populations abrogating the severity of lymphangiogenesis and

subsequent pathology observed (Ogata *et al.*, 2016). This suggests that increased, but lower secretions of lymphangiogenic molecules in T-cells may synergise with monocyte and macrophage secretions to directly mediate filarial induced lymphatic remodelling, while it cannot be ruled out that T-cell 'help' indirectly supports lymphangiogenic pathology by educating recruited monocytes and macrophages into a pro-lymphangiogenic phenotype following *BmL3* infection as well as induction of a primary adaptive immune response. A multitude of previous work has identified a key role for B-cells in remodelling of the lymph node lymphatic architecture following infection (Kumar *et al.*, 2010; Abe *et al.*, 2012). Immunostaining of infected LN's demonstrated B-cells as a major source of VEGF-A, and ablation of either B-cells or administration of VEGF-A blocking antibodies reversed lymphatic expansion of lymph nodes following infection (Angeli *et al.*, 2006). The previous work detailed therefore suggests that it is plausible that other contributing lymphangiogenic molecules that were observed in the data to be secreted by B-cells contribute to the filarial associated remodelling. It cannot, however be ruled out that the secretion of lymphangiogenic factors by B-cells is restricted to solely within the lymph node architecture facilitating lymph node expansion, as is observed following *BmL3* infection (Chapter 2), and is primarily to mediate appropriate immune responses rather mediating extra nodal filarial associated lymphatic remodelling. Further work utilising immune-staining and histology to locate-cell infiltrates near to areas of lymphatic remodelling may help to elucidate whether a lymphangiogenic role for B-cells in filarial driven lymphatic remodelling exists.

To further interrogate the importance of monocytes/macrophages in driving filarial associated lymphatic pathology *in vivo*, α -CCR2 antibody mediated Cd11b⁺Ly6C⁺CCR2⁺ monocyte depletion and CL mediated phagocyte depletion were administered to mice concurrent with *BmL3* infection. The effects of these treatments on severity of lymphatic remodelling and insufficiency were then investigated. α -CCR2 and CL treatment significantly decreased circulating Cd11b⁺Ly6C⁺CCR2⁺ monocyte populations by approximately 80% and 40% respectively, while local sdLN accumulation of Cd11b⁺Ly6C⁺CCR2⁺ monocytes were significantly reduced by approximately

80% following α -CCR2 treatment, confirming the efficacy of both treatments in ablating inflammatory monocytes.

BmL3+CL mice displayed no significant changes to PDE imaged ICG dye retention in the infected limb when compared to *BmL3* mice, however a significant reduction in Evan's blue dermal retention was observed. Additionally, via epifluorescence microscopy, the average lymphatic vessel aperture was significantly lower in *BmL3*+CL mice compared to *BmL3* mice suggesting amelioration of *BmL3* induced lymphatic vessel dilation, following CL mediated ablation of phagocytes local to *BmL3* infection. Higher retention of ICG dye, observed in the infected limb of *BmL3* infected mice, was significantly reduced in L3+ α CCR2 mouse cohorts suggesting that ablation of inflammatory monocytes reverses *BmL3* mediated lymphatic insufficiency. This was further corroborated by significantly lower dermal retention of Evan's Blue in L3+ α -CCR2 cohorts compared to the *BmL3*. Additionally, L3+ α CCR2 mouse cohorts presented a partial reversal of *BmL3* induced lymphatic vessel dilation, demonstrated by significantly smaller average aperture of Prox-1+ collecting vessels. Taken together, the data suggests that CL mediated ablation of phagocytic cells, such as Cd11b⁺MHCII⁺F480⁺ M Φ , or ablation of Cd11b⁺Ly6C⁺CCR2⁺ monocytes, which are likely the source of increased local M Φ populations, significantly ameliorated *BmL3* induced lymphatic dilation and pathological lymphatic insufficiency. This would indicate that the rapid expansion of pro-lymphangiogenic M Φ and inflammatory monocytes, observed following *BmL3* infection, play a driving role in inducing filarial associated lymphatic pathology partly by inducing local lymphatic insufficiency by mediating local lymphatic vessel dilation in response to *BmL3* infection.

Intravital PDE imaging in the intervention experiments demonstrated that neither L3+CL or L3+ α -CCR2 mouse cohorts displayed significant changes in quantity of aberrant lymphatics, when compared to *BmL3* infected mice alone, further, both L3+ α -CCR2 and L3+CL groups displayed significantly higher aberrant lymphatics across all imaged viewpoints, compared to sham infection controls. Together, this data would indicate that neither Cd11b⁺Ly6C⁺CCR2⁺ monocytes or Cd11b⁺MHCII⁺F480⁺ macrophages are

implicated in lymphatic remodelling/neovascularisation associated with filarial infection, thus are not the sole cellular drivers of filarial pathology. As residual populations of Cd11b⁺Ly6C⁺CCR2⁺ monocytes were observed in α -CCR2 and CL treated groups however, it cannot be discounted that the surviving populations may provide adequate numbers to initiate a level of filarial associated neovascularisation. Further, while potent depletion of inflammatory monocytes was observed in α -CCR2 and CL treated groups 2dpi, much lower levels of monocyte reduction was manifest at the 6dpi experimental endpoint, with monocyte accumulation only reduced by 50% at 6dpi, compared to 80% at 2dpi. The daily α -CCR2 and tri-daily CL treatment regimes utilised, would provide sufficient concentration of depleting antibody or clodronate throughout the 6 day experimental period. The drop in efficacy of monocyte depletion, therefore, could suggest a transient nature to monocyte depletion in both treatment groups, with resistance to ablating antibodies a well characterised phenomenon (Villamor, Montserrat and Colomer, 2003) The transient depletion could suggest there was sufficient time for the influx of ablation antibody-resistant to provide sufficient lymphangiogenic signalling to induce filarial lymphatic remodelling. Alternatively, and as demonstrated above by secretion of lymphangiogenic molecules from T and B-cells following BmL3 infection, other cellular sources are likely to contribute to the released lymphangiogenic milieu in the microenvironment surrounding larval infection, with T and B cell derived lymphangiogenic molecules either offering redundancy/compensation in the face of monocyte/macrophage ablation- driving neovascularisation type lymphatic remodelling in their absence- or are themselves more significant mediators of the neovascularisation observed.

Treatment with CL and α -CCR2 markedly reduced the accumulation of sdLN CD4⁺ T-cells compared to *BmL3* infected cohorts alone while, additionally, α -CCR2 treatment significantly reduced B220⁺ B-cell sdLN populations. Such reductions may infer a role for Cd11b⁺Ly6C⁺CCR2⁺ monocytes and/or Cd11b⁺MHCII⁺F480⁺ M Φ in effective immune priming to filarial infection, with monocyte derived dendritic cells and M Φ both demonstrated to be necessary for efficient priming of T-cells to a variety of infectious agents (Schlienger *et*

et al., 2000; Randolph, Jakubzick and Qu, 2008; Iijima, Mattei and Iwasaki, 2011; Bernhard *et al.*, 2015; Sánchez-Paulete *et al.*, 2017; Kurup *et al.*, 2019) and B-cells (Tosato *et al.*, 1988; Mueller *et al.*, 2007; Harwood and Batista, 2010). Alternatively, CCR2 receptor expression has been reported both on T-cells (Connor *et al.*, 2004) and B-cells (Frade *et al.*, 1997) and “off target” ablation of these T and B-cell subsets by α -CCR2 administration cannot be discounted. Regardless of the mechanism reducing T and B-cell populations, data demonstrating both T and B-cells secrete significant quantities of highly lymphangiogenic molecules would suggest a partial role for both cell types in the induction of filarial lymphatic pathology, while an indirect role for inflammatory monocytes or macrophages in contributing to filarial associated lymphatic pathology, by priming T and B-cells into pro-lymphangiogenic phenotypes, cannot be discounted. Future studies could utilise CCR2 monocyte conditional knockout murine strains in the developed *BmL3* infection to more specifically demonstrate a role for CCR2 inflammatory monocytes in the induction of lymphatic pathology. Additionally, use of inducible conditional, or traditional knockout murine strains that effectively deplete T or B cell populations in the developed model may more effectively elucidate the role for T and B-cells in mediating filarial lymphatic pathology.

With inflammatory monocytes and monocyte derived macrophages recruited to areas of *BmL3* infection being shown to play an important role in development of filarial lymphatic pathology, the capability of monocyte derived M ϕ to directly mediate LEC cell activation, upon stimulation with live *BmL3* or *BmL3* material was assessed. An *in vitro* co-culture system was developed in which human THP-1 monocyte derived macrophages, previously stimulated with live L3 or L3 extract (*BmL3E*) were co-cultured with Lymphatic Endothelial Cells (LECs) to investigate their potential to induce LEC proliferation. Unstimulated macrophages (M0) co-cultured in the presence of LECs in basal media did not significantly stimulate LEC proliferation compared with basal media LEC cultures alone (Basal) suggesting that recruited monocyte derived M ϕ initially fail to display a “pro-lymphangiogenic” phenotype that can drive LEC proliferation. In contrast, M0

stimulated with BmL3E or live L3, followed by subsequent co-culture with LECs, yielded significantly higher levels of LEC proliferation than either M0 co-cultured with LECs or basal media cultured LECs alone. This infers monocyte derived M ϕ , receiving local stimulatory cues from the invading filarial larvae, become polarised into a lymphangiogenic phenotype that can mediate significantly higher proliferation of LECs. LEC proliferation is an important part of lymphangiogenesis, driving post-natal lymphatic remodelling. As the co-culture system utilised cell insets, preventing physical contact between the LEC monolayer and the M ϕ , the increased proliferation observed is resultant of increased secretion of factors from L3/BmL3E polarised M ϕ that directly induce LEC proliferation. Studies providing corroboratory evidence to this data, were human PBMCs cultured in the presence of *Brugia malayi* adult filarial material induced significant secretion of growth factors such as VEGF-C. LEC cultures spiked with comparable concentrations of these growth factors resulted in significant lymphangiogenesis as measured by a number of *in vitro* 2D and 3D cell based assays (Weinkopff *et al.*, 2014).

Data from this chapter extends this phenomenon to products generated and secreted by the initial invading L3 of *B. malayi*. Future work could define the lymphangiogenic molecules secreted by L3/BmL3E polarised M ϕ that drives LEC proliferation by assaying the conditioned media of M ϕ exposed to filarial material. Cross referencing the presence of identified lymphangiogenic molecules with those demonstrated to be locally secreted by monocytes/macrophages in the filarial leg infection model or are systemically upregulated following *BmL3* infection (Chapter 3) could strengthen evidence of the molecular mechanisms that drive early filarial lymphatic pathology. It is important to note, however, that the developed co-culture model likely oversimplifies the early immunological niche encompassing filarial infection, as macrophages are likely to receive a variety of immunological cues through local uptake of chemokines, cytokines and other molecules released by other immune cells/other cell types in the microenvironment. It is likely that recruited monocytes undergoing differentiation into macrophages receives a variety of both parasite-derived, as well as host immune-cell derived stimuli

which ultimately shapes the pro-lymphangiogenic M ϕ phenotype that contributes to filarial lymphatic pathology.

The novel role for monocytes and M ϕ in mediating filarial lymphatic pathology highlights the potential of novel therapeutic strategies ,which aim to target monocyte/M ϕ lymphangiogenic signalling. Blocking the recruitment of monocyte derived, TAMs, demonstrating a highly lymphangiogenic phenotype, is an active area of research interest to inhibit vascularisation and metastasis of tumours (Qian *et al.*, 2011). Further, chemokine receptor antagonists, neutralising antibodies targeting the chemokines responsible for monocyte recruitment, or even pharmacological small molecule inhibitors blocking TAM recruitment to the tumour microenvironment has yielded promising pre-clinical results against a range of cancers(Gazzaniga *et al.*, 2007; Loberg *et al.*, 2007). The manipulation of recruited monocyte/macrophage phenotype is also an area of ongoing research, with prevention of 'M2 angiogenic/lymphangiogenic' M ϕ polarisation at tumours sites, by utilising Cyclo oxygenase-2 (COX-2) inhibitors, yielding interesting results (Na *et al.*, 2013). A similar rationale to prevent recruitment of inflammatory monocytes to the immunological niche proximal to filarial infection, or modifying the lymphangiogenic M ϕ phenotype associated with *BmL3* infection may represent an attractive target to reduce excessive lymphatic remodelling and development of lymphatic insufficiency.

4.5- Chapter Concluding Remarks

The primary objective of this chapter was to identify the cellular source of the milieu of highly lymphangiogenic molecules that are released following *BmL3* infection and are therefore likely implicated in the development of filarial lymphatic pathology. Given the established evidence demonstrating a role for monocytes/macrophages in lymphatic remodelling, both in reparatory and pathological settings, it was hypothesised that monocytes and macrophages may be implicated in filarial driven aberrant lymphatic remodelling and associated lymphatic dysfunction. The data in this chapter provides evidence that monocytes play an important role in the induction of lymphatic remodelling, that is highly associated with lymphatic dysfunction. The data successfully demonstrates that Cd11b⁺Ly6C⁺CCR2⁺ monocytes are rapidly recruited following filarial infection and, in addition to themselves secreting significant quantities of a range of pro-lymphangiogenic molecules, are also likely to differentiate into M Φ phenotypes that further add to the pro-lymphangiogenic milieu, implicated in the induction of filarial pathology. Further, other cellular sources, mainly B and T-cells were demonstrated to secrete lymphangiogenic molecules either following monocyte/macrophage priming or as an independent cellular mechanism of filarial pathology. Filarial exposed monocytes/M ϕ directly induced LEC proliferation, while targeted depletion of either monocyte or M ϕ populations significantly ameliorated filarial associated lymphatic insufficiency, providing strong evidence for a significant role for both monocytes/M ϕ in the induction of filarial lymphatic pathology. The novel role demonstrated suggests that specific targeting of lymphangiogenic monocytes/M ϕ may be a novel therapeutic strategy to prevent development of LF pathology.

Chapter 5

The role of host adaptive immune responses in induction of filarial inflammatory-associated lymphatic pathology.

The role of adaptive immunity in development of Lymphatic Filariasis (LF) related pathology is poorly understood. The nature of local adaptive immune responses following larval infection and the possible role of adaptive immune responses in the induction of filarial-associated lymphatic pathology was investigated. The murine leg pathology model was employed to characterize early local adaptive immune responses to *BmL3* inoculation. Severe Combined Immuno-Deficiency (SCID), Interleukin (IL)-4 receptor alpha deficient (IL-4R α ^{-/-}) and immunocompetent wild type (WT) mouse cohorts were utilized to compare severity of lymphatic remodeling and insufficiency in settings of varying adaptive immunological deficiency. At 14 days post *BmL3* infection, significant expansion of Th2 associated IL-4, IL-13 and IL-10 expressing CD4⁺ T-cells were observed in skin draining lymph nodes (sdLN) and connecting lymphatic channels proximal to infection site. Concurrently, there was evidence that expanded local F4/80⁺MHCII⁺ M ϕ populations expressed significantly increased levels of the alternatively activated (AA) markers (CD206 and Relm- α) typical of IL-4 / IL-13 conditioning. Total ablation of adaptive immune responses (SCID) or dysfunctional Th2 adaptive responses (IL-4R α ^{-/-}) resulted in significant amelioration of infection-induced lymphatic remodeling and insufficiency. Th2 ablation was associated with significantly attenuated release of lymphangiogenic molecules associated with induction of lymphatic pathologies, whilst significantly decreased recruitment of monocytes and M ϕ were observed in local lymphoid/lymphatic tissues proximal to infection. Human monocyte-derived M ϕ conditioned with recombinant IL-4 and 13 were able to induce significant increased LEC proliferation in a co-culture model. In conclusion, an IL-4R dependent, Th2 adaptive immune response is critical to mediate the induction of filarial-associated lymphatic pathology, promoting pro-lymphangiogenic secretions

and AAM ϕ that are functionally important in lymphatic remodelling. This demonstrates that dysregulated Th2-type responses contribute to pathological manifestations of LF.

5.1- Introduction

The previous chapters have defined rapid onset lymphatic remodelling, associated with lymphatic insufficiency, following filarial *Brugia malayi* L3 (*Bm*L3) larval infection. Data demonstrated a vigorous induction of inflammatory immune cell activation as little as 6 days post infection (6dpi), with characterised recruitment of Cd11b⁺Ly6C⁺CCR2⁺ monocytes and significant expansion of CD3⁺ T-cells and Cd11b⁺MHCII⁺F480⁺ macrophages in lymphoid / lymphatic tissues proximal to the site of initial larval invasion. Further a functional role of Cd11b⁺Ly6C⁺CCR2⁺ monocytes and/or Cd11b⁺MHCII⁺F480⁺ macrophages in mediating lymphatic insufficiency and pathology was identified . Together with data demonstrating differences in the severity of lymphatic alterations and pathology between two inbred murine strains with well characterised differences in anti-filarial adaptive immune responses, the underlying immune response to infection may play a key role to the induction of filarial associated lymphatic pathology.

Adaptive Immune responses following filarial nematode infection have been extensively studied, both in terms of immunity to infection as well as implications for pathogenesis. There is general consensus that filarial infection is associated with the induction of strong host Th2 adaptive immune responses (Hoerauf *et al.*, 2005; Babu and Nutman, 2014), as a key arm of anti-parasitic host defence and parasite expulsion. *In vivo* models have elegantly demonstrated that dysfunctional Th2 responses, such as in IL-4R α knockout (KO) mice, render mice permissive to chronic adult filarial infection, while wild type counterparts remain protected (Howells *et al.*, 1983; Devaney *et al.*, 2002; Turner *et al.*, 2018). Recent evidence, however, has characterised a mixed Th1/Th2 adaptive immune response following infection with evidence that early immune responses to filarial invasion is Th1 dominated (Babu *et al.*, 2000; Babu and Nutman, 2003), while it has been shown Th1 responses are also necessary for parasite expulsion in murine

models (Saefteel *et al.*, 2001, 2003). Additionally, there is evidence of compartmentalised adaptive responses which are Th2 dominant towards filarial nematodes, while proinflammatory Th1 responses are triggered against their endosymbiotic bacteria *Wolbachia* (Gentil, Hoerauf and Pearlman, 2012). It has been proposed successful establishment of chronic filarial infection is reliant on a 'modified', highly regulatory and anti-inflammatory Th2 response, dominated by high numbers of regulatory T-cells (Tregs) (Metenou *et al.*, 2010; Metenou and Nutman, 2013). Despite these well characterised adaptive immune responses to filarial infection, the role of adaptive immunity to the development of filarial pathology is less well defined. Early work involving severe combined immune deficiency (SCID) or nude athymic mice, displaying loss of functional adaptive immune responses, demonstrated a role for adaptive immunity in filarial-associated pathology (Vincent *et al.*, 1984; Nelson *et al.*, 1991). SCID mice were observed to develop patent infection, with early manifestation of pathological changes, such as lymphangiectasia, yet failed to progress to more severe lymphoedematous pathology. Progression to acute pathologies were only observed following adoptive transfer of immune competent splenocytes or T-cells, which recapitulated adaptive immune responses (Vickery *et al.*, 1991), suggesting an important role for adaptive immunity in the onset of severe filarial pathology. Further, clinical studies have demonstrated that the type of adaptive immune response initiated upon filarial infection is important for pathological outcome, with asymptomatic patient cohorts displaying a skewed highly regulatory adaptive immune response dominated by the presence of Tregs and secretion of high levels of IL-10 and TGF- β (Taylor *et al.*, 2005; Metenou *et al.*, 2010; Babu and Nutman, 2014), while symptomatic patients demonstrate a mixed inflammatory Th1, Th2 and Th17 response characterised by significantly higher concentrations of relevant cytokines (Babu *et al.*, 2009) as well as an increased, mixed, heightened parasite specific effector T-cell response .

The heterogeneous adaptive immune response outlined above demonstrates that the role of adaptive immunity in mediating, or protecting from, pathological manifestations of LF is still poorly defined. Additionally, the

majority of research has focused on characterisation of adaptive responses in the presence of chronic fecund adult filarial infections, including host responses to systemic circulating mf. Moreover, clinical studies of adaptive immune responses in symptomatic patient groups are highly variable in terms of type (hydrocele, limb LE) and extent (grade) of overt pathology. It is challenging to define precisely the initiating polarised adaptive immune responses that induce pathology considering the variation in patient cohorts and also the further confounding impact of latter secondary microbial skin infections. In chapter 2, the rapid manifestation of pathological lymphatic remodelling and associated lymphatic dysfunction following invasion by the infective L3 larval stage was detailed. This suggests the less well characterised adaptive immune responses to early invasion of L3 larvae may play a more significant role in the development of later pathological outcomes than was previously appreciated. The aims of this chapter will therefore be to characterise the early adaptive immune responses, locally and systemically, following *Brugia malayi* L3 (*BmL3*) infection. Additionally, a key aim will be to investigate the role of adaptive immune responses in the development of filarial-associated lymphatic pathology.

These research questions will be addressed using the following objectives:

1. Utilise the developed pathology model to investigate if lymphatic remodelling and associated insufficiency is modified between WT and SCID mice.
2. Characterise the type of adaptive immune response, both local to *BmL3* infection as well as systemically, at time-points where there is demonstrable lymphatic pathologies: (6-14dpi)
3. Utilise a selective knockout mouse system, dependent on identification of immune-polarisation defined in (2), to investigate the impact on infection-associated lymphatic pathologies.
4. Investigate associations between magnitude and type of adaptive immune response and previously identified molecular and/or cellular mechanisms of infection-associated lymphatic pathology.

5.2- Methods

5.2.1-Mouse maintenance, Murine hind-limb infection model and associated pathological readouts

Male BALB/c SCID mice were purchased from Charles River (Margate, UK) . Male BALB/c IL-4 receptor alpha ($R\alpha$)^{-/-} knockout mice were purchased from Jackson Laboratories (USA) and subsequently bred in house for experimental use, while C57BL/6J IL-4 α ^{-/-} breeding pairs were a kind gift from Dr Cecile Benezech (University of Edinburgh) and subsequently bred in house for experimental use. Breeding C57BL/6J IL-4 α ^{-/-} mice were phenotyped for loss of IL-4R α expression utilising flow cytometric analysis of lymphocytes and myeloid cell populations from relevant tail bleeds (data not shown) Both IL-4R α ^{-/-} strains of mice were 6-12 weeks at the start of each experiment and age matched with Wild Type (WT) immunocompetent mice (BALB/c and C57BL/6J) purchased from Charles river (Margate,UK) in appropriate experiments.

The murine experimental model of filarial-induced lymphatic remodelling and insufficiency, along with relevant readouts, were utilised throughout this chapter, methods can be accessed from chapter 2.2.1-2.2.7.

5.2.2-Skin draining Lymph Node (sdLN) Flow cytometry and Immunophenotyping

sdLNs, and the surrounding connecting lymphatic vasculature, of the infected left hind limb (popliteal, iliac and sub-iliac) were excised and processed as previously detailed (Chapter 2.2.1-2.2.7). Fc regions of prepared single cell suspensions were blocked through a twenty minute incubation with CD16/32 Fc-block (eBioscience, Hatfield UK). Live/dead cell differentiation was undertaken by 30-minute incubation of samples with efluor 450 fixable viability dye (eBioscience, Hatfield UK) on all samples. Following live/dead cell differentiation and a subsequent wash and centrifugation, cell surface staining was undertaken for 30 minutes with the following surface markers used: Ly6G PE (eBioscience, Hatfield), Ly6C PerCyP5.5 (eBioscience,

Hatfield), Rat IgG1 APC Isotype control (eBioscience, Hatfield), Rat IgG1 FITC Isotype control (eBioscience, Hatfield), CD4 APC (eBioscience, Hatfield), CD4 PerCyP Cy5.5 (eBioscience, Hatfield), CCR2 PE-Cy7 (eBioscience, Hatfield), Cd11b AF488 (eBioscience, Hatfield), Cd11b PerCyP Cy5.5 (ebioscience, Hatfield) B220 APC (eBioscience, Hatfield), MHCII Alexa Fluor 700 (AF700) (ebioscience, Hatfield), Tim-4 PE-Cy7 (ebioscience, Hatfield), SiglecF PE (ebioscience, Hatfield), F480 Brilliant Violet 711 (BV711) (Biolegend, London), CD206 APC (ebioscience, Hatfield). Following surface staining, cells were fixed for 40 minutes using the FoxP3 Fixation/Permeabilisation Kit (eBioscience, Hatfield) followed by either: acquisition, undertaken on a BD LSRII Flow cytometer (BD Biosciences, Berkshire, UK) or further intracellular staining utilising, rabbit polyclonal anti-RELM- α (Peprotech) or polyclonal rabbit anti-IgG (peprotech) fluorescently labelled with Zenon Rabbit IgG AF488 labelling kit (ThermoFisher, UK) for 40 minutes.

In other experiments, extracted single cell lymph node suspensions underwent a 5 hour incubation in cell stimulation cocktail (ebioscience Hatfield) as per manufacturer's instructions, followed by blocking of Fc regions and Live/Dead differentiation as described above. Cell surface staining of CD4 expression was then undertaken for 40 minutes followed by fixation/permeabilization as previously described. Fixed and permeabilised cells then underwent intracellular cytokine labelling utilising the antibodies: IFN- γ PE-Cy7 (eBioscience, Hatfield), IL-10 APC (eBioscience, Hatfield or Biolegend, London), IL-13 AF488 (eBioscience, Hatfield), IL-4 PE (eBioscience, Hatfield). All intracellular staining was undertaken in the FoxP3 permeabilization buffer as per manufacturer's protocol. Data was analysed using Flowjo software (BD Biosciences, Berkshire, UK).

5.2.3-Multiplex analysis of plasma or human cell secretion samples

Plasma was harvested from all relevant mouse groups as detailed in chapter two. Plasma samples were analysed for a panel of angiogenic/lymphangiogenic analytes using the MAGMAP-24k milliplex full panel (mouse plasma) or HAGP1MAG-12K full panel (human cell secretion)

(Merck Millipore, East Midlands) as per manufacturer's instructions and read on a Bio-Plex (Biorad, Deeside). Analyte expression was analysed by plotting the mean fold change of the individual analyte in infected mouse groups from the mean concentration of relevant sham infected controls. Cell secretion samples were normalised to media only controls to account for possible analyte contaminants in serum supplemented media.

5.2.4-Cell culture and maintenance

Cell lines utilised in this chapter were maintained and cultured as previously described in chapter 4.2.6.

5.2.5-Macrophage/ LEC co-culture proliferation assay

THP-1 monocytes were plated into the cell inset of 6 well trans-well plates (Sigma, Dorset) at 1×10^6 cells/well and differentiated into adherent non-polarised "M0" macrophages using 10ng/ml PMA (Sigma, Dorset) for 24 hours. Following differentiation, macrophage insets were washed in PBS before stimulation with either 5ng/ml of recombinant human Interferon-gamma (IFN- γ) (Peprotech), 5ng/ml recombinant human interleukin-4 (Peprotech) (IL-4) + 5 ng/ml recombinant human interleukin 13 (Peprotech) (IL-13) or media only (M0) for 48 hours. On the intermediate day, LECs were seeded separately on the bottom of fresh 6 well trans-well plates at 8×10^4 cells/well. Following 48-hour stimulation, cytokine polarised macrophage insets and LEC adherent layers were washed, before addition of the inserts onto the top of LEC wells, creating a LEC/Macrophage co-culture. A 20% EGM-2, 80% Endothelial basal media (EGM-2 without addition of any growth supplements, +0.1% FBS only) mix was used as the culture media. LEC wells without macrophage inserts plated in: 80:20 basal media alone or full EGM-2 were used as negative (negligible growth) and positive (maximal growth) controls respectively. All LEC/Macrophage co-culture wells and LEC control wells were incubated for 72 hours at 37°C, 5% CO₂. Following incubation, macrophage inserts were discarded and LEC cells dissociated from wells using 1x Trypsin/EDTA solution (Thermofisher, UK). All LEC samples were manually counted using a haemocytometer in a 1:1 cell

sample: 2% Trypan Blue (Sigma, Dorset) solution for Live/Dead cell differentiation. A schematic summary of the assay can be found in figure 5.7A

In other experiments, differentiated M0's were plated at 1×10^6 cells/well followed by polarisation with rIL-4 + rIL-13 or M0 as outlined above. Following 48 hours, polarised macrophages were carefully washed in PBS, followed by addition of fresh media and incubated for a further 72 hours. The 72 hour conditioned media containing secretions of polarised macrophages were then either added to plated 8×10^4 cells/well LECs as a proliferation assay as described above, or frozen to undergo multiplex analysis of lymphangiogenic factors.

5.2.6-Splenocyte recall assays

14 days following *BmL3* infection, harvested spleens from sham or infected mice were dissected and a single cell suspension created by teasing apart of spleens on top of a 40 μm cell sieve (Sigma, Dorset) followed by maceration of remaining spleen tissue through the sieve using the handle of 2ml syringes (Sigma, Dorset). The resultant single cell suspension was depleted of red blood cells utilising RBC lysis buffer (Biolegend, UK) as per manufacturer's instructions, followed by resuspension in Roswell Park Memorial Institute (RPMI) 1640 media (Sigma, Dorset) supplemented with 10% Foetal Bovine Serum (Sigma, Dorset), Penicillin / Streptomycin 100 I.U./mL (Sigma, Dorset) and Amphotericin B 2.5mg/L

Resuspended splenocytes were plated at a concentration of 2.5×10^5 cells/well onto 96 well plates (Starlab, UK) previously coated with 1.25 $\mu\text{g}/\text{ml}$ anti-CD3 (Biolegend, UK) for a minimum of 2 hours. Following plating, wells were supplemented with 2 $\mu\text{g}/\text{ml}$ soluble CD28 (Biolegend, UK) and incubated for 72 hours at 37°C and 5% CO₂. Following incubation, plates were centrifuged and supernatants harvested and stored at -20°C until assayed.

Splenocyte supernatants were thawed slowly and assayed for: Interleukin (IL)-4, IL-13, IL-10 and Interferon-gamma (IFN- γ) utilising appropriate Duo-

set enzyme-linked immunosorbent (ELISA) assays (R&D systems, Abingdon) as per manufacturer's protocol.

5.2.7-Statistical Analysis

All continuous data was tested for normal distribution using the Kolmogorov-Smirnov test for equal variance. Where data was normally distributed, a two-tailed independent student's t-Test was used to test for significant differences between two groups. Where data was found to be not normally distributed, a log transformation was first attempted and data re-tested for equal variance. If data remained non-parametric, a two-tailed Mann-Whitney U test was utilised to test for significant differences between two groups. Where more than 2 groups were being compared, a One-way ANOVA was utilised with a Tukey's post-hoc comparisons test to measure differences in parametric data, while a Kruskal-Wallis test was used for non-parametric data with Dunn's post-hoc multiple comparisons test. The mean along with the standard error of the mean (SEM) are reported in all data unless otherwise stated. Significance is indicated as $*=P<0.05$, $**=P<0.01$, $***=P<0.001$ in all figures unless stated otherwise.

5.3- Results

5.3.1- Ablation of adaptive immune responses results in significantly reduced lymphatic remodelling and insufficiency.

To investigate a possible role of adaptive immune responses in the rapid onset of lymphatic pathologies observed following *BmL3* infection, BABL/c SCID and BALB/c WT were inoculated in the left hind limb with 100 *BmL3* or sham inoculations and aberrant lymphatics and lymphatic insufficiency quantified, at both 14dpi and 35dpi (infection schematic in figure 5.1A) using PDE imaging and other readouts detailed in Chapter 2.2.1-2.2.7.

Compared to WT Sham controls, WT *BmL3* infected mice demonstrated significantly increased aberrant lymphatics in: dorsal (67.4 ± 25.7 vs 0.2 ± 0.2 A.U. $P < 0.05$), ventral (168.5 ± 24.6 vs 0.2 ± 0.1 A.U., $P < 0.01$) and Left (186.6 ± 63.8 vs 0.2 ± 0.2 A.U. $P < 0.01$; viewpoints, comparing *BmL3* inoculated vs sham inoculated animal limbs at 14dpi (Figure 5.1B-C) . SCID mice infected with *BmL3* displayed no significant difference in aberrant lymphatics across all imaged viewpoints, compared to SCID sham-infected counterparts.(Figure 5.1B-C) Further, WT *BmL3* mice demonstrated significantly higher aberrant lymphatics in the ventral viewpoint (168.5 ± 24.6 A.U vs 67.9 ± 39.2 A.U., $P < 0.05$), compared to SCID *BmL3* counterparts (Figure 5.1B&C).

At 14dpi, WT *BmL3* mice displayed significantly higher ICG retention in *BmL3* inoculated left limb compared to WT sham counterparts (Figure 5.1D; 0.44 ± 0.08 vs 1.0 ± 0.02 R/L Leg ratio, $P < 0.001$). ICG retention in SCID *BmL3* mice compared to SCID sham counterparts was not as profound and did not gain statistical significance (Figure 5.1D). Additionally, WT *BmL3* mice demonstrated significantly higher Evan's Blue dermal retention, measured at OD⁶²⁰, than WT Sham counterparts (Figure 5.1E; 0.1 ± 0.01 vs 0.08 ± 0.01 OD⁶²⁰, $P < 0.05$) while no significant difference in Evan's Blue dermal retention was observed between SCID *BmL3* and sham inoculated mice (Figure 5.1E).

At 5 weeks post-infection, WT *BmL3* mice demonstrated significantly higher levels of aberrant lymphatics in the ventrally PDE imaged viewpoint, compared to SCID counterparts, (Representative image in Figure 5.1F, Figure 5.1G; 143.4 ± 57.4 vs 27 ± 27 A.U, $P < 0.05$).

5.3.2- *BmL3* infection induces significant expansion of IL-4, IL-13 and IL-10 expressing CD4⁺ T-cells in local draining lymph nodes.

Local adaptive immune responses to *B. malayi* L3 (*BmL3*) larval infection were characterised at 14dpi. WT mice were inoculated with 100 *BmL3* and lymphoid cells from skin draining lymph nodes (sdLN- popliteal (pLN, iliac (iLN), sub-iliac (siLN)) proximal to inoculation site in the left limb were extracted. Subsequent intracellular cytokine flow cytometry of harvested sdLNs from *BmL3*- and sham-inoculated groups was undertaken to characterise CD4⁺ T-cell cytokine expression. Simultaneously, systemic adaptive immune responses were interrogated by preparing splenocyte cell suspensions from *BmL3*- and sham-inoculated groups 14dpi before undertaking splenocyte recall immuno-assays.

Compared to sham control mice, *BmL3*-infected mice demonstrated significant expansions of IL-4 (0.8 ± 0.12 vs 2.95 ± 0.32 %IL-4⁺ CD4⁺ T-cells, $P < 0.01$) IL-13 (0.86 ± 0.11 vs 2.7 ± 0.3 %IL-13⁺ CD4⁺ T-cells, $P < 0.05$), and IL-10 (0.76 ± 0.08 vs 1 ± 0.07 %IL-10⁺ CD4⁺ T-cells, $P < 0.01$) expressing CD4⁺ T-cells in sdLNs proximal to infection site (Figure 5.2A&B). No significant difference in IFN- γ expressing CD4⁺ T-cells was observed between sham controls and *BmL3* infected mice at 14dpi (Figure 5.2A&B). Further, polyclonal α CD3/CD28 splenocyte recall responses were significantly increased post-*BmL3* infection compared with sham-inoculated mice in terms of IL-4 (1.45 ± 0.43 vs 0.35 ± 0.02 ng/ml, $P < 0.05$), IL-13 (2.3 ± 1.1 vs 0.3 ± 0.02 ng/ml, $P < 0.01$), IL-10 (896.9 ± 389.3 vs 71.2 ± 12.8 pg/ml, $P < 0.01$) and IFN- γ secretion (13.0 ± 2.5 vs 2.9 ± 0.47 ng/ml $P < 0.01$) (Figure 5.2C). While no statistical significance was attained, there was a trend to suggest expansions

of splenocyte CD4⁺ t-cell expressing IL-4, IL-13 and IL-10 splenocytes (Figure 5.2D).

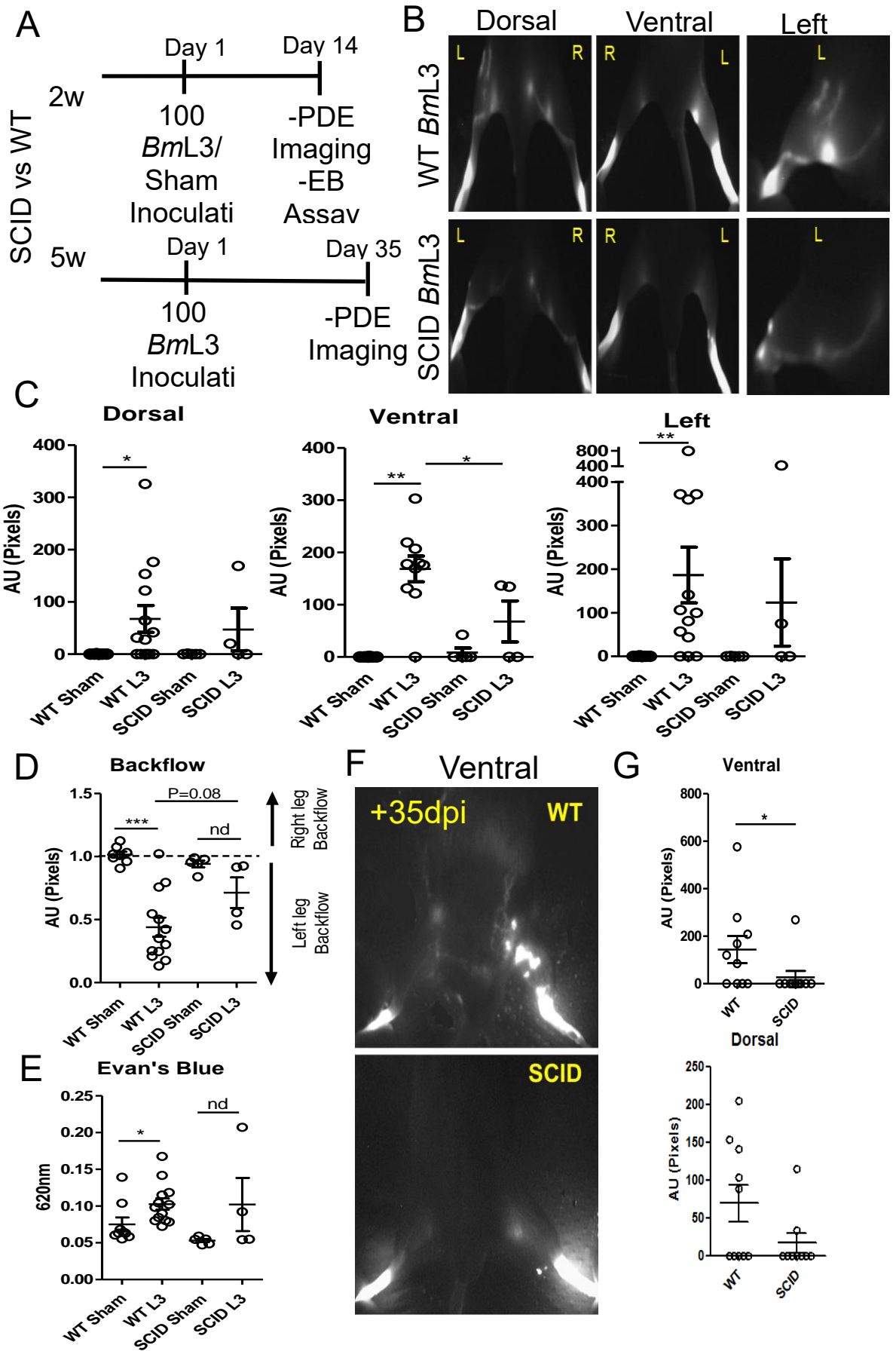


Figure 5.1: Defective adaptive Immune responses in Severe Combined Immuno-Deficient (SCID) mice results in significantly lower severity of lymphatic remodelling and insufficiency compared to Wild Type (WT) mouse counterparts, following filarial *BmL3* infection.

A) Schematic of infection experiments involving inoculation of 100 *BmL3* into left hindlimb of BALB/c Wild type (WT) and BALB/c adaptive immune response deficient Severe Combined Immune-Deficiency (SCID) mice **B)** Representative 14dpi PDE imaging of WT *BmL3* vs SCID *BmL3* mouse cohorts **C)** Quantification of PDE imaged: : aberrant lymphatic remodelling in dorsal, ventral and left leg viewpoints and **D)** PDE measured lymphatic insufficiency from quantification of ICG fluorescence retention in ROI lower hind limb between sham infected (SCID Sham, WT SCID) vs SCID *BmL3* and WT *BmL3* groups. **E)** Quantification of lymphatic insufficiency utilising Evan's Blue dermal retention assay. Evan's Blue was measured at OD⁶²⁰ following 14dpi in indicated groups **F)** Representative 35dpi PDE imaging of ventral viewpoint WT *BmL3* vs SCID *BmL3* mouse cohorts **G)** Quantification of PDE imaged aberrant lymphatic remodelling in ventral viewpoint 35dpi. Horizontal bars plot the mean \pm SEM. Data pooled from 2 individual experiments (WT 14dpi) (N=5 per group) or a single experiment (SCID 14dpi) (N=4 per group) (WTvsSCID 35dpi N=10 per group). Significance is indicated as *P<0.05 **P<0.01 ***P<0.001 nd=non-significant, derived from a one way ANOVA followed by Tukey's multiple comparisons post-hoc test, between indicated groups.

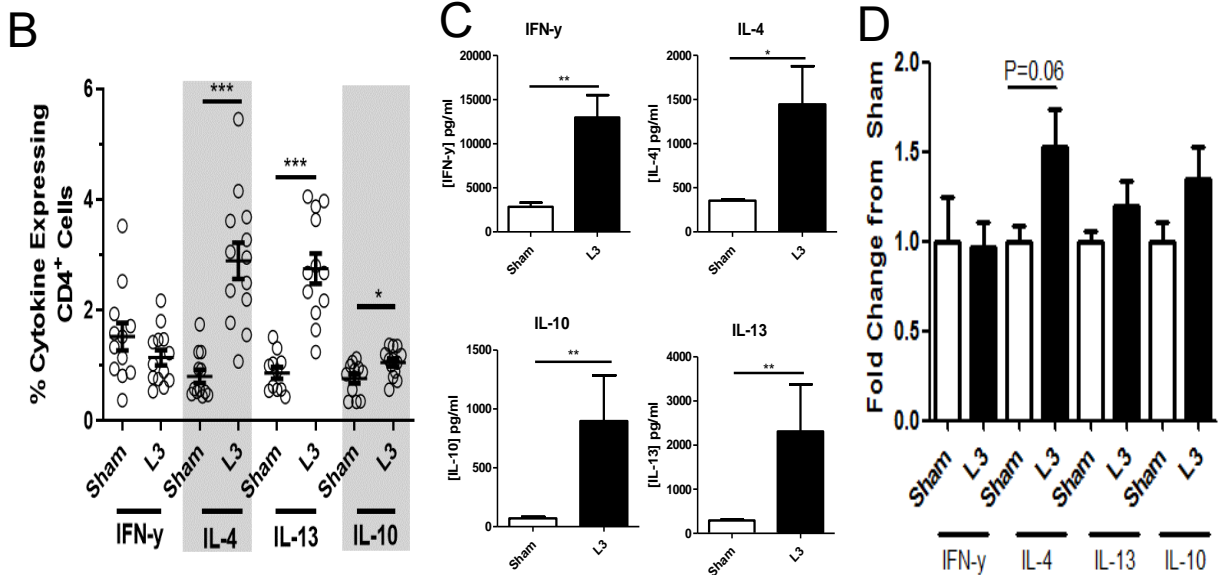
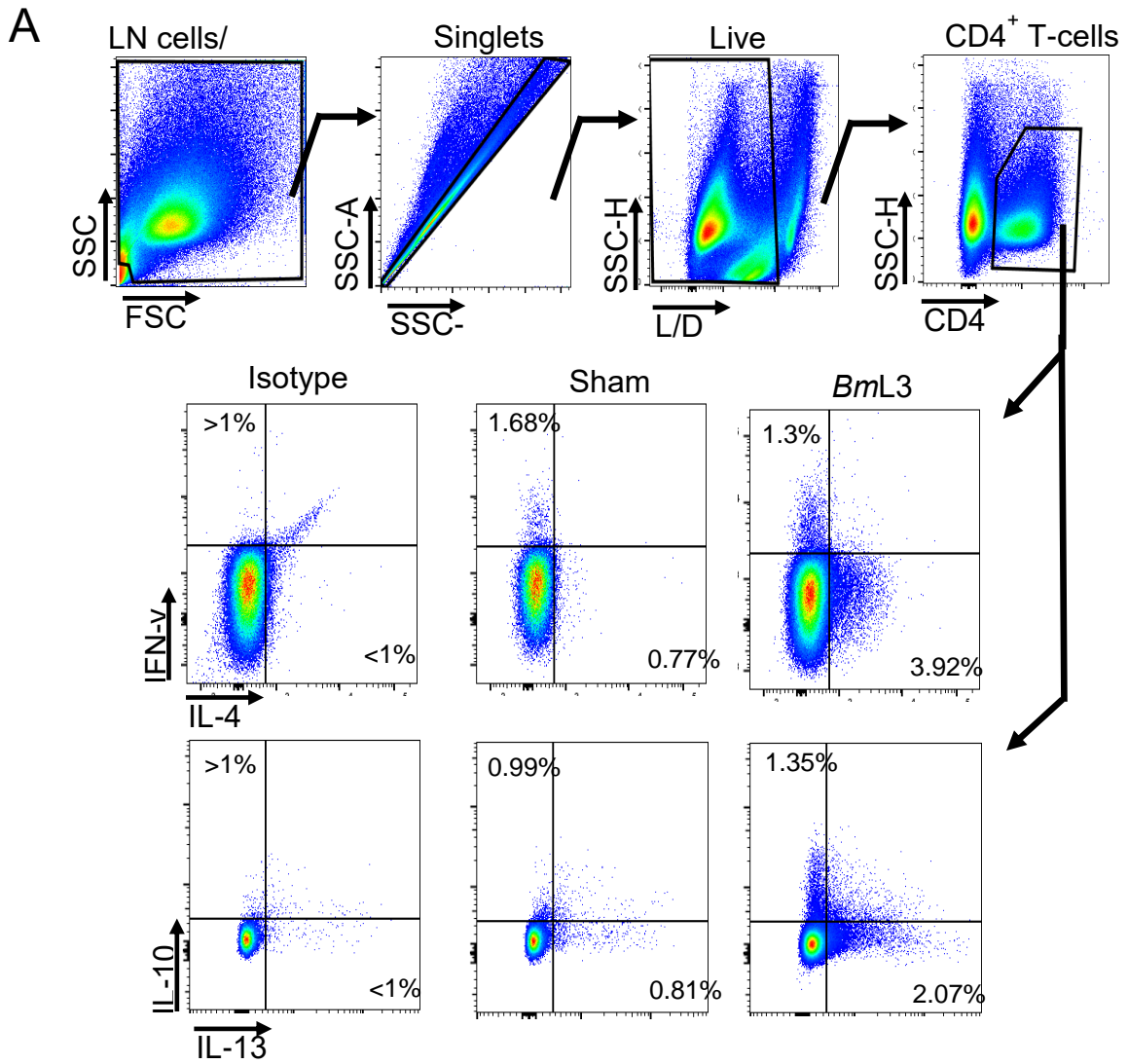


Figure 5.2: BmL3 infection induces a strong local Th2 adaptive immune response, 14dpi in sdLNs proximal to inoculation site concurrent with a mixed Th1/Th2 systemic response.

A) Intracellular cytokine staining gating strategy and representative flow cytometry plots of sdLN/splenocytes CD4⁺ T cells from sham- vs *BmL3*-infected C57BL/6J mouse groups at 14dpi **B)** Quantification of sdLN IL-4⁺, IL-13⁺, IFN- γ ⁺ and IL-10⁺ expressing CD4⁺ T-cells, between sham and *BmL3*-infected mouse cohorts, 14dpi.. **C)** Splenocyte recall responses from *BmL3* and sham infected mouse groups, following a 72hour stimulation with immobilised anti-CD3 and soluble anti-CD28. Bar graphs demonstrate cytokine concentrations derived from ELISAs undertaken on cell supernatants. **D)** Quantification of splenocyte IL-4⁺, IL-13⁺, IFN- γ ⁺ and IL-10⁺ expressing CD4⁺ t-cells, between sham and *BmL3*-infected mouse cohorts, 14dpi, data is normalised to mean fold change of cytokine expression from relevant sham infected cohorts. All graphs plot the mean \pm SEM, each data point plotted represents a single mouse (B). Data represents data pooled from 3 individual experiments (A + B n=9-13 mice per group) or a single experiment of 5 mice per group (C+D). Statistical significance is indicated as *=P<0.05 **=P<0.01 ***=P<0.001, derived from Student two-tailed t-tests comparing sham- vs *BmL3*-inoculated mice for individual cytokines.

5.3.3- Impaired Th2 Adaptive immune responses in IL-4R α ^{-/-} mice abrogates filarial induced lymphatic remodelling and insufficiency following *BmL3* infection.

Because adaptive immunity was implicated as necessary for the full development of lymphatic pathology, together with Th2 adaptive immune responses appearing to be upregulated locally in the sdLNs following infection, the role of Th2 adaptive immune responses was investigated. IL-4R α ^{-/-} mouse cohorts were infected alongside WT counterparts with 100 *BmL3*/sham control SC in the left hind limb. 14dpi, lymphatic remodelling and insufficiency was quantified (as described in Chapter 2.2.2-2.2.7). Both BALB/c/ BALB/C IL-4R α ^{-/-} and C57BL/6J/ C57BL/6J IL-4R α ^{-/-} mouse strains were investigated due to the strain-dependency of lymphatic pathology (detailed in Chapter 2.).

Fourteen days following *BmL3* infection, BALB/c IL-4R α ^{-/-} mouse cohorts displayed significantly reduced expansion of sdLN CD4⁺ cells expressing IL-4 (1±0.05 vs 2.5±0.66 fold change from sham, P<0.01) IL-13 (1.0±0.15 vs 2.5±0.4 fold change from sham, P<0.05), and IL-10 (1.6±0.43 vs 3.8±0.43 fold change from sham, P<0.01), compared with WT counterparts (Figure 5.3B).

Post-infection at 14 days, BALB/C IL-4R α ^{-/-} mice also displayed significantly reduced aberrant lymphatics in ventral (12.4±8.5 vs 231.6±33.0 A.U, P<0.001) and left (0.07±0.07 vs 150.8±44.4 A.U., P<0.01) aspects of infected limbs determined by contrast imaging of ICG lymphatic flow (Figure 5.3A&C). C57BL/6J IL-4R α ^{-/-} mice, 14dpi with 100 *BmL3* larvae, also displayed significantly reduced aberrant lymphatics in the ventral (243.8 ± 97.6 vs 611.6±101.6 A.U, P<0.01) aspect of infected limbs by ICG imaging (Figure 5.3A&C).

BALB/C IL-4R α ^{-/-} mice infected with *BmL3* exhibited significantly decreased retention of ICG in the left infected limb (0.84±0.16 vs 0.44± 0.01 R/L leg fluorescence ratio, P<0.05, Figure 5.3A&D) compared to WT counterparts.

Further, in BALB/C IL-4R α ^{-/-} mice, there was no significant alteration in ICG retention level between IL-4R α ^{-/-} *BmL3*- and sham-infection controls.

On the C57BL/6J background, whilst WT mice displayed significantly increased retention of ICG in the left infected limb compared to sham controls at 14 dpi (0.57±0.09 vs 0.99±0.034 R/L leg fluorescence ratio, P<0.001), no significant difference was observed between *BmL3*- and sham-infection groups in IL-4R α ^{-/-} mice (Figure 5.3A+D).

BALB/c WT mice had significantly increased retention of Evan's Blue at 14dpi with *BmL3* compared to sham-infection controls (Figure 5.3E; 0.11±0.01 vs 0.08±0.01 OD⁶²⁰, P<0.001), determined at end point via the Evan's Blue dermal retention assay. Corresponding, BALB/c IL-4R α ^{-/-} mice infected with *BmL3* displayed significantly decreased retention of Evan's Blue (Figure 5.3E; 0.09±0.01 OD⁶²⁰, P<0.05 vs WT BALB/c infected mice).

C57BL/6J mice, 14dpi, also displayed significantly increased Evan's Blue retention compared to C57BL/6J WT sham-infection controls (Figure 5.3E; 0.17±0.03 vs 0.07±0.01 OD⁶²⁰, P<0.001). No significant difference in Evan's Blue dermal retention was observed between corresponding C57BL/6J IL-4R α ^{-/-} mouse groups (Figure 5.3E).

5.3.4- Lymphangiogenic mediators in circulation following *BmL3* infection are altered in IL-4R α ^{-/-} mice.

The circulatory profile of a panel of lymphangiogenic markers, including those shown to be significantly associated with filarial-associated lymphatic pathology (Chapter 3), was investigated in WT and IL-4R α ^{-/-} mice from BALB/c and C57BL/6J strains following inoculations with 100 *BmL3*.

In C57BL/6J mice (Figure 5.4A&B), *BmL3* infected WT mice displayed significantly increased circulating serum levels of: VEGF-C (2.47±1.3-4.3 IQR median fold-change, P<0.01), sALK-1 (1.47± 0.8-2.9 IQR median fold-change, P<0.05) and TNF- α (1.39± 1.1-2.1 IQR median fold-change, P<0.05) compared to sham-infection controls. Contrastingly, Endoglin was significantly decreased compared to sham-infection controls (0.83± 0.51-0.96

IRQ median fold- change, $P < 0.05$). In comparison, *BmL3* infected $IL-4R\alpha^{-/-}$ mice demonstrated significantly lower levels of circulating VEGF-C ($0.58 \pm 0.47-1.5$ IQR median fold-change, $P < 0.05$), sALK-1 ($0.67 \pm 0.5-1.9$ IQR median fold-change, $P < 0.05$), TNF- α ($0.69 \pm 0.14-1.3$ IQR median fold-change, $P < 0.05$), FGF-2 ($0.7 \pm 0.48-0.84$ IQR median fold-change, $P < 0.05$) compared to *BmL3* infected WT mice. Additionally, there was a significant increase in Endoglin in *BmL3* infected $IL-4R\alpha^{-/-}$ ($0.97 \pm 0.9-1.2$ IQR median fold-change) compared to WT *BmL3* infected mice. Further, comparing circulating levels between *BmL3*- and sham-infected $IL-4R\alpha^{-/-}$ mice, a decreased level of FGF-2 was discernible ($0.7 \pm 0.48-0.84$ IQR median fold-change, $P < 0.05$), whilst there was no significant difference in VEGF-C, sALK-1, TNF- α or Endoglin between *BmL3*- and sham-infected $IL-4R\alpha^{-/-}$ mice (Figure 5.4A-B).

In BALB/c mice (Figure 5.4A&C), compared to sham-infections, *BmL3*-infected mice displayed significant increased circulatory sALK-1 ($1.35 \pm 1-1.7$ IQR median fold-change, $P < 0.001$), Follistatin ($1.36 \pm 0.84-2.1$ IQR median fold-change, $P < 0.01$), PLGF-2 ($1.16 \pm 0.8-2$ IQR median fold-change, $P < 0.05$) and Leptin ($1.14 \pm 0.9-1.6$ IQR median fold-change, $P < 0.05$). Comparatively, $IL-4R\alpha^{-/-}$ *BmL3* infected BALB/c mice displayed significantly reduced sALK-1 ($0.9 \pm 0.7-1.4$ IQR median fold-change, $P < 0.05$), Follistatin ($0.7 \pm 0.6-1.4$ IQR median fold- change, $P < 0.05$), PLGF-2 ($0.69 \pm 0.6-0.9$ IQR median fold-change, $P < 0.01$), Leptin ($0.82 \pm 0.4-1$ IQR median fold-change, $P < 0.01$), FGF-2 ($0.64 \pm 0.3-0.9$ IQR median fold-change, $P < 0.01$) and VEGF-A ($0.75 \pm 0.5-0.9$ IQR median fold-change, $P < 0.05$) compared with fold-changes in WT *BmL3* infected mice (Figure 5.4A&C).

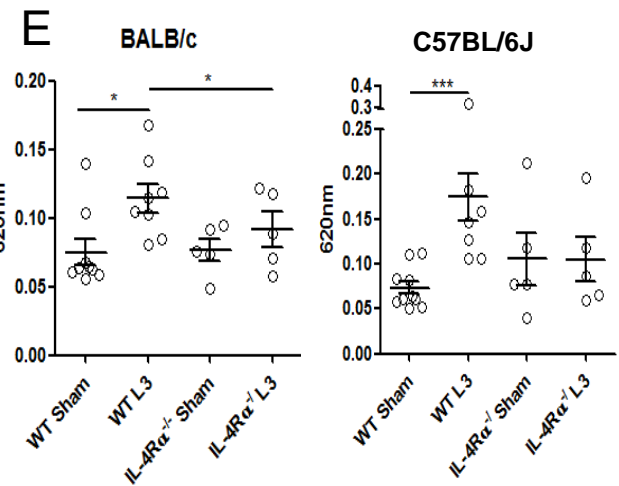
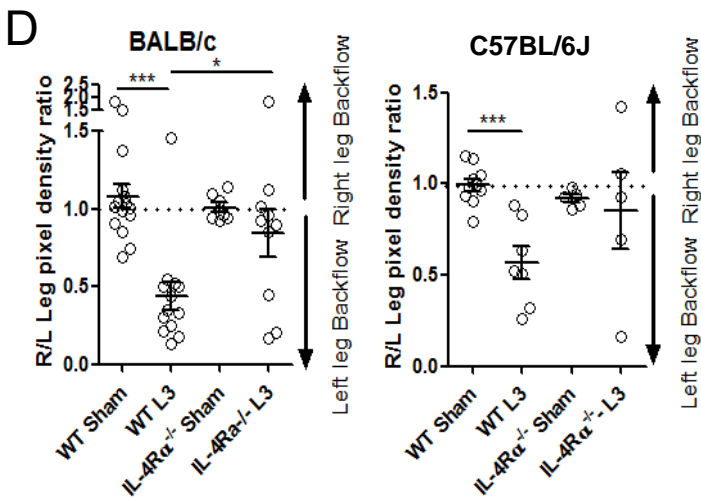
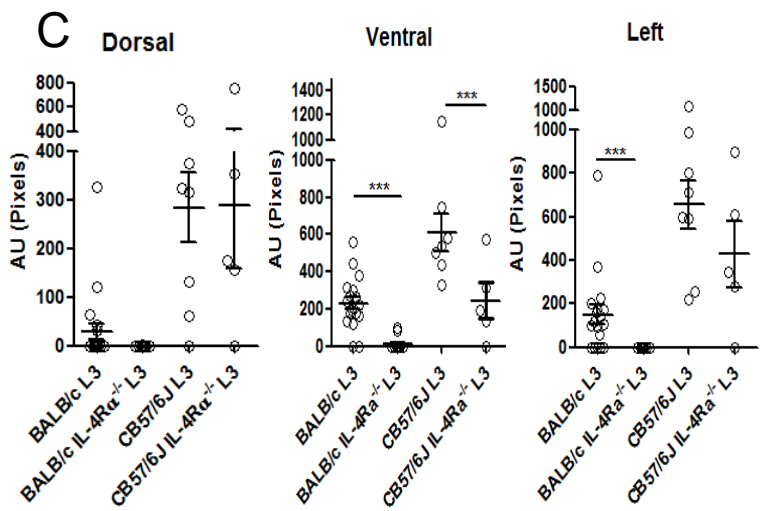
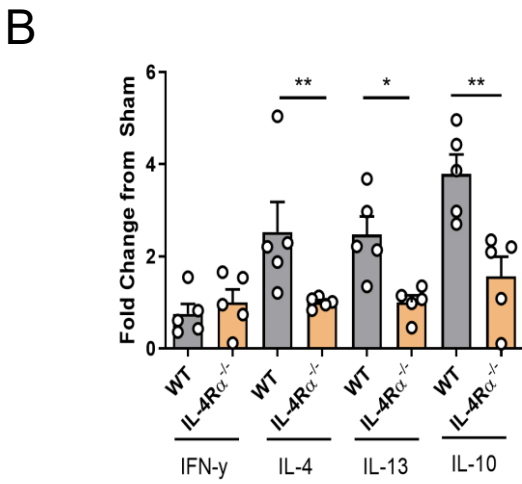
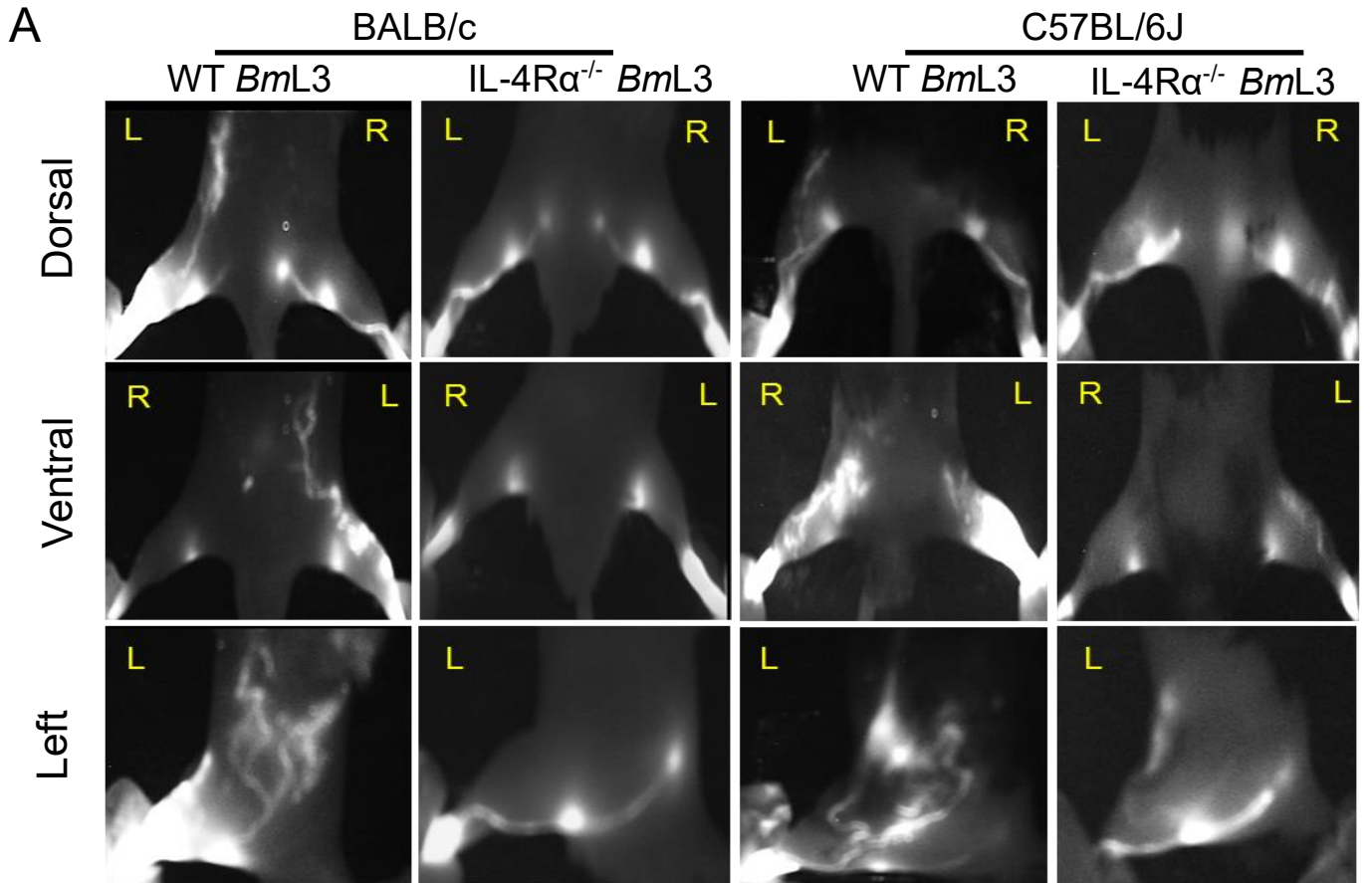


Figure 5.3: Development of lymphatic remodelling and insufficiency following *BmL3* filarial infection are ameliorated in the absence of IL-4R α immune responses.

A) Representative PDE lymphangiograms of mice groups **B)** BALB/c CD4⁺ cytokine expressing T-cells in sdLN's proximal to inoculation site were quantified using intracellular cytokine staining flow cytometry, graph plots mean fold change of the cytokine expressing T-cells populations from relevant sham inoculated control groups **C)** Quantified lymphatic remodelling, measured by aberrant lymphatics in: left, dorsal and ventral views from PDE imaging **D)** Quantified lymphatic insufficiency from PDE imaging, measured by ICG fluorescence retention in the ROI of lower hind-limbs, s. **E)** Dermal lymphatic backflow quantified utilising the Evan's Blue dermal retention assay at 14dpi experimental endpoint. Graph bars in B and horizontal bars in C-E plot the mean \pm SEM with data pooled from 3 separate experiments (C-E, n=5-20 per group- data for C57BL/6J WT sham and *BmL3* infected data has been reused from figure 2.2B&C) or a single experiment (B, n=4-5 per group). Statistical significance is indicated *P<0.05 **P<0.01 ***P<0.001 derived from a two-tailed student t-test comparing fold change of individual cytokines of infected groups (B) or a one-way ANOVA with Tukey's multiple comparisons post hoc test (C-E)

In addition, levels of sALK-1, Follistatin, PLGF-2 or VEGF-A were not significantly altered between IL-4R α ^{-/-} *BmL3*- and sham-infected mice, while there was a significant decrease in Leptin (1.14 \pm 0.9-1.6 IQR median fold-change, P<0.01) and FGF-2 (0.64 \pm 0.3-0.9 IQR median fold-change, P<0.01) (Figure 5.4A&C).

5.3.5- C57BL/6J IL-4R α ^{-/-} mice demonstrate significantly lower expansions of M Φ 's, T and B-cells in lymphoid tissue local to inoculation sites following *BmL3* infection, than WT *BmL3* infected counterparts.

The impact of IL-4R α ^{-/-} ablation on leukocyte cellular recruitment and/or proliferation in the local immune microenvironment, proximal to *BmL3* infection was investigated. Cells derived from local sdLNs and the connecting major afferent / efferent lymphatic channels were isolated 14dpi with 100 *BmL3* into the left hind limb of C57BL6/J WT and IL-4R α ^{-/-} mice. While both WT and IL-4R α ^{-/-} *BmL3*-infected mice demonstrated significant increases in total sdLN cellularity compared with sham-inoculated controls, WT *BmL3*-infected mice displayed a significantly higher total cellularity than IL4R α ^{-/-} mice (5.5 \times 10⁷ \pm 5.5 \times 10⁶ cells vs 2.4 \times 10⁷ \pm 4.9 \times 10⁶, P<0.001 Figure 5.5B).

Compared to Sham controls, within the local lymphatic / lymphoid cell suspension, WT *BmL3*-infected mice demonstrated significantly higher increases of CD3⁺ T-cells (3.36 \pm 0.32 vs 1.97 \pm 0.51 mean fold-change, P<0.05), B220⁺ (CD45R) B-cells (7.4 \pm 1.42 vs 2.53 \pm 0.67 mean fold-change, P<0.05) and F480⁺ M Φ 's (2.94 \pm 0.51 vs 0.56 \pm 0.16 mean fold-change, P<0.001) compared to IL-4R α ^{-/-} *BmL3*-infected mice (Figure 5.5A&C).

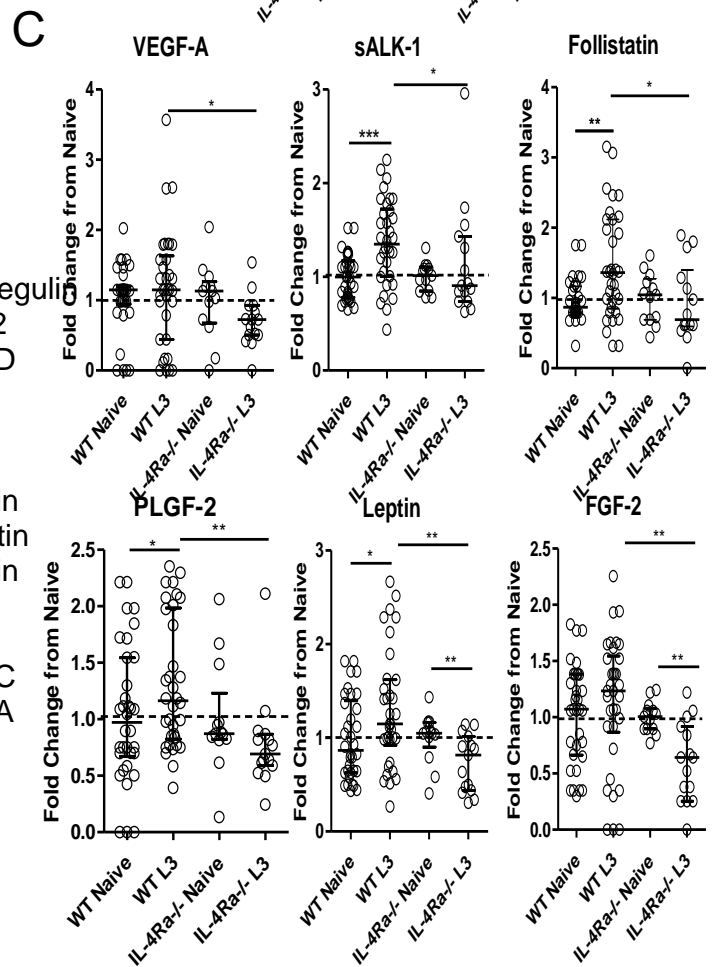
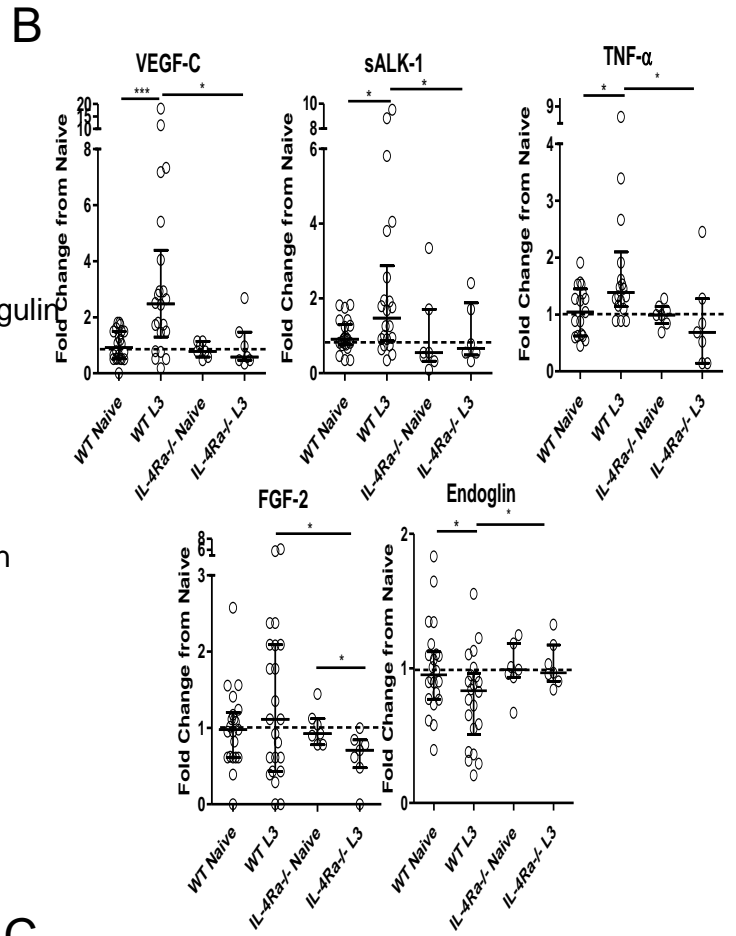
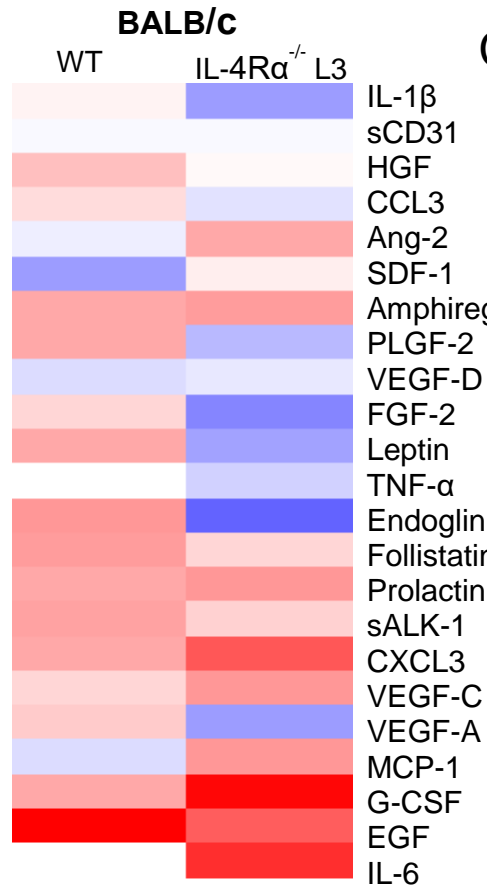
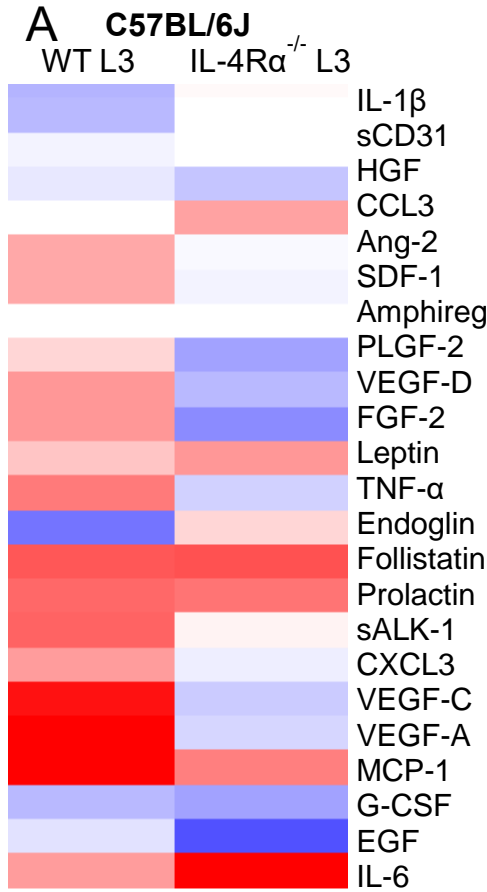


Figure 5.4: IL-4R α ^{-/-} mediated deficiency of Th2 adaptive immune responses significantly attenuates secretion of lymphangiogenic molecules linked with pathological filarial associated lymphatic remodelling, following *BmL3* infection.

A) Heatmap depicting mean fold-change increases (red) or decreases (blue), compared to sham-infected controls, in circulating serum lymphangiogenic/angiogenic factors in WT and IL-4R α ^{-/-} mice following *BmL3* infection determined by luminex multiplex immunoassay. Separate heatmaps are plotted for C57BL/6J and BALB/c strains **B&C)** serum analytes with statistically significant changes between WT and IL-4R α ^{-/-} *BmL3* infected mice, plotted as fold-change from the mean levels in relevant strain sham control groups. **B)** C57BL/6J strain **C)** BALB/c strain. Horizontal bars represent median \pm Interquartile range with data pooled from 3 separate experiments, with WT data reused from figure 3.3. (n=4-27 per group). Statistical significance is represented as *P<0.05 **P<0.01 ***P<0.001 derived from a Mann-Whitney U-test or a Kruskal Wallis test with Dunn's multiple comparisons post hoc test.

5.3.6- Macrophages in draining lymphoid tissues local to inoculation site express significantly higher levels of the alternatively activated macrophage markers CD206 and Relm- α .

To investigate if expanded macrophage populations local to the *BmL3* infection site demonstrate a 'Th2-associated alternative activation (AAM ϕ) phenotype, expression of two markers of alternative activation of macrophages (mannose receptor; CD206 and RELM α) were compared between C57BL/6J sham- and *BmL3*-infected mice at 14dpi, using flow cytometry.

C57BL/6J *BmL3* infected cohorts were observed to display significantly increased expression of CD206 and RELM α in draining lymphatic/lymphoid tissues, compared to sham infected controls (Figure 5.6A&B; CD206: 85.6 \pm 2.2 vs 55.8 \pm 2.5%, P<0.001, RELM α : 15.7 \pm 1.6 vs 1.3 \pm 0.2% P<0.001,).

5.3.7- Human monocyte derived macrophages polarised with recombinant IL-4 and IL-13 induce significant LEC proliferation and secrete higher concentrations of lymphangiogenic molecules *in vitro*.

Analysis of the *in vivo* data presented above indicates a Th2 adaptive immune response predominates in the infection microenvironment with associated IL-4R-dependent increases in lymphatic remodelling, lymphatic dysfunction and systemic circulating lymphangiogenic mediators. Further an AAM ϕ expansion is apparent at the site of infection and lymphatic pathology. Considering data from previous chapters implicating monocytes/macrophages with the induction of lymphatic pathology, the potential of differential, cytokine conditioned macrophages to induce LEC proliferation was investigated. The co-culture system developed in chapter 4 was utilised as shown in figure 5.7A with human THP-1 monocyte-derived macrophages stimulated with either Th1-associated recombinant (r)IFN- γ or Th2-associated rIL4 and rIL-13.

The proliferation of LECs co-cultured in the presence of M ϕ 's stimulated with rIL-4 and rIL-13 (M(IL-4/13)) was significantly higher than LECs cultured

alone in an 80% basal, 20% full growth medium (80:20) (Figure 5.7B; 1.85 ± 0.12 vs 1.0 ± 0.03 mean fold-change, $P < 0.001$), LECs co-cultured with macrophages receiving no cytokine stimulation (M0) (1.13 ± 0.04 mean fold-change from 80:20, $P < 0.001$) or LECs co-cultured in the presence of M ϕ 's conditioned with rIFN- γ (M(IFN γ)) (1.14 ± 0.08 mean fold-change from 80:20, $P < 0.001$) (Figure 5.7B). No significant difference in LEC proliferation was observed between LECs co-cultured with M(IFN- γ) and LECs cocultured with either M0 or 80:20 media alone (Figure 5.7B). Conditioned media from M ϕ 's stimulated with rIL-4 and rIL-13 contained significantly increased concentrations of the lymphangiogenic molecules: VEGF-A (2.1 ± 0.4 vs 1 ± 0.2 , $P < 0.05$), Follistatin (1.2 ± 0.02 vs 1 ± 0.02 , $P < 0.01$) and HGF (1.2 ± 0.05 vs 1.0 ± 0.03 , $P < 0.001$) compared to undifferentiated M ϕ 's (M0), while significantly decreased endoglin concentrations (0.89 ± 0.03 vs 1.0 ± 0 , $P < 0.01$) were observed (Figure 5.7C).

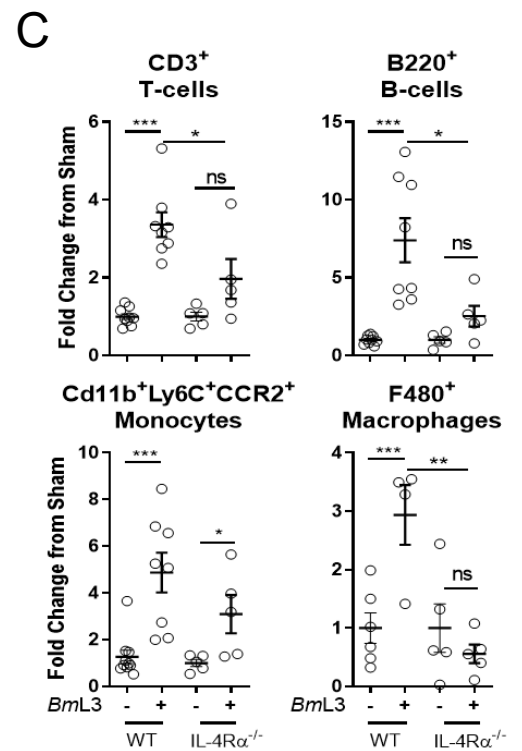
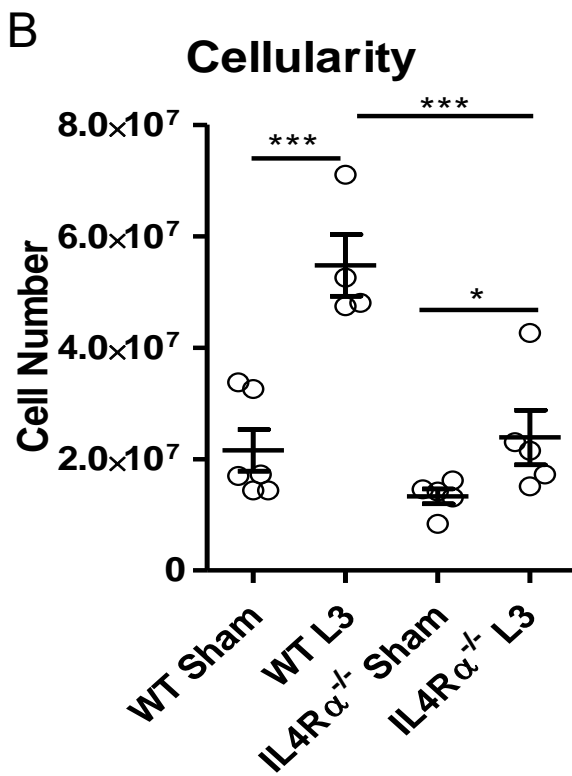
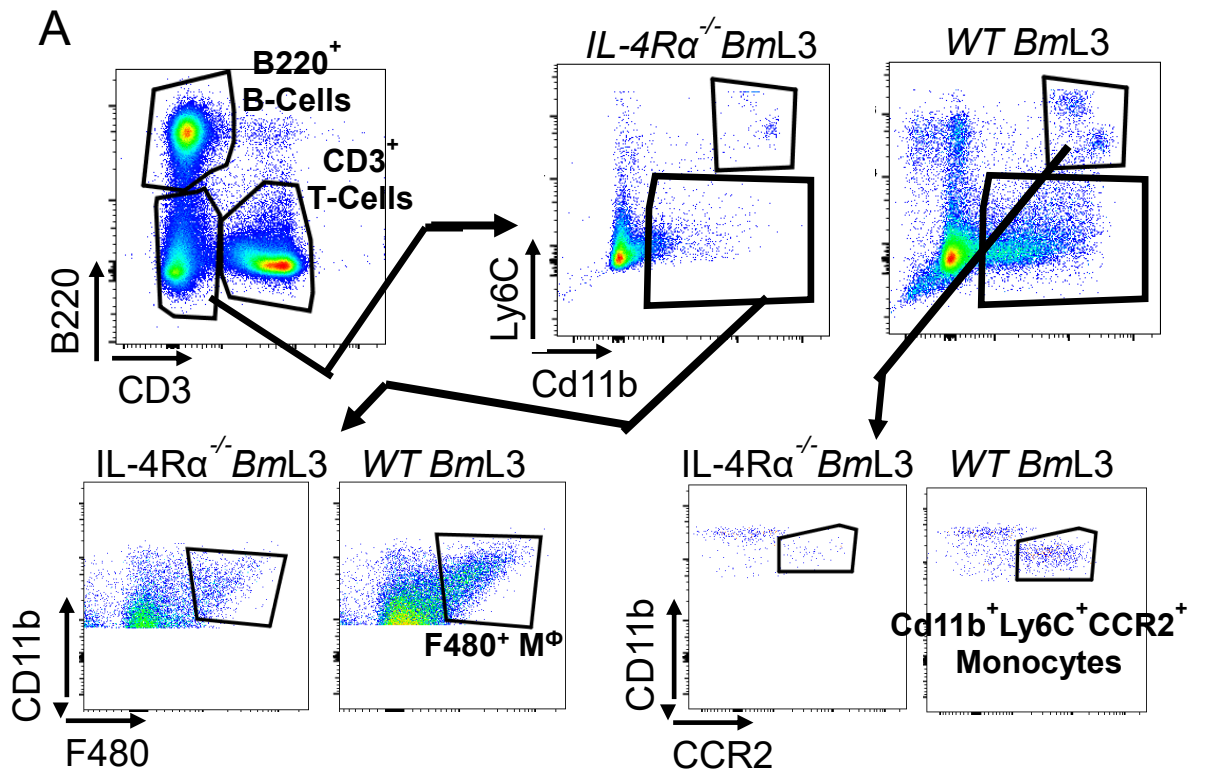


Figure 5.5: IL-4R α ^{-/-} deficiency in C57BL/6J mice results in significantly reduced proliferation/recruitment of specific immune cells to local lymphatic / lymphoid tissues following *BmL3* infection.

A) Gating strategy utilised to phenotype immune cell populations, strategy depicted previously gated on live, single cell LN populations **B)** Quantification of total cellularity of pooled sdLNs and associated lymphatics through total cell count **C)** Quantified changes in local lymphatic / lymphoid cell populations, plotted as a mean fold-change from relevant sham control, after immuno-phenotyping C57BL/6J sdLN suspensions using flow cytometry. Bars represent mean \pm SEM with data from a single experiment. Statistical significance is represented as *P<0.05 **P<0.01 ***P<0.001 derived from a one-way ANOVA with Tukey's multiple comparison post-hoc test (B) or two tailed student t-test (C).

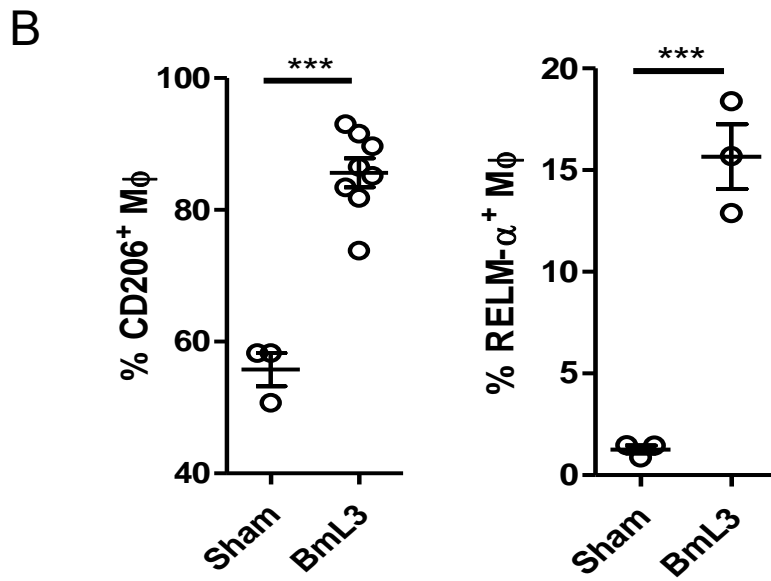
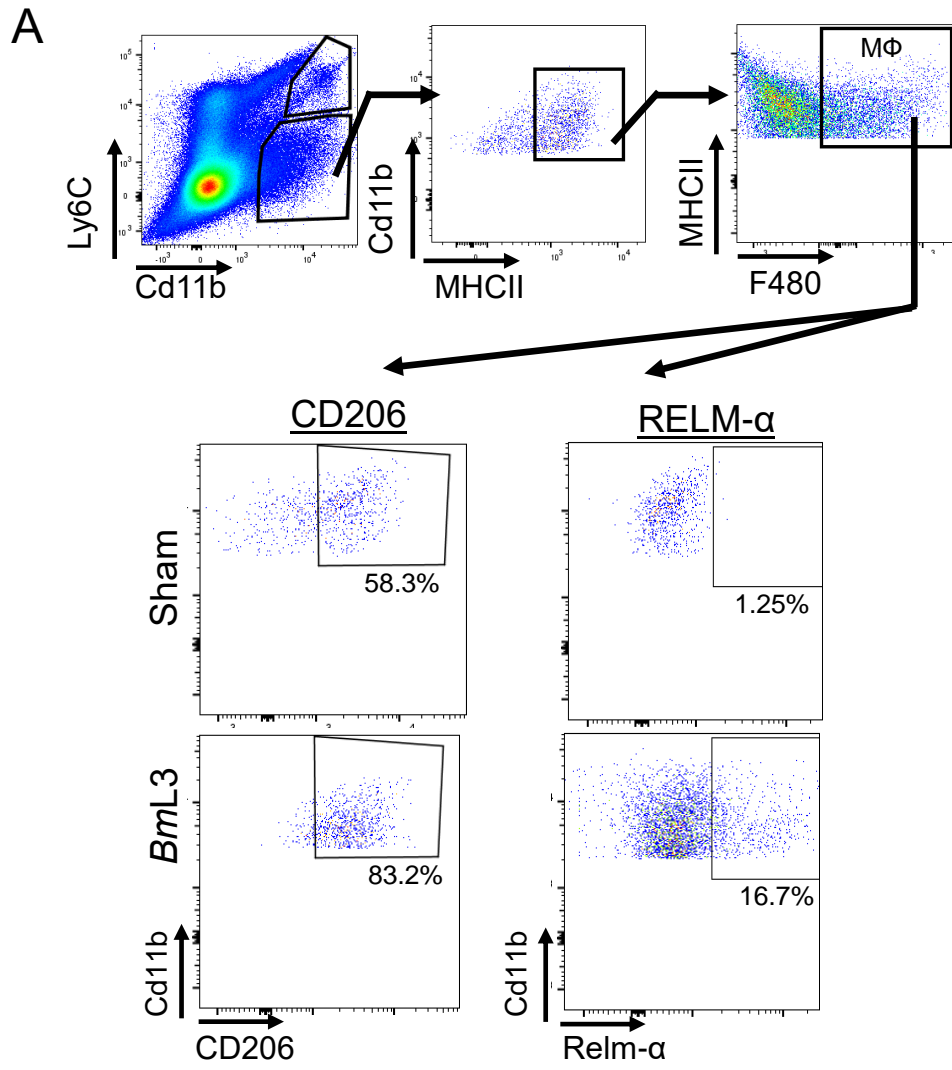
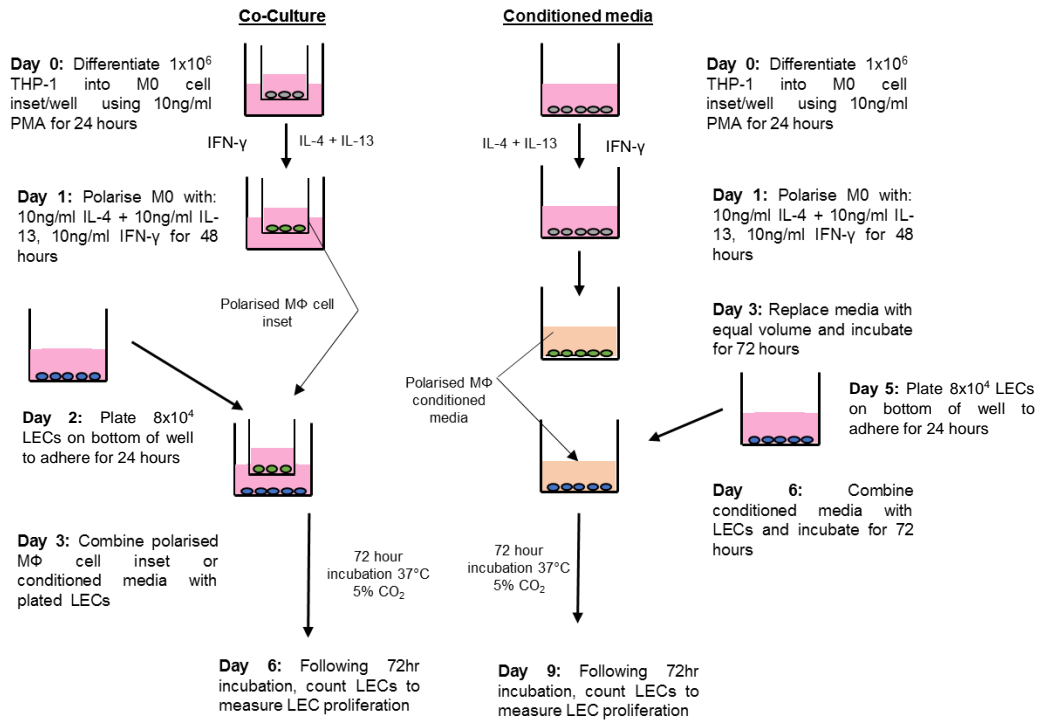


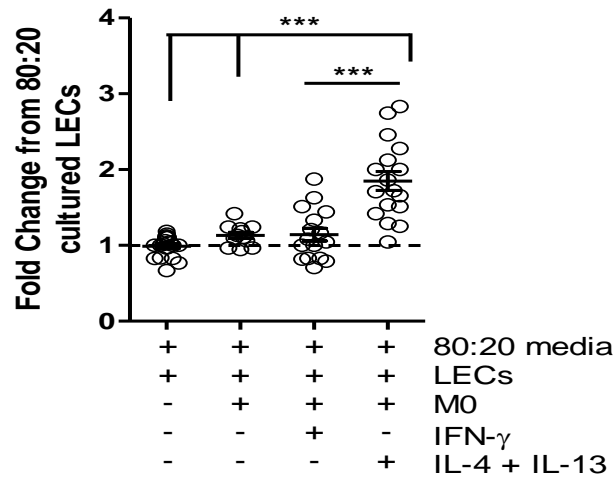
Figure 5.6: *BmL3* infection in C57BL/6J mice induces an ‘Alternatively Activated Macrophage (AAM ϕ)’ phenotype in lymphatic / lymphoid tissues local to the *BmL3* infection site.

A) Gating strategy and representative flow cytometry dot plots. Gating strategy applies to samples previously gated on live, single cells **B)** CD206⁺ and RELM- α ⁺ expression as a percentage of total macrophages from C57BL/6J *BmL3*- or sham-infected mice. Horizontal bars represent the mean \pm SEM with data pooled from two separate experiments (CD206) (n=11) or one individual experiment (RELM- α) (n=6). Statistical significance is indicated as ***=P<0.001, derived from a two-tailed student’s t-test.

A



B



C

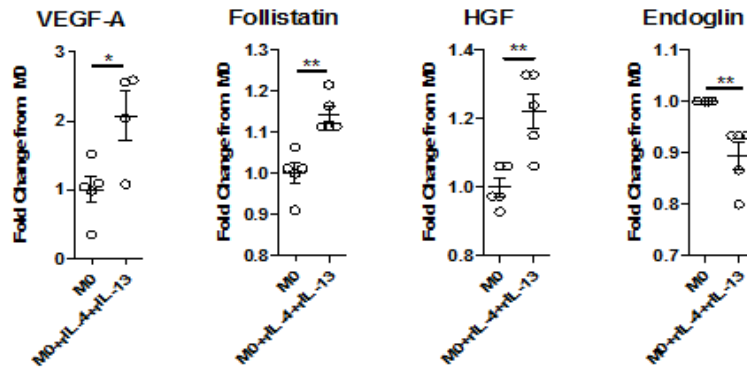


Figure 5.7: Exposure of monocyte derived macrophages to rIL-4 and rIL-13 induces significant proliferation of LECs *in vitro*

A) Schematic of developed co-culture system utilised **B)** Quantified survival/proliferation of LEC cells when co-cultured with differential-cytokine conditioned macrophages: differentiated macrophages with no further stimulation (M0), conditioned with rIFN- γ (IFN- γ) or conditioned with rIL-4 and rIL-13 (IL4+IL-13) in cell insets. Data is plotted as fold-change in LEC number from LECs cultured in 80:20 (basal media) only. **C)** Conditioned media from experiments in **B)** were assayed using a multiplex panel, of known lymphangiogenic molecules with analytes attaining statistically significant concentrations shown Data is plotted as the fold change in LEC number from LECs cultured in basal media only (B) or fold change in analyte concentration from undifferentiated M0 controls (C). Horizontal bars represent mean \pm SEM with data pooled from three separate experiments (N=15-19 per group) (B) or two individual experiments (N=5 per group) (C) Statistical significance is represented as *=P<0.05, **=P<0.01 ***=P<0.001 derived from a one- way ANOVA with Tukey's multiple comparison post-hoc test (B) or a student's two-tailed t-test (D).

5.4- Discussion

Th2 responses are critical for eosinophil-predominated worm attrition and resistance to filarial re-infection in animal models of infection (Osborne, Hunter and Devaney, 1996; Babu *et al.*, 2000; Spencer, Shultz and Rajan, 2001; Taylor *et al.*, 2005; Turner *et al.*, 2018). Successful establishment of chronic filarial infections appear dependent on modifying and suppressing these overt anti-parasite Th2 responses. Clinically, asymptomatic, microfilaraemic patients presenting with patent infection commonly exhibit a 'modified' Th2 response coincident with increased adaptive immunomodulatory regulatory T-cell responses (Metenou *et al.*, 2010; Babu and Nutman, 2012). PBMCs from permissive microfilaraemic individuals can be stimulated to produce elevated Th1 and Th2 cytokines to filarial antigens if regulatory cytokines, IL-10 and TGF- β , are neutralised in culture (King *et al.*, 1993). Further, in permissive rodent models of filariasis, depletion of regulatory T cells reverses Th2 hyporesponsiveness and mediates increased resistance against chronic adult infection (Taylor, 2005).

The role of anti-parasite Th2 responses in induction of filarial pathology are less well-defined. Filarial LE patients exhibit increased serum concentrations of Th2 associated cytokines (Anuradha *et al.*, 2012). In an Athymic (nude) mouse model of intra-lymphatic brugian filariasis, reconstitution of adaptive immunity is necessary for the development of severe LF lymphoedematous pathology (Vickery *et al.*, 1991). Further in a recently published ferret model of lymphatic filariasis, expression of mixed Th1 and Th2 responses was associated with development of lymphoedematous pathology (Jackson-Thompson *et al.*, 2018).

Data presented in chapter two demonstrated that substantial lymphatic pathology occurs far earlier in the infection time-course than previously realised, with rapid onset observed as little as 6 days following primary *B. malayi* larval infection. An important objective of this chapter, therefore, was to investigate adaptive immune control of the initiation of filarial-infection induced lymphatic pathology. Utilising the developed pathology model, SCID

mice, with impaired adaptive immune responses ((Bosma and Carroll, 1991; Nelson *et al.*, 1991)) were compared against immune-competent counterparts to measure differences in lymphatic remodelling and associated lymphatic dysfunction. SCID mice were less prone to initiation of lymphatic pathologies post-infection. Additionally, lymphatic insufficiency was shown to be partially ameliorated in SCID mice post-infection. Taken together, these data promote a role for the initial adaptive immune response, to larval lymphatic infection, in mediating lymphatic remodelling and associated lymphatic dysfunction. This partially emulates studies of adult *Brugia* infections within T-lymphocyte deficient (athymic) nude mice, demonstrating LF related pathology only occurs following adoptive transfer of adaptive immune competent splenocytes/T-cells (Vickery *et al.*, 1991) but indicates that larval infection can trigger pathology much earlier in the *B. malayi* infection time-course. Interestingly, a non-significant trend may suggest that early lymphatic pathology was not completely abrogated in SCID mice. Localised lymphatic dilation (lymphangectasia) has been detailed in lymphopenic mice post-infection with *B. malayi* (Vincent *et al.*, 1984; Nelson *et al.*, 1991; Vickery *et al.*, 1991). Therefore, either filarial-induced changes and/or innate immune processes may contribute to a minor degree in development of lymphatic activation post-filarial parasitism. Indeed, in chapter 4, it was determined that *B. malayi* live L3 or L3 extracts (*BmL3E*) could activate human monocyte-derived M ϕ to trigger LEC proliferation.

It was thus important to characterise the type of adaptive immune responses that were initiated by *B. malayi* larval intra-lymphatic infections. Intracellular cytokine staining of sdLN's proximal to inoculation sites demonstrated significant upregulation of IL-4, IL-13 and IL-10 CD4⁺ expressing T-cells in *BmL3* infected mice, compared to sham controls. The presence of an IL-4, IL-13 and IL-10 dominated local environment is highly indicative of a localised Th2 polarised adaptive immune response (Corthay, 2006)(Osborne, Hunter and Devaney, 1996; Osborne and Devaney, 1998; Babu *et al.*, 2000; Spencer, Shultz and Rajan, 2001; Babu and Nutman, 2014). Systemic immune responses, examined using splenocyte recall responses indicated a more mixed Th1/Th2 response, with significantly

higher secretion of Th1 related IFN- γ as well as IL-4, IL-13 and IL-10 observed in *BmL3* infected mice. Whilst it is presently unclear why splenic adaptive immune responses may be more mixed, previous studies have noted similar, mixed Th1/Th2 observations following filarial infection (Babu *et al.*, 2000; Saeftel *et al.*, 2003). Mixed adaptive immune responses may be potentially driven by parasite (Th2) stimulation, including responses to their secretions, concurrently with inflammatory (Th1) antigenic stimulation to the intracellular symbionts *Wolbachia* (Gentil, Hoerauf and Pearlman, 2012; Nutman, 2013) following death and disintegration of larvae. Further evidence for this hypothesis comes from studies showing that addition of *Wolbachia* derived lipoprotein alone was sufficient to deviate the strong Th-2 polarising potential of filarial material in dendritic cells (Turner *et al.*, 2009). *BmL3* larval death has been demonstrated to occur at the early 6-day time point in the developed model whilst there is no evidence of patent adult infections in immune-intact mice (Chapter 2) demonstrating that murine hosts would be subjected to both Th2 polarising filarial material, as well as Th1 polarising *Wolbachia* antigens at the time points analysed.

The known role of Th2 responses in anti-filarial immunity, together with evidence of strong Th2 responses in areas local to infection, remodelling and insufficiency, resulted in a hypothesis that Th2 responses may be necessary in the full induction of filarial-associated lymphatic pathology. To investigate this, IL-4R $\alpha^{-/-}$ mice, deficient in IL-4 and IL-13 signalling and thus displaying severely dysfunctional Th2 responses (Barner *et al.*, 1998)(Stanton *et al.*, 2015), from both C57BL/6J and BALB/c strains were utilised. Both strains were selected in experiments because of the pronounced strain-variation in degree of lymphatic pathology identified in chapter 2. The IL-4R $\alpha^{-/-}$ mice displayed significantly reduced Th2 adaptive immune responses, in terms of IL-4 and IL-13, compared to WT controls, post-infection. Together these data confirmed ablation of Th2 responses in IL-4R $\alpha^{-/-}$ mice local to infection, presumably due to nullification of autocrine IL-4/IL-13 –IL-4R positive feedback during the polarisation of Th2 CD4⁺ T cells. Via NIR optical imaging of infected limbs and ICG lymphangiography, significantly lower lymphatic remodelling, determined by a significantly lower level of aberrant lymphatic

channels, was apparent in the absence of IL-4R α signalling. Concomitantly, IL-4R α deficient mice displayed significantly less lymphatic dysfunction in terms of impeded lymphatic drainage / dermal backflow patterning usually observable in WT mice post-infection. Together, the data suggests polarised Th2 responses local to the infection site are functionally important in mediating aberrant lymphatic remodelling and insufficiency, induced by *BmL3* infection. The reproducibility of these findings across the 'high pathology' C57BL/6J, as well as the 'low pathology' BALB/c strains further strengthens the primacy of IL-4/13-IL-4R adaptive immune response to filarial infection as necessary for the initiation of lymphatic pathology.

Th2 adaptive immune responses have been shown to be important in wound healing and tissue repair, particularly as a primary defence to the overt damage inflicted by a range of extracellular parasites, including helminths (Taylor *et al.*, 2006). Migrating *BmL3* larvae and their death within lymphatic tissues will cause a level of tissue damage which will presumably invoke a local Th2 immune response. The data suggests however, that these repair mechanisms may be a double-edged sword, with the results suggesting 'runaway' Th2 stimulation results in off-target lymphatic remodelling events that induce a state of lymphatic dysfunction. The 'runaway' magnitude of the localised Th2 response, inducing pathological consequences, might also be positively influenced by the delivery of a rich Th2 polarising potential (ie a bolus of somatic and excreted/secreted filarial helminth antigens) 'delivered, en masse' into and immediately adjacent to the local skin draining lymphoid tissues. While ablation of Th2 responses appears protective from early induction of filarial-associated lymphatic pathology, further work is required to investigate the long-term consequences, particularly how an absence of early Th2 mediated tissue repair could contribute to potential later development of pathology. Of more importance to future therapeutic strategies, regulation / modulation of the 'strength' of the Th2 response following initial infection may be of interest, as pre-clinical and clinical data suggests a strong correlation between asymptomatic, lack of clinical pathology, patient outcome and a skewed, highly immunoregulatory Th2 response (Hoerauf *et al.*, 2005; Taylor *et al.*, 2005; O'Regan *et al.*, 2014).

Inducing a more balanced, modified Th2-based immunity with correct levels of wound healing, may be important for preventing the induction of LE pathology. The mechanisms by which filarial larvae can induce these 'modified' Th2 responses, particularly on effector immune cells may also be an area of future interest, as shown by previous findings (Allen and Loke, 2001; O'Regan *et al.*, 2014), along with work highlighted in chapter four demonstrating how parasite material can induce monocytes and macrophages to induce lymphatic endothelial proliferation directly. Interestingly, utilisation of parasite material has been shown to strongly induce regulatory immune responses, with potential therapeutic applications against autoimmune disorders currently an area of intense research (Hewitson, Grainger and Maizels, 2009; McSorley, Hewitson and Maizels, 2013). Utilisation of immunoregulatory parasite materials, or increasing the availability of filarial derived immunomodulatory proteins may prove useful in "resetting" immune responses or modulating "runaway" Th2 immune responses responsible for lymphatic pathology. As these proteins are mechanisms used by helminths for immune evasion, however it will be important to achieve a balance between controlling "wound healing" Th2 responses, while still achieving sufficient levels of anti-parasitic Th2 responses to allow worm expulsion

The cellular and molecular mechanisms by which Th2 responses induce lymphatic pathology remain to be fully defined. Alongside data presented in chapter 3 demonstrating strong upregulation of a milieu of circulating lymphangiogenic factors following *BmL3* infection, it was hypothesised that Th2 adaptive immune signalling may be necessary to induce the secretion of lymphangiogenic factors, local to infection, that are important in inducing lymphangiogenesis and dilation. To investigate this, IL-4R $\alpha^{-/-}$ and WT mouse serum lymphangiogenic profiles were compared following *BmL3* infection. Lymphangiogenic factors associated with induction of lymphatic pathology in WT mice failed to show similar levels of upregulation in *BmL3* infected IL-4R $\alpha^{-/-}$ mice. Specifically, upregulation of VEGF-A, C, sALK-1, Follistatin TNF- α , Leptin, PLGF-2, Endoglin and FGF-2 were significantly attenuated in the absence of IL-4R signalling. Some of these factors were impaired in both

background strains in the absence of IL-4R signalling (ALK-1 and VEGFs) whilst others were strain-dependent, suggesting a complex inter-dependent or redundant series of receptor-ligand pathways in inducing pathological lymphatic remodelling. Nevertheless, the data supports a requirement for IL-4R Th2 immune signalling to mediate the release of a complex milieu of lymphangiogenic factors, some of which alone or in combination may be fundamental to induce activation, sprouting, migration and even trans-differentiation of lymphatic endothelium/ progenitors leading to pathological remodelling.

Chapter four discussed data demonstrating *BmL3* infection results in expansion of monocytes and macrophages in sites proximal to infection and secrete significant concentrations of multiple lymphangiogenic molecules. This identified a potential role of monocytes/macrophages in the induction of lymphatic dysfunction, as depletion of either monocytes or macrophages lead to the amelioration of pathology. Macrophages express IL-4R (Weng *et al.*, 2018), which once ligated by IL-4 or IL-13, result in polarisation to a functionally distinct AAM ϕ phenotype (Gordon and Martinez, 2010). AAM ϕ are defined by strong downregulation of nitric oxide production (Mills, 2012), concurrent with strong expression of arginase enzyme (Rath *et al.*, 2014). Additionally, expression of the secreted molecules chitinase-like 3 (Ym-1) and Resistin-like molecule alpha (RELM- α) are only observed following polarisation to a AAM ϕ phenotype (Raes *et al.*, 2002). AAM ϕ are shown to be strongly induced following helminth infection including filarial *Brugia malayi* (Loke *et al.*, 2002; Hoerauf *et al.*, 2005; Babu, Kumaraswami and Nutman, 2009; Turner *et al.*, 2018), as well as *Heligmosomoides polygyrus*, *Nippostrongylus Brasiliensis* and *Litomosoides sigmondontis* (Anthony *et al.*, 2006; Nair, Guild and Artis, 2006; Taylor *et al.*, 2006). AAM ϕ play a key role as effector cells in the host response to helminth infection, inducing Th2 inflammatory responses which, following *Brugia malayi* infection, are key to parasite clearance and worm expulsion (Turner *et al.*, 2018). AAM ϕ , particularly following helminth infections, also play a key role in tissue repair and wound healing directly (Freedman *et al.*, 1994; Allen and Wynn, 2011; Chen *et al.*, 2012), through the secretion of factors such as matrix

metalloproteases (MMP's) (Krzyszczuk *et al.*, 2018) and members of the vascular endothelial growth factor (VEGF) family (Vannella and Wynn, 2017). Indirectly, AAM ϕ contribute to tissue repair by preventing excessive damage following inflammation, orchestrating its resolution through release of a milieu of anti-inflammatory/immunoregulatory molecules such as TGF- β , PDL-1 and IL-10 (Wynn and Barron, 2010; Wynn, Chawla and Pollard, 2013). In the context of helminth infection, it has been recently shown that AAM ϕ expression of Ym-1 and RELM- α is vital in lung tissue repair following the migratory stage of *N. brasiliensis* infection. IL-4R α deficient mice, thus lacking AAM ϕ induction, demonstrated more severe lung tissue damage following infection compared to WT, while this was reversed with adoptive transfer of WT macrophages to IL-4R α deficient mice.(Sutherland *et al.*, 2018)

A preliminary question was to understand if ablation of Th2 responses significantly impacted on increased populations of macrophages and monocytes following filarial infection. At the local lymphatic and lymphoid tissues proximal to lymphatic invasion sites of *BmL3* infection, IL-4R-deficiency resulted in a significantly lower expansion in macrophages. This would suggest that Th2 adaptive responses are important in either mediating the recruitment of monocytes following filarial infection or activating macrophages as an effector mechanism to respond to filarial infection. The reduced macrophage/monocyte populations coincident with reduced lymphatic pathology in IL-4R α ^{-/-} mice, together with the previously identified role for monocytes/macrophages in induction of lymphatic insufficiency (Chapter 4), suggests a role for Th2 adaptive responses in positively regulating the monocyte/macrophage cellular mechanism of pathology. When examining the phenotype of macrophages in lymphatic / lymphoid tissues proximal to sites of infection, significantly increased expression levels of the alternatively activated macrophage markers: CD206 (mannose receptor) and RELM α were evident, suggesting the significantly expanded macrophage population following *BmL3* infection are polarising to an alternatively activated phenotype.

Mannose receptor and MHCII have prior been identified as markers of inflammatory monocyte recruited populations of AAM ϕ in situations of serous cavity and hepatic helminth-mediated Th2 inflammation, including filarial infection (Smith *et al.*, 2004; Anthony *et al.*, 2006; Mylonas *et al.*, 2009; Jenkins and Allen, 2010). Whilst more experiments would be required (such as development of bone marrow chimeras) to formally prove the provenance of AAM ϕ at the filarial lymphatic pathology site, high MHCII and MR expression, together with a significantly decreased expression of tissue residence marker (Tim-4⁻)(Chapter 4) are evidence that these macrophages are recruited from the blood prior to alternative-activation and thus may be derived from CCR2⁺ recruited monocytes.

To further interrogate the ability of IL-4/13 activated AAM ϕ to directly induce lymphatic remodelling, monocyte-derived macrophages conditioned with IL-4/IL-13 recombinant cytokines were scrutinised for their ability to stimulate LEC proliferation in an *in vitro* co-culture system (see chapter 4). Monocytes recently differentiated to macrophages with no further stimulation, or conditioned with the Th-1 associated cytokine, IFN- γ , did not mediate significant proliferation of LEC cells, In contrast, monocyte derived macrophages, conditioned with rIL-4 and rIL-13 induced ~2-fold increases in LEC proliferation. This suggests that in a local environment dominated by Th2 adaptive responses, such as following early filarial infection, IL4/13 conditioned AAM ϕ can induce LEC proliferation, enabling lymphatic remodelling to occur. Assaying of media conditioned by M ϕ 's stimulated with rIL-4 and rIL-13 demonstrated significantly increased secretion of a milieu of lymphangiogenic molecules, identified to be increased systemically in the murine model (Chapter 3) including: VEGF-A, Follistatin, HGF as well as significantly decreased Endoglin. While the replication from the murine model to the human *in vitro* system further highlights a role for these factors in mediating remodelling, it also demonstrates AAM ϕ 's actively secrete lymphangiogenic products that drive lymphatic remodelling and downstream insufficiency, presumably in a Th2 dominated environment. The data presented concurs with observations in oncology, where tumours can 'hijack' recruited macrophages into 'tumour associated macrophages' (TAM's)- a

modified macrophage phenotype sharing characteristics with alternatively activated macrophages (Mantovani *et al.*, 2002; Sousa *et al.*, 2015; Yamaguchi *et al.*, 2016). These modified 'AAM like' TAM's mediate tumour survival through vascularisation of tumours (both through induction of angiogenesis and lymphangiogenesis (Lin *et al.*, 2006; Du *et al.*, 2008; Mazziari *et al.*, 2011; Riabov *et al.*, 2014)) as well as metastasis (Sangaletti *et al.*, 2008; Zhang *et al.*, 2009; Qian and Pollard, 2010). This, together with the data discussed strengthens the assertion that the strong local Th2 response that monocyte/macrophage effector cells are exposed to following *BmL3* infection induces the AAM ϕ phenotype which is functionally important in lymphatic remodelling post-filarial infection. Additionally, in concert with highly polarised Th2 responses, filarial larvae may be able to directly polarise monocytes and/or macrophages into a lymphangiogenic phenotype through parasite-host signalling (ie release of excretory secretory vesicles (Weinkopff *et al.*, 2014; Jothi *et al.*, 2016)). Evidence of this, concurring with the highlighted work above, was demonstrated in the same co-culture system in chapter 4.

With data demonstrating a mechanism whereby Th2 adaptive immune signalling leads to recruitment and development of a pro-lymphangiogenic monocyte-macrophage lineage to induce lymphatic pathology, new therapeutic strategies that target or modulate Th2 responses/signalling may become of interest. While still in it's infancy, nanoparticles that specifically target TAMs (such as through CD206 uptake), and deliver immunomodulatory molecules such as anti-IL10 or siRNA's against $\text{ik}\beta\alpha$ were successful in cancer preclinical models at "re-educating" TAMs to an "M1" phenotype, which correlated with tumour regression (Huang *et al.*, 2012; Ortega *et al.*, 2016). As eluded to above, it is possible that overstimulation of the Th2 anti-parasite response, potentially as a consequence of macro-parasitic infection within the 'heart' of the lymphatic system, may result in undesirable off-target effects such as overstimulated tissue repair pathways, leading to aberrant lymphatic remodelling. Therapeutic targets that aim to modulate the strength of Th2 responses to filarial infection, such as administration of anti-inflammatory medications or

blocking/depleting antibodies specific for Th2 responses, may be useful in preventing the overstimulation of the Th2 mediated lymphangiogenic pathways. Important consideration of such methods is necessary, however, with Th2 responses clearly an important facet of host defence to filarial infection, while later 'regulated / modified' Th2 responses even seem to be common in asymptomatic patient cohorts. This suggests the temporal induction, appropriate strength and type of Th2 responses may be key determinants of a pathological or asymptomatic outcome. Targeting the specific cellular or molecular effector mechanisms regulated by Th2 signalling that mediate lymphatic pathology induction may therefore be a more promising approach. 'Re-education' of local monocyte/macrophage populations- as hypothesised in tumour associated macrophages (Noy and Pollard, 2014; Josephs, Bax and Karagiannis, 2015; Huber-Ruano *et al.*, 2017)- may help to prevent excessive remodelling, thus modifying the maintenance and progression to a state of LE, through limitation of the pool of lymphangiogenic mediators in the microenvironment back to levels more appropriate for wound healing only.

5.5- Chapter concluding remarks

The objective of this chapter was to investigate the types of host adaptive immune responses present in the early time frame following filarial larval infection. More pertinently, it was important to understand if there was any association between induction of identified adaptive immune responses and the observed lymphatic remodelling and insufficiency post experimental *B. malayi* larval infection. Finally, the research aimed to investigate whether host adaptive responses are functionally important in the development of filarial-associated lymphatic pathology. The data clearly identifies a strong induction of localised Th2 adaptive immune responses following larval infection that it is temporally and spatially coincident with the induction of lymphatic dysfunction and concomitant increases in pro-lymphangiogenic mediators. Further, the data presented demonstrates Th2 signalling induces the expansion of a local population of AAM ϕ and provides *in vitro* evidence that IL-4/13 conditioned macrophages can directly stimulate lymphatic endothelial proliferation.

While host Th2 adaptive immune responses are crucial for defence to filarial infection, off-target 'runaway' Th2 mediated mechanisms can contribute to pathology. Inappropriately strong induction of Th2 mediated 'tissue repair' pathways, can lead to aberrant lymphatic remodelling that contributes to filarial-infection lymphatic dysfunction. Consequently, Th2 adaptive responses can be viewed as a 'double edged sword' and the temporal induction, strength of and type of Th2 responses induced following filarial larval infection may act as key determinants to later manifestations of pathology in patients. Ultimately, this reveals potential novel therapeutic strategies whereby modulation of Th2 anti-filarial responses could be targeted to ameliorate pathological LF outcomes.

Chapter 6

Concluding remarks

6.1- A new perspective on the role of lymphatic remodelling in filarial associated lymphatic pathology.

Lymphatic remodelling is a “hallmark” of filarial infection, with alterations to the lymphatic architecture observed in both symptomatic and asymptomatic patient groups. It is therefore not certain what role lymphatic remodelling plays in the development of future filarial pathology, with evidence in other models of lymphatic disease suggesting not only a contributing role to pathology, but also a possible compensatory “wound healing” response by the host to repair lymphatic damage and restore homeostatic lymphatic function. A major obstacle to investigating the mechanism and consequences of filarial lymphatic remodelling is the lack of animal models that allows longitudinal interrogation of changes to the lymphatic architecture, following filarial infection. While recent development of a ferret limb pathology model (Jackson-Thompson *et al.*, 2018) has provided promising insights, the lack of reagents or genetic knockout strains in ferrets limits findings to temporal development of lymphatic remodelling, with a lack of ability to adequately investigate the mechanisms driving filarial lymphatic remodelling.

The development of the novel murine inflammatory leg pathology model in immune-competent strains in this thesis demonstrated that profound alterations to the lymphatic architecture can be observed rapidly (as little as 6 days) following infection, and in response to the infective L3 larval stage of filarial infection. Further, lymphatic remodelling was concomitant with lymphatic dilation and significant lymphatic insufficiency, all of which persisted long-term and post-clearance of filarial infection. It was previously hypothesised that lymphatic remodelling is a consequence of long term habitation of adult worms in lymphatic channels and, when combined with subsequent death events initiating inflammatory reactions, results in lymphatic alterations which contributes to a pathological outcome (Rajan *et al.*, 1999; Figueredo-Silva *et al.*, 2002; Bennuru and Nutman, 2009b). In contrast, the evidence presented within this thesis suggests lymphatic remodelling occurs far earlier than previously anticipated, with significant

remodelling occurring in response to initial infective larval stage of filarial infection. The accompanying pathology, the consistency with which these lymphatic alterations were observed (almost 100% of infected animals displayed degrees of remodelling and pathology) and persistence long term, post clearance of infection, suggests this early subclinical pathology is an important feature of filarial infection. A number of clinical studies have demonstrated significant lymphatic alterations, even in asymptomatic LF patients (Noroës *et al.*, 1996; Shenoy *et al.*, 2008; Kar *et al.*, 2017). Further, subclinical, pathological changes to the lymphatics and changes in tissue fluid retention in clinically asymptomatic patients have also been observed (Douglass *et al.*, 2017). Together, the work in this thesis demonstrates a previously underappreciated role of infective L3 filarial Larvae in the rapid induction of lymphatic remodelling which quickly results in “covert” subclinical pathological lymphatic insufficiency.

[6.2- *BmL3* infection induces changes in expression of lymphangiogenic molecules which are implicated in lymphatic remodelling and pathology.](#)

With the successful development of a novel murine leg pathology model, a primary objective of the thesis was to characterise the mechanisms that induce the rapid lymphatic remodelling and pathology, observed following filarial infection. Assaying plasma against a focused panel of 27 growth factors and other molecules implicated in angiogenesis / lymphangiogenesis in various inbred murine strains and immune deficient animals revealed a milieu of factors which display significant upregulation/downregulation, concurrent with filarial lymphatic pathology. Further evidence strengthening a role for these lymphangiogenic factors was demonstrated by clear associations between: number of infection events or severity of lymphatic remodelling (with confirmed differences between inbred murine strains) and levels of upregulation/downregulation of these molecules. A summary of the key molecules that are most consistently altered, and thus demonstrate importance in mediating filarial lymphatic pathology can be seen in Table 1.

Clinical studies have previously characterised increases of lymphangiogenic molecules such as: VEGF's, Angiopoietins and FGF-2 in response to filarial

infection in humans (A Y Debrah *et al.*, 2007; Debrah *et al.*, 2009; Bennuru *et al.*, 2010). The work in this thesis reasserts the importance of these identified molecules, with the same lymphangiogenic molecules observed to be significantly upregulated in the murine model. Interestingly, the data also reveals an important role for less well characterised lymphangiogenic molecules such as: TGF- β superfamily members (ie sALK-1), Prolactin and Follistatin in driving filarial associated lymphatic remodelling and pathology.

SEVERITY OF LYMPHATIC REMODELLING

	C57BL/6J <i>BmL3x2</i> WT	C57BL/6J WT	BALB/c WT	C57BL/6J <i>IL-4Rα^{-/-}</i>	BALB/c <i>IL-4Rα^{-/-}</i>
VEGF-C	/	+++ ***	+ *	-	+
VEGF-A	/	+++	+	-	-
sALK-1	++++ *	+++ *	+ ***	/	/
Prolactin	++++ *	+++ *	++	+++	+++ *
Follistatin	++	++ *	+ **	++ *	/
Angiopoietin II	/	++ *	/	/	+ *
FGF-2	+	++ *	+	- *	-- **
Endoglin	-	- *	-	/	-
TNF- α	/	++ *	/	-	-
CXCL3	-- **	+	+	/	++ **
HGF	++++ *	-	+ *	--	/
SDF-1	+	++	- *	-	/
Leptin	++	+	+	++	- **
PLGF-2	-	/	+ *	- *	-

Chapter 3		Chapter 5			
++++	+++	++	+	/	--

*=P<0.05, **=P<0.01, ***=P<0.001 vs sham control counterparts

Lymphangiogenic molecules displaying consistent changes in circulating serum concentrations are summarised across all the varying murine wild type (WT) and Th2 deficient (IL-4R α ^{-/-}) strains. Red and blue shadings demonstrate varying degrees of upregulation or downregulation compared to sham controls.

6.3- Host inflammatory Th2 adaptive immune responses to filarial infection- too much of a good thing?

Investigation into the cellular mechanisms of filarial associated lymphatic remodelling and pathology in this thesis provided evidence for a role for immune inflammatory cells namely: Inflammatory monocytes, macrophages and, to a lesser extent, B and T-cells in secreting significant concentrations of lymphangiogenic molecules that contribute toward the milieu that potentially drives filarial associated lymphatic remodelling and pathology. An abundance of work has characterised innate and adaptive immune responses to filarial infection, with skewing of responses to inflammatory Th-1/Th-2/Th-17 responses correlating with a pathological outcome while “modified/regulatory/anti-inflammatory” Th-2 responses is more frequently observed in asymptomatic patients (Babu and Nutman, 2012). However, with the previously underappreciated role of the ability of infective larval infection to drive profound lymphatic remodelling, contributing to pathological lymphatic insufficiency, a final objective of the thesis was to better understand how early immune responses to filarial larval infection may contribute to the development of the rapid lymphatic remodelling and pathology observed.

Significant local expansions of IL-4⁺,IL-13⁺ and IL-10⁺ CD4⁺ T-cells, indicative of a strong Th2 adaptive immune response, were demonstrated as little as 14 days post infection with BmL3 larvae. Comparing immunocompetent wild type infected mice to heavily adaptive Th-2 deficient IL-4R α ^{-/-} infected counterparts demonstrated significant amelioration of lymphatic remodelling and pathology. Further many of the key lymphangiogenic signals showing consistent upregulation in Wild Type infected mice fail to show measurable changes following infection in IL-4R α ^{-/-} infected counterparts. This provided associative evidence that adaptive Th2

immune responses play a role, likely through specific recruitment/polarisation of “Th-2 effector” immune cells that secrete significant quantities of lymphangiogenic molecules, in driving filarial lymphatic pathology. With previous work showing a vital role for Th2 responses in anti-filarial immunity (Babu and Nutman, 2014; Turner *et al.*, 2018), the “strength” of the initiated Th-2 response and the extent to which regulatory responses are coincidentally triggered (inflammatory Th-2 vs anti-inflammatory/immunoregulatory Th-2) might be important in the severity of observed filarial lymphatic remodelling and pathology. This can be demonstrated by the significant difference in severity of remodelling and pathology observed between the higher lymphatic pathology C57BL/6J murine strain (which has a well characterised, more “vigorous” or strengthened immune response- making them resistant- to filarial infection (Shenoy *et al.*, 1998; Rajan *et al.*, 2002) and lower lymphatic magnitude BALB/c murine strain (demonstrating a more “immune-regulatory” Th-2 skewed phenotype which makes them permissive to certain filarial infections (Graham *et al.*, 2005; Taylor *et al.*, 2005; Campbell *et al.*, 2018). Thus, stronger, less well-regulated “runaway” inflammatory Th-2 adaptive immune responses appear to be implicated in filarial associated lymphatic remodelling and pathology. A balance, therefore, seems to be important between initiation of appropriate Th2 responses, necessary for worm expulsion, and appropriate immune-regulatory pathways to limit “collateral” lymphatic pathology that occurs in response to strengthened Th2 responses.

[6.4- Induction of filarial associated lymphatic remodelling and pathology- a conceptual model.](#)

The data presented throughout the thesis has provided evidence for a conceptual model that summarises how filarial lymphatic pathology is induced in response to filarial infective larvae. Filarial infected mosquitoes take a blood meal resulting in delivery of *BmL3* infective larvae into host dermal tissues. The larvae rapidly migrate into main pre-collector or collector lymphatic vessels proximal to the original infection site (as little as 3 hours after infection; Chapter 2) which results in activation of robust host adaptive Th2 immune responses, both in the local microenvironment of worm

habitation and to a lesser extent systemically (Chapter 5). The local, microenvironment encompassing the larvae residing in lymphatic pre-collector/collector channels will therefore be highly Th2 dominated with high local concentrations of Th-2 associated IL-4, IL-13 and IL-10 cytokines and related chemokines (Chapter 5). Filarial habitation of these vessels results in rapid recruitment of inflammatory CCR2⁺ monocytes into the microenvironment (Chapter 4). While these inflammatory monocytes themselves secrete significant quantities of lymphangiogenic molecules (Chapter 4), differentiation from monocytes to macrophages (M ϕ) rapidly occurs (Chapter 4). The newly differentiated macrophages will be exposed to the local, Th2 dominated, microenvironment proximal to larval habitation, ligation of these Th2 IL-4 and IL-13 cytokines to the IL-4R α receptor on M ϕ results in M ϕ polarisation to the “type 2” associated alternatively activated macrophage (AAM ϕ) (Chapter 5). The resultant *BmL3* polarised ‘*BmL3AAM ϕ* ’ secretes high concentrations of lymphangiogenic molecules (Chapter 4) and, together with other Th2 effector cells (such as T and B-cells) contribute to a localised, concentrated milieu of lymphangiogenic molecules which are shown to be highly upregulated following *BmL3* infection, concurrent with high levels of lymphatic remodelling and pathology (Chapter 3).

The resultant localised Th-2 dominant environment, together with Th-2 associated effector cell release of high concentrations of lymphangiogenic molecules, results in significant alterations to the local lymphatic architecture. Additionally, signalling from the larvae themselves (i.e. larval excretory secretory extracellular vesicles (Weinkopff *et al.*, 2014) may promote filarial-specific M ϕ activation which can also drive lymphatic proliferation (chapter 4). This strong “runaway” lymphangiogenic signalling results in inappropriate levels of lymphatic remodelling, ultimately contributing to observed pathological lymphatic insufficiency and dysfunction (Chapter 2). Figure 6.1 summarises the conceptual model graphically.

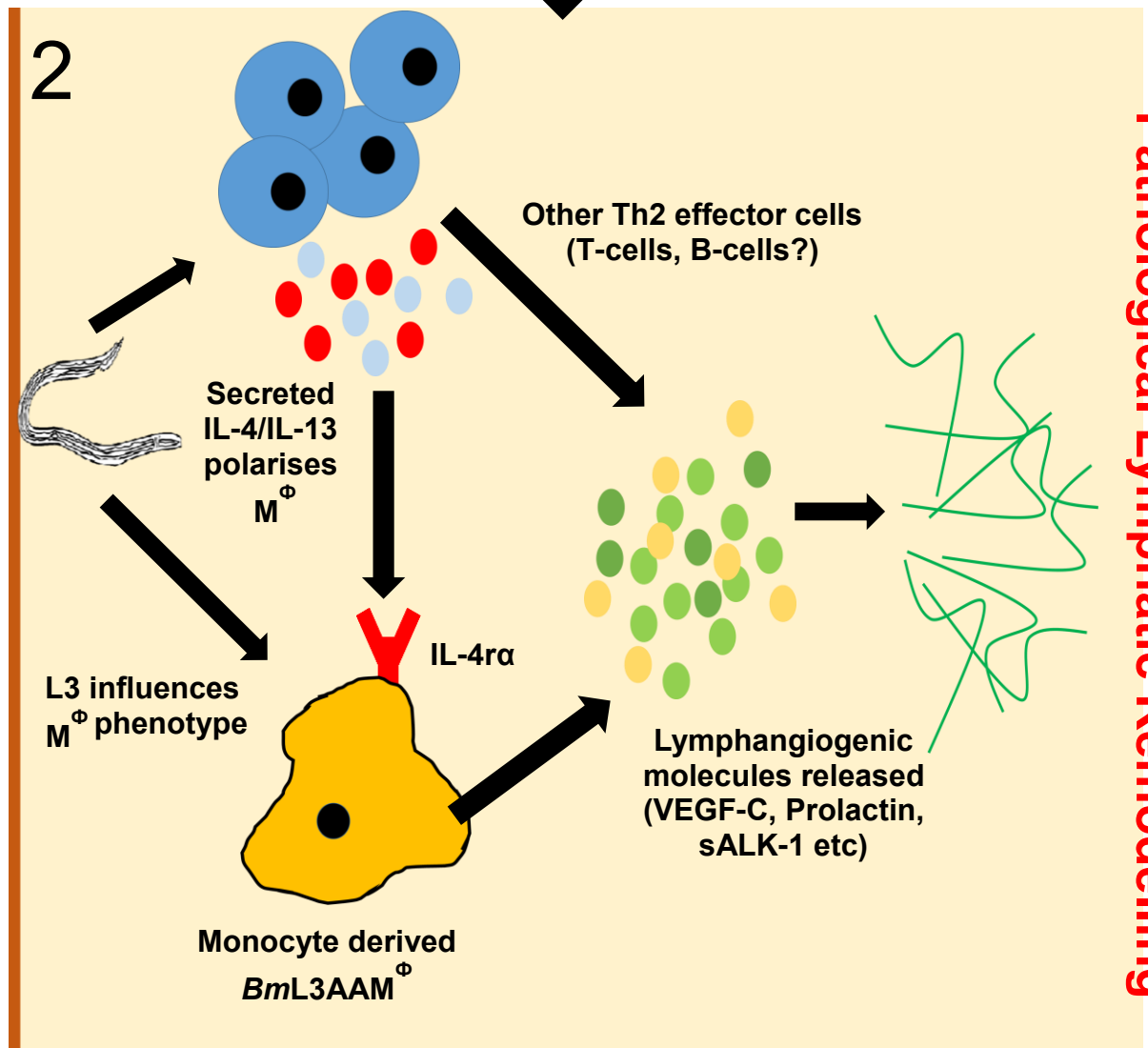
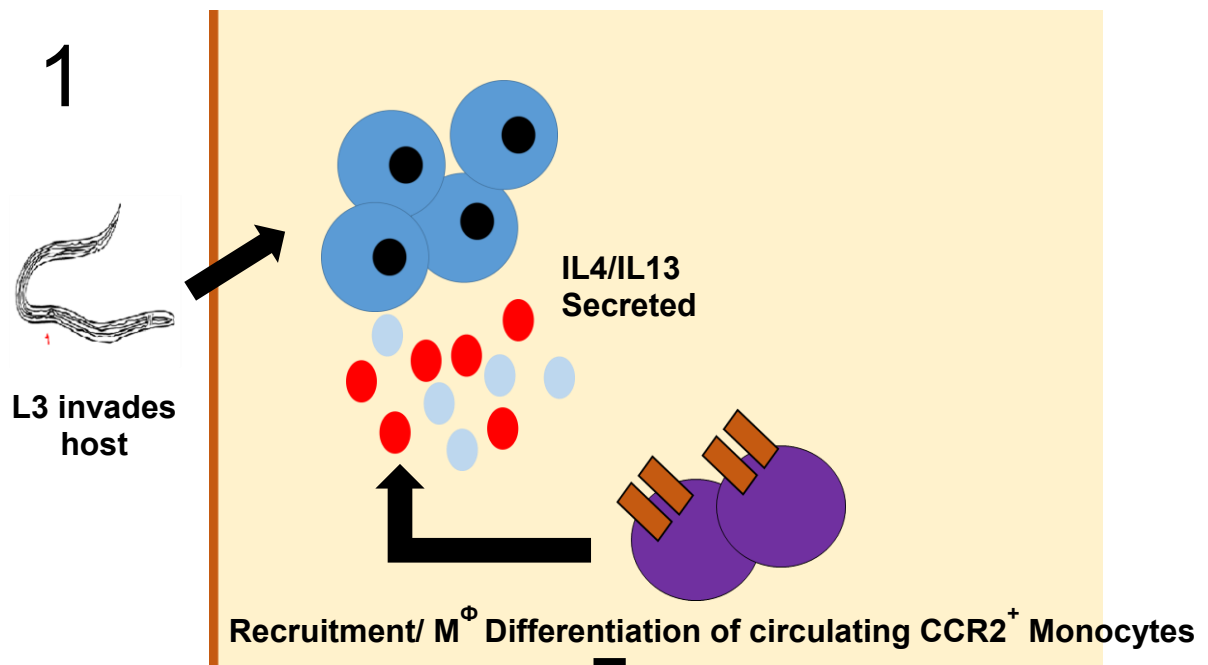


Figure 6.1: A conceptual model of early *BmL3* associated lymphatic remodelling and pathology

6.5- Future directions

6.5.1 Future experimental work to further characterise the drivers of filarial lymphatic pathology

The work described in this thesis has described a novel murine filarial infection model that enabled detailed investigation of the interaction between the early infecting larvae and the lymphatic architecture. Further the thesis describes a novel Th2/IL-4R α – Monocyte/Macrophage – lymphangiogenic signalling (VEGF-C,sALK-1, Prolactin) signalling axis that is crucial for the development of early filarial lymphatic remodelling and pathology. Filarial larval infection consistently resulted in significant levels of remodelling and lymphatic pathology in all infected mice, yet none displayed clinical manifestations such as observable lymphoedema- strengthening the idea of a “Stage 0” ‘covert’ or sub-clinical level of pathology in which levels of lymphatic dysfunction/pathology exist, and may be at future risk to develop clinical symptoms especially considering vulnerability to repeat filarial infectious challenges (Freedman *et al.*, 1995; Noroes *et al.*, 1996; R K Shenoy *et al.*, 2007; Douglass *et al.*, 2017). While work in the thesis demonstrated the importance of this “seeding” covert pathology, emulating clinical manifestations such as lymphoedema was beyond the scope of the project. Long term 12-week single infections demonstrated no clear pathology was manifest and after clearance of infection, however future work may want to drive larger levels of “covert” pathology utilising “trickle infection” (multiple weekly infections for example) methods to drive observable clinical pathologies. Such methods has recently driven clinical pathology in a ferret model (Jackson-Thompson *et al.*, 2018) yet driving these levels of pathology in the murine model provides a much easier platform to further investigate the driving mechanisms lymphatic pathology, building upon findings in this thesis. Longitudinal characterisation of the circulating lymphangiogenic

milieu, as well as local and systemic immunophenotyping in this transition between covert to clinical pathology may yield a better mechanistic understanding of filarial lymphatic pathology.

With it now apparent that “covert” pathologies manifest rapidly and are much more common in filarial infected patients than previously appreciated, a key future research question centres around the concept of what are the diverging mechanisms/events that determine whether patients fully progress to clinically apparent pathologies (the symptomatic patient cohorts) and those who are arrested at this covert pathology, but clinically asymptomatic stage. The characterisation of a “low pathology” BALB/c murine strain and “high pathology” C57BL/6J strain in this thesis provides a viable model to begin to study the differences between those who may be assumed to represent this asymptomatic cohort (BALB/c) and those at higher risk of developing overt pathology (C57BL/6J). While preliminary work has identified strain-dependent differences in terms of: strength of immune responses/immune cell recruitment and lymphangiogenic molecule secretion, which may relate to levels of pathology, future work aiming to thoroughly characterise immunological, molecular and even genetic differences could yield a better understanding of the mechanisms which are risk factors for a lymphoedematous pathological outcome.

A large lymphangiogenic multiplex panel was utilised in the model to begin to investigate molecular mechanisms of filarial lymphatic remodelling and pathology, yet this is limited to what is relatively a small number of well-defined mediators of angiogenesis/lymphangiogenesis. Future work could employ the model and utilise far more expansive transcriptomic and signalling pathway analysis of tissues/immune cells local to infection to far more comprehensively investigate molecular regulation of filarial associated remodelling. Additionally, cell sorting techniques employed in the model to isolate possible cellular mediators could be utilised to employ single cell RNA sequence analysis, thus far more accurately characterise the role of examined cells in regulating filarial lymphatic remodelling. Finally, work detailed in this thesis focused on the role of only a limited number of immune cell populations and future work may utilise the model and further cell sorting

experiments to isolate a more comprehensive pool of local cell populations. Together with the aforementioned transcriptomic, pathway and single cell RNA sequence analysis, this could yield a better understanding of the role of immune (and other) cell populations in regulating filarial lymphatic pathology.

6.5.2 Potential for novel anti-morbidity strategies against LF

The work undertaken in this thesis would advocate a novel therapeutic strategy to prevent development of, or even reverse, clinical LF pathology using interventions designed to block further development of, or even repair, filarial associated lymphatic pathology at the “covert”, sub clinical stage. Strengthening of this rationale has been demonstrated in studies in which early intervention at the “covert” LF pathology stage resulted in marked amelioration of tissue fluid retention as well as other early markers of lymphatic pathology (Douglass *et al.*, 2019). The consistency and reproducibility of the described novel *in vivo* model provides a tractable platform to begin to screen or test the efficacy of therapeutic interventions towards this purpose, as candidates that are able to ameliorate the observed lymphatic pathology could become novel anti- morbidity drugs against LF pathology, even perhaps within patients who have already developed \geq stage 1 LE. A whole milieu of upregulated circulating lymphangiogenic factors are observed, coincident with development of filarial associated pathology and strategies aiming to inhibit the signalling of these lymphangiogenic molecules could be a promising starting point. Previous studies have already demonstrated that doxycycline treatment reduces VEGF-C/A plasma concentrations and this was associated with reversal of lower grade LE in filarial infected patients. (Debrah *et al.*, 2006, 2009; Mand *et al.*, 2012). Doxycycline intervention studies utilising the developed model to investigate its effect on VEGF signalling and early filarial lymphatic pathology may strengthen the evidence for repurposing doxycycline or other next generation tetracyclines as a future LF anti-morbidity drug. Further, “anti-angiogenic/anti-lymphangiogenic” drugs which target a host of lymphangiogenic molecules are already used with success in the clinic against a range of pathologies including cancer and Age-related Macular

Degeneration (AMD). The targets of these treatments significantly overlap with lymphangiogenic mediators demonstrated to be upregulated following filarial infection, including VEGF-A/C/D (Holash *et al.*, 2002; Hurwitz *et al.*, 2004; Ferrara and Adamis, 2016 (Ferrara, Hillan and Novotny, 2005; COHEN, 2009)) and ALK-1 (Jimeno *et al.*, 2016; Burger *et al.*, 2018). Repurposing such drugs(or development of novel drugs against the less well characterised lymphangiogenic mediators of filarial pathology (such as those shown in Table 1) to prevent filarial associated lymphatic remodelling/neovascularisation could yield a novel anti-morbidity mode of action for LF. Utilisation of such drugs as interventions in the developed model could provide proof of principal for further downstream drug development.

With a Th2/IL-4R – monocyte/AAM ϕ signalling pathway clearly implicated as an important mediator of early filarial pathology, therapeutic strategies aimed at modifying the strength, or even type of immune responses that occur following filarial infection could provide another attractive novel anti-morbidity strategy. Administration of anti-inflammatories with the intention of modulating the strength of ‘runaway’ Th-1/Th-2 adaptive immune responses observed following filarial infection may be beneficial to ameliorate filarial lymphatic pathology. A potential anti-inflammatory/immunomodulatory mode of action for doxycycline and other tetracyclines has been reported (Griffin *et al.*, 2010; Bahrami, L. Morris and H. Pourgholami, 2012) which may explain its efficacy in reversing low grade filarial pathologies as already discussed. Future utilisation of anti-inflammatories, such as non-steroidal anti-inflammatory drugs (NSAID), steroids, or even tetracyclines in the model to investigate any effect on both the development of filarial lymphatic pathology and the characterised immune response, may provide proof-of-concept for this therapeutic strategy. Conversely, more targeted inhibition of inflammatory pathways such as cyclo-oxygenase-2 (COX-2), prostaglandins and leukotrienes may show promise, due to their potential role in lymphangiogenic pathways, with preliminary work showing reversal of secondary lymphoedema in a mouse model following intervention against these targets (Tian *et al.*, 2017) and any effects of compounds targeted at

these pathways on development of filarial lymphatic pathology in the model may be of great interest. Manipulation of the type of immune responses has recently shown clinical promise in cancer, specifically “immune re-education” of Th-2 associated AAM ϕ ’ like Tumour associated M ϕ into a Th-1 ‘M1’ phenotype reduces metastasis and vascular remodelling (Josephs, Bax and Karagiannis, 2015; Ortega *et al.*, 2016). Targeting of specific AAM ϕ surface markers, such as mannose receptor, may be beneficial in this regard. Similar strategies that attempt to modify the “runaway” Th-2 responses or the “Th-2 effector cells” observed following filarial infection may show success. Future work could attempt to blockade Th-2 cytokines with biological therapies as a therapeutic strategy in the model as a follow on from the experiments showing lack of filarial lymphatic pathology in Th-2 deficient mice, thus providing proof-of-concept. Finally, attempts to characterise immune evasion mechanisms utilised by helminths to enable chronic infection has yielded a host of parasite derived proteins which are highly immunomodulatory (Hewitson, Grainger and Maizels, 2009; McSorley, Hewitson and Maizels, 2013). Parasite excretory secretory proteins results in strong induction of regulatory T-cells (Tregs), dampening both Th1 and Th2 immune responses (Grainger *et al.*, 2010; Johnston *et al.*, 2017). Utilising parasite derived immunomodulatory materials to regulate “runaway” Th2 responses could therefore result in a therapeutic approach were, the very same parasites that induce filarial lymphatic pathology, could contain the materials necessary to halt, or even reverse filarial LE.

Appendices

Appendix 1- Table of utilised flow cytometry and fc fusion chimeras with relevant manufacturers and clones.

Antibody	Fluorophore	Clone	Manufacturer
CD3	PerCpCy5.5	17A2	ebioscience
Ly6C	PerCpCy5.5	Hk1.4	ebioscience
CD11b	PerCpCy5.5	M1/70	ebioscience
IFN- γ	PE-Cy7	XMG1.2	ebioscience
Tim-4	PE-Cy7	RMT4-54	ebioscience
CCR2	PE-Cy7	SA203G11	ebioscience
IgG1 Rat isotype	PE-Cy7	eBRG1	ebioscience
CCR2	AlexaFluor700	SA203G11	Biolegend
Ly6C	APCeFluor780	Hk1.4	ebioscience
F480	BV711	BM8	ebioscience
IgG1 Rat isotype	APC	eBGR1	ebioscience
IgG2A	APC	eBR2a	ebioscience
CD206	APC	MR6F3	Invitrogen
CD11b	APC	M1/70	ebioscience
B220	APC	RA3-6B2	ebioscience
MHCII	APC	M5/114.15.2	ebioscience
SiglecF	APC	ES22-10D8	Miltenyi
IL-10	APC	JES5-16E3	Biolegend
IgG1	PE	eBRG1	ebioscience
IgG2A	PE	TRFK5	ebioscience
CD3	PE	145-2c11	ebioscience
IL-4	PE	11b11	ebioscience
SiglecF	PE	E50-2440	BD Bioscience
Ly6G	PE	RB6-8C5	ebioscience
IgG1	AlexaFluor 488	eBRG-1	ebioscience
IgG2a	AlexaFluor 488	eBR2a	ebioscience
CD11b	AlexaFluor 488	M1/70	ebioscience
CD11c	AlexaFluor 488	N418	ebioscience
CD206	AlexaFluor 488	C068C2	Biolegend
IL-10	AlexaFluor 488	JES5-16F3	ebioscience
IL-13	AlexaFluor 488	eBio13A	ebioscience
RELM- α	N/A	500-P214	Peprtech
Mouse sVEGFR-3-Fc Chimera	N/A	N/A	R&D Systems
Mouse ALK-1-Fc Chimera	N/A	N/A	R&D Systems

Appendix 2- USB drive of relevant representative movies.

The attached USB drive in this thesis contains an electronic PDF copy of this thesis, along with representative movies of lymphangiogram PDE intravital imaging which were utilised to quantify lymphatic remodelling and insufficiency.

Also included is representative movies of filarial worms filmed inside lymphatic channels 24 hours post SC infection into the left hind limb.

REFERENCES

- Abe, J. *et al.* (2012) 'B cells regulate antibody responses through the medullary remodeling of inflamed lymph nodes', *International Immunology*. Narnia, 24(1), pp. 17–27. doi: 10.1093/intimm/dxr089.
- Abouelkheir, G. R., Upchurch, B. D. and Rutkowski, J. M. (2017) 'Lymphangiogenesis: fuel, smoke, or extinguisher of inflammation's fire?', *Experimental Biology and Medicine*. SAGE Publications Sage UK: London, England, 242(8), pp. 884–895. doi: 10.1177/1535370217697385.
- Adamczyk, L. A. *et al.* (2016) 'Lymph vessels: the forgotten second circulation in health and disease', *Virchows Archiv*. Springer, 469(1), pp. 3–17. doi: 10.1007/s00428-016-1945-6.
- Addiss, D. G. and Brady, M. A. (2007) 'Morbidity management in the Global Programme to Eliminate Lymphatic Filariasis: a review of the scientific literature', in *Filaria J*. WHO Collaborating Center for Control and Elimination of Lymphatic Filariasis in the Americas, Division of Parasitic Diseases, Centers for Disease Control and Prevention, Mailstop F-22, 4770 Buford Highway, Atlanta, Georgia, 30341, USA Fetzter Institute, 92, p. 2. doi: 10.1186/1475-2883-6-2.
- Ah, H. S. and Thompson, P. E. (1973) 'Brugia pahangi: infections and their effect on the lymphatic system of Mongolian jirds (*Meriones unguiculatus*)', *Exp Parasitol*. 1973/12/01, 34(3), pp. 393–411.
- Ahmed, S. S. (1967) 'Studies on the laboratory transmission of sub-periodic *Brugia malayi* and *B. pahangi*. II. Transmission to intact and splenectomized rats and cotton rats.', *Annals of tropical medicine and parasitology*, 61(4), pp. 432–6. Available at: <http://www.ncbi.nlm.nih.gov/pubmed/5634132> (Accessed: 11 February 2019).
- Al-Qaoud, K. M. *et al.* (2000) 'A new mechanism for IL-5-dependent helminth control: neutrophil accumulation and neutrophil-mediated worm encapsulation in murine filariasis are abolished in the absence of IL-5', *International Immunology*. Narnia, 12(6), pp. 899–908. doi: 10.1093/intimm/12.6.899.
- Alexander, J. S. *et al.* (2010) 'Emerging roles of lymphatics in inflammatory bowel disease', *Annals of the New York Academy of Sciences*. John Wiley & Sons, Ltd (10.1111), 1207, pp. E75–E85. doi: 10.1111/j.1749-6632.2010.05757.x.
- Alexander, N. D. E. (2015) 'Are we nearly there yet? Coverage and compliance of mass drug administration for lymphatic filariasis elimination.', *Transactions of the Royal Society of Tropical Medicine and Hygiene*. Oxford University Press, 109(3), pp. 173–4. doi: 10.1093/trstmh/tru204.
- Alitalo, K. (2011) 'The lymphatic vasculature in disease', *Nature Medicine*. Nature Publishing Group, 17(11), pp. 1371–1380. doi: 10.1038/nm.2545.
- Allen, J. E. and Loke, P. (2001) 'Divergent roles for macrophages in

- lymphatic filariasis', *Parasite Immunology*, 23(7), pp. 345–352. doi: 10.1046/j.1365-3024.2001.00394.x.
- Allen, J. E. and Maizels, R. M. (2011) 'Diversity and dialogue in immunity to helminths', *Nature Reviews Immunology*. Nature Publishing Group, 11(6), pp. 375–388. doi: 10.1038/nri2992.
- Allen, J. E. and Wynn, T. A. (2011) 'Evolution of Th2 immunity: a rapid repair response to tissue destructive pathogens.', *PLoS pathogens*. Public Library of Science, 7(5), p. e1002003. doi: 10.1371/journal.ppat.1002003.
- Amaral, F. *et al.* (1994) 'Live adult worms detected by ultrasonography in human Bancroftian filariasis', *Am J Trop Med Hyg.* 1994/06/01. Hospital de Restauracao, Recife, Brasil., 50(6), pp. 753–757.
- Angeli, V. *et al.* (2006) 'B cell-driven lymphangiogenesis in inflamed lymph nodes enhances dendritic cell mobilization.', *Immunity*. Elsevier, 24(2). doi: 10.1016/j.immuni.2006.01.003.
- Anthony, R. M. *et al.* (2006) 'Memory T(H)2 cells induce alternatively activated macrophages to mediate protection against nematode parasites.', *Nature medicine*. NIH Public Access, 12(8), pp. 955–60. doi: 10.1038/nm1451.
- Anuradha, R. *et al.* (2012) 'Altered Circulating Levels of Matrix Metalloproteinases and Inhibitors Associated with Elevated Type 2 Cytokines in Lymphatic Filarial Disease', *Plos Neglected Tropical Diseases*. [Anuradha, Rajamanickam George, Jovvian P. Pavankumar, Nathella Babu, Subash] Natl Inst Hlth, Int Ctr Excellence Res, Chennai, Tamil Nadu, India. [Kumaraswami, Vasanthapuram] TB Res Ctr, Chennai, Tamil Nadu, India. [Nutman, Thomas B.] NIAID, Parasit Dis L, 6(6), p. 9. doi: 10.1371/journal.pntd.0001681.
- Aspelund, A. *et al.* (2014) 'The Schlemm's canal is a VEGF-C/VEGFR-3-responsive lymphatic-like vessel.', *The Journal of clinical investigation*. American Society for Clinical Investigation, 124(9), pp. 3975–86. doi: 10.1172/JCI175395.
- Attout, T. *et al.* (2009) 'Lymphatic Vascularisation and Involvement of Lyve-1⁺ Macrophages in the Human Onchocerca Nodule', *PLoS ONE*, 4(12), p. e8234. doi: 10.1371/journal.pone.0008234.
- Babu, S. *et al.* (2000) 'Role of gamma interferon and interleukin-4 in host defense against the human filarial parasite *Brugia malayi*.', *Infection and immunity*. American Society for Microbiology Journals, 68(5), pp. 3034–5. doi: 10.1128/IAI.68.5.3034-3035.2000.
- Babu, S. *et al.* (2009) 'Filarial Lymphedema Is Characterized by Antigen-Specific Th1 and Th17 Proinflammatory Responses and a Lack of Regulatory T Cells', *PLoS Neglected Tropical Diseases*. Edited by R. T. Fujiwara. Public Library of Science, 3(4), p. e420. doi: 10.1371/journal.pntd.0000420.
- Babu, S. *et al.* (2012) 'Toll-Like Receptor- and Filarial Antigen-Mediated, Mitogen-Activated Protein Kinase- and NF-κB-Dependent Regulation of

Angiogenic Growth Factors in Filarial Lymphatic Pathology', *Infection and Immunity*. Edited by J. F. Urban, 80(7), pp. 2509–2518. doi: 10.1128/IAI.06179-11.

Babu, S., Kumaraswami, V. and Nutman, T. B. (2009) 'Alternatively Activated and Immunoregulatory Monocytes in Human Filarial Infections', *Journal of Infectious Diseases*, 199(12), pp. 1827–1837. doi: 10.1086/599090.

Babu, S. and Nutman, T. B. (2003) 'Proinflammatory cytokines dominate the early immune response to filarial parasites.', *J Immunol*, 171, pp. 6723–6732. doi: 10.4049/jimmunol.171.12.6723.

Babu, S. and Nutman, T. B. (2012) 'Immunopathogenesis of lymphatic filarial disease', *Seminars in Immunopathology*, 34(6), pp. 847–861. doi: 10.1007/s00281-012-0346-4.

Babu, S. and Nutman, T. B. (2014) 'Immunology of lymphatic filariasis', *Parasite Immunology*. [Babu, S.] NIAID NIRT ICER, Madras, Tamil Nadu, India. [Nutman, T. B.] NIAID, Helminth Immunol Sect, Parasit Dis Lab, Bethesda, MD 20892 USA. Babu, S (reprint author), Natl Inst Res TB, 1 Mayor Sathiyamurthy Rd, Madras 600031, Tamil Nadu, India. sbabu@mai, 36(8), pp. 338–346. doi: 10.1111/pim.12081.

Bahrami, F., L. Morris, D. and H. Pourgholami, M. (2012) 'Tetracyclines: Drugs with Huge Therapeutic Potential', *Mini-Reviews in Medicinal Chemistry*, 12(1), pp. 44–52. doi: 10.2174/138955712798868977.

Bain, C. C. *et al.* (2016) 'Long-lived self-renewing bone marrow-derived macrophages displace embryo-derived cells to inhabit adult serous cavities', *Nature Communications*, 7(1), p. ncomms11852. doi: 10.1038/ncomms11852.

Baluk, P. *et al.* (2005) 'Pathogenesis of persistent lymphatic vessel hyperplasia in chronic airway inflammation.', *The Journal of clinical investigation*. American Society for Clinical Investigation, 115(2), pp. 247–57. doi: 10.1172/JCI22037.

Bandi, C., Trees, A. J. and Brattig, N. W. (2001) 'Wolbachia in filarial nematodes: evolutionary aspects and implications for the pathogenesis and treatment of filarial diseases', *Veterinary Parasitology*, 98(1–3), pp. 215–238. doi: 10.1016/s0304-4017(01)00432-0.

Bao, P. *et al.* (2009) 'The Role of Vascular Endothelial Growth Factor in Wound Healing', *Journal of Surgical Research*, 153(2), pp. 347–358. doi: 10.1016/j.jss.2008.04.023.

Barner, M. *et al.* (1998) 'Differences between IL-4R α -deficient and IL-4-deficient mice reveal a role for IL-13 in the regulation of Th2 responses', *Current Biology*. Cell Press, 8(11), pp. 669–672. doi: 10.1016/S0960-9822(98)70256-8.

Bazigou, E. *et al.* (2014) 'Primary and secondary lymphatic valve development: molecular, functional and mechanical insights.', *Microvascular research*. NIH Public Access, 96, pp. 38–45. doi: 10.1016/j.mvr.2014.07.008.

- Bellini, C. *et al.* (2006) 'Congenital pulmonary lymphangiectasia', *Orphanet Journal of Rare Diseases*. BioMed Central, 1(1), p. 43. doi: 10.1186/1750-1172-1-43.
- Benedito, R. *et al.* (2012) 'Notch-dependent VEGFR3 upregulation allows angiogenesis without VEGF-VEGFR2 signalling', *Nature*, 484(7392), pp. 110–114. doi: 10.1038/nature10908.
- Benjamin, D. B. and Soulsby, E. J. (1976) 'The homocytotropic and hemagglutinating antibody responses to *Brugia pahangi* infection in the multimammate rat (*Mastomys natalensis*).', *The American journal of tropical medicine and hygiene*, 25(2), pp. 266–72. Available at: <http://www.ncbi.nlm.nih.gov/pubmed/1259087> (Accessed: 11 February 2019).
- Bennuru, S. *et al.* (2010) 'Elevated levels of plasma angiogenic factors are associated with human lymphatic filarial infections', *The American journal of tropical medicine and hygiene*, 83(4), pp. 884–890. doi: 10.4269/ajtmh.2010.10-0039.
- Bennuru, S. and Nutman, T. B. (2009a) 'Lymphangiogenesis and lymphatic remodeling induced by filarial parasites: implications for pathogenesis', *Lymphatic research and biology*. Mary Ann Liebert, Inc., 7(4), pp. 215–219. doi: 10.1089/lrb.2009.0022.
- Bennuru, S. and Nutman, T. B. (2009b) 'Lymphatics in human lymphatic filariasis: in vitro models of parasite-induced lymphatic remodeling', *Lymphatic research and biology*, 7(4), pp. 215–219. doi: 10.1089/lrb.2009.0022.
- Bernhard, C. A. *et al.* (2015) 'CD169+ macrophages are sufficient for priming of CTLs with specificities left out by cross-priming dendritic cells.', *Proceedings of the National Academy of Sciences of the United States of America*. National Academy of Sciences, 112(17), pp. 5461–6. doi: 10.1073/pnas.1423356112.
- Böhmer, R. *et al.* (2010) 'Regulation of Developmental Lymphangiogenesis by Syk+ Leukocytes', *Developmental Cell*, 18(3), pp. 437–449. doi: 10.1016/j.devcel.2010.01.009.
- Bosma, M. J. and Carroll, A. M. (1991) 'The SCID mouse mutant: definition, characterization, and potential uses', *Annu Rev Immunol*. 1991/01/01. Institute for Cancer Research, Fox Chase Cancer Center, Philadelphia, Pennsylvania 19111., 9, pp. 323–350. doi: 10.1146/annurev.iy.09.040191.001543.
- Brice, G. *et al.* (2005) 'Milroy disease and the VEGFR-3 mutation phenotype.', *Journal of medical genetics*. BMJ Publishing Group Ltd, 42(2), pp. 98–102. doi: 10.1136/jmg.2004.024802.
- Brouillard, P., Boon, L. and Vikkula, M. (2014) 'Genetics of lymphatic anomalies.', *The Journal of clinical investigation*. American Society for Clinical Investigation, 124(3), pp. 898–904. doi: 10.1172/JCI71614.
- Burger, R. A. *et al.* (2018) 'Phase II evaluation of dalantercept in the

treatment of persistent or recurrent epithelial ovarian cancer: An NRG Oncology/Gynecologic Oncology Group study', *Gynecologic Oncology*, 150(3), pp. 466–470. doi: 10.1016/j.ygyno.2018.06.017.

Byrne, A. *et al.* (2013) 'Vascular Endothelial Growth Factor-Trap Decreases Tumor Burden, Inhibits Ascites, and Causes Dramatic Vascular Remodeling in an Ovarian Cancer Model', *Clinical Cancer Research*. American Association for Cancer Research, 9(15), pp. 5721–5728. doi: 10.1158/1078-0432.ccr-12-2911.

Campbell, S. M. *et al.* (2018) 'Myeloid cell recruitment versus local proliferation differentiates susceptibility from resistance to filarial infection', *eLife*, 7. doi: 10.7554/eLife.30947.

Cardones, A. R. and Banez, L. L. (2006) 'VEGF inhibitors in cancer therapy.', *Current pharmaceutical design*, 12(3), pp. 387–94. Available at: <http://www.ncbi.nlm.nih.gov/pubmed/16454752> (Accessed: 10 April 2019).

Carlson, J. A. (2014) 'Lymphedema and subclinical lymphostasis (microlymphedema) facilitate cutaneous infection, inflammatory dermatoses, and neoplasia: A locus minoris resistentiae', *Clinics in Dermatology*, 32(5), pp. 599–615. doi: 10.1016/j.clindermato1.2014.04.007.

Carreño, P. C. *et al.* (2005) 'Prolactin affects both survival and differentiation of T-cell progenitors', *Journal of Neuroimmunology*, 160(1–2), pp. 135–145. doi: 10.1016/j.jneuroim.2004.11.008.

Case, T. *et al.* (1991) 'Vascular abnormalities in experimental and human lymphatic filariasis', *Lymphology*. 1991/12/01. Department of Surgery, University of Arizona., 24(4), pp. 174–183.

Case, T. C. *et al.* (1992) 'LYMPHATIC IMAGING IN EXPERIMENTAL FILARIASIS USING MAGNETIC-RESONANCE', *Investigative Radiology*, 27(4), pp. 293–297. doi: 10.1097/00004424-199204000-00006.

Chakraborty, S. *et al.* (2013) 'Lymphatic filariasis: perspectives on lymphatic remodeling and contractile dysfunction in filarial disease pathogenesis', *Microcirculation (New York, N.Y. : 1994)*, 20(5), pp. 349–364. doi: 10.1111/micc.12031.

Chakraborty, S., Davis, M. J. and Muthuchamy, M. (2015) 'Emerging trends in the pathophysiology of lymphatic contractile function.', *Seminars in cell & developmental biology*. NIH Public Access, 38, pp. 55–66. doi: 10.1016/j.semcd.2015.01.005.

Chan, M. S. *et al.* (1998) 'EPIFIL: A dynamic model of infection and disease In lymphatic filariasis', *American Journal of Tropical Medicine and Hygiene*. Univ Oxford, Dept Zool, Wellcome Trust Ctr Epidemiol Infect Dis, Oxford OX1 3PS, England. Vector Control Res Ctr, Med Complex, Pondicherry 605006, India. Chan, MS (reprint author), Univ Oxford, Dept Zool, Wellcome Trust Ctr Epidemiol Infect Dis, S Parks R, 59(4), pp. 606–614.

Chandy, A. *et al.* (2011) 'A review of neglected tropical diseases: filariasis', *Asian Pacific Journal of Tropical Medicine*. [Chandy, Anish Thakur, Alok Singh Singh, Mukesh Pratap] Chouksey Engn Coll, Sch Pharm, Bilaspur,

- Chattishgarh, India. [Manigauha, Ashish] NRI Coll Pharm, Bhopal, India. Chandy, A (reprint author), Chouksey Engn Coll, Sch Pharm, Bilaspur, Chattishgarh, Ind, 4(7), pp. 581–586. doi: 10.1016/s1995-7645(11)60150-8.
- Chang, J. E. and Turley, S. J. (2015) 'Stromal infrastructure of the lymph node and coordination of immunity.', *Trends in immunology*. Elsevier, 36(1), pp. 30–9. doi: 10.1016/j.it.2014.11.003.
- Chavez-Rueda, K. *et al.* (2005) 'Prolactin effect on CD69 and CD154 expression by CD4+ cells from systemic lupus erythematosus patients.', *Clinical and experimental rheumatology*, 23(6), pp. 769–77. Available at: <http://www.ncbi.nlm.nih.gov/pubmed/16396693> (Accessed: 14 March 2019).
- Chen, F. *et al.* (2012) 'An essential role for TH2-type responses in limiting acute tissue damage during experimental helminth infection', *Nature Medicine*. Nature Publishing Group, 18(2), pp. 260–266. doi: 10.1038/nm.2628.
- Cheun, H. I. *et al.* (2009) 'Successful Control of Lymphatic Filariasis in the Republic of Korea', *Korean J Parasitol*. Division of Malaria and Parasitic Diseases, National Institute of Health, Seoul 122-701, Korea. Department of Molecular Parasitology and Samsung Research Institute, Sungkyunkwan University College of Medicine, Suwon 440-746, Korea. Department of Parasitol, 47(4), pp. 323–335. doi: 10.3347/kjp.2009.47.4.323.
- Chirgwin, S. R. *et al.* (2005) 'Profiling the cellular immune response to multiple *Brugia pahangi* infections in a susceptible host', *The Journal of parasitology*. Department of Pathobiological Sciences, Louisiana State University School of Veterinary Medicine, Baton Rouge, Louisiana 70803, USA., 91(4), pp. 822–829. doi: 10.1645/ge-400r.1.
- Chirgwin, S. R. *et al.* (2006) 'TISSUE MIGRATION CAPABILITY OF LARVAL AND ADULT BRUGIA PAHANGI', *Journal of Parasitology*, 92(1), pp. 46–51. doi: 10.1645/GE-599R.1.
- Choi, I. *et al.* (2011) 'Visualization of lymphatic vessels by Prox1-promoter directed GFP reporter in a bacterial artificial chromosome-based transgenic mouse.', *Blood*. American Society of Hematology, 117(1), pp. 362–5. doi: 10.1182/blood-2010-07-298562.
- Chow, L. Q. M. and Eckhardt, S. G. (2007) 'Sunitinib: from rational design to clinical efficacy.', *Journal of clinical oncology : official journal of the American Society of Clinical Oncology*. American Society of Clinical Oncology, 25(7), pp. 884–96. doi: 10.1200/JCO.2006.06.3602.
- COHEN, S. Y. (2009) 'ANTI-VEGF DRUGS AS THE 2009 FIRST-LINE THERAPY FOR CHOROIDAL NEOVASCULARIZATION IN PATHOLOGIC MYOPIA', *Retina*, 29(8), pp. 1062–1066. doi: 10.1097/IAE.0b013e3181b1bb1a.
- Connor, S. J. *et al.* (2004) 'CCR2 expressing CD4+ T lymphocytes are preferentially recruited to the ileum in Crohn's disease.', *Gut*. BMJ Publishing Group, 53(9), pp. 1287–94. doi: 10.1136/gut.2003.028225.
- Corthay, A. (2006) 'A three-cell model for activation of naive T helper cells',

Scand J Immunol. 2006/07/27. Institute of Immunology, University of Oslo and Rikshospitalet-Radiumhospitalet Medical Center, Oslo, Norway. alexandre.corthay@medisin.uio.no, 64(2), pp. 93–96. doi: 10.1111/j.1365-3083.2006.01782.x.

Coso, S., Bovay, E. and Petrova, T. V. (2014) 'Pressing the right buttons: signaling in lymphangiogenesis', *Blood*. American Society of Hematology, 123(17), pp. 2614–2624. doi: 10.1182/BLOOD-2013-12-297317.

da Cunha Castro, E. C. and Galambos, C. (2009) 'Prox-1 and VEGFR3 Antibodies Are Superior to D2–40 in Identifying Endothelial Cells of Lymphatic Malformations—A Proposal of a New Immunohistochemical Panel to Differentiate Lymphatic from other Vascular Malformations', *Pediatric and Developmental Pathology*, 12(3), pp. 187–194. doi: 10.2350/08-05-0471.1.

Cursiefen, C. *et al.* (2004) 'VEGF-A stimulates lymphangiogenesis and hemangiogenesis in inflammatory neovascularization via macrophage recruitment.', *The Journal of clinical investigation*. American Society for Clinical Investigation, 113(7), pp. 1040–50. doi: 10.1172/JCI20465.

Davies, L. C. *et al.* (2011) 'A quantifiable proliferative burst of tissue macrophages restores homeostatic macrophage populations after acute inflammation', *European Journal of Immunology*, 41(8), pp. 2155–2164. doi: 10.1002/eji.201141817.

De-Jian, S., Xu-Li, D. and Ji-Hui, D. (2013) 'The history of the elimination of lymphatic filariasis in China', *Infectious diseases of poverty*, 2(1), p. 30. doi: 10.1186/2049-9957-2-30.

Debrah, A. Y. *et al.* (2006) 'Doxycycline reduces plasma VEGF-C/sVEGFR-3 and improves pathology in lymphatic filariasis', *PLoS pathogens*, 2(9), pp. e92–e92. doi: 10.1371/journal.ppat.0020092.

Debrah, Alexander Yaw *et al.* (2007) 'Plasma vascular endothelial growth Factor-A (VEGF-A) and VEGF-A gene polymorphism are associated with hydrocele development in lymphatic filariasis.', *The American journal of tropical medicine and hygiene*, 77(4), pp. 601–8. Available at: <http://www.ncbi.nlm.nih.gov/pubmed/17978056> (Accessed: 14 June 2019).

Debrah, A Y *et al.* (2007) 'Plasma vascular endothelial growth Factor-A (VEGF-A) and VEGF-A gene polymorphism are associated with hydrocele development in lymphatic filariasis', *Am J Trop Med Hyg.* 2007/11/06. Institute for Medical Microbiology, Immunology and Parasitology, University of Bonn, Bonn, Germany., 77(4), pp. 601–608.

Debrah, A. Y. *et al.* (2009) 'Reduction in levels of plasma vascular endothelial growth factor-A and improvement in hydrocele patients by targeting endosymbiotic Wolbachia sp. in *Wuchereria bancrofti* with doxycycline', *Am J Trop Med Hyg.* 2009/05/30. Institute for Medical Microbiology, Immunology and Parasitology, University Hospital Bonn, Bonn, Germany., 80(6), pp. 956–963.

Devaney, E. *et al.* (2002) 'Interleukin-4 influences the production of microfilariae in a mouse model of *Brugia* infection', *Parasite Immunology*.

John Wiley & Sons, Ltd (10.1111), 24(1), pp. 29–37. doi: 10.1046/j.0141-9838.2001.00433.x.

DiSipio, T. *et al.* (2013) 'Incidence of unilateral arm lymphoedema after breast cancer: a systematic review and meta-analysis', *The Lancet Oncology*. Elsevier, 14(6), pp. 500–515. doi: 10.1016/S1470-2045(13)70076-7.

Douglass, J. *et al.* (2017) 'Lymphatic Filariasis Increases Tissue Compressibility and Extracellular Fluid in Lower Limbs of Asymptomatic Young People in Central Myanmar', *Tropical Medicine and Infectious Disease*, 2(4), p. 50. doi: 10.3390/tropicalmed2040050.

Douglass, J. *et al.* (2019) 'Preventive chemotherapy reverses covert, lymphatic-associated tissue change in young people with lymphatic filariasis in Myanmar', *Tropical Medicine & International Health*, 24(4), pp. 463–476. doi: 10.1111/tmi.13212.

Douglass, J., Graves, P. and Gordon, S. (2016) 'Self-Care for Management of Secondary Lymphedema: A Systematic Review', *PLoS neglected tropical diseases*. College of Public Health, Medical and Veterinary Sciences, Division of Tropical Health and Medicine, James Cook University, Townsville, Queensland, Australia., 10(6), p. e0004740. doi: 10.1371/journal.pntd.0004740.

Dreyer, G. *et al.* (2000) 'Pathogenesis of lymphatic disease in bancroftian filariasis: A clinical perspective', *Parasitology Today*, 16(12), pp. 544–548. doi: 10.1016/s0169-4758(00)01778-6.

Dreyer, G. *et al.* (2001) *Lymphoedema Staff Manual Treatment and Prevention of Problems Associated with Lymphatic Filariasis World Health Organization Geneva Part 1. Learner's Guide*. Available at: https://apps.who.int/iris/bitstream/handle/10665/67224/WHO_CDS_CPE_CEE_2001.26a.pdf?sequence=1&isAllowed=y (Accessed: 12 June 2019).

Du, R. *et al.* (2008) 'HIF1alpha induces the recruitment of bone marrow-derived vascular modulatory cells to regulate tumor angiogenesis and invasion.', *Cancer cell*. NIH Public Access, 13(3), pp. 206–20. doi: 10.1016/j.ccr.2008.01.034.

Durrheim, D. N. *et al.* (2004) 'Editorial: Lymphatic filariasis endemicity - an indicator of poverty?', *Tropical Medicine and International Health*. John Wiley & Sons, Ltd (10.1111), 9(8), pp. 843–845. doi: 10.1111/j.1365-3156.2004.01287.x.

Ellis, L. M. and Hicklin, D. J. (2008) 'VEGF-targeted therapy: mechanisms of anti-tumour activity', *Nature Reviews Cancer*. Nature Publishing Group, 8(8), pp. 579–591. doi: 10.1038/nrc2403.

Emami-Naeini, P. *et al.* (2014) 'Soluble vascular endothelial growth factor receptor-3 suppresses allosensitization and promotes corneal allograft survival.', *Graefe's archive for clinical and experimental ophthalmology = Albrecht von Graefes Archiv fur klinische und experimentelle Ophthalmologie*. NIH Public Access, 252(11), pp. 1755–62. doi:

10.1007/s00417-014-2749-5.

Enholm, B. *et al.* (2001) 'Adenoviral Expression of Vascular Endothelial Growth Factor-C Induces Lymphangiogenesis in the Skin', *Circulation Research*. Lippincott Williams & Wilkins, 88(6), pp. 623–629. doi: 10.1161/01.RES.88.6.623.

Esther, C. R. and Barker, P. M. (2004) 'Pulmonary lymphangiectasia: Diagnosis and clinical course', *Pediatric Pulmonology*. John Wiley & Sons, Ltd, 38(4), pp. 308–313. doi: 10.1002/ppul.20100.

Evans, A. L. *et al.* (2003) 'Identification of eight novel VEGFR-3 mutations in families with primary congenital lymphoedema.', *Journal of medical genetics*. BMJ Publishing Group Ltd, 40(9), pp. 697–703. doi: 10.1136/JMG.40.9.697.

FAUL, J. L. *et al.* (2000) 'Thoracic Lymphangiomas, Lymphangiectasis, Lymphangiomatosis, and Lymphatic Dysplasia Syndrome', *American Journal of Respiratory and Critical Care Medicine*. American Thoracic Society New York, NY, 161(3), pp. 1037–1046. doi: 10.1164/ajrccm.161.3.9904056.

Ferrara, N. and Adamis, A. P. (2016) 'Ten years of anti-vascular endothelial growth factor therapy', *Nature Reviews Drug Discovery*. Nature Publishing Group, 15(6), pp. 385–403. doi: 10.1038/nrd.2015.17.

Ferrara, N., Hillan, K. J. and Novotny, W. (2005) 'Bevacizumab (Avastin), a humanized anti-VEGF monoclonal antibody for cancer therapy', *Biochemical and Biophysical Research Communications*. Academic Press, 333(2), pp. 328–335. doi: 10.1016/J.BBRC.2005.05.132.

Ferrell, R. *et al.* (1998) 'Hereditary lymphedema: evidence for linkage and genetic heterogeneity', *Human Molecular Genetics*. Oxford University Press, 7(13), pp. 2073–2078. doi: 10.1093/hmg/7.13.2073.

Figueredo-Silva, J. *et al.* (2002) 'The histopathology of bancroftian filariasis revisited: the role of the adult worm in the lymphatic-vessel disease', *Annals of Tropical Medicine and Parasitology*. Univ Fed Pernambuco, Hosp Clin, Dept Cirurgia, BR-50740900 Recife, PE, Brazil. Univ Fed Pernambuco, Dept Patol, LIKA, BR-50740900 Recife, PE, Brazil. Univ Fed Sao Paulo, Disciplina Urol, Lab Reprod Humana, BR-04025010 Sao Paulo, Brazil. Fiocruz MS, Ctr Pe, 96(6), pp. 531–541. doi: 10.1179/000349802125001348.

Flister, M. J. *et al.* (2010) 'Inflammation induces lymphangiogenesis through up-regulation of VEGFR-3 mediated by NF-kappaB and Prox1.', *Blood*. American Society of Hematology, 115(2), pp. 418–29. doi: 10.1182/blood-2008-12-196840.

Frade, J. M. *et al.* (1997) 'Characterization of the CCR2 chemokine receptor: functional CCR2 receptor expression in B cells.', *Journal of immunology (Baltimore, Md. : 1950)*. American Association of Immunologists, 159(11), pp. 5576–84. Available at: <http://www.ncbi.nlm.nih.gov/pubmed/9548499> (Accessed: 3 May 2019).

Freedman, D. O. *et al.* (1994) 'Lymphoscintigraphic analysis of lymphatic abnormalities in symptomatic and asymptomatic human filariasis', *J Infect Dis*. 1994/10/01. Division of Geographic Medicine, University of Alabama at

Birmingham 35294-2170., 170(4), pp. 927–933.

Freedman, D. O. *et al.* (1995) 'Abnormal lymphatic function in presymptomatic bancroftian filariasis', *J Infect Dis.* 1995/04/01. Division of Geographic Medicine, University of Alabama at Birmingham., 171(4), pp. 997–1001.

Gale, N. W. *et al.* (2002) 'Angiopoietin-2 Is Required for Postnatal Angiogenesis and Lymphatic Patterning, and Only the Latter Role Is Rescued by Angiopoietin-1', *Developmental Cell.* Elsevier, 3(3), pp. 411–423. doi: 10.1016/S1534-5807(02)00217-4.

Gazzaniga, S. *et al.* (2007) 'Targeting tumor-associated macrophages and inhibition of MCP-1 reduce angiogenesis and tumor growth in a human melanoma xenograft.', *The Journal of investigative dermatology.* Elsevier, 127(8), pp. 2031–41. doi: 10.1038/sj.jid.5700827.

Gentil, K., Hoerauf, A. and Pearlman, E. (2012) 'Differential induction of Th2- and Th1-associated responses by filarial antigens and endosymbiotic Wolbachia in a murine model of river blindness.', *European journal of microbiology & immunology.* Akadémiai Kiadó, 2(2), pp. 134–9. doi: 10.1556/EuJMI.2.2012.2.6.

Ghalamkarpour, A. *et al.* (2006) 'Hereditary lymphedema type I associated with VEGFR3 mutation: the first de novo case and atypical presentations', *Clinical genetics.* Laboratory of Human Molecular Genetics, Christian de Duve Institute of Cellular Pathology, Universite Catholique de Louvain, Brussels, Belgium., 70(4), pp. 330–335. doi: 10.1111/j.1399-0004.2006.00687.x.

Gillespie, S. H. (2004) 'Basic lymphoedema management: treatment and prevention of problems associated with lymphatic filariasis', *International Journal of Infectious Diseases.* Elsevier, 8(5), p. 321. doi: 10.1016/j.ijid.2004.02.003.

Le Goff, L. *et al.* (2002) 'IL-4 is required to prevent filarial nematode development in resistant but not susceptible strains of mice.', *International journal for parasitology*, 32(10), pp. 1277–84. Available at: <http://www.ncbi.nlm.nih.gov/pubmed/12204227> (Accessed: 22 February 2019).

Goldman, J. *et al.* (2005) 'Overexpression of VEGF-C Causes Transient Lymphatic Hyperplasia but Not Increased Lymphangiogenesis in Regenerating Skin', *Circulation Research.* Lippincott Williams & Wilkins, 96(11), pp. 1193–1199. doi: 10.1161/01.RES.0000168918.27576.78.

Gordon, K. *et al.* (2013) 'Mutation in Vascular Endothelial Growth Factor-C, a Ligand for Vascular Endothelial Growth Factor Receptor-3, Is Associated With Autosomal Dominant Milroy-Like Primary Lymphedema', *Circulation Research*, 112(6), pp. 956–960. doi: 10.1161/CIRCRESAHA.113.300350.

Gordon, S. and Martinez, F. O. (2010) 'Alternative Activation of Macrophages: Mechanism and Functions', *Immunity.* Cell Press, 32(5), pp. 593–604. doi: 10.1016/j.immuni.2010.05.007.

Gousopoulos, E. *et al.* (2017) 'An Important Role of VEGF-C in Promoting Lymphedema Development', *Journal of Investigative Dermatology*. Elsevier, 137(9), pp. 1995–2004. doi: 10.1016/J.JID.2017.04.033.

Grada, A. A. and Phillips, T. J. (2017) 'Lymphedema: Pathophysiology and clinical manifestations.', *Journal of the American Academy of Dermatology*. Elsevier, 77(6), pp. 1009–1020. doi: 10.1016/j.jaad.2017.03.022.

Graham, A. L. *et al.* (2005) 'Quantitative appraisal of murine filariasis confirms host strain differences but reveals that BALB/c females are more susceptible than males to *Litomosoides sigmodontis*', *Microbes Infect*. 2005/04/12. Institute of Evolution, School of Biological Sciences, University of Edinburgh, King's Buildings, Ashworth Laboratories, Edinburgh EH9 3JT, UK., 7(4), pp. 612–618. doi: 10.1016/j.micinf.2004.12.019.

Graham, H. and Peng, C. (2006) 'Activin receptor-like kinases: structure, function and clinical implications.', *Endocrine, metabolic & immune disorders drug targets*, 6(1), pp. 45–58. Available at: <http://www.ncbi.nlm.nih.gov/pubmed/16611164> (Accessed: 11 March 2019).

Grainger, J. R. *et al.* (2010) 'Helminth secretions induce de novo T cell Foxp3 expression and regulatory function through the TGF- β pathway', *The Journal of Experimental Medicine*, 207(11), pp. 2331–2341. doi: 10.1084/jem.20101074.

Grenfell, B. T., Michael, E. and Denham, D. A. (1991) 'A model for the dynamics of human lymphatic filariasis', *Parasitol Today*. 1991/11/01. Department of Zoology, Cambridge University, Downing Street, Cambridge CB2 3EJ, UK., 7(11), pp. 318–323.

Griffin, M. O. *et al.* (2010) 'Tetracyclines: a pleiotropic family of compounds with promising therapeutic properties. Review of the literature', *American Journal of Physiology-Cell Physiology*. American Physiological Society Bethesda, MD, 299(3), pp. C539–C548. doi: 10.1152/ajpcell.00047.2010.

Grosdemouge, I. *et al.* (2003) 'Effects of deletion of the prolactin receptor on ovarian gene expression.', *Reproductive biology and endocrinology : RB&E*. BioMed Central, 1, p. 12. doi: 10.1186/1477-7827-1-12.

Guilliams, M., Mildner, A. and Yona, S. (2018) 'Developmental and Functional Heterogeneity of Monocytes', *Immunity*. Cell Press, 49(4), pp. 595–613. doi: 10.1016/J.IMMUNI.2018.10.005.

Gyapong, J. O. *et al.* (2005) 'Treatment strategies underpinning the global programme to eliminate lymphatic filariasis', *Expert Opinion on Pharmacotherapy*, 6(2), pp. 179–200. doi: 10.1517/14656566.6.2.179.

Haiko, P. *et al.* (2008) 'Deletion of vascular endothelial growth factor C (VEGF-C) and VEGF-D is not equivalent to VEGF receptor 3 deletion in mouse embryos.', *Molecular and cellular biology*. American Society for Microbiology Journals, 28(15), pp. 4843–50. doi: 10.1128/MCB.02214-07.

Hajrasouliha, A. R. *et al.* (2012) 'Vascular Endothelial Growth Factor-C Promotes Alloimmunity by Amplifying Antigen-Presenting Cell Maturation and Lymphangiogenesis', *Investigative Ophthalmology & Visual Science*. The

Association for Research in Vision and Ophthalmology, 53(3), p. 1244. doi: 10.1167/iovs.11-8668.

Hall, K. L. *et al.* (2012) 'New Model of Macrophage Acquisition of the Lymphatic Endothelial Phenotype', *PLoS ONE*. Edited by R. Bonecchi. Public Library of Science, 7(3), p. e31794. doi: 10.1371/journal.pone.0031794.

Hanahan, D. and Weinberg, R. A. (2011) 'Hallmarks of Cancer: The Next Generation', *Cell*, 144(5), pp. 646–674. doi: 10.1016/j.cell.2011.02.013.

Harwood, N. E. and Batista, F. D. (2010) 'Antigen presentation to B cells.', *F1000 biology reports*. Faculty of 1000 Ltd, 2, p. 87. doi: 10.3410/B2-87.

Hewitson, J. P., Grainger, J. R. and Maizels, R. M. (2009) 'Helminth immunoregulation: The role of parasite secreted proteins in modulating host immunity', *Molecular and Biochemical Parasitology*, 167(1), pp. 1–11. doi: 10.1016/j.molbiopara.2009.04.008.

Higazi, T. B. *et al.* (2003) 'Angiogenic activity of an *Onchocerca volvulus* *Ancylostoma* secreted protein homologue', *Molecular and Biochemical Parasitology*, 129(1), pp. 61–68. doi: 10.1016/s0166-6851(03)00094-x.

Hines, S. A. *et al.* (1989) 'LYMPHATIC FILARIASIS - BRUGIA-MALAYI INFECTION IN THE FERRET (MUSTELA-PUTORIUS-FURO)', *American Journal of Pathology*, 134(6), pp. 1373–1376.

Hirosue, S. *et al.* (2014) 'Steady-state antigen scavenging, cross-presentation, and CD8+ T cell priming: a new role for lymphatic endothelial cells.', *Journal of immunology (Baltimore, Md. : 1950)*. The American Association of Immunologists, Inc., 192(11), pp. 5002–11. doi: 10.4049/jimmunol.1302492.

Hoerauf, A. *et al.* (2005) 'Immunomodulation by filarial nematodes', *Parasite Immunol.* 2005/09/24. Institute for Medical Parasitology, University Clinic Bonn, Sigmund Freud Strasse 25, 53105 Bonn, Germany. hoerauf@parasit.meb.uni-bonn.de, 27(10–11), pp. 417–429. doi: 10.1111/j.1365-3024.2005.00792.x.

Hoerauf, A. (2006) 'New strategies to combat filariasis', *Expert review of anti-infective therapy*. Institute of Medical Microbiology, Immunology and Parasitology, University Clinic Bonn, 53105 Bonn, Germany. hoerauf@parasit.meb.uni-bonn.de, 4(2), pp. 211–222. doi: 10.1586/14787210.4.2.211.

Holash, J. *et al.* (2002) 'VEGF-Trap: A VEGF blocker with potent antitumor effects', *Proceedings of the National Academy of Sciences*, 99(17), pp. 11393–11398. doi: 10.1073/pnas.172398299.

Hotez, P. J. *et al.* (2007) 'Current concepts - Control of neglected tropical diseases', *New England Journal of Medicine*. George Washington Univ, Sabin Vaccine Inst, Washington, DC 20037 USA. George Washington Univ, Dept Microbiol Immunol & Trop Med, Washington, DC 20037 USA. Univ Liverpool Liverpool Sch Trop Med, Lymphat Filariasis Support Ctr, Liverpool, Merseyside, Englan, 357(10), pp. 1018–1027. doi: 10.1056/NEJMra064142.

Hotez, P. J. *et al.* (2008) 'The neglected tropical diseases of Latin America and the Caribbean: a review of disease burden and distribution and a roadmap for control and elimination', *PLoS neglected tropical diseases*, 2(9), pp. e300–e300. doi: 10.1371/journal.pntd.0000300.

Hotez, P. J. and Kamath, A. (2009) 'Neglected Tropical Diseases in Sub-Saharan Africa: Review of Their Prevalence, Distribution, and Disease Burden', *Plos Neglected Tropical Diseases*, 3(8). doi: 10.1371/journal.pntd.0000412.

Hotez, P. J., Savioli, L. and Fenwick, A. (2012) 'Neglected tropical diseases of the Middle East and North Africa: review of their prevalence, distribution, and opportunities for control', *PLoS neglected tropical diseases*, 6(2), pp. e1475–e1475. doi: 10.1371/journal.pntd.0001475.

Howells, R. E. *et al.* (1983) 'The susceptibility of BALB/C and other inbred mouse strains to *Brugia pahangi*.', *Acta tropica*, 40(4), pp. 341–50. Available at: <http://www.ncbi.nlm.nih.gov/pubmed/6142632> (Accessed: 22 February 2019).

Huang, S. *et al.* (2002) 'Contributions of stromal metalloproteinase-9 to angiogenesis and growth of human ovarian carcinoma in mice.', *Journal of the National Cancer Institute*, 94(15), pp. 1134–42. Available at: <http://www.ncbi.nlm.nih.gov/pubmed/12165638> (Accessed: 3 May 2019).

Huang, Z. *et al.* (2012) 'Targeted delivery of oligonucleotides into tumor-associated macrophages for cancer immunotherapy', *Journal of Controlled Release*. Elsevier, 158(2), pp. 286–292. doi: 10.1016/J.JCONREL.2011.11.013.

Huber-Ruano, I. *et al.* (2017) 'An antisense oligonucleotide targeting TGF- β 2 inhibits lung metastasis and induces CD86 expression in tumor-associated macrophages', *Annals of Oncology*, 28(9), pp. 2278–2285. doi: 10.1093/annonc/mdx314.

Hurwitz, H. *et al.* (2004) 'Bevacizumab plus Irinotecan, Fluorouracil, and Leucovorin for Metastatic Colorectal Cancer', *New England Journal of Medicine*, 350(23), pp. 2335–2342. doi: 10.1056/NEJMoa032691.

Hussain, R. and Ottesen, E. A. (1985) 'IgE responses in human filariasis. III. Specificities of IgE and IgG antibodies compared by immunoblot analysis.', *Journal of immunology (Baltimore, Md. : 1950)*. American Association of Immunologists, 135(2), pp. 1415–20. Available at: <http://www.ncbi.nlm.nih.gov/pubmed/3891853> (Accessed: 22 March 2019).

Iijima, N., Mattei, L. M. and Iwasaki, A. (2011) 'Recruited inflammatory monocytes stimulate antiviral Th1 immunity in infected tissue', *Proceedings of the National Academy of Sciences*, 108(1), pp. 284–289. doi: 10.1073/pnas.1005201108.

Jackson-Thompson, B. M. *et al.* (2018) 'Brugia malayi infection in ferrets – A small mammal model of lymphatic filariasis', *PLOS Neglected Tropical Diseases*. Edited by B. L. Makepeace. Public Library of Science, 12(3), p. e0006334. doi: 10.1371/journal.pntd.0006334.

- James, J. M., Nalbandian, A. and Mukouyama, Y. (2013) 'TGF β signaling is required for sprouting lymphangiogenesis during lymphatic network development in the skin.', *Development (Cambridge, England)*. Company of Biologists, 140(18), pp. 3903–14. doi: 10.1242/dev.095026.
- Jenkins, S. J. and Allen, J. E. (2010) 'Similarity and diversity in macrophage activation by nematodes, trematodes, and cestodes', *Journal of biomedicine & biotechnology*, 2010, p. 262609. doi: 10.1155/2010/262609.
- Jensen, M. R. *et al.* (2015) 'Higher vascular endothelial growth factor-C concentration in plasma is associated with increased forearm capillary filtration capacity in breast cancer-related lymphedema', *Physiological Reports*, 3(6), p. e12403. doi: 10.14814/phy2.12403.
- Jimeno, A. *et al.* (2016) 'A phase 2 study of dalantercept, an activin receptor-like kinase-1 ligand trap, in patients with recurrent or metastatic squamous cell carcinoma of the head and neck', *Cancer*, 122(23), pp. 3641–3649. doi: 10.1002/cncr.30317.
- Jin da, P. *et al.* (2009) 'Therapeutic responses to exogenous VEGF-C administration in experimental lymphedema: immunohistochemical and molecular characterization', *Lymphat Res Biol.* 2009/03/24. Lymphatic Research and Medicine, Stanford University School of Medicine, Falk Cardiovascular Research Center, Stanford, California 94305, USA., 7(1), pp. 47–57. doi: 10.1089/lrb.2009.0002.
- Johnston, C. J. C. *et al.* (2017) 'A structurally distinct TGF- β mimic from an intestinal helminth parasite potently induces regulatory T cells', *Nature Communications*. Nature Publishing Group, 8(1), p. 1741. doi: 10.1038/s41467-017-01886-6.
- Jones, R. T. (2014) 'Non-endemic cases of lymphatic filariasis', *Tropical Medicine & International Health*, 19(11), pp. 1377–1383. doi: 10.1111/tmi.12376.
- Josephs, D. H., Bax, H. J. and Karagiannis, S. N. (2015) 'Tumour-associated macrophage polarisation and re-education with immunotherapy.', *Frontiers in bioscience (Elite edition)*, 7, pp. 293–308. Available at: <http://www.ncbi.nlm.nih.gov/pubmed/25553381> (Accessed: 5 March 2019).
- Jothi, J. *et al.* (2016) 'Brugia malayi Asparaginyl - tRNA Synthetase Stimulates Endothelial Cell Proliferation, Vasodilation and Angiogenesis', *PloS one*. Center for Biotechnology, Anna University, Chennai-25, Tamil Nadu, India., 11(1), p. e0146132. doi: 10.1371/journal.pone.0146132.
- Jungmann, P., Figueredo-Silva, J. and Dreyer, G. (1991) 'Bancroftian lymphadenopathy: a histopathologic study of fifty-eight cases from northeastern Brazil', *Am J Trop Med Hyg.* 1991/09/01. Laboratório de Imunopatologia Keizo Asami, Universidade Federal de Pernambuco, Recife, Brazil., 45(3), pp. 325–331.
- Kar, S. K. *et al.* (2017) 'Lymphatic pathology in asymptomatic and symptomatic children with *Wuchereria bancrofti* infection in children from Odisha, India and its reversal with DEC and albendazole treatment.', *PLoS*

neglected tropical diseases. Public Library of Science, 11(10), p. e0005631. doi: 10.1371/journal.pntd.0005631.

Kar, S. K., Mania, J. and Kar, P. K. (no date) 'Humoral immune response during filarial fever in Bancroftian filariasis.', *Transactions of the Royal Society of Tropical Medicine and Hygiene*, 87(2), pp. 230–3. Available at: <http://www.ncbi.nlm.nih.gov/pubmed/8337737> (Accessed: 28 January 2019).

Karkkainen, M. J. *et al.* (2000) 'Missense mutations interfere with VEGFR-3 signalling in primary lymphoedema', *Nature Genetics*. Nature Publishing Group, 25(2), pp. 153–159. doi: 10.1038/75997.

Karkkainen, M. J. *et al.* (2004) 'Vascular endothelial growth factor C is required for sprouting of the first lymphatic vessels from embryonic veins', *Nature Immunology*, 5(1), pp. 74–80. doi: 10.1038/ni1013.

Kasten, J. L. *et al.* (2009) 'TGF-beta inhibits lymphatic regeneration and dedifferentiates LECs via knockdown of Prox1', *Journal of the American College of Surgeons*. Elsevier, 209(3), p. S76. doi: 10.1016/j.jamcollsurg.2009.06.186.

Kataru, R. P. *et al.* (2009) 'Critical role of CD11b+ macrophages and VEGF in inflammatory lymphangiogenesis, antigen clearance, and inflammation resolution.', *Blood*. American Society of Hematology, 113(22), pp. 5650–9. doi: 10.1182/blood-2008-09-176776.

Kazenwadel, J. *et al.* (2012) 'Loss-of-function germline GATA2 mutations in patients with MDS/AML or MonoMAC syndrome and primary lymphedema reveal a key role for GATA2 in the lymphatic vasculature.', *Blood*. The American Society of Hematology, 119(5), pp. 1283–91. doi: 10.1182/blood-2011-08-374363.

Kesler, C. T. *et al.* (2013) 'Lymphatic vessels in health and disease.', *Wiley interdisciplinary reviews. Systems biology and medicine*. NIH Public Access, 5(1), pp. 111–24. doi: 10.1002/wsbm.1201.

Kilarski, W. W. *et al.* (2019) 'Inherent biomechanical traits enable infective filariae to disseminate through collecting lymphatic vessels', *Nature Communications*. Nature Publishing Group, 10(1). doi: 10.1038/s41467-019-10675-2.

Kim, H., Kataru, R. P. and Koh, G. Y. (2014) 'Review series Inflammation-associated lymphangiogenesis: a double-edged sword?', *The Journal of Clinical Investigation*, 124. doi: 10.1172/JCI71607.

Kim, T. H. *et al.* (2010) 'Remodelling of nasal mucosa in mild and severe persistent allergic rhinitis with special reference to the distribution of collagen, proteoglycans, and lymphatic vessels', *Clinical & Experimental Allergy*. John Wiley & Sons, Ltd (10.1111), 40(12), pp. 1742–1754. doi: 10.1111/j.1365-2222.2010.03612.x.

Kinet, V. *et al.* (2011) 'The Angiostatic Protein 16K Human Prolactin Significantly Prevents Tumor-Induced Lymphangiogenesis by Affecting Lymphatic Endothelial Cells', *Endocrinology*. Oxford University Press, 152(11), pp. 4062–4071. doi: 10.1210/en.2011-1081.

- King, C. L. *et al.* (1993) 'Cytokine control of parasite-specific anergy in human lymphatic filariasis. Preferential induction of a regulatory T helper type 2 lymphocyte subset.', *The Journal of clinical investigation*. American Society for Clinical Investigation, 92(4), pp. 1667–73. doi: 10.1172/JCI116752.
- Ko, J.-Y., Ahn, Y.-L. and Cho, B.-N. (2003) 'Angiogenesis and white blood cell proliferation induced in mice by injection of a prolactin-expressing plasmid into muscle.', *Molecules and cells*, 15(2), pp. 262–70. Available at: <http://www.ncbi.nlm.nih.gov/pubmed/12803491> (Accessed: 14 March 2019).
- Krishnamoorthy, K. (1999) 'Estimated costs of acute adenolymphangitis to patients with chronic manifestations of bancroftian filariasis in India.', *Indian journal of public health*, 43(2), pp. 58–63. Available at: <http://www.ncbi.nlm.nih.gov/pubmed/11243067> (Accessed: 28 January 2019).
- Krzyszczczyk, P. *et al.* (2018) 'The Role of Macrophages in Acute and Chronic Wound Healing and Interventions to Promote Pro-wound Healing Phenotypes.', *Frontiers in physiology*. Frontiers Media SA, 9, p. 419. doi: 10.3389/fphys.2018.00419.
- Kubo, H. *et al.* (2002) 'Blockade of vascular endothelial growth factor receptor-3 signaling inhibits fibroblast growth factor-2-induced lymphangiogenesis in mouse cornea.', *Proceedings of the National Academy of Sciences of the United States of America*. National Academy of Sciences, 99(13). doi: 10.1073/pnas.062040199.
- Kumar, V. *et al.* (2010) 'Global lymphoid tissue remodeling during a viral infection is orchestrated by a B cell-lymphotoxin-dependent pathway', *Blood*, 115(23), pp. 4725–4733. doi: 10.1182/blood-2009-10-250118.
- Kunsthfeld, R. *et al.* (2004) 'Induction of cutaneous delayed-type hypersensitivity reactions in VEGF-A transgenic mice results in chronic skin inflammation associated with persistent lymphatic hyperplasia'. doi: 10.1182/blood-2003-08-2964.
- Kurup, S. P. *et al.* (2019) 'Monocyte-Derived CD11c + Cells Acquire Plasmodium from Hepatocytes to Prime CD8 T Cell Immunity to Liver-Stage Malaria', *Cell Host and Microbe*, 25(4), pp. 565-577.e6. doi: 10.1016/j.chom.2019.02.014.
- Lähteenvuo, M. *et al.* (2011) 'Growth Factor Therapy and Autologous Lymph Node Transfer in Lymphedema', *Circulation*, 123(6), pp. 613–620. doi: 10.1161/CIRCULATIONAHA.110.965384.
- Lawrence, R. A. *et al.* (1995) 'Infection of IL-4-deficient mice with the parasitic nematode *Brugia malayi* demonstrates that host resistance is not dependent on a T helper 2-dominated immune response.', *Journal of immunology (Baltimore, Md. : 1950)*, 154(11), pp. 5995–6001. Available at: <http://www.ncbi.nlm.nih.gov/pubmed/7751642> (Accessed: 15 May 2019).
- Lawrence, R. A. (1996) 'Lymphatic filariasis: what mice can tell us', *Parasitol Today*. 1996/07/01. Department of Biology, Imperial College of Science,

Technology and Medicine, Prince Consort Road, London, UK.
ral1@bio.ic.ac.uk, 12(7), pp. 267–271.

Lawrence, R. A. and Denham, D. A. (1993) 'STAGE AND ISOTYPE-SPECIFIC IMMUNE-RESPONSES IN A RAT MODEL OF FILARIASIS', *Parasite Immunology*, 15(8), pp. 429–439. doi: 10.1111/j.1365-3024.1993.tb00628.x.

Lee, J. Y. *et al.* (2010) 'Podoplanin-expressing cells derived from bone marrow play a crucial role in postnatal lymphatic neovascularization', *Circulation*, 122(14), pp. 1413–1425. doi: 10.1161/CIRCULATIONAHA.110.941468.

Lee, S. *et al.* (2007) 'Autocrine VEGF Signaling Is Required for Vascular Homeostasis', *Cell*, 130(4), pp. 691–703. doi: 10.1016/j.cell.2007.06.054.

Legorreta-Haquet, M. V *et al.* (2012) 'Prolactin down-regulates CD4+CD25hiCD127low/- regulatory T cell function in humans', *Journal of Molecular Endocrinology*, 48(1), pp. 77–85. doi: 10.1530/JME-11-0040.

Levet, S. *et al.* (2013) 'Bone morphogenetic protein 9 (BMP9) controls lymphatic vessel maturation and valve formation.', *Blood*. The American Society of Hematology, 122(4), pp. 598–607. doi: 10.1182/blood-2012-12-472142.

Lewis, J. S. *et al.* (2000) 'Expression of vascular endothelial growth factor by macrophages is up-regulated in poorly vascularized areas of breast carcinomas.', *The Journal of pathology*, 192(2), pp. 150–8. doi: 10.1002/1096-9896(2000)9999:9999<::AID-PATH687>3.0.CO;2-G.

Liao, S. *et al.* (2015) 'Lymphatic system: an active pathway for immune protection.', *Seminars in cell & developmental biology*. NIH Public Access, 38, pp. 83–9. doi: 10.1016/j.semcdb.2014.11.012.

Liao, S. and Padera, T. P. (2013) 'Lymphatic function and immune regulation in health and disease.', *Lymphatic research and biology*. Mary Ann Liebert, Inc., 11(3), pp. 136–43. doi: 10.1089/lrb.2013.0012.

Liebl, J. *et al.* (2015) 'Cdk5 controls lymphatic vessel development and function by phosphorylation of Foxc2', *Nature Communications*. Nature Publishing Group, 6(1), p. 7274. doi: 10.1038/ncomms8274.

Liew, S.-C. *et al.* (2012) 'Differential expression of the angiogenesis growth factors in psoriasis vulgaris.', *BMC research notes*. BioMed Central, 5, p. 201. doi: 10.1186/1756-0500-5-201.

Lin, E. Y. *et al.* (2006) 'Macrophages Regulate the Angiogenic Switch in a Mouse Model of Breast Cancer', *Cancer Research*, 66(23), pp. 11238–11246. doi: 10.1158/0008-5472.CAN-06-1278.

Linares, P. M. and Gisbert, J. P. (2010) 'Role of Growth Factors in the Development of Lymphangiogenesis Driven by Inflammatory Bowel Disease: A Review'. doi: 10.1002/ibd.21554.

Liu, N. F., Yan, Z. X. and Wu, X. F. (2012) 'Classification of Lymphatic-system Malformations in Primary Lymphoedema based on MR

Lymphangiography', *European Journal of Vascular & Endovascular Surgery*, 44, pp. 345–349. doi: 10.1016/j.ejvs.2012.06.019.

Loberg, R. D. *et al.* (2007) 'Targeting CCL2 with Systemic Delivery of Neutralizing Antibodies Induces Prostate Cancer Tumor Regression *In vivo*', *Cancer Research*. American Association for Cancer Research, 67(19), pp. 9417–9424. doi: 10.1158/0008-5472.CAN-07-1286.

Lohela, M. *et al.* (2009) 'VEGFs and receptors involved in angiogenesis versus lymphangiogenesis', *Current opinion in cell biology*. Molecular/Cancer Biology Laboratory, Biomedicum Helsinki and Department of Pathology, Haartman Institute, University of Helsinki, Helsinki, Finland., 21(2), pp. 154–165. doi: 10.1016/j.ceb.2008.12.012.

Loke, P. *et al.* (2002) 'IL-4 dependent alternatively-activated macrophages have a distinctive in vivo gene expression phenotype.', *BMC immunology*. BioMed Central, 3, p. 7. doi: 10.1186/1471-2172-3-7.

Lund, A. W. *et al.* (2012) 'VEGF-C Promotes Immune Tolerance in B16 Melanomas and Cross-Presentation of Tumor Antigen by Lymph Node Lymphatics', *Cell Reports*. Cell Press, 1(3), pp. 191–199. doi: 10.1016/J.CELREP.2012.01.005.

Ly, L. V. *et al.* (2010) 'In Aged Mice, Outgrowth of Intraocular Melanoma Depends on Proangiogenic M2-Type Macrophages', *The Journal of Immunology*, 185(6), pp. 3481–3488. doi: 10.4049/jimmunol.0903479.

Maertens, L. *et al.* (2014) 'Bone marrow-derived mesenchymal stem cells drive lymphangiogenesis.', *PloS one*. Public Library of Science, 9(9), p. e106976. doi: 10.1371/journal.pone.0106976.

Malaguarnera, L. *et al.* (2004) 'Prolactin increases HO-1 expression and induces VEGF production in human macrophages', *Journal of Cellular Biochemistry*, 93(1), pp. 197–206. doi: 10.1002/jcb.20167.

Mand, S. *et al.* (2009) 'Macrophilicidal activity and amelioration of lymphatic pathology in bancroftian filariasis after 3 weeks of doxycycline followed by single-dose diethylcarbamazine', *The American journal of tropical medicine and hygiene*, 81(4), pp. 702–711. doi: 10.4269/ajtmh.2009.09-0155.

Mand, S. *et al.* (2012) 'Doxycycline Improves Filarial Lymphedema Independent of Active Filarial Infection: A Randomized Controlled Trial', *Clinical Infectious Diseases*, 55(5), pp. 621–630. doi: 10.1093/cid/cis486.

Mantovani, A. *et al.* (2002) 'Macrophage polarization: tumor-associated macrophages as a paradigm for polarized M2 mononuclear phagocytes.', *Trends in immunology*. Elsevier, 23(11), pp. 549–55. doi: 10.1016/S1471-4906(02)02302-5.

Maruyama, K. *et al.* (2005) 'Inflammation-induced lymphangiogenesis in the cornea arises from CD11b-positive macrophages.', *The Journal of clinical investigation*. American Society for Clinical Investigation, 115(9), pp. 2363–72. doi: 10.1172/JCI23874.

Mazzieri, R. *et al.* (2011) 'Targeting the ANG2/TIE2 Axis Inhibits Tumor

Growth and Metastasis by Impairing Angiogenesis and Disabling Rebounds of Proangiogenic Myeloid Cells', *Cancer Cell*. Elsevier, 19(4), pp. 512–526. doi: 10.1016/j.ccr.2011.02.005.

McCall, J. W. *et al.* (1973) 'Mongolian jirds (*Meriones unguiculatus*) infected with *Brugia pahangi* by the intraperitoneal route: a rich source of developing larvae, adult filariae, and microfilariae.', *The Journal of parasitology*, 59(3), p. 436. Available at: <http://www.ncbi.nlm.nih.gov/pubmed/4711663> (Accessed: 11 February 2019).

McSorley, H. J., Hewitson, J. P. and Maizels, R. M. (2013) 'Immunomodulation by helminth parasites: Defining mechanisms and mediators', *International Journal for Parasitology*. Pergamon, 43(3–4), pp. 301–310. doi: 10.1016/J.IJPARA.2012.11.011.

Mellor, R. H. *et al.* (2011) 'Mutations in FOXC2 in Humans (Lymphoedema Distichiasis Syndrome) Cause Lymphatic Dysfunction on Dependency', *Journal of Vascular Research*. Karger Publishers, 48(5), pp. 397–407. doi: 10.1159/000323484.

Mertlitz, S. *et al.* (2017) 'Lymphangiogenesis is a feature of acute GVHD, and VEGFR-3 inhibition protects against experimental GVHD.', *Blood*. American Society of Hematology, 129(13), pp. 1865–1875. doi: 10.1182/blood-2016-08-734210.

Metenou, S. *et al.* (2010) 'At Homeostasis Filarial Infections Have Expanded Adaptive T Regulatory but Not Classical Th2 Cells', *J Immunol*, 184(9), pp. 5375–5382. doi: 10.4049/jimmunol.0904067.

Metenou, S. and Nutman, T. B. (2013) 'Regulatory T cell subsets in filarial infection and their function', *Front Immunol*. 2013/10/19. Helminth Immunology Section, Laboratory of Parasitic Diseases, National Institutes of Health, Bethesda, MD, USA., 4, p. 305. doi: 10.3389/fimmu.2013.00305.

Michael, E. and Bundy, D. A. P. (1997) 'Global mapping of lymphatic filariasis', *Parasitology Today*, 13(12), pp. 472–476. doi: 10.1016/s0169-4758(97)01151-4.

Michael, E., Bundy, D. A. P. and Grenfell, B. T. (1996) 'Re-assessing the global prevalence and distribution of lymphatic filariasis', *Parasitology*, 112, pp. 409–428.

Mihara, M. *et al.* (2012) 'Indocyanine green (ICG) lymphography is superior to lymphoscintigraphy for diagnostic imaging of early lymphedema of the upper limbs.', *PloS one*. Public Library of Science, 7(6), p. e38182. doi: 10.1371/journal.pone.0038182.

Mills, C. D. (2012) 'M1 and M2 Macrophages: Oracles of Health and Disease.', *Critical reviews in immunology*, 32(6), pp. 463–88. Available at: <http://www.ncbi.nlm.nih.gov/pubmed/23428224> (Accessed: 4 March 2019).

Mitchell, D. *et al.* (2010) 'ALK1-Fc inhibits multiple mediators of angiogenesis and suppresses tumor growth', *Molecular Cancer Therapeutics*. American Association for Cancer Research Inc., 9(2), pp. 379–388. doi: 10.1158/1535-7163.MCT-09-0650.

- Moldobaeva, A. *et al.* (2017) 'Lymphangiogenesis in rat asthma model.', *Angiogenesis*. NIH Public Access, 20(1), pp. 73–84. doi: 10.1007/s10456-016-9529-2.
- Mor, F., Quintana, F. J. and Cohen, I. R. (2004) 'Th1 Polarization Secreted by Activated T Cells and Induces Vascular Endothelial Growth Factor Is Angiogenesis-Inflammation Cross-Talk', *J Immunol References*, 172, pp. 4618–4623. doi: 10.4049/jimmunol.172.7.4618.
- Mortimer, P. (2013) 'Arm lymphoedema after breast cancer', *The Lancet Oncology*. Elsevier, 14(6), pp. 442–443. doi: 10.1016/S1470-2045(13)70097-4.
- Mortimer, P. S. and Rockson, S. G. (2014) 'New developments in clinical aspects of lymphatic disease.', *The Journal of clinical investigation*. American Society for Clinical Investigation, 124(3), pp. 915–21. doi: 10.1172/JCI171608.
- Mueller, C. G. *et al.* (2007) 'Critical role of monocytes to support normal B cell and diffuse large B cell lymphoma survival and proliferation', *Journal of Leukocyte Biology*, 82(3), pp. 567–575. doi: 10.1189/jlb.0706481.
- Myers, A. L. (2018) 'Localized Lymphadenitis, Lymphadenopathy, and Lymphangitis', *Principles and Practice of Pediatric Infectious Diseases*. Elsevier, pp. 158-163.e1. doi: 10.1016/B978-0-323-40181-4.00020-7.
- Mylonas, K. J. *et al.* (2009) 'Alternatively Activated Macrophages Elicited by Helminth Infection Can Be Reprogrammed to Enable Microbial Killing', *The Journal of Immunology*, 182(5), pp. 3084–3094. doi: 10.4049/jimmunol.0803463.
- Na, Y.-R. *et al.* (2013) 'Cyclooxygenase-2 inhibition blocks M2 macrophage differentiation and suppresses metastasis in murine breast cancer model.', *PloS one*. Public Library of Science, 8(5), p. e63451. doi: 10.1371/journal.pone.0063451.
- Nadarajah, N. *et al.* (2018) 'A Novel Splice-Site Mutation in VEGFC Is Associated with Congenital Primary Lymphoedema of Gordon', *International Journal of Molecular Sciences*, 19(8), p. 2259. doi: 10.3390/ijms19082259.
- Nair, M. G., Guild, K. J. and Artis, D. (2006) 'Novel effector molecules in type 2 inflammation: lessons drawn from helminth infection and allergy.', *Journal of immunology (Baltimore, Md. : 1950)*. NIH Public Access, 177(3), pp. 1393–9. Available at: <http://www.ncbi.nlm.nih.gov/pubmed/16849442> (Accessed: 4 March 2019).
- Narushima, M. *et al.* (2015) 'Indocyanine Green Lymphography Findings in Limb Lymphedema', *Journal of Reconstructive Microsurgery*, 32(01), pp. 072–079. doi: 10.1055/s-0035-1564608.
- Nelson, F. K. *et al.* (1991) 'The immunodeficient scid mouse as a model for human lymphatic filariasis', *J Exp Med*. 1991/03/01. Department of Pathology, University of Connecticut Health Center, Farmington 06030., 173(3), pp. 659–663.
- Newman, B. *et al.* (2012) 'Possible genetic predisposition to lymphedema

after breast cancer', *Lymphatic research and biology*. Institute of Health and Biomedical Innovation and School of Public Health, Queensland University of Technology, Brisbane, Australia., 10(1), pp. 2–13. doi: 10.1089/lrb.2011.0024.

Niessen, K. *et al.* (2010) 'ALK1 signaling regulates early postnatal lymphatic vessel development.', *Blood*. The American Society of Hematology, 115(8), pp. 1654–61. doi: 10.1182/blood-2009-07-235655.

Noroës, J. *et al.* (1996) 'Ultrasonographic evidence of abnormal lymphatic vessels in young men with adult *Wuchereria bancrofti* infection in the scrotal area', *The Journal of Urology*. 1996/08/01. Hospital das Clinicas, UFPE, Centro de Pesquisas Aggeu Magalhaes-FIOCRUZ, Recife, Brasil.: No longer published by Elsevier, 156(2 Pt 1), pp. 409–412. doi: 10.1016/S0022-5347(01)65862-2.

Noy, R. and Pollard, J. W. (2014) 'Tumor-associated macrophages: from mechanisms to therapy.', *Immunity*. NIH Public Access, 41(1), pp. 49–61. doi: 10.1016/j.immuni.2014.06.010.

Nutman, T. B. (2013) 'Insights into the pathogenesis of disease in human lymphatic filariasis', *Lymphatic research and biology*. Laboratory of Parasitic Diseases, National Institute of Allergy and Infectious Diseases, Bethesda, Maryland., 11(3), pp. 144–148. doi: 10.1089/lrb.2013.0021.

O'Farrell, A. M. *et al.* (2003) 'SU11248 is a novel FLT3 tyrosine kinase inhibitor with potent activity in vitro and in vivo', *Blood*, 101(9), pp. 3597–3605. doi: 10.1182/blood-2002-07-2307.

O'Regan, N. L. *et al.* (2014) 'Brugia malayi microfilariae induce a regulatory monocyte/macrophage phenotype that suppresses innate and adaptive immune responses.', *PLoS neglected tropical diseases*. Public Library of Science, 8(10), p. e3206. doi: 10.1371/journal.pntd.0003206.

Ochi, N. *et al.* (2007) 'Vascular Endothelial Growth Factor-C Secreted by Pancreatic Cancer Cell Line Promotes Lymphatic Endothelial Cell Migration in an In Vitro Model of Tumor Lymphangiogenesis', *Pancreas*, 34(4), pp. 444–451. doi: 10.1097/mpa.0b13e31803dd307.

Ogata, F. *et al.* (2016) 'Excess Lymphangiogenesis Cooperatively Induced by Macrophages and CD4+ T Cells Drives the Pathogenesis of Lymphedema', *Journal of Investigative Dermatology*. Elsevier, 136(3), pp. 706–714. doi: 10.1016/J.JID.2015.12.001.

Oh, S.-J. *et al.* (1997) 'VEGF and VEGF-C: Specific Induction of Angiogenesis and Lymphangiogenesis in the Differentiated Avian Chorioallantoic Membrane', *Developmental Biology*. Academic Press, 188(1), pp. 96–109. doi: 10.1006/DBIO.1997.8639.

Ortega, R. A. *et al.* (2016) 'Manipulating the NF-κB pathway in macrophages using mannosylated, siRNA-delivering nanoparticles can induce immunostimulatory and tumor cytotoxic functions.', *International journal of nanomedicine*. Dove Press, 11, pp. 2163–77. doi: 10.2147/IJN.S93483.

Osborne, J. and Devaney, E. (1998) 'The L3 of *Brugia* induces a Th2-

polarized response following activation of an IL-4-producing CD4-CD8-alpha-beta T cell population', *International Immunology*, 10(10), pp. 1583–1590. doi: 10.1093/intimm/10.10.1583.

Osborne, J., Hunter, S. J. and Devaney, E. (1996) *Anti-Interleukin-4 Modulation of the Th2 Polarized Response to the Parasitic Nematode Brugia pahangi*, *INFECTION AND IMMUNITY*. Available at: <https://www.ncbi.nlm.nih.gov/pmc/articles/PMC174249/pdf/643461.pdf> (Accessed: 22 February 2019).

Ottesen, E. A. (1992) 'INFECTION AND DISEASE IN LYMPHATIC FILARIASIS - AN IMMUNOLOGICAL PERSPECTIVE', *Parasitology*, 104, pp. S71–S79.

Ottesen, E. A. (2000) 'Editorial: The Global Programme to Eliminate Lymphatic Filariasis', *Tropical Medicine and International Health*. John Wiley & Sons, Ltd (10.1111), 5(9), pp. 591–594. doi: 10.1046/j.1365-3156.2000.00620.x.

Ottesen, E. A. (2006) 'Lymphatic filariasis: Treatment, control and elimination', *Advances in parasitology*. Lymphatic Filariasis Support Centre, The Task Force for Child Survival and Development, 750 Commerce Drive Decatur, GA 30030, USA., 61, pp. 395–441. doi: 10.1016/s0065-308x(05)61010-x.

Paavonen, K. *et al.* (2002) 'Vascular endothelial growth factors C and D and their VEGFR-2 and 3 receptors in blood and lymphatic vessels in healthy and arthritic synovium.', *The Journal of rheumatology*, 29(1), pp. 39–45. Available at: <http://www.ncbi.nlm.nih.gov/pubmed/11824969> (Accessed: 11 March 2019).

Paily, K. P., Hoti, S. L. and Das, P. K. (2009) 'A review of the complexity of biology of lymphatic filarial parasites', *Journal of parasitic diseases : official organ of the Indian Society for Parasitology*. Springer, 33(1–2), pp. 3–12. doi: 10.1007/s12639-009-0005-4.

De Palma, M. *et al.* (2005) 'Tie2 identifies a hematopoietic lineage of proangiogenic monocytes required for tumor vessel formation and a mesenchymal population of pericyte progenitors', *Cancer Cell*, 8(3), pp. 211–226. doi: 10.1016/j.ccr.2005.08.002.

Pani, S. P. *et al.* (1995) 'Episodic adenolymphangitis and lymphoedema in patients with bancroftian filariasis.', *Transactions of the Royal Society of Tropical Medicine and Hygiene*, 89(1), pp. 72–4. Available at: <http://www.ncbi.nlm.nih.gov/pubmed/7747314> (Accessed: 28 January 2019).

Pani, S. P. and Srividya, A. (1995) 'Clinical manifestations of bancroftian filariasis with special reference to lymphoedema grading', *Indian J Med Res*, 102, pp. 114–118. Available at: <http://www.ncbi.nlm.nih.gov/pubmed/8543349> (Accessed: 28 January 2019).

Park, C., Lee, J. Y. and Yoon, Y. (2011) 'Role of bone marrow-derived lymphatic endothelial progenitor cells for lymphatic neovascularization.', *Trends in cardiovascular medicine*. NIH Public Access, 21(5), pp. 135–40.

doi: 10.1016/j.tcm.2012.04.002.

Partanen, T. A. and Paavonen, K. (2001) 'Lymphatic versus blood vascular endothelial growth factors and receptors in humans', *Microscopy Research and Technique*, 55(2), pp. 108–121. doi: 10.1002/jemt.1162.

Partono, F. (1987) 'THE SPECTRUM OF DISEASE IN LYMPHATIC FILARIASIS', *Ciba Foundation Symposia*, 127, pp. 15–31. Available at: <http://www.ncbi.nlm.nih.gov/pubmed/3297555> (Accessed: 28 January 2019).

Petrova, T. V *et al.* (2004) 'Defective valves and abnormal mural cell recruitment underlie lymphatic vascular failure in lymphedema distichiasis', *Nature Medicine*. Nature Publishing Group, 10(9), pp. 974–981. doi: 10.1038/nm1094.

Pfarr, K. M. *et al.* (2009) 'Filariasis and lymphoedema', *Parasite immunology*, 31(11), pp. 664–672. doi: 10.1111/j.1365-3024.2009.01133.x.

Qi, H., Kastenmüller, W. and Germain, R. N. (2014) 'Spatiotemporal Basis of Innate and Adaptive Immunity in Secondary Lymphoid Tissue', *Annual Review of Cell and Developmental Biology*. Annual Reviews, 30(1), pp. 141–167. doi: 10.1146/annurev-cellbio-100913-013254.

Qian, B.-Z. *et al.* (2011) 'CCL2 recruits inflammatory monocytes to facilitate breast-tumour metastasis', *Nature*, 475(7355), pp. 222–225. doi: 10.1038/nature10138.

Qian, B.-Z. and Pollard, J. W. (2010) 'Macrophage diversity enhances tumor progression and metastasis.', *Cell*. NIH Public Access, 141(1), pp. 39–51. doi: 10.1016/j.cell.2010.03.014.

Radu, M. and Chernoff, J. (2013) 'An in vivo assay to test blood vessel permeability.', *Journal of visualized experiments : JoVE*. MyJoVE Corporation, (73), p. e50062. doi: 10.3791/50062.

Raes, G. *et al.* (2002) 'Differential expression of FIZZ1 and Ym1 in alternatively versus classically activated macrophages', *Journal of Leukocyte Biology*, 71(4), pp. 597–602.

Rajan, T. . *et al.* (2002) 'Brugian infections in the peritoneal cavities of laboratory mice: kinetics of infection and cellular responses', *Experimental Parasitology*. Academic Press, 100(4), pp. 235–247. doi: 10.1016/S0014-4894(02)00015-2.

Rajan, T. V. *et al.* (1999) 'Life and Death of *Brugia malayi* in the Mammalian Host: Passive Death vs Active Killing', *Experimental Parasitology*. Academic Press, 93(2), pp. 120–122. doi: 10.1006/EXPR.1999.4447.

Rajan, T. V *et al.* (1996) 'Role of nitric oxide in host defense against an extracellular, metazoan parasite, *Brugia malayi*.', *Infection and immunity*. American Society for Microbiology (ASM), 64(8), pp. 3351–3. Available at: <http://www.ncbi.nlm.nih.gov/pubmed/8757874> (Accessed: 22 March 2019).

Ramaiah, K. D. *et al.* (1998) 'Direct and indirect costs of the acute form of lymphatic filariasis to households in rural areas of Tamil Nadu, south India.', *Tropical medicine & international health : TM & IH*, 3(2), pp. 108–15.

Available at: <http://www.ncbi.nlm.nih.gov/pubmed/9537272> (Accessed: 28 January 2019).

Ramaiah, K. D. and Ottesen, E. A. (2014) 'Progress and Impact of 13 Years of the Global Programme to Eliminate Lymphatic Filariasis on Reducing the Burden of Filarial Disease', *PLoS Neglected Tropical Diseases*. Edited by M. Bockarie. Public Library of Science, 8(11), p. e3319. doi: 10.1371/journal.pntd.0003319.

Ran, S. and Montgomery, K. E. (2012) 'Macrophage-mediated lymphangiogenesis: the emerging role of macrophages as lymphatic endothelial progenitors.', *Cancers*. Multidisciplinary Digital Publishing Institute (MDPI), 4(3), pp. 618–57. doi: 10.3390/cancers4030618.

Randolph, G. J. *et al.* (2017) 'The Lymphatic System: Integral Roles in Immunity.', *Annual review of immunology*. NIH Public Access, 35, pp. 31–52. doi: 10.1146/annurev-immunol-041015-055354.

Randolph, G. J., Jakubzick, C. and Qu, C. (2008) 'Antigen presentation by monocytes and monocyte-derived cells.', *Current opinion in immunology*. NIH Public Access, 20(1), pp. 52–60. doi: 10.1016/j.coi.2007.10.010.

Rath, M. *et al.* (2014) 'Metabolism via Arginase or Nitric Oxide Synthase: Two Competing Arginine Pathways in Macrophages', *Frontiers in Immunology*. Frontiers, 5, p. 532. doi: 10.3389/fimmu.2014.00532.

Reuwer, A. Q. *et al.* (2012) 'Functional consequences of prolactin signalling in endothelial cells: a potential link with angiogenesis in pathophysiology?', *Journal of Cellular and Molecular Medicine*, 16(9), pp. 2035–2048. doi: 10.1111/j.1582-4934.2011.01499.x.

Riabov, V. *et al.* (2014) 'Role of tumor associated macrophages in tumor angiogenesis and lymphangiogenesis.', *Frontiers in Physiology*, 5, p. 75. doi: 10.3389/fphys.2014.00075.

Ricard, N. *et al.* (2012) 'BMP9 and BMP10 are critical for postnatal retinal vascular remodeling', *Blood*, 119(25), pp. 6162–6171. doi: 10.1182/blood-2012-01-407593.

Rockson, S. G. and Rivera, K. K. (2008) 'Estimating the Population Burden of Lymphedema', *Annals of the New York Academy of Sciences*, 1131(1), pp. 147–154. doi: 10.1196/annals.1413.014.

Rosas, M. *et al.* (2014) 'The Transcription Factor Gata6 Links Tissue Macrophage Phenotype and Proliferative Renewal', *Science*, 344(6184), pp. 645–648. doi: 10.1126/science.1251414.

Roskoski, R. (2007) 'Sunitinib: A VEGF and PDGF receptor protein kinase and angiogenesis inhibitor', *Biochemical and Biophysical Research Communications*, 356(2), pp. 323–328. doi: 10.1016/j.bbrc.2007.02.156.

Saaristo, A. *et al.* (2002) 'Adenoviral VEGF-C overexpression induces blood vessel enlargement, tortuosity, and leakiness but no sprouting angiogenesis in the skin or mucous membranes', *The FASEB Journal*. Federation of American Societies for Experimental Biology, 16(9), pp. 1041–1049. doi:

10.1096/fj.01-1042com.

Saaristo, A. *et al.* (2006) 'Vascular Endothelial Growth Factor-C Accelerates Diabetic Wound Healing', *The American Journal of Pathology*. Elsevier, 169(3), pp. 1080–1087. doi: 10.2353/AJPATH.2006.051251.

Sabine, A. *et al.* (2012) 'Mechanotransduction, PROX1, and FOXC2 cooperate to control connexin37 and calcineurin during lymphatic-valve formation.', *Developmental cell*. Elsevier, 22(2), pp. 430–45. doi: 10.1016/j.devcel.2011.12.020.

Saefteel, M. *et al.* (2001) 'Lack of interferon- γ confers impaired neutrophil granulocyte function and imparts prolonged survival of adult filarial worms in murine filariasis', *Microbes and Infection*. Elsevier Masson, 3(3), pp. 203–213. doi: 10.1016/S1286-4579(01)01372-7.

Saefteel, M. *et al.* (2003) 'Synergism of gamma interferon and interleukin-5 in the control of murine filariasis.', *Infection and immunity*. American Society for Microbiology (ASM), 71(12), pp. 6978–85. doi: 10.1128/IAI.71.12.6978-6985.2003.

Sánchez-Paulete, A. R. *et al.* (2017) 'Antigen cross-presentation and T-cell cross-priming in cancer immunology and immunotherapy', *Annals of Oncology*. Narnia, 28(suppl_12), pp. xii44–xii55. doi: 10.1093/annonc/mdx237.

Sangaletti, S. *et al.* (2008) 'Macrophage-Derived SPARC Bridges Tumor Cell-Extracellular Matrix Interactions toward Metastasis', *Cancer Research*. American Association for Cancer Research, 68(21), pp. 9050–9059. doi: 10.1158/0008-5472.CAN-08-1327.

Schlienger, K. *et al.* (2000) 'Efficient priming of protein antigen-specific human CD4(+) T cells by monocyte-derived dendritic cells.', *Blood*, 96(10), pp. 3490–8. Available at: <http://www.ncbi.nlm.nih.gov/pubmed/11071646> (Accessed: 3 May 2019).

Semo, J., Nicenboim, J. and Yaniv, K. (2016) 'Development of the lymphatic system: new questions and paradigms', *Development*. Oxford University Press for The Company of Biologists Limited, 143(6), pp. 924–935. doi: 10.1242/DEV.132431.

Shaw, T. N. *et al.* (2018) 'Tissue-resident macrophages in the intestine are long lived and defined by Tim-4 and CD4 expression', *The Journal of Experimental Medicine*, 215(6), pp. 1507–1518. doi: 10.1084/jem.20180019.

Sheik, Y. *et al.* (2015) 'FOXC2 and FLT4 Gene Variants in Lymphatic Filariasis', *Lymphatic Research and Biology*, 13(2), pp. 112–119. doi: 10.1089/lrb.2014.0025.

Shenoy, R. K. *et al.* (1998) 'Prevention of acute adenolymphangitis in brugian filariasis: comparison of the efficacy of ivermectin and diethylcarbamazine, each combined with local treatment of the affected limb', *Annals of Tropical Medicine and Parasitology*, 92(5), pp. 587–594.

Shenoy, R. K. *et al.* (2007) 'Doppler ultrasonography reveals adult-worm

nests in the lymph vessels of children with brugian filariasis', *Annals of Tropical Medicine & Parasitology*. Taylor & Francis, 101(2), pp. 173–180. doi: 10.1179/136485907X154566.

Shenoy, R K *et al.* (2007) 'Preliminary findings from a cross-sectional study on lymphatic filariasis in children, in an area of India endemic for *Brugia malayi* infection', *Ann Trop Med Parasitol*. 2007/03/17. Filariasis Chemotherapy Unit, T.D. Medical College Hospital, Alappuzha - 688 011, Kerala, India. drrkshenoy@gmail.com, 101(3), pp. 205–213. doi: 10.1179/136485907x154548.

Shenoy, R. K. (2008) 'Clinical and pathological aspects of filarial lymphedema and its management', *The Korean journal of parasitology*. Filariasis Chemotherapy Unit, T. D. Medical College Hospital, Alappuzha-688 011, Kerala, India. drrkshenoy@gmail.com, 46(3), pp. 119–125. doi: 10.3347/kjp.2008.46.3.119.

Shenoy, R. K. *et al.* (2008) 'Lymphoscintigraphic evidence of lymph vessel dilation in the limbs of children with *Brugia malayi* infection.', *The Journal of communicable diseases*, 40(2), pp. 91–100. Available at: <http://www.ncbi.nlm.nih.gov/pubmed/19301693> (Accessed: 6 February 2019).

Shi, C. and Pamer, E. G. (2011) 'Monocyte recruitment during infection and inflammation.', *Nature reviews. Immunology*. NIH Public Access, 11(11), pp. 762–74. doi: 10.1038/nri3070.

Singh, N. *et al.* (2013) 'Soluble vascular endothelial growth factor receptor 3 is essential for corneal alymphaticity', *Blood*. American Society of Hematology, 121(20), pp. 4242–4249. doi: 10.1182/BLOOD-2012-08-453043.

Skobe, M. *et al.* (2001) 'Induction of tumor lymphangiogenesis by VEGF-C promotes breast cancer metastasis', *Nature Medicine*. Nature Publishing Group, 7(2), pp. 192–198. doi: 10.1038/84643.

Smith, P. *et al.* (2004) 'Schistosoma mansoni Worms Induce Anergy of T Cells via Selective Up-Regulation of Programmed Death Ligand 1 on Macrophages', *The Journal of Immunology*, 173(2), pp. 1240–1248. doi: 10.4049/jimmunol.173.2.1240.

Soderberg, K. A. *et al.* (2005) 'Innate control of adaptive immunity via remodeling of lymph node feed arteriole', *Proceedings of the National Academy of Sciences*, 102(45), pp. 16315–16320. doi: 10.1073/pnas.0506190102.

Sousa, S. *et al.* (2015) 'Human breast cancer cells educate macrophages toward the M2 activation status', *Breast Cancer Research*. BioMed Central, 17(1), p. 101. doi: 10.1186/s13058-015-0621-0.

Spencer, L., Shultz, L. and Rajan, T. V (2001) 'Interleukin-4 receptor-Stat6 signaling in murine infections with a tissue-dwelling nematode parasite.', *Infection and immunity*. American Society for Microbiology (ASM), 69(12), pp. 7743–52. doi: 10.1128/IAI.69.12.7743-7752.2001.

- Stanton, M. C. *et al.* (2015) 'Exploring hydrocoele surgery accessibility and impact in a lymphatic filariasis endemic area of southern Malawi', *Transactions of the Royal Society of Tropical Medicine and Hygiene*, 109(4), pp. 252–261. doi: 10.1093/trstmh/trv009.
- Su, J.-L. *et al.* (2007) 'The role of the VEGF-C/VEGFR-3 axis in cancer progression.', *British journal of cancer*. Nature Publishing Group, 96(4), pp. 541–5. doi: 10.1038/sj.bjc.6603487.
- Sutherland, T. E. *et al.* (2018) 'Ym1 induces RELM α and rescues IL-4R α deficiency in lung repair during nematode infection', *PLoS Pathogens*. Edited by W. C. Gause. Public Library of Science, 14(11), p. e1007423. doi: 10.1371/journal.ppat.1007423.
- Sweet, D. T. *et al.* (2015) 'Lymph flow regulates collecting lymphatic vessel maturation in vivo.', *The Journal of clinical investigation*. American Society for Clinical Investigation, 125(8), pp. 2995–3007. doi: 10.1172/JCI79386.
- Takahashi, S. (2011) 'Vascular endothelial growth factor (VEGF), VEGF receptors and their inhibitors for antiangiogenic tumor therapy.', *Biological & pharmaceutical bulletin*, 34(12), pp. 1785–8. Available at: <http://www.ncbi.nlm.nih.gov/pubmed/22130231> (Accessed: 27 March 2019).
- Tamarozzi, F. *et al.* (2016) 'Wolbachia endosymbionts induce neutrophil extracellular trap formation in human onchocerciasis', *Scientific Reports*. Nature Publishing Group, 6(1), p. 35559. doi: 10.1038/srep35559.
- Tammela, T. and Alitalo, K. (2010) 'Lymphangiogenesis: Molecular Mechanisms and Future Promise', *Cell*. Cell Press, 140(4), pp. 460–476. doi: 10.1016/J.CELL.2010.01.045.
- Tammela, T., Petrova, T. V and Alitalo, K. (2005) 'Molecular lymphangiogenesis: new players', *Trends in Cell Biology*, 15(8), pp. 434–441. doi: 10.1016/j.tcb.2005.06.004.
- Taylor, M. D. *et al.* (2005) 'Removal of regulatory T cell activity reverses hyporesponsiveness and leads to filarial parasite clearance in vivo.', *Journal of immunology (Baltimore, Md. : 1950)*, 174(8), pp. 4924–33. Available at: <http://www.ncbi.nlm.nih.gov/pubmed/15814720> (Accessed: 22 February 2019).
- Taylor, M. D. *et al.* (2006) 'F4/80(+) alternatively activated macrophages control CD4(+) T cell hyporesponsiveness at sites peripheral to filarial infection', *Journal of Immunology*, 176(11), pp. 6918–6927.
- Taylor, M. J., Hoerauf, A. and Bockarie, M. (2010) 'Lymphatic filariasis and onchocerciasis', *Lancet (London, England)*, 376(9747), pp. 1175–1185. doi: 10.1016/s0140-6736(10)60586-7.
- Tian, W. *et al.* (2017) 'Leukotriene B₄ antagonism ameliorates experimental lymphedema', *Science Translational Medicine*, 9(389), p. eaal3920. doi: 10.1126/scitranslmed.aal3920.
- Ton, T. G. N., Mackenzie, C. and Molyneux, D. H. (2015) 'The burden of mental health in lymphatic filariasis', *Infectious Diseases of Poverty*. BioMed

Central, 4(1), p. 34. doi: 10.1186/s40249-015-0068-7.

Tosato, G. *et al.* (1988) 'Stimulation of EBV-activated human B cells by monocytes and monocyte products. Role of IFN-beta 2/B cell stimulatory factor 2/IL-6.', *Journal of immunology (Baltimore, Md. : 1950)*. American Association of Immunologists, 140(12), pp. 4329–36. Available at: <http://www.ncbi.nlm.nih.gov/pubmed/2836512> (Accessed: 3 May 2019).

Turner, J. D. *et al.* (2009) 'Wolbachia lipoprotein stimulates innate and adaptive immunity through Toll-like receptors 2 and 6 to induce disease manifestations of filariasis.', *The Journal of biological chemistry*. American Society for Biochemistry and Molecular Biology, 284(33), pp. 22364–78. doi: 10.1074/jbc.M901528200.

Turner, J. D. *et al.* (2018) 'Interleukin-4 activated macrophages mediate immunity to helminth infection by sustaining CCR3-dependent eosinophilia', *PLOS Pathogens*. Submitted.

Vannella, K. M. and Wynn, T. A. (2017) 'Mechanisms of Organ Injury and Repair by Macrophages', *Annual Review of Physiology*. Annual Reviews , 79(1), pp. 593–617. doi: 10.1146/annurev-physiol-022516-034356.

Veikkola, T. *et al.* (2003) 'Intrinsic versus microenvironmental regulation of lymphatic endothelial cell phenotype and function', *The FASEB Journal*, 17(14), pp. 2006–2013. doi: 10.1096/fj.03-0179com.

Venneri, M. A. *et al.* (2007) 'Identification of proangiogenic TIE2-expressing monocytes (TEMs) in human peripheral blood and cancer.', *Blood*. American Society of Hematology, 109(12), pp. 5276–85. doi: 10.1182/blood-2006-10-053504.

Vickery, A. C. *et al.* (1991) 'Histopathology of *Brugia malayi*-infected nude mice after immune-reconstitution', *Acta Trop*. 1991/04/01. College of Public Health, University of South Florida, Tampa 33612., 49(1), pp. 45–55.

Villamor, N., Montserrat, E. and Colomer, D. (2003) 'Mechanism of action and resistance to monoclonal antibody therapy.', *Seminars in oncology*, 30(4), pp. 424–33. Available at: <http://www.ncbi.nlm.nih.gov/pubmed/12939711> (Accessed: 3 May 2019).

Vincent, A. L. *et al.* (1984) 'The lymphatic pathology of *Brugia pahangi* in nude (athymic) and thymic mice C3H/HeN', *J Parasitol*. 1984/02/01, 70(1), pp. 48–56.

Vincent, A. L., Sodeman, W. A. and Winters, A. (1980) 'Development of *Brugia pahangi* in normal and nude mice.', *The Journal of parasitology*, 66(3), p. 448. Available at: <http://www.ncbi.nlm.nih.gov/pubmed/6967111> (Accessed: 17 May 2019).

Visuri, M. T. *et al.* (2015) 'VEGF-C and VEGF-C156S in the pro-lymphangiogenic growth factor therapy of lymphedema: a large animal study', *Angiogenesis*. Springer Netherlands, 18(3), pp. 313–326. doi: 10.1007/s10456-015-9469-2.

Vranova, M. and Halin, C. (2014) 'Lymphatic Vessels in Inflammation',

Journal of Clinical & Cellular Immunology. OMICS International, 05(04), pp. 1–11. doi: 10.4172/2155-9899.1000250.

Wang, J. F., Zhang, X. and Groopman, J. E. (2004) *Activation of VEGF Receptor-3 and Its Downstream Signaling Promote Cell Survival Under Oxidative Stress* Downloaded from. JBC Papers in Press. Available at: <http://www.jbc.org/> (Accessed: 10 April 2019).

Wang, Y. and Oliver, G. (2010) 'Current views on the function of the lymphatic vasculature in health and disease.', *Genes & development*. Cold Spring Harbor Laboratory Press, 24(19), pp. 2115–26. doi: 10.1101/gad.1955910.

Warren, A. G. *et al.* (2007) 'Lymphedema', *Annals of Plastic Surgery*, 59(4), pp. 464–472. doi: 10.1097/01.sap.0000257149.42922.7e.

Wauke, K. *et al.* (2002) 'Expression and localization of vascular endothelial growth factor-C in rheumatoid arthritis synovial tissue.', *The Journal of rheumatology*, 29(1), pp. 34–8. Available at: <http://www.ncbi.nlm.nih.gov/pubmed/11824968> (Accessed: 11 March 2019).

Weinkopff, T. *et al.* (2014) 'Filarial Excretory-Secretory Products Induce Human Monocytes to Produce Lymphangiogenic Mediators', *Plos Neglected Tropical Diseases*, 8(7). doi: 10.1371/journal.pntd.0002893.

Weinkopff, T. and Lammie, P. (2011) 'Lack of evidence for the direct activation of endothelial cells by adult female and microfilarial excretory-secretory products', *PloS one*. Department of Cell Biology, University of Georgia, Athens, Georgia, United States of America. tiffany.weinkopff@unil.ch, 6(8), p. e22282. doi: 10.1371/journal.pone.0022282.

Weiss, M. G. (2008) 'Stigma and the social burden of neglected tropical diseases.', *PLoS neglected tropical diseases*. Public Library of Science, 2(5), p. e237. doi: 10.1371/journal.pntd.0000237.

Weng, S.-Y. *et al.* (2018) 'IL-4 Receptor Alpha Signaling through Macrophages Differentially Regulates Liver Fibrosis Progression and Reversal.', *EBioMedicine*. Elsevier, 29, pp. 92–103. doi: 10.1016/j.ebiom.2018.01.028.

Wynn, T. A. and Barron, L. (2010) 'Macrophages: Master Regulators of Inflammation and Fibrosis', *Seminars in Liver Disease*, 30(3), pp. 245–257. doi: 10.1055/s-0030-1255354.

Wynn, T. A., Chawla, A. and Pollard, J. W. (2013) 'Macrophage biology in development, homeostasis and disease.', *Nature*. NIH Public Access, 496(7446), pp. 445–55. doi: 10.1038/nature12034.

Xu, Y. *et al.* (2010) 'Neuropilin-2 mediates VEGF-C–induced lymphatic sprouting together with VEGFR3', *The Journal of Cell Biology*, 188(1), pp. 115–130. doi: 10.1083/jcb.200903137.

Yamaguchi, T. *et al.* (2016) 'Tumor-associated macrophages of the M2 phenotype contribute to progression in gastric cancer with peritoneal

dissemination.’, *Gastric cancer: official journal of the International Gastric Cancer Association and the Japanese Gastric Cancer Association*. Springer, 19(4), pp. 1052–1065. doi: 10.1007/s10120-015-0579-8.

Yamamoto, T. *et al.* (2011) ‘Characteristic Indocyanine Green Lymphography Findings in Lower Extremity Lymphedema: The Generation of a Novel Lymphedema Severity Staging System Using Dermal Backflow Patterns’, *Plastic and Reconstructive Surgery*, 127(5), pp. 1979–1986. doi: 10.1097/PRS.0b013e31820cf5df.

Yoon, Y. S. *et al.* (2003) ‘VEGF-C gene therapy augments postnatal lymphangiogenesis and ameliorates secondary lymphedema’, *J Clin Invest*. 2003/03/06. Department of Vascular Medicine, St. Elizabeth’s Medical Center, Tufts University School of Medicine, Boston, Massachusetts, USA., 111(5), pp. 717–725. doi: 10.1172/jci15830.

Yoshimatsu, Y. *et al.* (2013) ‘Bone morphogenetic protein-9 inhibits lymphatic vessel formation via activin receptor-like kinase 1 during development and cancer progression’, *Proceedings of the National Academy of Sciences of the United States of America*, 110(47), pp. 18940–18945. doi: 10.1073/pnas.1310479110.

Zampell, J. C. *et al.* (2012) ‘CD4+ Cells Regulate Fibrosis and Lymphangiogenesis in Response to Lymphatic Fluid Stasis’, *PLoS ONE*. Edited by N. O. S. Câmara. Public Library of Science, 7(11), p. e49940. doi: 10.1371/journal.pone.0049940.

Zawieja, D. C. (2009) ‘Contractile physiology of lymphatics.’, *Lymphatic research and biology*. Mary Ann Liebert, Inc., 7(2), pp. 87–96. doi: 10.1089/lrb.2009.0007.

Zawieja, S. D. *et al.* (2012) ‘Impairments in the intrinsic contractility of mesenteric collecting lymphatics in a rat model of metabolic syndrome.’, *American journal of physiology. Heart and circulatory physiology*. American Physiological Society, 302(3), pp. H643-53. doi: 10.1152/ajpheart.00606.2011.

Zeldenryk, L. M. *et al.* (2011) ‘The Emerging Story of Disability Associated with Lymphatic Filariasis: A Critical Review’, *Plos Neglected Tropical Diseases*, 5(12). doi: 10.1371/journal.pntd.0001366.

Zhang, B. C. *et al.* (2009) ‘Alternatively Activated RAW264.7 Macrophages Enhance Tumor Lymphangiogenesis in Mouse Lung Adenocarcinoma’, *Journal of Cellular Biochemistry*. [Zhang, Bicheng Gao, Jianfei Rao, Zhiguo] Wuhan Gen Hosp Guangzhou Command PLA, Dept Oncol, Wuhan 430070, Peoples R China. [Zhang, Bicheng Wang, Jun Guo, Yan Chen, Xi Chen, Zhengtang] Third Mil Med Univ, Xinqiao Hosp, Canc Inst PLA, Chongqing, Peoples R C, 107(1), pp. 134–143. doi: 10.1002/jcb.22110.

Zhang, Q. *et al.* (2007) ‘Increased lymphangiogenesis in joints of mice with inflammatory arthritis’, *Arthritis Research & Therapy*. BioMed Central, 9(6), p. R118. doi: 10.1186/ar2326.

Zhao, T. *et al.* (2014) ‘Vascular endothelial growth factor-C: its unrevealed

role in fibrogenesis.', *American journal of physiology. Heart and circulatory physiology*. American Physiological Society, 306(6), pp. H789-96. doi: 10.1152/ajpheart.00559.2013.

Zumsteg, A. and Christofori, G. (2012) 'Myeloid cells and lymphangiogenesis.', *Cold Spring Harbor perspectives in medicine*. Cold Spring Harbor Laboratory Press, 2(6), p. a006494. doi: 10.1101/cshperspect.a006494.